

**Growth of oleaginous yeasts on mixed C5 and C6 sugar streams to generate lipid feedstocks
for renewable hydrocarbon production**

by

Damaris Chinwendu Okafor

A thesis submitted in partial fulfillment of the requirements for the degree of

Master of Science

in

Bioresource Technology

Department of Agricultural, Food and Nutritional Science
University of Alberta

© Damaris Chinwendu Okafor, 2022

Abstract

Microbial lipids are a promising feedstock to produce renewable fuels. Lignocellulosic feedstocks can provide multiple carbon sources for microbial growth, such as hexoses (C6) and pentoses (C5). Oleaginous yeasts can convert C5 and C6 sugars to microbial lipids that can be further processed into renewable fuels and value-added chemicals. The major challenge to the production of microbial lipids for biofuel production using mixed sugar streams is the inability of oleaginous yeasts and many other microbes to utilize the C5 and C6 sugars simultaneously. The challenge is caused by carbon catabolite repression (glucose repression), which is characterized by the global regulatory mechanism that prevents the transcription of genes responsible for the expression/synthesis of enzymes responsible for secondary carbon (C5) utilization in the presence of preferred primary carbon (C6).

Many preliminary screening research reports have identified some oleaginous microbes that can simultaneously utilize xylose and glucose for microbial lipid production. However, further studies to explore comparatively these non-conventional oleaginous yeasts endowed with the ability to simultaneously use C5 and C6 sugars for lipid production will add more knowledge to our understanding of the behavior of these oleaginous yeasts, and improve their industrial application in the renewable energy sector. The present study investigates the mixed sugar (i.e. C5 and C6) utilization abilities of *Pseudozyma tsukubaensis*, *Pseudozyma hubeiensis*, and *Cystobasidium iriomotense* in both shake flask and 5 L scale. The lipids extracted from biomass grown using nitrogen-limiting medium and fully automated 5 L bioreactors were subjected to lipid pyrolysis to generate renewable hydrocarbons. The products of lipid pyrolysis were then characterized.

Comparative studies of *P. tsukubaensis*, *P. hubeiensis*, and *C. iriomotense* grown in shake flasks and bioreactors using the fermentation strategy deployed in this study confirmed the gradual simultaneous assimilation of the xylose and glucose sugars, rather than the preferential utilization of glucose that is typically observed. This research revealed that *P. tsukubaensis* and *P. hubeiensis* efficiently utilized the mixed C5 and C6 carbon sources within 240 h. Conversely, *C. iriomotense* could not completely utilize both sugars within the same cultivation period. *P. hubeiensis* and *P. tsukubaensis* produced higher lipid levels, $59.0 \pm 2.3\%$ and $58.1 \pm 0.1\%$, respectively, than *C. iriomotense*, which displayed lipid yields of $27.0 \pm 0.7\%$. The *n*-hexane soluble extracts (recovered fatty acids) when derivatized were abundant in unsaturated fatty acid methyl esters (FAMES): 86.8% for *P. tsukubaensis*, 64.8% for *P. hubeiensis*, and 56.4% for *C. iriomotense*.

The composition of the renewable hydrocarbon products generated from lipid pyrolysis was identified. *n*-alkanes, *l*-alkenes, internal alkenes, branched hydrocarbons, aromatics, cyclics, and some fatty acids were present. These classes of hydrocarbons had a high C to H ratio indicating that some of the lipid feedstocks were subjected to saturation, decarbonylation, and/or decarboxylation reactions. The most abundant hydrocarbon was the *n*-alkanes series in both the gaseous and liquid fractions. The observed composition of renewable hydrocarbons in this research is consistent with fossil fuels and thus can be used in existing infrastructure where fossil fuels are already in operation. Thus, the hydrocarbon products generated in these studies are promising alternatives to fossil fuel towards reduced/zero carbon emissions, sustainability, and cost-effectiveness.

Taken together, this study provides a comparative study of three oleaginous yeasts and demonstrated that they could simultaneously use xylose and glucose in nitrogen-limiting (C: N = 100:1) fermentation conditions to generate large amounts of lipids. Pyrolysis experiments yielded liquid renewable hydrocarbons that could potentially be used as drop-in fuels. Finally, this research demonstrated that the microbes that are best candidates for simultaneously using C5 and C6 sugars from lignocellulosic feedstocks to generate lipids for biofuel applications were *P. tsukubaensis* and *P. hubeiensis*.

PREFACE

This thesis is an original work prepared by Damaris Chinwendu Okafor. No part of this thesis has been published but there are plans to publish these data immediately after the thesis completion. All experiments in this thesis served to meet the required expectations for MSc program completion as outlined and approved by my supervisor Dr. David C. Bressler and my committee members Dr. Michael Gaenzle and Dr. Jonathan Curtis. All the experiments concerning this research were conducted in the Biorefining Conversions and Fermentation lab and the Agricultural, Food, and Nutritional Science (AFNS) departmental chromatography suite at the University of Alberta. Dr. Michael Chae contributed to the thesis proofreading, revisions, and edits, and provided constructive feedback.

ACKNOWLEDGEMENTS

My sincere thanks go to my supervisor Dr. David C. Bressler who gave me the opportunity for this project. I am grateful for his guidance, support, and encouragement during this program. Thank you for creating this golden opportunity for me to join the renewable energy/green energy team and research. I greatly appreciated it. I also want to thank Dr. Michael Chae, our program manager for his suggestions on my research and his contribution to thesis editing. I would like to thank Dr. Jonathan Curtis as a member of my supervisory committee for his fatherly advice, encouragement on my research, and for allowing me to be here in Canada. I want to thank Dr. Michael Gaenzle as a supervisory committee member for your soothing words and advice in my worst moment in life helped me to be alive pushing. Thank you. Many thanks to Dr. Justice Asomaning for your technical support and troubleshooting when I ran into difficulty with some equipment.

Special thanks to Jingui Lan for being available 24/7 to troubleshoot when I ran into difficulty using the analytical equipment, your assistance, training, and patience are indelible and highly appreciated. I want to thank all my fellow lab mates in 2-38 for their support, advice, encouragement, and for making the lab a second home for us all. Keep it up. To Samuel K., Pahul, Benardo, and Bingxin, thanks for your assistance, time, and forbearing my disturbances, and questions while carrying out LTH experiments.

This research project was possible because of the Tertiary Education Trust Fund (TETFund), Nigerian sponsorship, I thank TETFund immensely for financing the tuition fees, travels, and living expenses for this program. This program would not have been possible without the Federal University of Technology, Owerri (FUTO) approval of the TETFund study fellowship, Thanks to FUTO Vice-Chancellors past and present, especially to Prof. F. C. Eze. I also want to

thank the Future Energy Systems and the Natural Sciences and Engineering Research Council of Canada (NSERC) for project support.

Finally, I want to thank my children, husband, family, and friends for their support and love. Special thanks to my loving husband Anthony and my children Adelaide, Franklin, and George (a.k.a Oto, my Kamsó baby, Juu-juu nwa m, and my mpo-mpo m de-jor-jor, respectively, for their unalloyed care, attention, kind support, and unconditional love. I am here today because you tolerated it. You guys are the best, my dearest friends, and God's precious gifts. To my parents, I am forever proud to be born and trained by you. Thank you for your love and listening ear any time any day. To my dearest siblings and the in-laws, thank you immensely for your support and for standing by me. My friends both in Nigeria and Canada, I appreciate all of you. Thank you.

My greatest thanks go to Jehovah the almighty who has sustained me through thick and thin during this program and saw me through the end. May your precious name be glorified forever and ever. Finally, I want to conclude this acknowledgment with a quote from the 2019 November Watchtower page 27 ~

“The outcome of the decision we make is like the destination of a journey. If you really want to succeed in that destination, you will keep going albeit a road is closed and you thus must change your route. Similarly, if we focus on the outcome of our set goals and decisions not minding the obstacles, we will not quit easily once we encounter setbacks or detours in life”.

Table of Contents

Chapter 1 Introduction

1.1	Background.....	1
1.2	Research objectives	4
1.2.1	Short-term objectives	5
1.3	Research justification	5

Chapter 2 Literature Review

2.1	Major drivers of biofuel production	7
2.2.	Feedstock for biofuel production	9
2.2.1	Oil-based feedstocks	10
2.3	Microbes for microbial lipid generation.....	12
2.4	Microbial biomass production from yeasts	13
2.5	Sugar uptake in yeasts.....	15
2.6	Yeast carbon metabolism.....	16
2.7	Simultaneous utilization of sugars (C5 and C6) in oleaginous yeasts	18
2.8	Lipid biosynthesis in oleaginous yeasts	24
2.9	Carbon catabolite repression	30
2.10	Xylose transporters.....	31
2.11	Yeast <i>Pseudozyma hubeiensis</i> and <i>Pseudozyma tsukubaensis</i>	33
2.11.1	Biology	34
2.11.2	Biotechnological applications of <i>P. hubeiensis</i> and <i>P. tsukubaensis</i>	34
2.12.	Yeast <i>Cystobasidium iriomotense</i>	35
2.12.1	Biology.....	35
2.12.2	Biotechnological applications of <i>C. iriomotense</i>	36
2.13	Factors that affect lipid accumulation	37
2.14	Approaches for the bioconversion of microbial biomass to biofuel production.....	38
2.14.1	Biofuel production through the extraction of the microbial intracellular components.....	40
2.14.1.1	Processing steps for the extraction of the contents of microbial biomass...	41
2.14.1.2	Microbial biomass harvesting operation.....	41
2.14.1.3	Drying of microbial biomass.....	50
2.14.1.4	Cell disruption operation.....	51
2.14.1.5	Lipid extraction.....	53
2.14.2	Whole biomass processing without microbial extraction.....	54
2.14.2.1	Biochemical conversion processes.....	54
2.14.2.2	Thermochemical conversion.....	56
2.14.2.2.1	Pyrolysis	56
2.14.2.2.2	Gasification.....	57
2.14.2.3	Direct biomass combustion.....	58
2.14.2.4	Thermochemical liquefaction.....	59
2.14.3	Chemical conversion processes	60
2.14.3.1	Transesterification.....	61
2.14.3.2	Esterification	63
2.14.4	Current microbial biomass conversion techniques	63
2.14.4.1	Microbial fuel cell (MFC) for electricity generation	63

2.14.4.2	Lipid-to-hydrocarbon (LTH) technology.....	66
Chapter 3 Materials and Methods.....		68
3.1	Materials	68
3.2	Methods	69
3.2.1	Yeast biomass production	69
3.2.1.1	Medium preparation	69
3.2.1.2	Growing the yeast cells.....	71
3.2.1.3	Starter culture preparation.....	72
3.2.1.4	Shake flask fermentation.....	73
3.2.1.5	Bioreactor fermentation.....	73
3.2.2	Analysis of fermentation.....	75
3.2.2.1	Quantification of residual glucose and xylose sugars	75
3.2.2.2	Growth	76
3.2.2.3	Cell dry weight determination.....	76
3.2.3	Microbial lipids quantification.....	77
3.2.4	Fatty acid methyl ester production	79
3.2.5	Gram staining	80
3.2.6	Hydrolysis.....	81
3.2.6.1	Post-hydrolysis treatment.....	82
3.2.6.2	Harvesting the products contained in the hydrolyzed reactors.....	82
3.2.7	Pyrolysis of hexane soluble fraction from oleaginous yeast slurry	82
3.2.8	Analysis of products.....	83
3.2.8.1	Chemical characterization of the hydrocarbon gaseous products	83
3.2.8.2	Chemical characterization of the hydrocarbon liquid products	84
3.2.8.3	Lipid profile analysis.....	85
3.2.9	Statistical analysis	87
Chapter 4: Results and discussion		88
4.1	Gram-stained oleaginous yeast strains.....	88
4.2 Characterization of oleaginous organisms grown in shake flasks.....		89
4.2.1	Growth of <i>P. hubeiensis</i> in 500 mL shake flasks.....	89
4.2.2	Time course of sugar consumption by <i>P. hubeiensis</i> IPM1-10	91
4.2.3	Biomass and lipid accumulation in small-batch shake flask by <i>P. hubeiensis</i> IPM1-10.....	93
4.2.4	Growth by <i>P. tsukubaensis</i> in 500 mL shake flask.....	94
4.2.5	Time course of sugar utilization profile of <i>P. tsukubaensis</i>	94
4.2.6	Biomass and lipid accumulation by <i>P. tsukubaensis</i>	96
4.2.7	Growth curve of <i>C. iriomotense</i> ISM28-8s ^T in 500 mL shake flasks.....	96
4.2.8	Time course utilization of glucose and xylose by <i>C. iriomotense</i> ISM28-8s ^T	98
4.2.9	Biomass and lipid accumulation by <i>C. iriomotense</i> ISM28-8s ^T	99
4.2.10	Summary of growth and lipid accumulation of oleaginous yeasts.....	99
4.3 Characterization of oleaginous organisms grown in 5 L bioreactors		100
4.3.1	Growth and time course of sugar utilization by <i>P. hubeiensis</i> IPM1-10 in bioreactors.....	101
4.3.2	Biomass and lipid accumulation by <i>P. hubeiensis</i> IPM1-10	103
4.3.3	Lipid accumulation by <i>P. hubeiensis</i> IPM1-10.....	104
4.3.4	Fatty acid composition of lipids from <i>P. hubeiensis</i> IPM1-10	105

4.3.5	Growth and time course of sugar utilization by <i>P. tsukubaensis</i> in bioreactors.....	108
4.3.6	Biomass and lipid accumulation by <i>P. tsukubaensis</i>	110
4.3.7	Time course of lipid accumulation in <i>P. tsukubaensis</i>	110
4.3.8	Fatty acid composition of lipids generated by <i>P. tsukubaensis</i>	111
4.3.9	Growth and time course of sugar utilization by <i>C. iriomotense</i> ISM28-8s ^T bioreactors	113
4.3.10	Biomass and lipid accumulation by <i>C. iriomotense</i>	115
4.3.11	Time course of lipid accumulation in <i>C. iriomotense</i> ISM28-8s ^T	115
4.3.12	Fatty acid profile of lipid produced by <i>C. iriomotense</i> ISM28-8s ^T	117
4.3.13	Comparison of yeast growth and lipid accumulation in 5 L bioreactors....	119
4.4	Characterization of the hydrolysis product generated from yeast slurries	120
4.4.1	Product distribution within yeast hydrolysates.....	120
4.4.2	Assessment of lipid classes in yeast hydrolysates through thin layer chromatography	121
4.4.3	Characterization of fatty acids extracted from yeast hydrolysates.....	123
4.5	Characterization of products generated through pyrolysis of hexane-extracted fatty acids	127
4.5.1	Quantification of liquid and gas fractions.....	127
4.5.2	Characterization of the gas fractions obtained through pyrolysis.....	128
4.5.3	Characterization of the liquid fractions obtained through pyrolysis	134
4.5.4	Characterization of the liquid pyrolysis product through FTIR-ATR.....	137
4.6	Overall conclusions from the integration of oleaginous yeasts into the LTH Process...	139
Chapter 5: General conclusions, recommendation, and future directions		139
5,1	General conclusion	139
5.2	Recommendations and future directions	140
References		143

List of Tables

Table 4.1	The % lipid and cell dry weight generated from shake flask cultivation ...	100
Table 4.2	Summary of results from three oleaginous yeasts grown in 5 L bioreactors	120
Table 4.3	Characterization of hydrolysis products generated from yeast slurries.....	121
Table 4.4	Fatty acid profiles of before and after hydrolysis of oleaginous yeasts...	125
Table 4.5	Pyrolysis product distribution.....	128
Table 4.6	Gas fraction components generated through pyrolysis of n-hexane-extracted fatty acids	130

List of Figures

Figure 2.1	Global energy consumption in quadrillion British thermal units and global percentage share of primary energy consumption by energy source. Source: U.S energy information administration, <i>International energy outlook 2021</i> (IEC2021)	8
Figure 2.2	Glycolytic pathway. Enzymes involved in this pathway are written in red color. Carbon numbers for compounds and phosphate positions in the ten steps of glycolysis are written in rectangular boxes. Adapted from Bender, 2013; Blanco & Blanco, (2017)	19
Figure 2.3	Pentose phosphate pathway linked with glycolysis Adapted from Gao et al., (2019) and Stincone et al., (2015).....	23
Figure 2.4	Lipid biosynthesis in yeast. Adapted from Dulermo et al., 2015; adjusted from Gonzalez, (2014) and Ratledge, (2004).....	28
Figure 2.5	Triacylglycerol synthesis from dihydroxyacetone phosphate (DHAP) Adapted from Blanco & Blanco, (2017).....	29
Figure 2.6	Conversion pathways for biofuel production from microbial biomass Adapted from Gonzalez, (2014).....	39
Figure 2.7	Process flow diagram for downstream processing of microbial biomass extracts during biodiesel production. Adapted from Gonzalez, 2014; Halim et al., (2012).....	42
Figure 2.8	Microbial biomass conversion technologies to biofuels. Adapted from Espinosa Gonzalez, (2014). H. Hassan et al., (2019) and Medipally et al., (2015).	55
Figure 2.9	Microbial fuel cell process diagram. Adapted from Moradian et al., (2021)	65
Figure 2.10	Lipid to hydrocarbon (LTH) process. Adapted from Gonzelez et al., (2014) and Asomaning <i>et al.</i> , (2014).....	67
Figure 3.1	Schematic of the fermentation procedure for biofuel production.....	74
Figure 3.2	Schematic diagram of the cell dry weight determination protocol using <i>P. hubeiensis</i> culture	77
Figure 3.3	Schematic diagram of the lipid extraction procedure in freeze-dried oleaginous yeasts.....	78
Figure 3.4	Schematic diagram of the derivatization of oleaginous extracted lipids (TAG) to fatty acid methyl esters.....	80
Figure 3.5	Schematic of thin-layer chromatography	87
Figure 4.1	Micrograph of Gram-stained <i>P. hubeiensis</i> IPM1-10	88
Figure 4.2	Micrograph of Gram-stained <i>P. tsukubaensis</i>	89
Figure 4.3	Micrographs of Gram-stained <i>C. iriomotense</i> ISM28-8s ^T	89
Figure 4.4	Growth curve for <i>P. hubeiensis</i> IPM1-10 in 500 mL Erlenmeyer shake flasks for 240 h using glucose and xylose as the carbon sources at a final concentration of 30 g/L (15 g/L each) and ammonium chloride at 0.5 g/L. The carbon to nitrogen ratio for these studies was 100:1.....	91
Figure 4.5	A time course of sugar consumption by <i>P. hubeiensis</i> IPM1-10 in 500 mL Erlenmeyer shake flasks for 240 h using glucose and xylose as the carbon sources at a final concentration of 30 g/L (15 g/L each) and ammonium chloride at 0.5 g/L. The carbon to nitrogen ratio for these studies was 100:1.....	93

Figure 4.6	Growth curve of <i>P. tsukubaensis</i> in 500 mL Erlenmeyer shake flasks over a 240 h period using glucose and xylose as the carbon sources at a final concentration of 30 g/L (15 g/L each) and ammonium chloride at 0.5 g/L. The initial carbon to nitrogen ratio of the medium was 100:1.....	95
Figure 4.7	The time course sugar consumption profile of <i>P. tsukubaensis</i> when grown in 500 mL Erlenmeyer shake flasks for 240 h using glucose (15 g/L) and xylose (15 g/L) as the carbon sources at a final sugar concentration of 30 g/L and ammonium chloride at 0.5 g/L. The initial carbon to nitrogen ratio of the medium was 100:1.....	95
Figure 4.8	Growth curve of <i>P. tsukubaensis</i> when grown in 500 mL Erlenmeyer shake flasks for 240 h using glucose and xylose as the carbon sources at a final concentration of 30 g/L (15 g/L each) and ammonium chloride at 0.5 g/L, achieving a carbon to nitrogen ratio of 100:1.....	97
Figure 4.9	Time course sugar consumption profile by <i>C. iriomotense ISM28-8s^T</i> in a 500 mL Erlenmeyer shake flask for 240 h using glucose and xylose at a final concentration of 30 g/L (15 g/L each) and ammonium chloride at 0.5 g/L, achieving a carbon to nitrogen ratio of 100:1.....	98
Figure 4.10	Substrate consumption by and growth profiles of <i>P. hubeiensis</i> IPM1-10 in a bioreactor. Cultures were grown for 240 h using an equimolar of glucose and xylose as the carbon sources at a final concentration of 30 g/L (15 g/L each) and ammonium chloride at 0.5 g/L for a carbon to nitrogen ratio of 100:1.....	100
Figure 4.11	Lipid production in <i>P. hubeiensis</i> IPM1-10 from 120 h to 240 h. Cells were grown in a medium containing glucose and xylose in a 1:1 ratio (15 g/L each) in a 5 L bioreactor under limiting nitrogen conditions (0.5 g/L ammonium chloride).....	105
Figure 4.12	Fatty acid profile of the lipids accumulated in <i>P. hubeiensis</i> IPM1-10	108
Figure 4.13	Substrate consumption by and growth profiles of <i>P. tsukubaensis</i> in a bioreactor for 240 h using glucose and xylose as the carbon source at a final concentration of 30 g/L (15 g/L each) and ammonium chloride at 0.5 g/L for a carbon to nitrogen ratio of 100:1.....	109
Figure 4.14	Time course of the experiment to monitor lipid production by <i>P. tsukubaensis</i> from simultaneous utilization of glucose and xylose in the ratio of 1:1 (15 g each) in a 5 L scale bioreactor under limiting nitrogen condition (0.5 g/L ammonium chloride)	111
Figure 4.15	Fatty acid profile of <i>P. tsukubaensis</i> before hydrolysis	112
Figure 4.16	Substrate consumption and growth profiles by <i>C. iriomotense ISM28-8s^T</i> in a 5 L bioreactor over a 240 h period. The medium contained equal amounts of glucose and xylose (15 g/L each, for a total of 30 g/L) and 0.5 g/L ammonium chloride, establishing a carbon to nitrogen ratio of 100:1.....	115
Figure 4.17	Time course of lipid production from 120 h to 240 h by <i>C. iriomotense ISM28-8s^T</i> from simultaneous utilization of glucose and xylose in the ratio of 1:1 (15 g each) in a 5 L scale bioreactor under limiting nitrogen condition (NH ₄ Cl 0.5 g/L).....	117
Figure 4.18	Fatty acid profile of <i>C. iriomotense ISM28-8s^T</i>	118

Figure 4.19	Thin-layer chromatography of yeast lipids after hydrolysis. The mobile phase was hexane, ether, and acetic acid in the ratio of 80:20:1	122
Figure 4.20	The fatty acid composition of the product obtained through hexane extraction of yeast hydrolysates from <i>P. tsukubaensis</i> , <i>P. hubeiensis</i> , and <i>C. iriomotense</i> grew in a 5 L scale bioreactor with glucose, xylose, and ammonium chloride.	124
Figure 4.21	The GC-FID chromatograms of hydrocarbons in the gas fraction generated through pyrolysis (410 °C) of the hexane-extracted fatty acids obtained from <i>P. hubeiensis</i> , <i>P. tsukubaensis</i> , and <i>C. iriomotense</i> hydrolysates.....	131
Figure 4.22	The GC-TCD chromatograms of hydrocarbons in the gas fraction generated through pyrolysis (410 °C) of the hexane-extracted fatty acids obtained from <i>P. hubeiensis</i> , <i>P. tsukubaensis</i> , and <i>C. iriomotense</i> hydrolysates.	132
Figure 4.23	The GC-FID chromatograms of hydrocarbons in the liquid fractions generated through pyrolysis (410 °C) of the hexane-extracted fatty acids obtained from <i>P. hubeiensis</i> , <i>P. tsukubaensis</i> , and <i>C. iriomotense</i> hydrolysates.	135
Figure 4.24	Classes of compounds in the liquid pyrolysis product generated from hexane extracted fatty acids from <i>P. hubeiensis</i> , <i>P. tsukubaensis</i> , and <i>C. iriomotense</i>	137
Figure 4.25	FTIR spectra of the liquid product generated through pyrolysis of fatty acids derived from <i>P. hubeiensis</i> , <i>P. tsukubaensis</i> , and <i>C. iriomotense</i>	138

List of equations

Equation 1	Conversion of citrate to acetyl-CoA and oxaloacetate in the cytosol by ATP-citrate lyase.....	25
Equation 2	Pyruvate conversion to acetyl-CoA by the pyruvate dehydrogenase complex enzyme.....	36
Equation 3	Cell dry weight.....	76

List of abbreviations

ACC	Acetyl-CoA carboxylase
ACP	Acyl carrier protein
ATP	adenosine triphosphate
AMP	Adenosine monophosphate
BDM	biomass-degrading microorganism
C5	5-carbon sugar
C6	6-carbon sugar
CCR	Carbon catabolite repression
CDW	Cell dry weight
CO ₂	Carbon dioxide
CoA	Coenzyme A
CoA-SH	Coenzyme A with sulfhydryl functional group
DHAP	Dihydroxyacetone phosphate
DNA	Deoxyribonucleic acids
DOM	dissolved organic matters
EAM	electroactive microorganism
EI	Electro ionization
EMP	Embden Meyerhof Parnas pathway
FAPs	Fatty acid profiles
FAS	Fatty acid synthesis
FFAs	Free fatty acids
FUTO	Federal University of technology Owerri
GA3P	Glyceraldehyde3phosphate
GAL2	Galectin 2 or galactose permease 2
GC	gas chromatography
GHG	Greenhouse gas
GXF1	Glucose and xylose facilitator 1
GXS1	Glucose and xylose symport 1
HPLC	high performance liquid chromatography
HXT	Hexose transporters
Hxt1-6	Hexose transporter 1 to 6
Hxt7	Hexose transporter 7 (high-affinity)
Hxt8-16	Hexose transporter 8-16
Hxt17	Hexose transporter 17
ICDH	Isocitrate dehydrogenase
LTH	lipid to hydrocarbon technology
ME	Malic enzyme
MEL	Mannosylerythritol lipid
MEL-A	Mannosylerythritol lipid-A

MEL-B	Mannosylerythritol lipid-B
MEL-C	Mannosylerythritol lipid-C
MFC	Microbial fuel cell
Mig1	Multicopy inhibitor of galactose gene expression
NADH	nicotinamide adenine dinucleotide (reduced)
NAD ⁺	nicotinamide adenine dinucleotide (oxidized)
NADPH	nicotinamide adenine dinucleotide phosphate
NIST	National Institute of Standards and Technology
OD600	optical density at 600 nm
PEM	proton exchange membrane
PEP	Phosphoenolpyruvate
pH	Potential of hydrogen
PPP	Pentose phosphate pathway
PUFA	Polyunsaturated fatty acid
RGT2	Restores glucose transport
RNA	Ribonucleic acid
SNF1	Sucrose non-fermenting 1
SNF3	Sucrose non-fermenting 3
SNF5	Sucrose non-fermenting 5
Ssn6	General transcriptional corepressor/glucose repression mediator protein
Sut1	Sterol Uptake 1
TAG	Triacylglyceride
TAGs	Triacylglycerides
TCA	tricarboxylic acid
TETFund	Tertiary education trust fund
Tup1	dTMP-Uptake ie deoxythymidine monophosphate
VVM	Vessel volume per minute
Xut4	Transcription repressor 4
Xut5	Transcription repressor 5
Xut6	Transcription repressor 6
Xut7	Transcription repressor 7
YEPD	Yeast extract peptone dextrose

Chapter 1

1 Introduction

1.1 Background

The increasing global energy demand and population growth have resulted in the constant depletion of fossil fuels. Fossil fuels utilization is one of the leading causes of excess carbon dioxide (CO₂) accumulation in the atmosphere (Lindsey, 2020). Over the last two decades, the world has witnessed the impacts of climate change resulting from the steady increases in temperature. To arrest these climate change issues, one of the Paris agreement's goals is to keep the global average temperature increase to below 2°C. (De Bhowmick, Sarmah & Sen, 2018a, Olatunji, Akinlabi & Madushele, 2020). Hence, this has necessitated global academic and industrial research on finding alternative, sustainable and cost-effective energy sources. For example, in support of the Paris climate accord, the European Union long term goal on environmental law is to reduce net CO₂ emission levels by 45% by 2030 and finally reach net zero by the year 2050 to mitigate greenhouse gases (GHGs) effects (i.e. climate change and global warming) (Amaniampong et al., 2020; Olatunji et al., 2020).

Consequently, for the objectives of the Paris accord to be met, a significant portion of the world's energy needs have to be sourced from renewable energy (fuel) sources, instead of fossil fuels (conventional oil derivatives) (Okafor & Daramola, 2020). Renewable fuels have emerged as the alternative to fossil fuels because it is sustainable, sufficient, and biomass-based (Akhundi et al., 2019; Lynd et al., 1999; Ragauskas et al., 2006; Tonda et al., 2018; Yuan & Xu, 2015). Biomass can be defined as any organic matter derived from plants or animals that are renewable (Demirbas, 2007; Javed et al., 2019; Okafor & Daramola, 2020). Biomass can be used as fuel to generate heat and electricity (Cheng, 2017; Mirza et al., 2008). Basically, biomass can be

transformed into solid (biochar), liquid (biodiesel, bioethanol), and/or gaseous forms (methane) (Cattaneo et al., 2019; Chen Chen et al., 2019; Guo et al., 2020; C. Huang et al., 2019; Z. Liu et al., 2013; Neto et al., 2019; Orr & Rehmann, 2016; S. Xu et al., 2019). Edible biomass feedstocks for biorefineries include grains (corn, wheat, sorghum), starchy crops (sugarcane, beets), oil or tree seeds (mustard, sunflower, coconut, jatropha, rapeseed, palm, soya), and aquatic biomass (algae and seaweeds). Non-edible biomass feedstocks for biofuels include organic residues (post-consumer wastes, industrial wastes, commercial wastes), lignocellulosic plants and crops (forestry woods, energy grasses, and reeds) that contain different compositions of lignin, hemicellulose, and cellulose (De Bhowmick et al., 2018, 2019; Javed et al., 2019; Takkellapati et al., 2018). Plant-based biofuels were originally produced using edible biomass (first generation) such as sugarcane, corn, etc., but have since transitioned to the use of non-edible biomass, such as lignocellulosic biomass. Lignocellulosic biomass has great potential to produce renewable fuels, chemicals, and other high-value in-demand products (Isikgor & Becer, 2015; F. Wang et al., 2021).

The use of oleaginous microbial biomass as an alternative biofuel feedstock has emerged (Octave & Thomas, 2009; B. Subhadra, 2011; B. G. Subhadra, 2010) and microbial lipid production has been reported by many researchers (Annamalai et al., 2018; Carsanba et al., 2018; Cho & Park, 2018; Javed et al., 2019; Lopes et al., 2018; Meeuwse et al., 2013; Parsons et al., 2018; Patel & Matsakas, 2019; Shields-Menard et al., 2017, 2018; Yellapu et al., 2018). Oils derived from microorganisms are often referred to as microbial lipids, microbial oils, or single-cell oils (Lopes et al., 2018). Oleaginous microorganisms for lipid accumulation include, but are not limited to, yeasts, bacteria, fungi, and microalgae. (Meng et al., 2009; Patel et al., 2020; Paul et al., 2020; I. Sitepu et al., 2014; I. R. Sitepu et al., 2014; Sreeharsha & Mohan, 2020). Among these classes of oleaginous microorganisms, yeasts are the most efficient in growing on a wide variety of renewable

substrates from both the industrial and agricultural sectors for lipid production (Patel et al., 2020).

It is important however to emphasize that different oleaginous yeasts have the potential to intake and utilize sugar carbon sources (C5 and C6) and non-sugar carbon sources (acetate, and glycerol (Patel & Matsakas, 2019; G.-C. Zhang et al., 2015b)). The ability to consume such hydrophilic substrates comes about via the *de novo* lipid synthesis pathway. *De novo* entails the utilization of hydrophilic substrates for lipid accumulation. On the other hand, the utilization of hydrophobic substrates (such as oil from cooking waste) for lipid production occurs due to the *ex novo* lipid synthesis pathway (Patel & Matsakas, 2019). *Ex novo* refers to the use of hydrophobic substances (such as glycerol) for lipid synthesis. *Ex novo* lipid accumulation also relates to the biomodification of fats and oils by oleaginous microorganisms (Lopes et al., 2018) prompting the production of varieties of fatty acid distinct from the original hydrophobic substrate (Patel & Matsakas, 2019). Undoubtedly, oleaginous yeasts are good candidates for microbial oil production and can be genetically engineered to create and/or improve fatty acid synthesis. Similarly, their ability to accumulate lipids above 20% of their cell dry weight and short proliferation time are other reasons for their acceptance and consideration for scale-up (Carsanba et al., 2018; Espinosa-Gonzalez, Parashar, Chae, et al., 2014; Javed et al., 2019; Shields-Menard et al., 2017, 2018). Also, the use of oleaginous microbes to meet global energy demand does not require the doubling of arable lands and the growth of oil crops (Younes et al., 2020). Optimal utilization of the C5 and C6 sugars from lignocellulosic biomass hydrolysate for lipid generation by oleaginous yeasts would improve future green energy, save cost and time, and reduce the environmental and social concerns associated with fossil fuel and first-generation feedstock.

Yarrowia lipolytica, *Rhodospiridium toruloids*, and *Lipomyces starkeyi* were subjected to extensive investigations for lipid accumulation by different researchers (Adams et al., 2013;

Kolouchová et al., 2016; Younes et al., 2020). For example, *Y. lipolytica* was reported to accumulate lipid above 70% (g lipid/g dry cell weight) when it was genetically engineered for xylose consumption, and *Cutaneotrichosporon oleaginosus* accumulated lipids at levels reaching 85% (g lipid/g dry cell weight) under stressful conditions and using different carbon and nitrogen sources (Gujjari et al., 2011; Masri et al., 2019; Younes et al., 2020). In light of this, extensive investigations and comparative studies on simultaneous utilization of C5 and C6 carbon sources and lipid generation capabilities of *Pseudozyma hubeiensis*, *Pseudozyma tsukubaensis*, and *Cystobasidium iriomotense* in nitrogen limiting M9 mineral medium for biofuel production is inevitable.

1.2 Research objectives

The research question is can *P. tsukubaensis*, *P. hubeiensis*, and *C. iriomotense* consume mixed C5 and C6 sugars simultaneously and efficiently in a limiting nitrogen medium to generate large quantities of lipid for biofuel production? The general research aim of this thesis is to use a fully automated 5 L scale bioreactor to ascertain the growth and simultaneous utilization capabilities of xylose and glucose sugars by these three yeasts in mixed sugar, nitrogen limiting media for microbial lipid production. This thesis studied the fatty acid profiles (FAPs) of the microbial lipids generated from simultaneous utilization of xylose and glucose sugars by *P. tsukubaensis* and *P. hubeiensis* in limiting nitrogen media. Furthermore, this research produced biofuel (renewable hydrocarbons) with the generated microbial lipids through the LTH technology conversion technique and characterized the biofuel. These aims were addressed through the following short-term objectives:

1.2.1 Short-term objectives

- ❖ To compare the simultaneous xylose and glucose utilization abilities of *P. tsukubaensis*, *P. hubeiensis*, and *C. iriomotense* in a limiting nitrogen M9 medium.
- ❖ To compare the microbial lipid accumulation levels of *P. tsukubaensis*, *P. hubeiensis*, and *C. iriomotense*.
- ❖ To convert the generated microbial lipids to renewable hydrocarbon products using the well-established lipid-to-hydrocarbon (LTH) lipid pyrolysis technology.
- ❖ To do chemical characterization of the pyrolysis products.
- ❖ To do a comparative study of the pyrolyzed *n*-hexane soluble lipid-extracts and characterized pyrolytic products of *P. tsukubaensis*, *P. hubeiensis*, and *C. iriomotense*.

1.3 Research justification

The purpose of this study is to examine the simultaneous utilization of mixed sugars by the aforementioned organisms for lipid production. The organisms will be grown under the same cultivation conditions in a bioreactor and then assessed with regards to sugar utilization and lipid production, as well as subsequent renewable hydrocarbon (biofuel) production. While some information has been identified in the literature concerning the simultaneous mixed sugar usage of *P. hubeiensis*, and *C. iriomotense* in a 100 ml shake flask screening experiment, there is a lack of knowledge about their behavior from a large-scale cultivation point of view. Published reports are also lacking on the conversion of *P. tsukubaensis*, *P. hubeiensis*, and *C. iriomotense* lipids to renewable hydrocarbons and the characteristics of renewable hydrocarbons generated. More importantly, there are no comparisons of these oleaginous yeasts when cultivated in a mixed sugar nitrogen-limited medium, nor a comparison of the generated renewable hydrocarbons. Extensive

investigations and comparative studies on simultaneous utilization of C5 and C6 carbon sources and lipid generation capabilities of *Pseudozyma hubeiensis*, *Pseudozyma tsukubaensis*, and *Cystobasidium iriomotense* in nitrogen limiting M9 mineral medium for biofuel production are inevitable because it will serve as fundamental research work for the bioconversion of lignocellulosic feedstock into biofuel using these organisms, help alleviate the economic viabilities and challenges associated with pentose utilization, tolerance of microorganism to inhibitors present in lignocellulosic hydrolysates, and circumvent petroleum constant depletion problem by being efficient in producing biofuel (green energy) from lignocellulosic materials for improved energy security (S.-M. Lee et al., 2015). This research may bridge these gaps that exist in bioresource technology.

As global interest is geared toward alternative energy sources to mitigate global energy demands and as 27% of global energy sources by 2050 are projected to come from renewable energy (*International energy outlook 2021*), this research may help to actualize these future energy-dependent goals. This research is promising to be useful to the industry in the sense that the optimal use of mixed sugars can improve future green energy, save time, and ultimately reduce environmental concerns. Comparative information generated from this project on the mixed sugar utilization by *P. tsukubaensis*, *P. hubeiensis*, and *C. iriomotense* may offer a plethora of information that may benefit and guide the bioenergy industries, researchers, and scholars.

Chapter 2

2 Literature Review

2.1 Major drivers of biofuel production

There are some major drivers for the generation and use of biomass for advanced biofuel production. One of them is energy security (Yousuf, 2012). Energy production from renewable sources ensures energy security in the sense that materials that are found locally are utilized for bioenergy production. Then, undue attention to petroleum-based energy sources is minimized and overdependence on the import of fossil energy is ameliorated. Favorable technologies for renewable fuel production that lower costs and favorable government policies are other drivers that are increasing interest in renewable fuels (Keasling et al., 2021; Yousuf, 2012). The environmental concerns of conventional energy are distinctively a major driver of biomass production and biomass utilization. Conventional fuel generation and usage result in the depletion of the ozone layer, global warming, and severe climate change from high CO₂ emissions and other greenhouse gases (GHG). The produced GHG tend to cause air pollution that creates ample public health safety risks and huge cost (Ritchie & Roser, 2017; Van der Ploeg, 2016). Renewable energy usage on the other hand mitigates the CO₂ emission concentration in the atmosphere (Ritchie & Roser, 2017; Sumiyoshi et al., 2017; Van der Ploeg, 2016). The fact that conventional fuels are not renewable is an important driver of renewable fuels. Additionally, the depletion of petroleum reservoirs has necessitated the need for alternative, sustainable, and renewable energy. It is important to mention that there is no unanimously agreed-on timeframe for the total depletion of fossil fuels. Nevertheless, if we fail to reduce our complete dependence and reliance on fossil energy and fossil by-products, regulate the fossil fuel burning rate, as well as discover new petroleum reservoirs (Adegboye et al., 2021), we are may run out of fossil reservoirs. An estimated time frame for the

complete depletion of fossil fuels could be by 2060 (<https://octopus.energy/blog/when-will-fossil-fuels-run-out/>). The consumption rate and global energy demands keep rising as time progresses (Ritchie & Roser, 2017), requiring alternative plans to mitigate the energy demand challenge. Over the past five decades, there has been a constant significant increase in energy consumption globally and this consumption has shifted from coal to high demand for gas and oil (Ritchie & Roser, 2017). Recently, the US energy information administration (Figure 2.1) confirmed that global energy consumption based on energy sources is largely dependent on liquid fuels, renewable fuels, and natural gas through coal still makes up a large fraction. By the year 2050, 27% of the global energy consumption is projected to come from renewable energy sources, increasing from 15% in the year 2020 (Figure 2.1). This roughly doubling in renewable energy consumption from the year 2020 to 2050 will approximately equalize renewable energy sources to petroleum and other liquids (Figure 2.1).

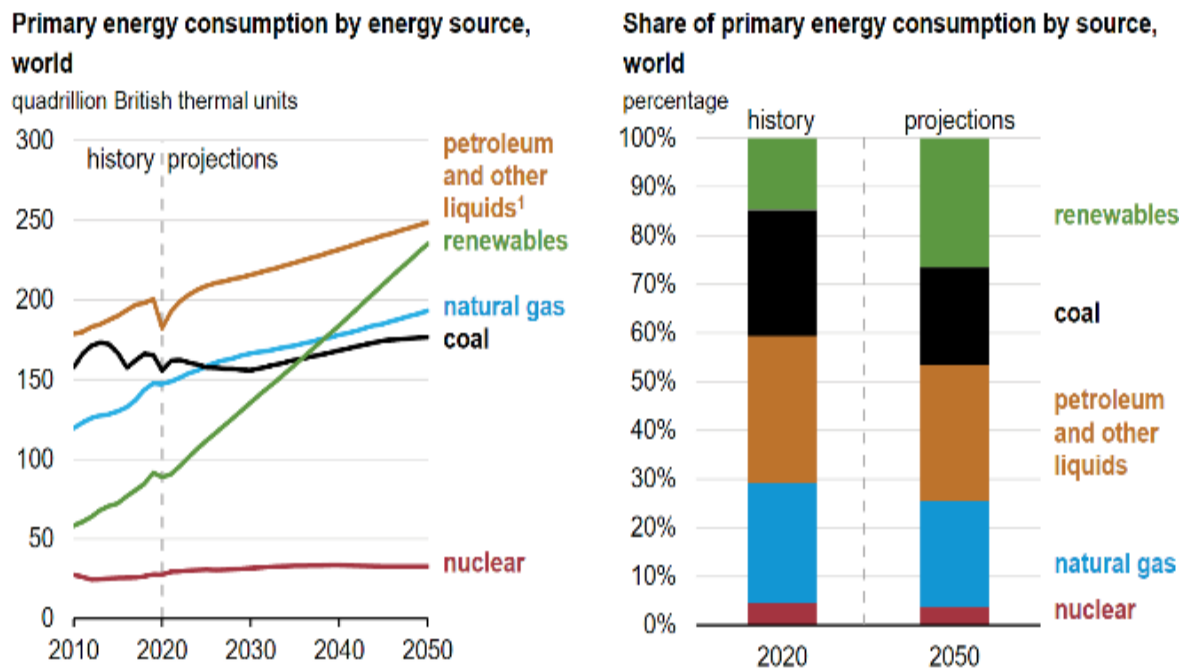


Figure 2.1: Global energy consumption in quadrillion British thermal units and global percentage share of primary energy consumption by energy source. Source: U.S energy information administration, *International energy outlook 2021* (IEC2021)

2.2 Feedstocks for biofuel production

Feedstocks in this context refer to raw materials directly or indirectly converted to biofuel. Feedstocks grouped in generations are the basis for biofuel classification. The first-generation biofuels are generated from edible feedstocks (Alalwan et al., 2019). Biogas, bioethanol and biodiesel are mostly produced using grasses and grains, edible starches and sugars, and oils, respectively (Lackner, 2017). The non-edible feedstocks such as lignocellulose and municipal solid wastes are used for the production of second-generation biofuels (Alalwan et al., 2019; Chintagunta et al., 2021). Some 1st generation biofuel platforms (starches and sugars) depend on microorganisms for the conversion of these organic compounds (energetic compounds) to biofuel while their high lipid counterparts are chemically, thermochemically, or hydrothermally treated to form bioenergy (Lackner, 2017; R. A. Lee & Lavoie, 2013). The use of microalgae for biofuel production is another class of feedstock for third-generation renewable fuel (Medipally et al., 2015). The drawbacks associated with the third-generation biofuel feedstocks include a low concentration of microalgal biomass, the tiny size of the microalgae that hinders proper harvesting, low lipid accumulation ability, the massive volume of water that must be dried to concentrate the algal biomass, and cost (such as photobioreactor costs) (Ge et al., 2017; Karim et al., 2020; R. A. Lee & Lavoie, 2013; Medipally et al., 2015; Scaife et al., 2015). Hence the need for fourth-generation biofuel feedstocks. Other microbes that use CO₂ as feedstock belongs to the third generation as well (R. A. Lee & Lavoie, 2013). Fourth-generation biofuels involve the use of algae in biofuel production technology, like in the third generation of biofuel, but the major difference between the third and fourth biofuel generation platforms is that 4th generation biofuels are produced from the genetic manipulation of oxygenic photosynthetic microorganisms (e.g. algae) to create genetically/metabolically modified microorganisms with novel function(s) and /or

improved feature(s) for biofuel production (Dutta et al., 2014; Lü et al., 2011) Some biomass crops that capture CO₂ and lock it in their parts (trunk, leaves, and branches) are part of fourth-generation biofuel platform and this captured CO₂ is further processed into biofuels (Abdullah et al., 2019; Shokravi et al., 2019). Also, solar fuels and electro fuels are 4th generation biofuels and electro fuels are formed when chemical energy is stored in the chemical bonds of liquids and gases while solar fuels are formed using sunlight, CO₂, and genetically/metabolically engineered microorganism in the solar converter model to form biofuels (Alalwan et al., 2019; Ben-Iwo et al., 2016; Lü et al., 2011; Oncel, 2013; Shokravi et al., 2019; J. Zhang & Zhang, 2019). The fourth biofuel generation platform is robust in CO₂ capture and sequestration, thereby reducing the CO₂ emissions (Abdullah et al., 2019; Alalwan et al., 2019). The end products of some 4th generation biofuels are exuded out or secreted out of the cell (extracellular storage) instead of being stored intracellularly requiring biomass feedstock processing (Lü et al., 2011).

2.2.1 Oil-based feedstocks

Vegetable oils both edible oils and non-edible oils, including waste oils from the restaurant industries, were used as feedstock for biodiesel production. The non-edible feedstocks for biofuel production include *Jatropha curcas* (jatropha), *Pongamia pinnata* (karanja), *Moringa oleifera* (moringa), *Hevea brasiliensis* (rubber), *Madhuca indica* (mahua), *Azadirachta indica* (neem), *Schleichera oleosa* (kusum), *Mesua ferrea* (Nahor), *Thietiva peruviana* (Karabi), *Pongamia glabra* (Karanja), and *Ricinus communis* (castor) (Chintagunta et al., 2021). Edible vegetable oils are comprised of the oils from plants (such as palm oil widely used in Asia), seeds oils (such as rapeseed, the most widely-used oil in Canada and USA for global biodiesel production,

Simmondsia chinensis (jojoba), *Gossypium hirsutum* (cottonseed), *Nicotiana tabacum* (tobacco), *Simarouba glauca* (Simarouba), and *Sapindus mukorossi* (soap nut), (Chintagunta et al., 2021), grain oil (such as corn oil), etc. The advantages of using oils as feedstocks for biofuel production stems from their good heating ability (high heating value), being very sustainable, low aromatic and sulfur content, and wide availability. However, vegetable oil chemical bonds are majorly made up of unsaturated bonds, leading to some of the disadvantages associated with the use of vegetable oils, which are the high reactivity of the unsaturated vegetable oils for saturation purposes (this is inevitable because of its unstable nature) and in some cases the high viscosity of the produced biofuel (i.e. viscous biodiesel).

Waste oils are used oils (such as yellow grease) that are no longer suitable for their original intended can be utilized for biodiesel and renewable biodiesel production. They are cheap feedstocks for biofuel production. The challenge of unsteady supply and high demand, and problems associated with the gathering of waste oils from the sources that are scattered here and there are currently circumvented by the creation of collection strategies. For instance, there are hauling services already in place to collect waste grease from various restaurants.

Animal fats (such as fish fat, lard, tallow, and poultry fat) also serve as feedstocks for biofuel production (specifically biodiesel). Desirable features of biodiesel from animal fats are the high cetane number, very high stability to oxidation, and high energy value (Chintagunta et al., 2021). The challenge it has comes from the high free fatty acids (FFA) present, which retards the transesterification reaction process leading to the saponification process for soap formation. High FFA content (FFA greater than 1%) in oil and fats creates negative effects and requires high alkali to neutralize the FFA. If water is present in the animal fats with high FFA, gel and foam formation occur during transesterification preventing the separation of glycerol from biodiesel

(Mathiyazhagan & Ganapathi, 2011). These negative effects retard transesterification in the sense that the catalyst effect is retarded or may be utilized for soap formation (saponification), more catalysts than normal may be required, and the quantity of methyl ester produced is reduced. These animal fats can be converted to renewable diesel if they were stripped of their glycerol backbone and their fatty acids recovered and pyrolyzed or co-pyrolyzed.

Oleaginous microorganisms (such as yeasts, bacteria, filamentous fungi or molds, and microalgae) generate microbial oils for biofuel production from diverse substrates. The oleaginous microbes are first cultivated on a favorable substrate under conditions that will enable them to grow and accumulate lipids for subsequent conversion to advanced biofuels. The outstanding feature of oleaginous microorganisms is that the problem of fuel versus food concern is resolved. Pretreated lignocellulosic materials are promising substrates for the cultivation of oleaginous microorganisms.

2.3 Microbes for microbial lipid generation

Microalgae is one of the oleaginous microbe utilized for biomass accumulation for biofuel production. Its lipid accumulation capacity ranges from 20-50% of cell dry weight (CDW) (Chintagunta et al., 2021). The classification of microalgae is based on its morphological variations (such as cylindrical, round), mode of energy source for growth and survival (such as heterotroph and autotroph), and projections (e.g. cilia). When organic compounds serve as the source of growth of microalgae, it is classified as heterotrophic organism. If the source of carbon for growth is generated from carbon dioxide reduced by light to release oxygen, the microalgae are regarded as autotrophic microalgae. Most microalgae belong to the autotrophic class. On the other hand, the mixotrophic class of microalgae uses both organic compounds and CO₂ for growth. This indicates

that both photosynthesis and cell respiration pathways exist in the mixotrophic microalgae for cell growth (Lackner, 2017).

Oleaginous fungi and molds also accumulate high lipids by growing on carbon substrates in a stressful environment (such as limiting nitrogen conditions). Unlike microalgae, they do not have the photosynthetic metabolic pathway. Bacteria are not known for being oleaginous when compared to other microbes but they are like yeasts uniquely known for being efficient for their genetic manipulation to achieve high lipid accumulation (Chintagunta et al., 2021). Although yeasts grow relatively fast, bacteria grow very fast. Some bacteria (*Rhodococcus opacus*) are endowed with the ability to degrade lignocellulosic feedstock and utilize the lignin, sugars, and other sugars to store lipids at levels of ~80% of their CDW (Chintagunta et al., 2021; Da Silva et al., 2016). Similar to microalgae, oleaginous yeasts are universally known for their oleaginous nature. Yeasts grow faster than microalgae with doubling time less than an hour unlike in microalgae and are used for biomass generation.

2.4 Microbial biomass production from yeasts

Yeasts are single-celled organisms that mostly reproduce asexually by budding (bump extends from the parent cell, grows, matures, and detaches), while a few of them divide by fission (parent cell divides into two equal cells) to produce daughter cells (Britannica, 2020; E. A. Johnson & Echavarri-Erasun, 2011; C. Kurtzman et al., 2011). Yeasts are a type of fungi and thus can also form or grow thread-like hyphae depending on the environmental conditions of the growth medium (E. A. Johnson & Echavarri-Erasun, 2011; C. Kurtzman et al., 2011). For example, growing yeasts

in a limiting (reduced) nitrogen condition causes the formation of pseudohyphae in yeasts (Gancedo, 2001).

Yeasts have a wide variety of uses. Common applications of yeasts are in food (such as in baking), brewing and beverage production (*Saccharomyces cerevisiae*, *Hanseniaspora uvarum*), scientific research, biofuel production (such as oleaginous yeasts), probiotics (such as *S. cerevisiae* var. *boulardi* for the alleviation of gastrointestinal disorders), agriculture (such as *Williopsis saturninus* isolated from maize root that produces indole-3-acetic acid and indole-3-pyruvic acid for direct and indirect crop health/plant growth promotion and bio-controlling activities), and medicine (such as *S. cerevisiae* EPY224 for antimalarial drug production) (E. A. Johnson, 2013b, 2013a; E. A. Johnson & Echavarri-Erasun, 2011; Mukherjee et al., 2020). The most studied yeast is the conventional yeast or model yeast *S. cerevisiae* (E. A. Johnson, 2013a, 2013b; Nandy & Srivastava, 2018). The biotechnological application of yeasts is completely immeasurable (extensive and broad) and closely related to their biodiversity (Nandy & Srivastava, 2018; Żymańczyk-Duda et al., 2017).

When the genome of *S. cerevisiae* was elucidated in 1996, it opened the door for the global study of other non-conventional yeasts (Żymańczyk-Duda et al., 2017). Other non-conventional yeasts have great potential and specific features for biotechnological applications. Non-conventional yeasts are less explored yeasts but new research findings have resulted in ample innovative scientific investigations (Żymańczyk-Duda et al., 2017). These non-conventional yeasts include *Yarrowia lipolytica* (known for being salt and oxidative stress-tolerant), *Pichia pastoris*, *Pichia stipitis*, and *Kluyveromyces marxianus* (known for their extreme thermotolerant/stability), *Ogataea polymorpha* (characterized for being heat tolerant), and the last but not the least, *Kluyveromyces lactis* (noted for its adaptabilities to different harsh environments and suitability

for different bioprocesses) (Rebello et al., 2018; Sharrel et al., 2018). In addition, *Basidiomycetes* were explored for enzyme synthesis, secondary metabolite production, and lipid accumulation (E. A. Johnson, 2013a; Nandy & Srivastava, 2018). Likewise, *Ascomycetes* synthesize fine chemicals and compounds of high value as well as proteins for both medical and nutritional usage (Flores et al., 2000; M. Hassan et al., 1994; E. A. Johnson, 2013b; Ayumi Tanimura et al., 2018). Yeast can grow in either bioreactor or shake flasks, which makes the production of yeast cultures possible in small- and large-scale production.

2.5 Sugar uptake in yeasts

Before carbon can be metabolized in yeasts, it must be transported from outside of the cell (extracellular) to inside of the cell (intracellular) through the cell membrane (plasma membrane) as sugars do not freely permeate the biological membrane (Lagunas, 1993). Thus sugar uptake requires the action of transporters (Compagno et al., 2014). *S. cerevisiae* has two transporters for monosaccharides which are glucose and galactose transporters (Lagunas, 1993). These transporters are known as hexose transporters (*HXT*) and act by the mechanism of facilitated diffusion (Compagno et al., 2014; Lagunas, 1993). In *S. cerevisiae*, twenty members of the *HXT* family were identified. They are *HXT1* to *HXT17*, sucrose non-fermenting 3 (*SNF3*), Galectin 2 (*GAL2*), and restores glucose transport 2 (*RGT2*), with specific degrees of affinity for monosaccharides (Compagno et al., 2014; Hamacher et al., 2002; O. mur Kayikci & Nielsen, n.d.; Lagunas, 1993; Liang & Gaber, 1996; Nijland et al., 2017). Only seven out of the 20 hexose transporters are responsible for functional glucose transport and any organism that lacks these seven hexose transporters will lack the ability to transport glucose (Özcan & Johnston, 1999). Low glucose levels are sensed by *SNF3* and *RGT2* (which restores glucose transport) acts as a sensor for high glucose

levels in the extracellular environment (Compagno et al., 2014). High-affinity glucose transporters in *S. cerevisiae* are expressed when glucose is scarce whereas low-affinity glucose transporters are expressed when the glucose level is high (Compagno et al., 2014; Kamrad et al., 2020; Ruchala & Sibirny, 2021), thereby controlling sugar uptake. D-xylose uptake is most relevantly transported into the cell via the high- or intermediate-affinity transporters, Hxt4, Hxt5, Hxt7, and Gal2 uptake systems (Ruchala & Sibirny, 2021), which are also glucose transporters. Once the hexose and pentose (C6 and C5) sugars are taken from outside of the microorganisms to the inside of the cell, they are ready to be metabolized. For the sugars (C6 and C5) to be transported into the cells using the above-mentioned uptake systems, facilitated diffusion is the mechanism used caused by the enzyme permeases. These multi-pass transport proteins ensure the diffusion of C6 and C5 specific molecules into the cell in the direction of the area of high concentration to an area of low concentration. Glucose-permease (Erni & Zanolari, 1986) and xylose-permease (Saloheimo et al., 2007) specifically mediate the sugar transportation in C6 and C5 sugars, respectively. Overall, sugar uptake in yeasts depends on the affinity of the transporters to the carbon source(s) present, expression of the appropriate transporter, and inactivation of the transporter actions by regulatory processes in response to extracellular glucose.

2.6 Yeast carbon metabolism

Carbon metabolism in yeasts depends on the source of carbon, the yeasts strain involved, and environmental physiochemical conditions (Käppeli, 1987). In heterotrophic organisms like yeasts, energy and carbon metabolism are interrelated. Glycolysis is the universally known biochemical pathway for carbon metabolism found in many organisms (Compagno et al., 2014). Adenosine triphosphate (ATP) is provided by the oxidation of organic molecules that serve as

carbon sources for biosynthesis and is used as energetic currency within the cell. The preferred carbon source for both conventional and non-conventional yeasts is sugar and the components of the pathways of sugar utilization in conventional yeast, *S. cerevisiae*, have been extensively studied (Compagno et al., 2014; Flores et al., 2000). Though the sugar utilization pathways for non-conventional yeasts are not fully known, they may be similar to the pathways in *S. cerevisiae*, with minor differences at some biochemical steps (Gonzalez, 2014).

Glycolysis is a ten reaction steps process that occurs in sequence, producing intermediates that are transformed to pyruvate (R. A. Bender, 2013; Blanco & Blanco, 2017; Feher, 2012; Smallbone et al., 2013). Generally speaking, glycolysis has two phases, the first phase is the chemical preparing or prompting or priming phase and the second is the energy-yielding phase. When D-glucose enters the cell, it is phosphorylated by hexokinase to form glucose 6-phosphate fueled by ATP. Glucose 6-phosphate is isomerized to fructose 6-phosphate by glucose 6-phosphate isomerase. Fructose 6-phosphate is converted to fructose 1,6 bisphosphate by the enzyme 6-phosphofruktokinase, fueled by ATP and it is the last stage of the chemical preparation phase (Figure 2.2) (R. A. Bender, 2013; Blanco & Blanco, 2017; Feher, 2012; Flores et al., 2000). Fructose 1, 6 bisphosphates are then converted to dihydroxyacetone phosphate (DHAP) and glyceraldehyde 3-phosphate (GA3P) by the aldolase enzyme. That said, DHAP and GA3P can be converted to each other (isomerization) by the action of triosephosphate isomerase. The second phase of glycolysis begins with the conversion of GA3P to 1,3-bisphosphoglycerate by GA3P dehydrogenase with NAD^+ to generate NADH. Having produced 1,3-bisphosphate, the enzyme phosphoglycerate kinase catalyzes the generation of 3 phosphoglycerates and produces ATP from ADP. 3 phosphoglycerate is then converted to 2 phosphoglycerates by the action of phosphoglycerate mutase, coupled with water released. Next, enolase directly converts 2

phosphoglycerates to phosphoenolpyruvate (PEP) yielding ATP. Subsequently, pyruvate kinase catalyzes the transformation of PEP to pyruvate (Blanco & Blanco, 2017; Feher, 2012; Flores et al., 2000).

2.7 Simultaneous utilization of sugars (C5 and C6) in oleaginous yeasts

Biochemicals and biofuels production from lignocellulosic biomass is gaining increased attention. The released sugars in the lignocellulosic hydrolysate are comprised mainly of glucose (36-60%) and xylose (18-30%) (Zhao et al., 2020), which can be utilized by microorganisms for the production of biofuels and biochemicals (Ryu & Trinh, 2018; B. Zhang et al., 2016; G.-C. Zhang et al., 2016). The simultaneous utilization of mixed C6 and C5 sugars for lipid production

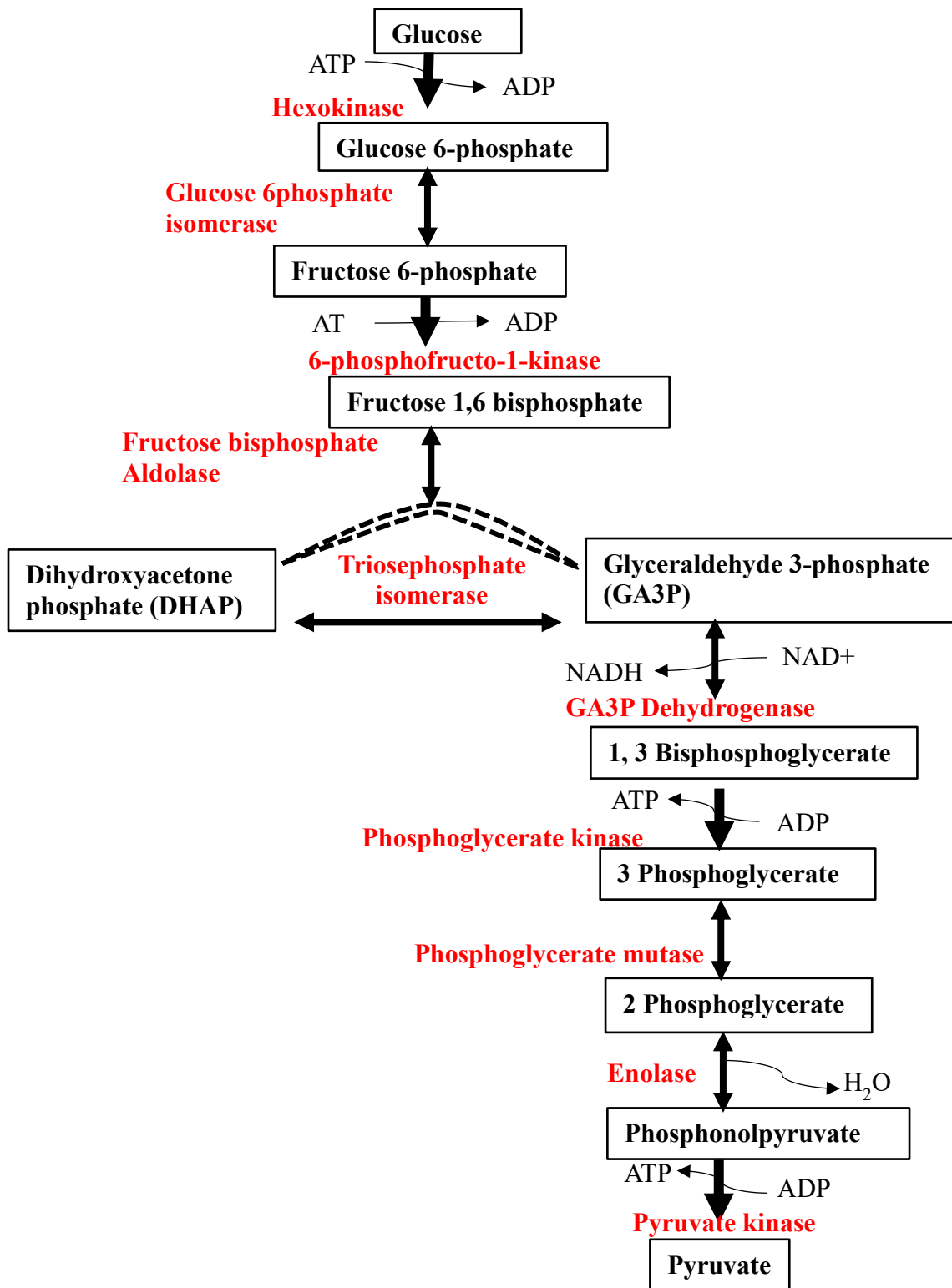


Figure 2.2 Glycolytic pathway. Enzymes involved in this pathway are written in red. Carbon numbers for compounds and phosphate positions in the ten steps of glycolysis are written within rectangular boxes.. (R. A. Bender, 2013; Blanco & Blanco, 2017).

has been studied in *Pseudozyma hubeiensis* (strains IPM1-7, IPM1-9, IPM1-10, IP068, IP045, IP026, and IP004), *Moesziomyces aphidis* (RS041), *Ustilago siamensis* (IP037), *Moesziomyces Antarctica* (IP040), Unidentified *Ustilaginales* (IP056), *Anthracoystis elionuri* (IPM46-16) (Ayumi Tanimura et al., 2016), *Cystobaesidium iriomotense* (strains IPM32-16, ISM28-8sT, and IPM46-17) (Ayumi Tanimura et al., 2018) in a non-limiting nitrogen medium, and *Trichosporon cutaneum* in limiting nitrogen medium (C. Hu et al., 2011). A non-limiting nitrogen medium contains a high level of nitrogen relative to carbon or a low ratio of carbon to nitrogen; a nitrogen limiting medium contains a high mole ratio of carbon relation to nitrogen. A high level or low level in this context refers to a high mole ratio and a low mole ratio of carbon relative to nitrogen.

Mixed sugar fermentations present some bottleneck challenges. The most outstanding challenge is the slow and inefficient fermentation of non-glucose sugars (L. Wang et al., 2020; G.-C. Zhang et al., 2015a). Another challenge is the inability to metabolize pentose sugars, such as xylose and L-arabinose by some microbes such as *S. cerevisiae* (Bertilsson et al., 2008; Bruder et al., 2018; Goncalves et al., 2014; Hou et al., 2017a; Jeffries, 2006; Y.-S. Jin et al., 2004; Karhumaa et al., 2005; Leandro et al., 2006; J. W. Lee et al., 2021; X. Li et al., 2016; Moysés et al., 2016; Nijland et al., 2017; Smallbone et al., 2013). As a result, innovative metabolic engineering schemes in the form of exogenous transporters insertions and metabolic pathways insertions were very necessary for simultaneous fermentation of C5 and C6 sugars (Hao Li et al., 2014; C. Ren et al., 2009; L. Wu et al., 2015; J. Xu et al., 2013; G.-C. Zhang et al., 2015b; Z. Zhang et al., 2019).

Fungi and bacteria have different approaches for the preparation of xylose for metabolism/assimilation in the pentose phosphate pathway (PPP) (Feng et al., 2018; Hou et al., 2017b; Jojima et al., 2010; Kuyper et al., 2004; J. W. Lee et al., 2021; Lynd et al., 1999; E. M. Young et al., 2012; G.-C. Zhang et al., 2015b). The bacterial xylose metabolic route involves the

use of only one enzyme, xylose isomerase, for the conversion of xylose directly into xylulose. In contrast, the fungal xylose metabolic approach requires the use of two enzymes (oxidoreductases), NADPH-linked xylose reductase and NAD-linked xylitol dehydrogenase, to convert xylose into xylulose (Abdel-Mawgoud & Stephanopoulos, 2018; G.-C. Zhang et al., 2015b) (Figure 2.3). Then, the phosphorylation of the xylulose into xylulose 5-phosphate occurs by the action of the xylulose kinase (G.-C. Zhang et al., 2015a). Xylulose 5-phosphate finally enters the non-oxidative pentose phosphate pathway for further metabolism.

Oleaginous yeasts are known to follow the fungal xylose pathway for xylose metabolism (Ryu & Trinh, 2018). Simultaneous utilization of C5 and C6 for lipid production mostly occurs in yeast using the pentose phosphate pathway (PPP), when xylose has been fully converted to xylulose 5-phosphate and is influenced greatly by nitrogen availability and source of nitrogen (Flores et al., 2000). The PPP can be divided into two steps, an irreversible oxidative step, and a reversible non-oxidative step. It is important, however, not to overemphasize that in PPP, glucose metabolism does not fully follow the glycolytic pathway for its metabolism. As glucose enters the cell and is phosphorylated to form glucose-6-phosphate, it is worthy to emphasize that in the PPP pathway, glucose-6-phosphate is in fact converted to 6-phosphogluconolactone instead of fructose-6-phosphate as the case in the glycolysis pathway (Carsanba et al., 2018; Flores et al., 2000; Gao et al., 2018; Y.-S. Jin et al., 2004; Karhumaa et al., 2005; Osorio-González et al., 2019; Papanikolaou & Aggelis, 2011).

Oxidation of glucose-6-phosphate to 6-phosphogluconolactone is catalyzed by glucose-6-phosphate dehydrogenase and the hydrolysis of 6-phosphogluconolactone to 6-phosphogluconate is directed by 6-phosphogluconolactonase. The oxidative decarboxylation of 6-phosphogluconate to ribulose 5-phosphate is catalyzed by 6-phosphogluconate dehydrogenase. Then, the next step in

PPP is the formation of ribose 5-phosphate from ribulose 5-phosphate by an isomerization catalyzed by ribulose 5-phosphate isomerase or xylulose 5-phosphate from ribulose 5-phosphate by an epimerization reaction catalyzed by ribulose 5-phosphate epimerase (Flores et al., 2000; Jeffries, 2006; M.-H. Shen et al., 2015). Transketolase catalyzes the transfer of two carbons (glycolaldehyde moiety) from xylulose 5-phosphate (ketose donor) to ribose 5-phosphate (an aldose acceptor) to generate glyceraldehyde 3-phosphate from the donor and sedoheptulose-7-phosphate from the acceptor. Transketolase action is a reversible reaction in that the transaldolase reverses the formation of glyceraldehyde-3-phosphate and sedoheptulose-7-phosphate by catalyzing the transferring of three carbon moieties from sedoheptulose-7-phosphate to glyceraldehyde-3-phosphate to form fructose 6-phosphate. Then, the remaining 4 carbon moieties from sedoheptulose-7-phosphate is a new PPP intermediate called erythrose 4-phosphate. Transketolase also catalyzes the transfer of a two-carbon moiety from xylulose 5-phosphate (donor) to erythrose 4-phosphate (acceptor) to form two products, fructose 6-phosphate and glyceraldehyde 3-phosphate (Flores et al., 2000; Gao et al., 2018; Jeffries, 2006). PPP generates nicotinamide adenine dinucleotide phosphate (NADPH) that meets the need of the organisms in building other molecules. It also produces ribose 5-phosphate essential for making both ribonucleic acid (RNA) and deoxyribonucleic acid (DNA). The non-oxidative PPP phase links to the glycolytic pathway and the PPP products that are shunted into the glycolytic pathway are NADPH and GA3P.

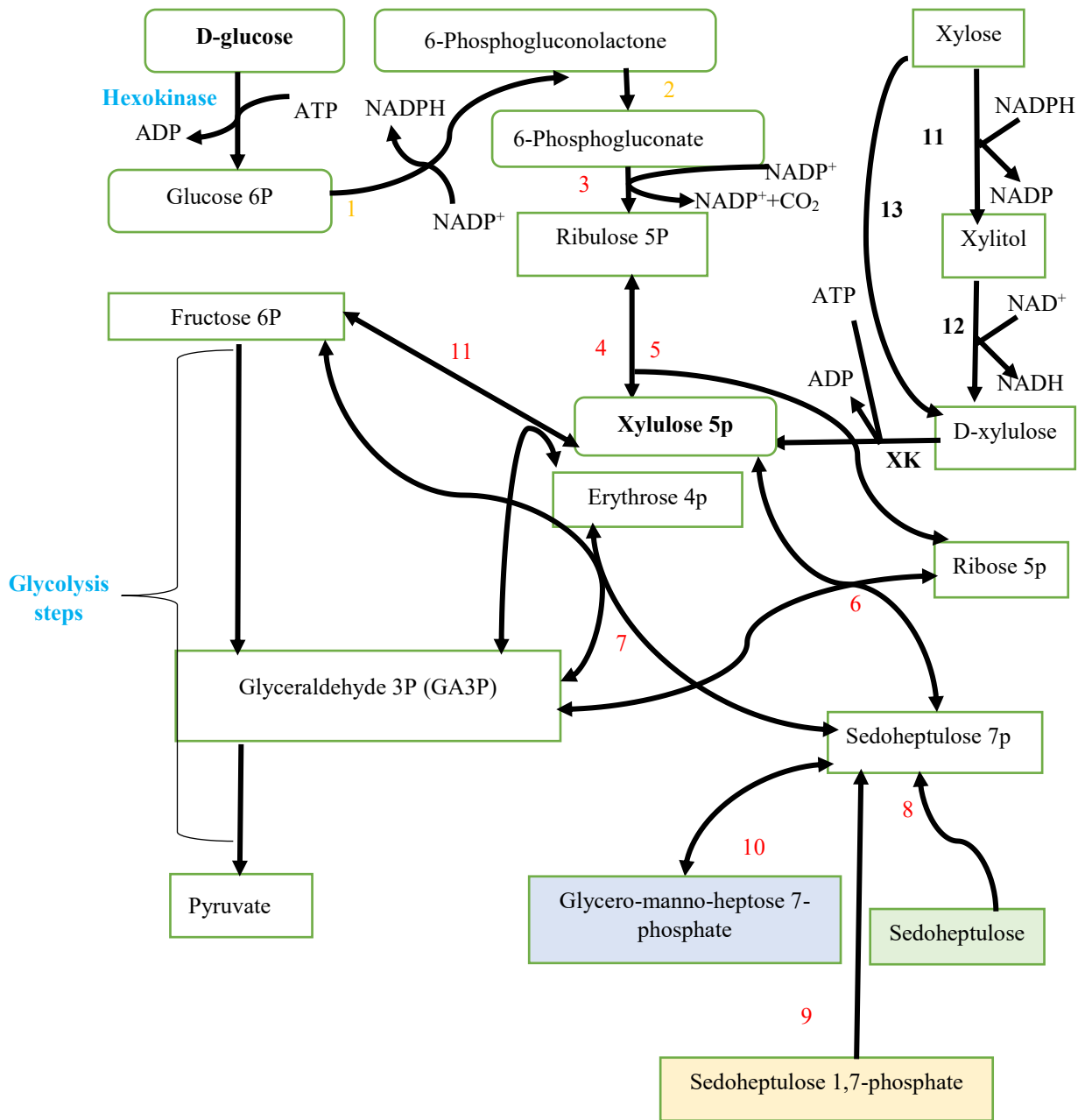


Figure 2.3: Pentose phosphate pathway linked with glycolysis. Enzymes 1 (Glucose 6-dehydrogenase) and 2 (6-Phosphogluconolactonase) are highlighted in yellow and indicate the oxidative branches of PPP. Enzymes 3 (Glucose 6-Phosphate dehydrogenase), 4 (Ribulose 5-phosphate epimerase), 5 (Ribulose 5-phosphate isomerase), 6 (Transketolase), 7 (Transaldolase), 8 (Sedoheptulose kinase), 9 (Sedoheptulose 1,7-bisphosphatase), 10 (Sedoheptulose 7-phosphate

isomerase), and 11 (Transketolase) are highlighted in red and represent the non-oxidative part of the PPP. Sedoheptulose 7-phosphate isomerase is found only in bacteria, sedoheptulose 1,7-bisphosphatase is only found in yeast and plants, and sedoheptulosekinase is found only in mammals). Enzymes 11 (xylose reductase) and 12 (xylitol dehydrogenase) are fungal enzymes and enzyme 13 (xylulokinase) is a bacterial enzyme that prepares xylose for PPP. The glycolysis pathway is linked to PPP indicating PPP products shunted back to the glycolytic pathway. Adopted in part from (Gao et al., 2019; Stincone et al., 2015).

2.8 Lipid biosynthesis in oleaginous yeasts

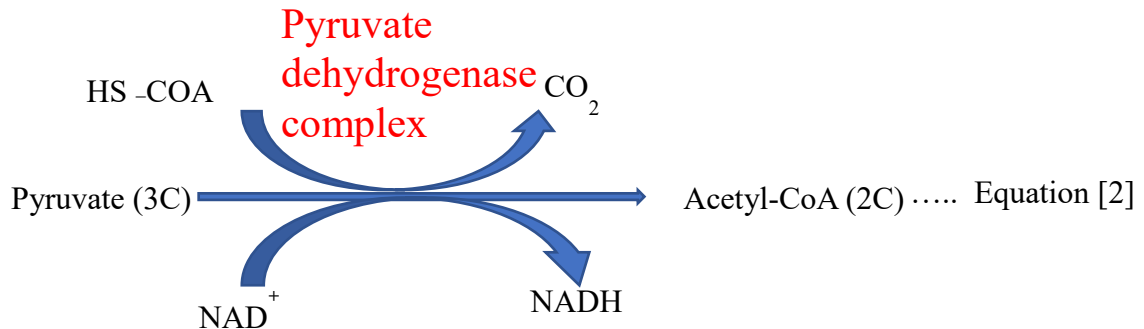
A comparison of the lipid metabolism in non-oleaginous and oleaginous yeasts showed that the biosynthetic pathways are similar, but with minor differences (Fakas, 2017; Mbuyane et al., 2021). The enzyme phosphatidic acid phosphatase is responsible for the control of triacylglyceride biosynthesis (Figure 2.5) in both oleaginous *Yarrowia lipolytica* and non-oleaginous *S. cerevisiae* (Fakas, 2017). Lipids in oleaginous microorganisms are not formed continuously, but rather is an adaptive reaction to particular environmental factors (Younes et al., 2020). When oleaginous microorganisms are grown in a medium rich in carbon, but deficient in certain specific nutrients like nitrogen, they tend to convert the excess carbon into fatty acids and incorporate them into triacylglycerides (TAGs) as energy storage. The TAGs are stored in specialized organelles called lipid bodies or lipid droplets (Ami et al., 2014; Fakas, 2017; Hall & Ratledge, 1977; Ratledge, 2004; Sijtsma et al., 2010; Younes et al., 2020). Under limiting nitrogen conditions, protein and nucleic acid synthesis stop resulting in the inhibition of isocitrate dehydrogenase (ICDH) (Sijtsma et al., 1998). Despite this, abundant carbon continues to be metabolized in oleaginous yeasts (Younes et al., 2020), leading to citrate accumulation in the mitochondria, which takes part in fatty acid

synthesis (FAS) (Saini et al., 2020). Intramitochondrial citrate accumulates specifically because of the decrease in intracellular adenosine monophosphate (AMP) concentration, resulting in a decrease in the activity of the isocitrate dehydrogenase (an AMP-dependent NAD⁺) in the mitochondria. This leads to citrate transport across the mitochondrial membrane in exchange for L-malate (Younes et al., 2020; Yuzbasheva et al., 2019). Citrate is then cleaved in the cytosol by ATP citrate lyase to yield acetyl-CoA and oxaloacetate (Bhagavan & Ha, 2015). ATP citrate lyase is not present in non-oleaginous yeasts (Equation 1) (Ratledge, 2004; Ratledge & Wynn, 2002).



The two reasons for oleaginicacy are the ability for cells to continuously produce acetyl-CoA in the cytosol of the cell, a precursor for fatty acid synthase, and the ability to produce an ample supply of NADPH, a reductant used in FAS (Ratledge, 2004; Ratledge & Wynn, 2002). The malate dehydrogenase enzyme converts oxaloacetate to malate while acetyl-CoA is utilized for fatty acid synthesis (Ratledge, 2004). Malate is further metabolized for the regeneration of oxaloacetate by NAD⁺ dependent malate dehydrogenase (D. A. Bender, 2003; Kumari, 2018). Oxaloacetate is first converted to malate before being converted back to oxaloacetate because oxaloacetate cannot pass through the mitochondria whereas malate can freely pass the mitochondria membrane into the cytoplasm where its conversion to oxaloacetate occurs. Similarly, acetyl-CoA can also be generated from the tricarboxylic acid (TCA) cycle and incorporated into FAS by direct conversion of pyruvate through a process called pyruvate decarboxylation, which is mediated by the pyruvate dehydrogenase complex found in mitochondria. Dihydrolipoamide dehydrogenase, pyruvate dehydrogenase, and dihydrolipoamide acetyltransferase are the three enzymes that form the pyruvate dehydrogenase complex. In the pyruvate decarboxylation process, carbon dioxide is produced by the action of the pyruvate dehydrogenase in the presence of coenzyme A with a sulfhydryl functional group (CoA-SH),

followed by the action of dihydrolipoamide acetyltransferase that yields acetyl-CoA. CoA-SH is the intermediate involved in the one-step synthesis of CoA substrates where the acetyl group is transferred to form acetyl-CoA (Equation 2) (Lindquist & Horton, 1993; Tager, 1993). Then, dihydrolipoamide dehydrogenase produces NADH by oxidation (Flores et al., 2000).



The acetyl-CoA from direct conversion of pyruvate is free to enter the TCA cycle within mitochondria. For FAS, this acetyl-CoA must be transferred to the cytosol. In the cytosol, acetyl-CoA undergoes a carboxylation reaction to generate malonyl CoA by the acetyl-CoA carboxylase (ACC) enzyme (Flores et al., 2000). The actual synthesis and assembly of the fatty acid chain are carried out by fatty acid synthase. Fatty acids are synthesized from acetyl-CoA and malonyl-CoA that are bound to an acyl carrier protein (ACP) (Ratledge, 2004; Saini et al., 2020). ACP are small acidic proteins that serve as cofactors and are involved in *de novo* fatty acid synthesis. Acetyl-CoA and malonyl-CoA are then directed toward the FAS complex, which then relocates to the endoplasmic reticulum. Acetyl-CoA and malonyl-CoA undergo NADPH-dependent desaturation and are then utilized for TAGs production.

Seven steps are involved in fatty acid elongation in humans, mice, and yeasts (Jump, 2009). In step one, the enzyme 3-keto acyl-CoA synthase catalyzes the condensation reaction of malonyl-CoA with a fatty acyl-CoA precursor, and then the resulting intermediate is reduced in step 2 by

3-keto acyl-CoA reductase. Step 3 is a dehydration reaction of the 3-hydroxy species catalyzed by 3-hydroxy acyl-CoA dehydratase and step 4 is a reduction reaction of the step 3 product catalyzed by trans -2, 3-enoyl-CoA reductase. Steps 5-7 are called the elongation steps because they are steps 2-4 repeated numerous times to promote elongation, producing a primary fatty acid, typically palmitic acid. Subsequently, further elongation rounds (modification) occur to achieve a wide variety of desired fatty acids in the endoplasmic reticulum (Flores et al., 2000; Ratledge, 2004; Ratledge & Wynn, 2002).

Three fatty acids can be linked to the three alcohol groups in glycerol to form TAG. The formation of unsaturated fatty acids is mediated by desaturase enzymes (Laoteng et al., 2011; Sijtsma et al., 1998). It is important to mention that TAGs can be synthesized from dihydroxyacetone phosphate (Figure 2.3). The conversion of dihydroxyacetone phosphate (DHAP) to glycerol 3-phosphate is achieved by the action of glycerol 3-phosphate dehydrogenase. Then, sequential acylation of the glycerol 3-phosphate yields TAGs. The first acylation of glycerol 3-phosphate by acyltransferase results in the formation of monoacylglycerol 3-phosphate. Monoacylglycerol 3-phosphate is converted to phosphatidate by acyltransferase in the second acylation step. Phosphatidate is then converted to 1,2 diacylglycerols by phosphatidate phosphatase. The third acylation, which is the last acylation step, converts 1,2 diacylglycerols to TAG. Both the formation of long-chain polyunsaturated fatty acids (PUFA) and lipid biosynthesis (TAG) occurs in the endoplasmic reticulum (Figure 2.4) (Sha, 2013; Takaku et al., 2020).

The oxidative PPP (Figure 2.3) and malic enzyme (ME) are the avenues that provide NADPH for lipid synthesis (Jump, 2009; Saini et al., 2020). The malic enzyme is a family of malate dehydrogenases that catalyze the oxidative decarboxylation of malate to pyruvate (Figure 2.4).

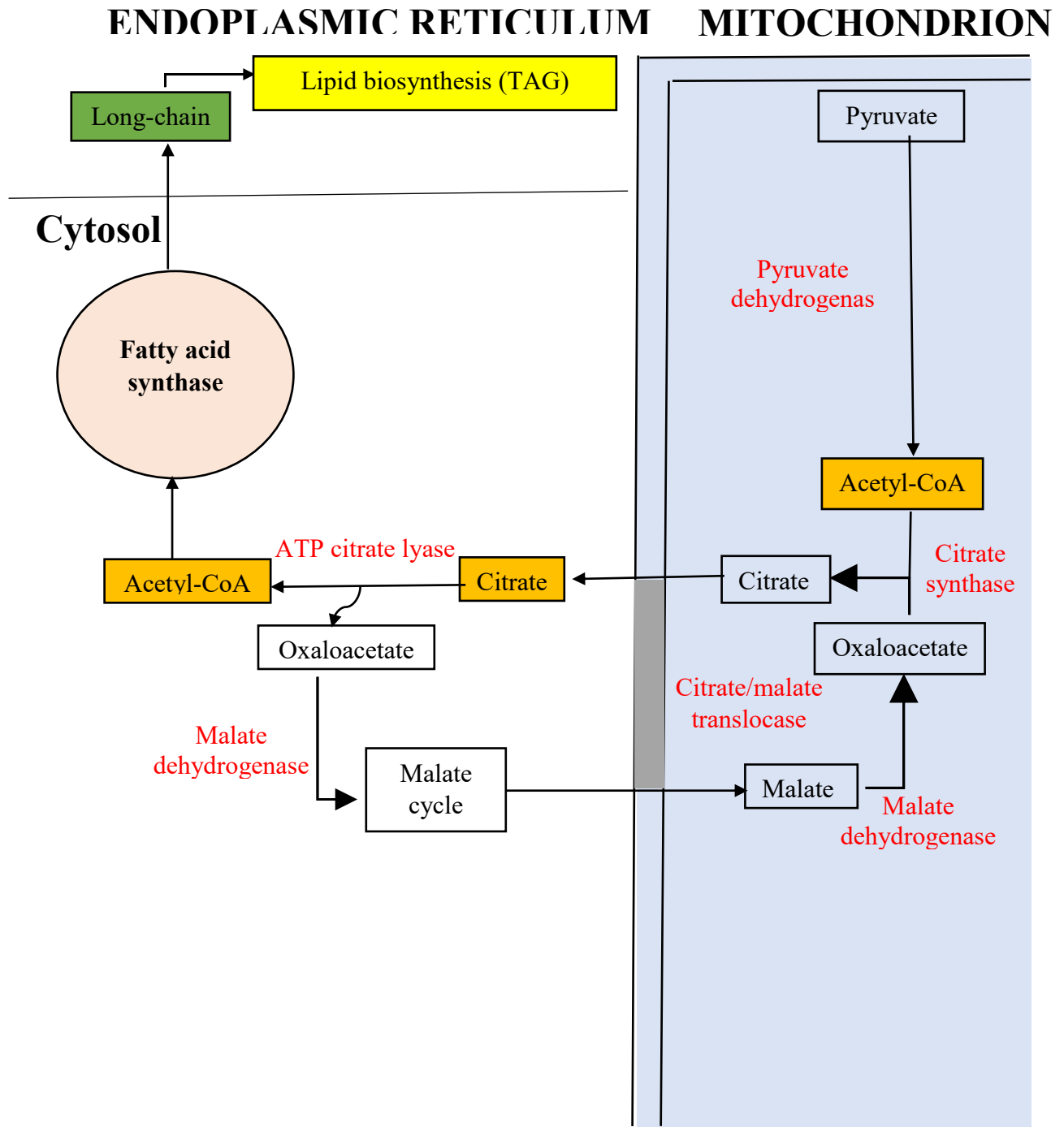


Figure 2.4: Lipid biosynthesis in yeast. Pyruvate migrates into mitochondria from the cytosol and is converted to acetyl-CoA via pyruvate dehydrogenase which in turn enters the TCA cycle. Citrate is an intermediate of the TCA cycle produced by citrate synthase. Limiting nitrogen conditions

prevents the production of isocitrate dehydrogenase, which is required for the TCA cycle and thus leads to citrate accumulation. As a result, ATP citrate lyase cleaves citrate in the cytosol to yield acetyl-CoA, a precursor for fatty acid synthesis, along with oxaloacetate. The enzymatic complex of fatty acid synthase mediates the production of fatty acids. Elongation and modification of the fatty acids to produce long-chain polyunsaturated fatty acids (PUFAs) and the formation of TAG from the fatty acids occur in the endoplasmic reticulum. The interconversion of oxaloacetate to malate occurs in the malate cycle using malate enzymes and cofactors (NAD⁺ or NADP⁺). Malate cycle adopted in part from (Dulermo et al., 2015; Gonzalez, 2014; Ratledge, 2004).

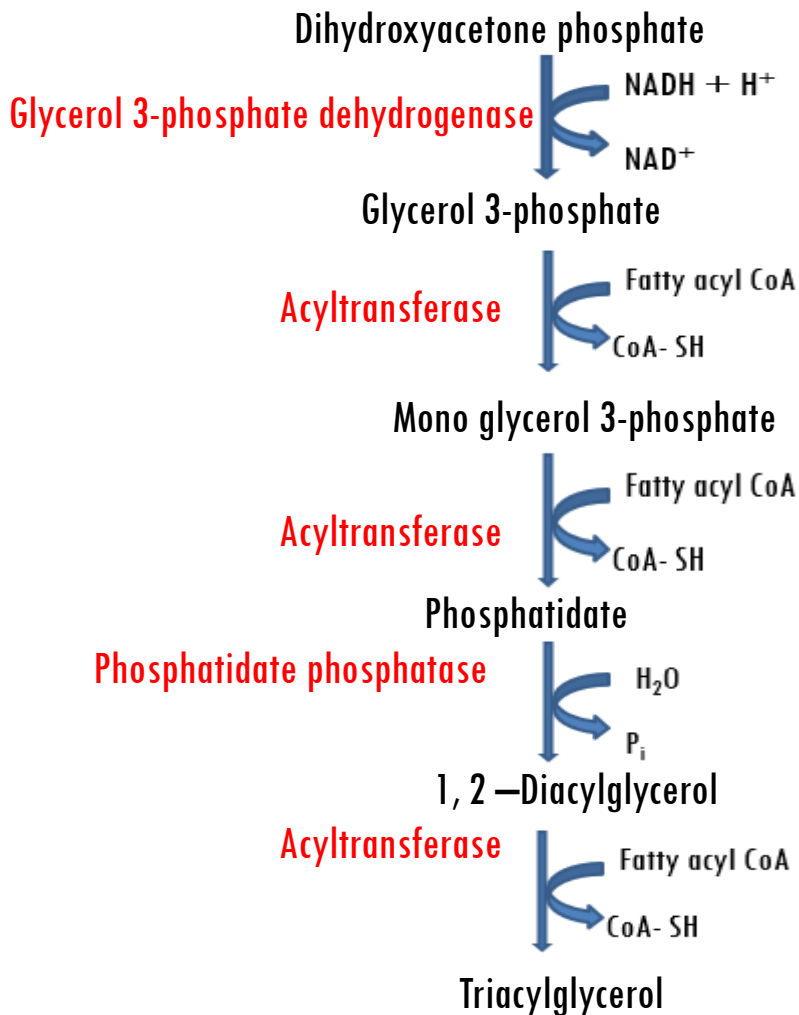


Figure 2.5: Triacylglycerol synthesis from dihydroxyacetone phosphate (DHAP) (Blanco & Blanco, 2017)

Saini *et al.*, (2020) reported that the oxidative PPP is the primary NADPH source for the biosynthesis of fatty acids in *Y. lipolytica* and *R. toruloides* (Ratledge & Wynn, 2002; Takaku *et al.*, 2020). The conversion of glucose to TAG can give the highest theoretical yield of 33% (w/w), but 22% (w/w) is the highest yield, in reality, obtainable from converting glucose to TAG (Ratledge & Cohen, 2008). This is because the theoretical efficiency does not put into consideration the glucose utilized by yeast for growth and maintenance.

2.9 Carbon catabolite repression

Carbon catabolite repression (CCR) is the preferential utilization of one carbon source when two or more carbon sources are present (Deutscher, 2008). It can also be defined as the regulatory mechanism by which the gene expression required for secondary carbon utilization is prevented by the presence of a preferred substrate (Stülke & Hillen, 1999). When glucose and xylose sugars are present, glucose is preferentially utilized before xylose in most microorganisms because the presence of glucose prevents or represses the transcription of the genes responsible for the utilization of the alternate carbon (xylose). CCR often occurs through either: 1. Mechanisms that affect the synthesis of catabolic enzymes by way of global or specific regulators; or 2. The inhibition of the uptake of a carbon source (Deutscher, 2008; Monedero *et al.*, 2008; New *et al.*, 2014).

In most bacteria, the enzymes involved in sugar transport play a significant role in CCR mechanisms (Siegal, 2015; Stülke & Hillen, 1999). In CCR, cells detect the presence of multiple carbon sources through the binding of signal molecules to a receptor protein, triggering a specific cellular response that prevents the transcription of genes encoding the enzymes and transporters for the uptake, catabolism, and utilization of the secondary or alternate carbon.

Yeasts thrive on different carbon sources but the most preferred ones are glucose and fructose (Gancedo, 1998). When glucose or fructose is present, the enzymes required for the utilization of other carbon sources are either not synthesized (inhibited) or synthesized at a slow rate (Gancedo, 1998; Siegal, 2015; Simpson-Lavy & Kupiec, 2019). Yeast carbon metabolism is governed by the extracellular and intracellular glucose levels detected and this governs the cell's activities. Snf3 and Rgt2 in yeasts detect the levels of extracellular glucose, which helps the cells to determine the time for glucose uptake and the induction of glucose repression (John L Celenza et al., 1988; JOHN L Celenza & Carlson, 1989; Gancedo, 1998). High levels of glucose inactivate Snf1 giving room for the action of non-phosphorylated Mig1 with the Ssn6 and Tupi complex to initiate repression of genes that facilitate the use of alternative carbon sources (Adnan et al., 2018; Gancedo, 1998). Conversely, limiting glucose levels results in the activation of Snf1, which keeps multicopy inhibitor of galactose 1 (Mig1) phosphorylated thereby releasing the repressed genes for alternate carbon sources utilization (Ö. Kayikci & Nielsen, 2015; Nair & Sarma, 2021). When CCR in yeast is brought about by the Mig1 complex, Snf1 relieves the repression (Gancedo, 1998). Overexpression of genes for pentose transporters and pentose metabolizing enzymes will improve both co-fermentation and simultaneous fermentation of pentoses in the presence of D-glucose (Subtil & Boles, 2012).

2.10 Xylose transporters

Lignocellulosic biomass feedstock contains cellulose, hemicellulose, and lignin. The cellulose is a polysaccharide homopolymer of glucose linked with beta 1-4 glycosidic bonds, whereas hemicellulose is a heteropolymer of pentoses (xylose and arabinose), hexoses (glucose, mannose, and galactose), and sugar acids (citric acids, galacturonic acids, etc.) (Duarte et al., 2017; Kumar et al., 2019; Seidl & Goulart, 2016; X. Zhou et al., 2016). When lignocellulose is pretreated

and hydrolyzed, monomers of C5 and C6 sugars are released into the hydrolysate (Ryu & Trinh, 2018). Efficient conversion of the sugar monomers present in the lignocellulosic biomass hydrolysates is required for biofuel and biochemical production by microorganisms. For industrial bio-catalysis, microbes capable of utilizing these C5 and C6 sugars without CCR are essential and desirable. Biofuel and biochemical production via biological routes require the molecular transfer of sugar into the cell. Xylose sugar transfer into the cell is a bottleneck issue as it is inhibited strongly by glucose (Gao et al., 2018; Hamacher et al., 2002; Saloheimo et al., 2007; E. M. Young et al., 2014; G.-C. Zhang et al., 2015b; Zhao et al., 2020). Thus, before yeasts can serve as efficient producers of biofuel and biochemical products, their xylose utilization must be improved. This is especially true when lignocellulose is the source of carbon because xylose is the most second abundant sugar in lignocellulosic hydrolysates.

Some transporters for xylose uptake can transport glucose as well. Many transporters have been identified in *Candida intermedia* (glucose/xylose facilitator 1 (Gxf1) and glucose/xylose symport 1 (Gxs1)), *S. cerevisiae* (Hxt1, Hxt2, Hxt5, and Hxt7), and *S. stipitis* (Xut4, Xut5, Xut6, Xut7, Rgt2, and Sut1) (Bueno et al., 2020; Gárdonyi et al., 2003; Leandro et al., 2006; Nijland & Driessen, 2020; N. K. Sharma et al., 2018; E. Young et al., 2011). The mechanism for xylose transport in *S. cerevisiae*, *Schizosaccharomyces pombe*, and *Kluyveromyces marxianus* is facilitated diffusion (Heiland et al., 2000; Mehta et al., 1998; N. K. Sharma et al., 2018). In *Calathea utilis*, *Scheffersomyces stipites*, and *M reukaufii*, xylose uptake is achieved through a proton symport mechanism (da Cunha-Pereira et al., 2011; Rouhollah et al., 2007; N. K. Sharma et al., 2018; Subtil & Boles, 2012). Both facilitated diffusion and proton symport mechanisms for xylose uptake occur in *Rhodotorula glutinis* and *Candida shehatae* (Höfer & Misra, 1978; Janda

et al., 1976; N. K. Sharma et al., 2018). Xylose uptake in yeast is affected by yeast growing conditions, the carbon sources available, and the yeast species.

Young *et al.*, (2014) reported that G-G/F-XXX-G is a general sequence protein motif conserved among functional transporters of many microbes and highly enriched in transporters that grant growth on xylose. The modification of this conserved protein motif rewires yeast sugar transporter preferences (E. M. Young et al., 2014). The G-G/F-XXX-G structural motif is used to determine specific xylose transporters in yeast. Two conserved amino acids, threonine, and asparagine, were found within the *S. cerevisiae* xylose transporter protein motif (Farwick et al., 2014; Jiang et al., 2020; Ryu & Trinh, 2018; E. M. Young et al., 2014). Conversely, the native xylose-specific transporter in *Yarrowia lipolytica* contains a G-F-L-L-F-G structural motif, with tyrosine replacing asparagine (Ryu & Trinh, 2018). Enhanced C5 assimilation in yeasts when glucose (C6) is available requires the engineering of pentose specific transporters or modification of other transporters to import xylose or symport glucose and xylose (Farwick et al., 2014) if the yeast is not naturally endowed with high-affinity xylose transporters for xylose uptake.

2.11 Yeast *Pseudozyma hubeiensis* and *Pseudozyma tsukubaensis*

2.11.1 Biology

The yeast *P. hubeiensis* belongs to the phylum *Basidiomycetes*, subphylum *Ustilaginomycotina*, class *Ustilaginomycetes*, order *Ustilaginales*, and family *Ustilaginaceae* (Boekhout et al., 2011; E. A. Johnson & Echavarri-Erasun, 2011; C. Kurtzman et al., 2011). The majority of *Pseudozyma* species assimilate inositol but *P. hubeiensis* is inositol assimilation negative, which is a distinguishing factor of *P. hubeiensis* over other species (Digambar Gokhale, 2018; Mhetras et al., 2016). *P. hubeiensis* also produces cellulase-free xylanase and beta-

xylosidase (xylanolytic complete system) (Adsul et al., 2009; Bastawde et al., 1994; D. V. Gokhale et al., 1998). Possession of the xylanolytic complex system enables *P. hubeiensis* to break down xylan found in agricultural waste materials that are rich in lignocellulosic materials (Digambar Gokhale, 2018). In this manner, the simple sugar xylose can be produced for *P. hubeiensis* consumption (Digambar Gokhale, 2018). By this approach, the released sugars can become carbon sources for the biosynthesis of lipids and chemicals of high value.

The yeast *P. tsukubaensis* belongs to the phylum *Basidiomycetes*, subphylum *Ustilaginomycotina*, class *Ustilaginomycetes*, order *Ustilaginales*, and family *Ustilaginaceae* (Kawashima et al., 2011; Morita et al., 2011; Tanaka & Honda, 2017). *P. tsukubaensis* is the anamorph (asexual reproductive stage) of *Macalpinomyces spermophorus* (Tanaka & Honda, 2017). *P. tsukubaensis* secretes extracellular lipases to hydrolyze triglycerides into free fatty acids and glycerol for cellular metabolism.

2.11.2 Biotechnological applications of *P. hubeiensis* and *P. tsukubaensis*

P. hubeiensis is an oleaginous yeast of great biotechnological interest. Two native xylanases named PhX20 and PhX33 with molecular masses of 20.1 kDa and 33.3 kDa, respectively, can be produced by *P. hubeiensis* (Adsul et al., 2009). Furthermore, *P. hubeiensis* can produce low amounts of mannosylerythritol (MEL), a microbial biosurfactant (Beck, Haitz, et al., 2019). This is interesting because MEL is a product of high value characterized by its strong interfacial and biochemical properties (Morita, Fukuoka, Imura, et al., 2015), which predisposes it to cosmetic applications, such as for the treatment of damaged hair and as a moisturizer (Yoshida et al., 2014). Additionally, it serves as a natural antioxidant (Morita et al., 2010; Yoshida et al., 2014).

P. tsukubaensis produces a MEL biosurfactant under specific culture conditions, which can be

used in cosmetics and household detergents as described in section 2.11.2 (Beck, Haitz, et al., 2019). MEL is a biosurfactant belonging to the glycolipids class. *P. tsukubaensis* is distinctly known for exclusive secretion of MEL-B (Beck, Haitz, et al., 2019; Morita et al., 2007; Morita, Fukuoka, Imura, et al., 2015; Yoshida et al., 2014) whereas other organisms produce different MEL homologs (i.e. - A, -B, and -C variants) (Beck, Haitz, et al., 2019; Fai et al., 2014). *P. tsukubaensis* has been used to produce prebiotic galactooligosaccharides from lactose (Fai et al., 2014). *P. tsukubaensis* also produces biological erythritol, a non-cariogenic sweetener, that is in high demand commercially due to its benefits, including the fact that it does not spike blood sugar and has no nasty side effects (Tanaka & Honda, 2017). Other nasty side effects of sweeteners are depression, unpleasant aftertaste, negative impact on gut health, increased diabetes risk, weight gain, and increased risks of cancer.

2.12 Yeast *Cystobasidium iriomotense*

2.12.1 Biology

The yeast *C. iriomotense* belongs to the phylum *Basidiomycetes*, subphylum *Pucciniomycotina*, class *Cystobasidiomycetes*, order *Cystobasidiales* and family *Cystobasidiaceae* (C. Kurtzman et al., 2011; C. P. Kurtzman et al., 2011). *C. iriomotense* is an asexual yeast with pink-colored colonies (E. A. Johnson & Echavarri-Erasun, 2011). Lack of fucose as a cell-wall carbohydrate is a distinct characteristic of *C. iriomotense* (E. A. Johnson & Echavarri-Erasun, 2011; C. Kurtzman et al., 2011; C. P. Kurtzman et al., 2011). Only about 5% of the basidiomycetes yeasts that exist in nature have been identified, that is around 50 genera and approximately 250 species, while 95% are still unidentified and unexplored (Chreptowicz et al., 2019).

2.12.2 Biotechnological application of *C. iriomotense*

As a basidiomycetous yeast, *C. iriomotense* has gained attention because of its biodiversity and ecological roles, agricultural and medical importance, as well as from an economic point of view. The use of bacteria in bioremediation has gained great attention, but the use of fungi has not been studied in great detail. Recently, Chreptowicz *et al.*, (2019) reported that several basidiomycetous yeasts have a great impact on the bio-control of plant diseases by possessing rapid multiplication ability, antibiotics producing ability, and enzymes production potentials that induce resistance to diseases and promote plant growth. Basidiomycetous yeast, such as *C. iriomotense*, can break down aromatic compounds, and as a result, can be a useful tool in bioremediation. Anastasi *et al.*, (2008) reported about a consortium of three basidiomycete mycelia that can degrade polycyclic aromatic hydrocarbons (Anastasi *et al.*, 2008). Another important biotechnological application of *C. iriomotense* is in their ability to accumulate lipids in lipid bodies (Chreptowicz *et al.*, 2019; Ayumi Tanimura *et al.*, 2018) accounting for up to 65% of their dry biomass. Microbial lipids, like plant oils, are of great interest to the cosmetics industry because of their emollient and lubricity (Chreptowicz *et al.*, 2019). In pharmaceutical applications, microbial lipids serve as delivery agents (Chreptowicz *et al.*, 2019; Parsons *et al.*, 2018; Pichler & Emmerstorfer-Augustin, 2018). For food applications, microbial lipids are used for more homogeneous and efficient transportation of active agents, and nutritional purposes (Caporusso *et al.*, 2021; Chreptowicz *et al.*, 2019; Pichler & Emmerstorfer-Augustin, 2018; Yellapu *et al.*, 2018; Younes *et al.*, 2020). Microbial lipids are also applied in biofuels (Chreptowicz *et al.*, 2019; Galafassi *et al.*, 2012; M. Jin *et al.*, 2015; Maza *et al.*, 2020; Shields-Menard *et al.*, 2018; Wagner *et al.*, 2014; Yellapu *et al.*, 2018). Some basidiomycetous yeasts such as *C. iriomotense* are known

best for their pigment production. For example, *Rhodotorula* spp. and *Sporobolomyces roseus* are typically known for the production of carotenoids (tetraterpenoids) such as torulene, torularhodin, and γ - and β -carotene. Similarly, *Phaffia rhodozyma* is known for astaxanthin production (Chreptowicz et al., 2019; Davoli & Weber, 2002). The pigments are natural and can be used to replace artificial food coloring and dyes, to combat the growing legal restrictions on the use of artificial food additives in both Europe and the USA (Chreptowicz et al., 2019; Manu et al., 2020; Schor et al., 2010). The global market value for natural carotenoids was nearly \$1.4 billion in 2018, reaching \$1.5–1.8 billion in 2019–2020 (Chreptowicz et al., 2019; McWilliams, 2018), and will continue to appreciate every year because of the quest for natural (organic) foods.

2.13 Factors that affect lipid accumulation

The main factors that affect lipid accumulation are surplus carbon and limiting nitrogen. Limiting nitrogen in the presence of excess carbon decreases the level of adenosine monophosphate through the conversion of adenosine to inosine by adenosine deaminases. High concentrations of adenosine monophosphate indicate that the cell is starved for energy, hence the need for rapid glycolysis to restore levels of ATP. Conversely, the reduction in adenosine monophosphate level signals that ATP (energy) is sufficient, causing the TCA cycle to proceed (Reece et al., 2011; Sha, 2013). Citrate is an intermediate of the TCA cycle and can be transported to the cytosol for lipid formation and accumulation as described in section 2.8 and figure 2.4.

Restriction of other nutrients such as sulfur, iron, calcium, magnesium, and potassium in the culture medium can also increase lipid accumulation. Deng *et al.*, 2011 cultivated *Chlamydomonas* and *Chlorella* for lipid accumulation in nutritionally restricted media and reported that there was a significant increase in lipid content in both microalgae species when

cultivated in a medium with excess carbon and limiting nitrogen and sulfur (Deng et al., 2011). Also, when *Coccomyxa sp.* was cultivated in a medium limited in sulfur, nitrogen, or potassium nutrients, increased lipid content was observed and higher lipid content was also reported for the synergistic effects of combined sulfur, nitrogen, and potassium nutrients starvation (Tripathi et al., 2021). Cultivation of *Rhodospiridium toruloides* in a medium limited in sulfate resulted in high lipid accumulation regardless of the concentration of nitrogen (S. Wu et al., 2011). When *Chlamydomonas reinhardtii* was grown under nitrogen and sulfur starvation, lipid levels and biomass volume increased, while cell division and chlorophyll levels significantly decreased (Cakmak et al., 2012). Furthermore, culture time, temperature, and pH affect cell growth and lipid content in yeasts (Bartley et al., 2014; Dourou et al., 2018; Fakhry & El Maghraby, 2015; V. Johnson et al., 1992; Mus et al., 2013; Su et al., 2011).

2.14. Approaches for the bioconversion of microbial biomass to biofuel production

Biofuel production from microbial biomass occurs through different methods (Figure 2.6). The direct microbial biomass bioconversion method uses microorganisms to transform organic substrates (raw materials) present in the feedstock directly into biofuels. The biofuel produced via the direct conversion approach can be used as an energy source without undergoing more processing techniques (Espinosa Gonzalez, 2014). In some cases, the microbial biomass can be utilized directly by other microorganisms as feedstock for biofuel production. This is the entire biomass utilization approach to biofuel production. When the content of the microbial biomass is drawn out, it is called the microbial excerpts or extracts approach. These excerpts (extracts) can be fractionated using different processing routes (Espinosa Gonzalez, 2014), before being converted to biofuels (Karatzos et al., 2017; Okafor & Daramola, 2020). For instance, accumulated

lipids that are stored intracellularly in microbial biomass can be extracted using solvents before their conversion to biofuel. Similarly, microbial biomass can also be hydrolyzed first to liberate the fatty acids in the lipids before they are extracted for subsequent conversion to biofuel.

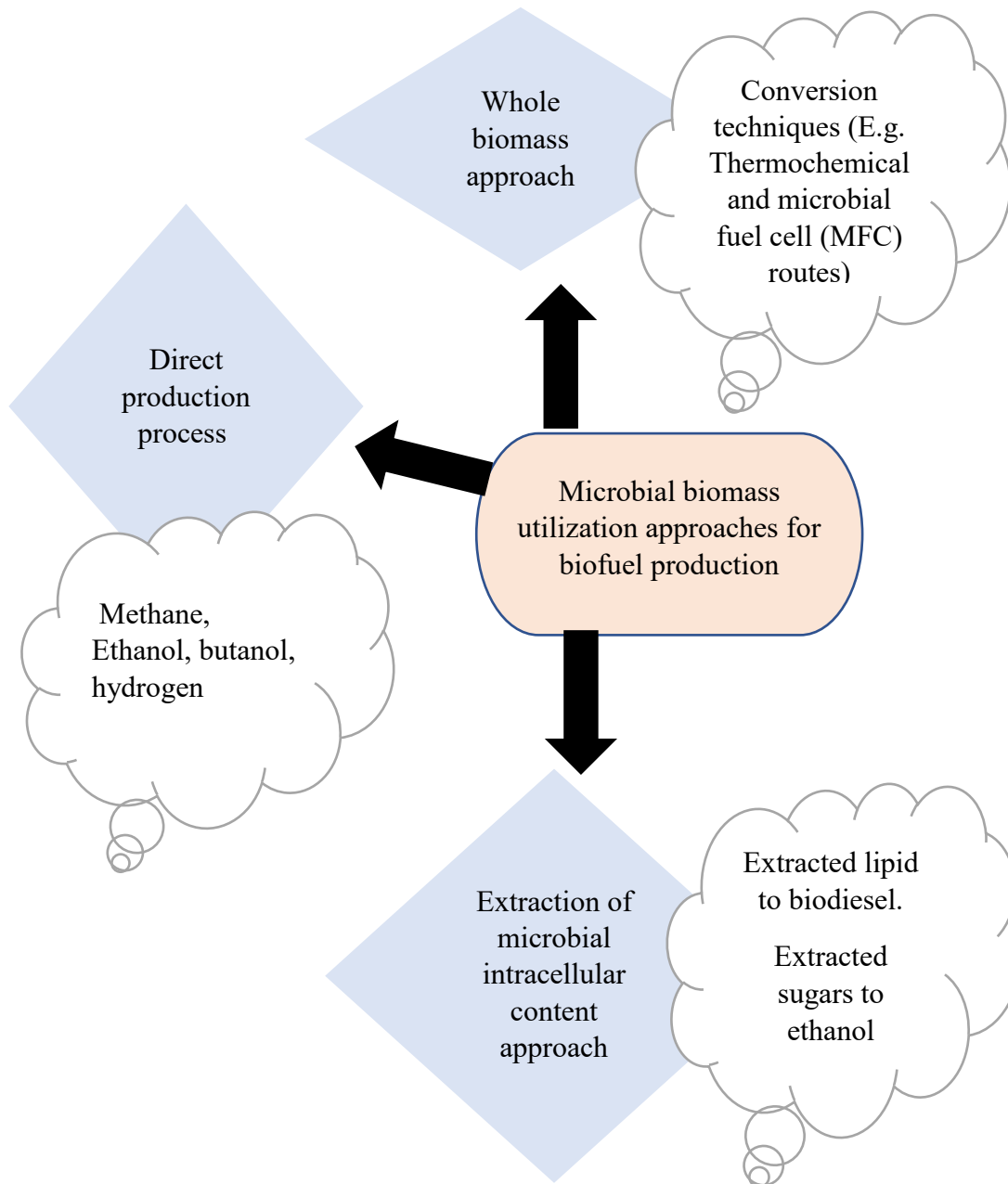


Figure 2.6. Conversion pathways for biofuel production from microbial biomass. Adopted in part from (Gonzalez, 2014)

2.14.1 Biofuel production through the extraction of the microbial intracellular components

Microbial cells are endowed with various components and the separation of the individual components from microorganisms offers a wider range of products and great opportunities for by-product utilization (Maddi, 2019). Lipids stored inside the microbial biomass of fungi, yeast, bacteria, microalgae, and macroalgae mostly are extracted for biodiesel, renewable diesel, and/or oleochemical production. Biodiesel burns clean and better than its fossil fuel counterpart (Karatzos et al., 2017). It is non-toxic and is biodegradable (Arvindnarayan et al., 2017; Halim et al., 2012). Compression ignition engines can utilize biodiesel as their fuel source. Twenty percent of biodiesel can be blended with 80% of petroleum diesel to form B20 (Furimsky, 2013; B. K. Sharma et al., 2009).

Figure 2.7 shows the lipid extraction process for biodiesel and renewable diesel production. Lipid extraction from microbial biomass for biodiesel production accounts for $\leq 50\%$ of the total production cost of biodiesel (Karatzos et al., 2017). The lipids extracted from microbial biomass can then be processed into biofuel. But the dewatering of the microbial culture to concentrate the microbial biomass, to get dry cells, or both is very expensive and energy-demanding, especially during large-scale production (Espinosa Gonzalez, 2014; Halim et al., 2012). Dewatering of microbial biomass can be achieved by mechanical processes such as centrifugation or filtration. To completely dry all the water in the microbial biomass requires the deployment of other drying operations (i.e. spray drying) that may be capital intensive. Dewatering is an issue of serious concern to the industrial-scale/commercial production of biofuel using microbial cultures (Gonzalez, 2014; Karatzos et al., 2017).

2.14.1.1 Processing steps for the extraction of the contents of microbial biomass

2.14.1.2. Microbial biomass harvesting operation

Biofuel generated from oleaginous organisms requires the harvest of microbial biomass. To harvest the oleaginous biomass from the culture, the culture has to be concentrated by removing the excess water. This concentrated microbial slurry is required before embarking on downstream processing (Gonzalez, 2014; Karatzos et al., 2017; Ndikubwimana et al., 2016; Uduman et al., 2010). Some methods used to achieve the concentration of the microbial liquid cultures are decantation, filtration, flocculation, flotation, centrifugation, and sedimentation (Gonzalez, 2014).

The process of allowing the liquid culture to pass through a permeable membrane that allows only the media (fluid) to pass but retains the microorganisms (solid particles) in the culture is called filtration (Espinosa Gonzalez, 2014; Halim et al., 2012; Uduman et al., 2010). Achieving an efficient filtration process is dependent mainly on the pressure from either the vacuum, centrifuge, or gravitational forces used for this unit operation (Espinosa Gonzalez, 2014; Ndikubwimana et al., 2016; Uduman et al., 2010). The filtration separation technique has some drawbacks, which are blocked membrane problems, being a time-consuming process, the high need for membrane replacement, and disposal costs associated with membrane replacement (Danquah et al., 2009; Espinosa Gonzalez, 2014; Raheem et al., 2015).

Sedimentation refers to a separation technique that involves specifically the use of gravitational forces, centrifugal acceleration, or electromagnetism to separate the biomass from the suspension or fluid. This way, the biomass tends to settle out of the culture. Though sedimentation has negative aspects, such as the sedimentation equipment occupying a large space and being a time-consuming technique, it is still in use today (Espinosa Gonzalez, 2014).

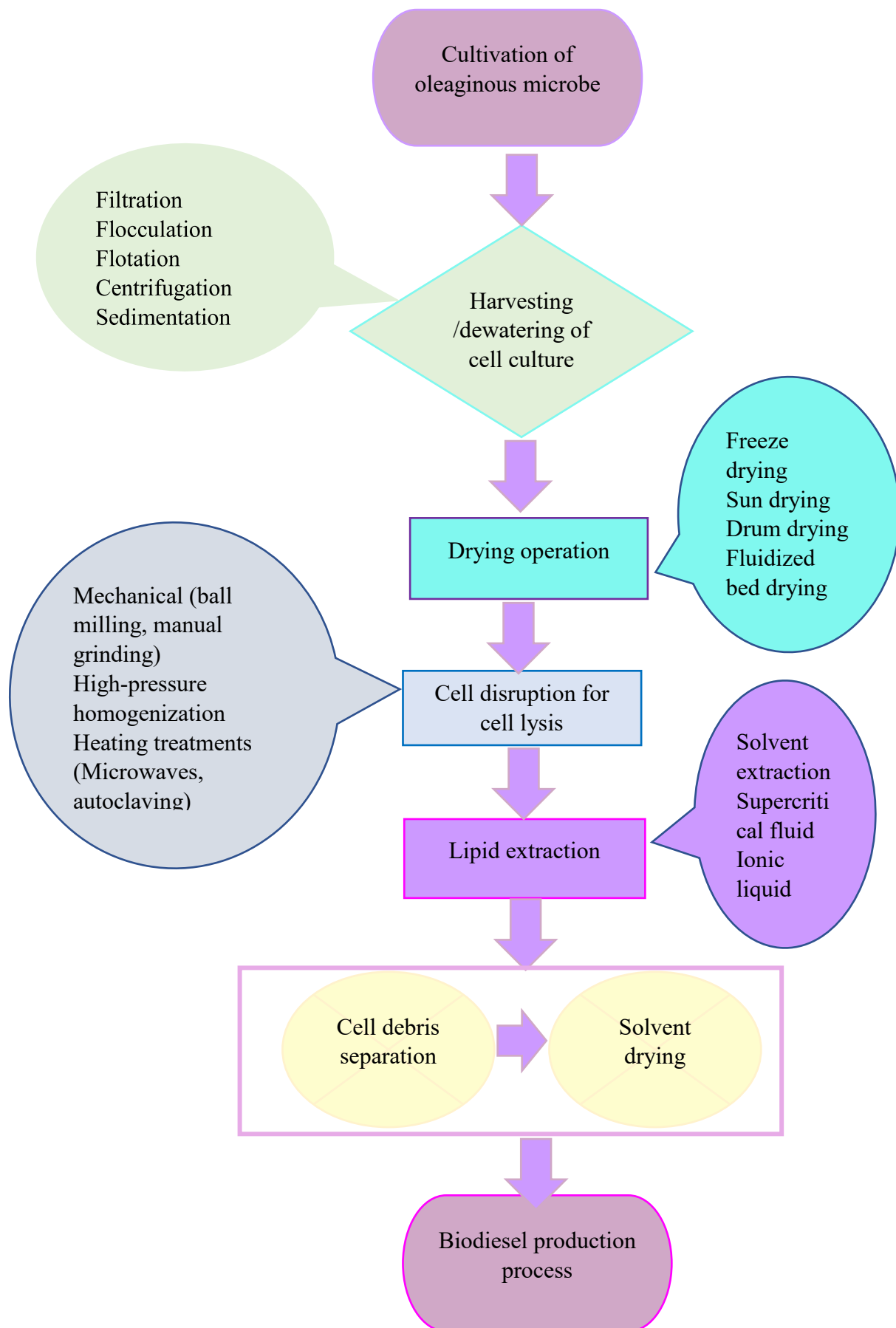


Figure 2.7. Process flow diagram for downstream processing of microbial biomass extracts during biodiesel production. Adopted in part from (Gonzalez, 2014; Halim et al., 2012).

Unlike the sedimentation technique, the flotation separation technique involves the action of using air or gas on the microorganisms to assist them to float to the surface. The particle size of the microbial biomass and contact area (Espinosa Gonzalez, 2014; Halim et al., 2012; Uduman et al., 2010) affect the efficiency of the flotation separation method.

Flocculation is another separation technique that ensures the coming together of microbial cells to form large-size clusters of flakes or flocs by contact through collision and adhesion. Flocculation can be achieved spontaneously or through the addition of clarifying agents which are chemical coagulants that facilitate the bonding of particles to form flakes, aggregates, or flocs. (Bratby, 2016; Danquah et al., 2009; Halim et al., 2012; Uduman et al., 2010). Clay-based flocculants, inorganic flocculants, and cation flocculants can be employed to achieve microbial biomass flocculation (Chunyi Chen et al., 2018; Gonzalez, 2014).

The use of the centrifugal separation method is also useful for the separation of biomass from the medium. It is the most used separation technique used in laboratories. Separation by centrifugation makes use of high speed, is fast, does not lead to product degradation, and is efficient in product recovery. Centrifugation makes use of centrifugal forces to separate particles based on size, shape, viscosity, rotor speed, and density. No wonder it is a technique of choice for the recovery of high-value metabolites. Notwithstanding, it is energy and capital-intensive for microbial harvest.

2.14.1.3 Drying of microbial biomass

Drying is a technique that ensures that water is removed from solid, semi-solid, and liquid substances through evaporation. There are different techniques by which drying can be accomplished. They include but are not limited to, the use of sun drying, low-pressure drying, spray

drying, drum drying, fluidized bed drying, or freeze-drying (Fonseca et al., 2019; Gonzalez, 2014). The objective of these drying processes is to completely reduce the moisture content of microbial biomass to a safe level to either extend the shelf life or prepare biomass for the next steps of operation (Espinosa Gonzalez, 2014).

Amongst all the techniques, sun drying is not a capital intensive method, though it leads to material loss, consumes longer time, and requires larger surfaces (Baloch et al., 2018; Biller & Ross, 2016; Fonseca et al., 2019; Heidenreich et al., 2016; Monlau et al., 2015; Naghdi et al., 2016). In addition, sun drying depends on the climatic condition and is not available all year round in some regions. The drying method to be used depends on the nature of the sample to dry, the value of the product, and the desired final product (Espinosa Gonzalez, 2014; J. Jin et al., 2016).

Freeze drying is a common drying technique used in the laboratory setting for drying oleaginous microbial biomass because it saves time and preserves the accumulated lipids in the microbial cells. Freeze-drying is not often used commercially for large-scale production because it is capital intensive and difficult to maximize profit.

2.14.1.4 Cell disruption operation

The manipulation of living organisms by accessing their cell components to produce useful products requires an important unit operation known as microbial cell disruption (Harrison, 1991). The objective of cell disruption is specifically to weaken the cell wall of the microbial biomass to remove/break the cell wall's protective power, allowing extraction materials (such as solvents) to gain free access to the intracellularly stored lipid facilitating their recovery (Dong et al., 2016). Some examples of commercial high-value bio-molecules/products are enzymes, pigments, lipids, organic acids, and proteins (Espinosa Gonzalez, 2014; Gomes et al., 2020; D. Liu et al., 2016).

Cell disruption can be achieved by mechanical methods (glass shear, osmotic shock, pressing, and sonication), physical methods (thermolysis, osmotic shock), chemical methods (acids, bases, enzymes), or biological processes (Dong et al., 2016; Espinosa Gonzalez, 2014; Harrison, 1991; Salazar & Asenjo, 2007). The drawbacks associated with the use of different cell disruption techniques include energy consumption, the interaction of disruption methods with downstream operations, product degradation, and profit optimization (Günerken et al., 2015; D. Liu et al., 2016).

Mechanical cell disruption techniques are used when high recovery is required. The mechanical cell disruption method is a poor selective technique, expensive, and can increase sample handling risks (Goldberg, 2008; Rivera et al., 2018). For example, high-pressure homogenization results in emulsion formation during oil extraction (Dong et al., 2016). Bead milling applied on microalgae before hexane extraction of oil led to the recovery of 4 times higher oil than achieved through Soxhlet extraction, though it is not a cost-efficient cell-disruption method (Dong et al., 2016; Voloshin et al., 2016). Conversely, non-mechanical techniques are mild, gentle, and effective in the selection for bio-active extraction (Günerken et al., 2015; D. Liu et al., 2016). The effect of six cell disruption methods on yeast cells was investigated by Kot *et al.*, 2020, who observed that the cell disruption method had a significant effect on the quality and quantity of lipid extracted. When homogenization was done with zirconium balls, it led to the degradation of the oleic and linolenic fatty acids (Kot et al., 2020). Desired recovery level, selectivity of cell contents, and energy consumption specifically influence the choice of cell disruption method. Protocols used for extraction in the laboratory but are not optimal for industrial application (scale-up) include microwaving, freeze-drying, cell homogenization, sonication, autoclaving, osmotic shock, or pulverization (Halim et al., 2012; Patel et al., 2020)

2.14.1.5. Lipid extraction

After cell disruption, extraction of bioproducts from microorganisms is done mostly by using solvents. Hexane, methanol, chloroform, and diethyl ether are some of the most common solvents that can be used for lipid extraction (Mercer & Armenta, 2011). The use of solvents in lipid extraction is cheap and gives reproducible results, but it can leave residual solvent on the extracted bioproducts (Espinosa Gonzalez, 2014; Mercer & Armenta, 2011).

The use of supercritical fluids for lipid extraction and separation of substances has gained popular acceptance in recent years (Mercer & Armenta, 2011). Separation is achieved based on the solvating power of gases above their critical points (McHugh & Krukoniš, 2013). The use of a supercritical fluid separation technique provides ample benefits such as the production of highly purified extracts free of harmful solvents residues, safe separation of heat-labile products, quick extraction and separation of bioproducts, reduced separation costs, and reduced greenhouse gas effects from industries by utilizing the CO₂ generated (Baloch et al., 2018; Hewavitharana et al., 2020; Karmakar & Halder, 2019; Mercer & Armenta, 2011; Park et al., 2018; Patil et al., 2018; Posmanik et al., 2017). Furthermore, supercritical fluids are non-toxic, non-flammable, and involve a simple operation and some supercritical fluids are green solvents (Abas et al., 2018; Catchpole et al., 2018; Du et al., 2015; Halim et al., 2012; Hrnčič et al., 2016; Mercer & Armenta, 2011; Patil et al., 2017; Remón et al., 2018).

Other extraction techniques utilized in lipid production are pulsed electric field processing, enzymatic treatment, and ultrasound. They have improved lipid extraction performance and yields (Espinosa Gonzalez, 2014; Hao et al., 2021; Picó et al., 2018; Z. Wang et al., 2019; Zuorro et al., 2018). Similarly, ionic liquids (liquid organic salts) have been for lipid extraction on microalgal biomass (Espinosa Gonzalez, 2014; Ho et al., 2016; Krishnan et al., 2020; Pan et al., 2016; Shankar

et al., 2017; Tang & Ho Row, 2020; W. Zhou et al., 2019). In brief, the choice of the extraction technique to apply depends significantly on the purpose of the recovery, desired purity, quality, and the structural characteristics of the microbe that contains the intracellular biomolecules (bioactive components).

2.14.2. Whole biomass processing without microbial extraction

Advanced biofuel production can be done without extracting the content of the microbial biomass and the concept is to reduce some of the preprocessing steps and their corresponding costs incurred when using the microbial extract method. The whole biomass processing method involves thermochemical, chemical, and biochemical conversions (Figure 2.8) (Arvindnarayan et al., 2017; W.-H. Chen & Lin, 2019; Demirbas, 2007; Demirel, 2018; Espinosa Gonzalez, 2014; Hossain, 2019; Rezaei & Mehrpooya, 2018; Yazan et al., 2016). The selection of the processing method depends on the type of biofuel desired, quality of biofuel, type of bio-feedstock, and economic considerations (Hossain, 2019). Direct combustion of dried whole biomass into heat to generate electricity or steam is also a route in the whole biomass processing techniques.

2.14.2.1 Biochemical conversion processes

Biochemical conversion processes use biological enzymes or biochemicals to produce intermediates, biofuels, chemical building blocks, and/or value-added products. These processes often involve fermentation with special operational conditions applied, such as anaerobic conditions, aerobic conditions, illumination, etc. (Atsonios et al., 2015; Gouveia & Passarinho, 2017; Zhao et al., 2020). Lignocellulosic material or microbial biomass can serve as feedstocks for biochemical conversions (Gouveia & Passarinho, 2017). For microbial biomass or lignocellulosic feedstocks to be used by microorganisms in biochemical conversions, they must be pretreated to

hydrolyze/break down the feedstocks to liberate simple sugars and other nutrients. Then, bacteria, cyanobacteria, and yeasts can utilize (ferment) the sugars or the gas phase intermediates into biofuels. For example, employing anaerobic digestion, algal biomass can be converted into methane and carbon dioxide (Gonzalez, 2014; Gouveia & Passarinho, 2017; H. Hassan et al., 2019).

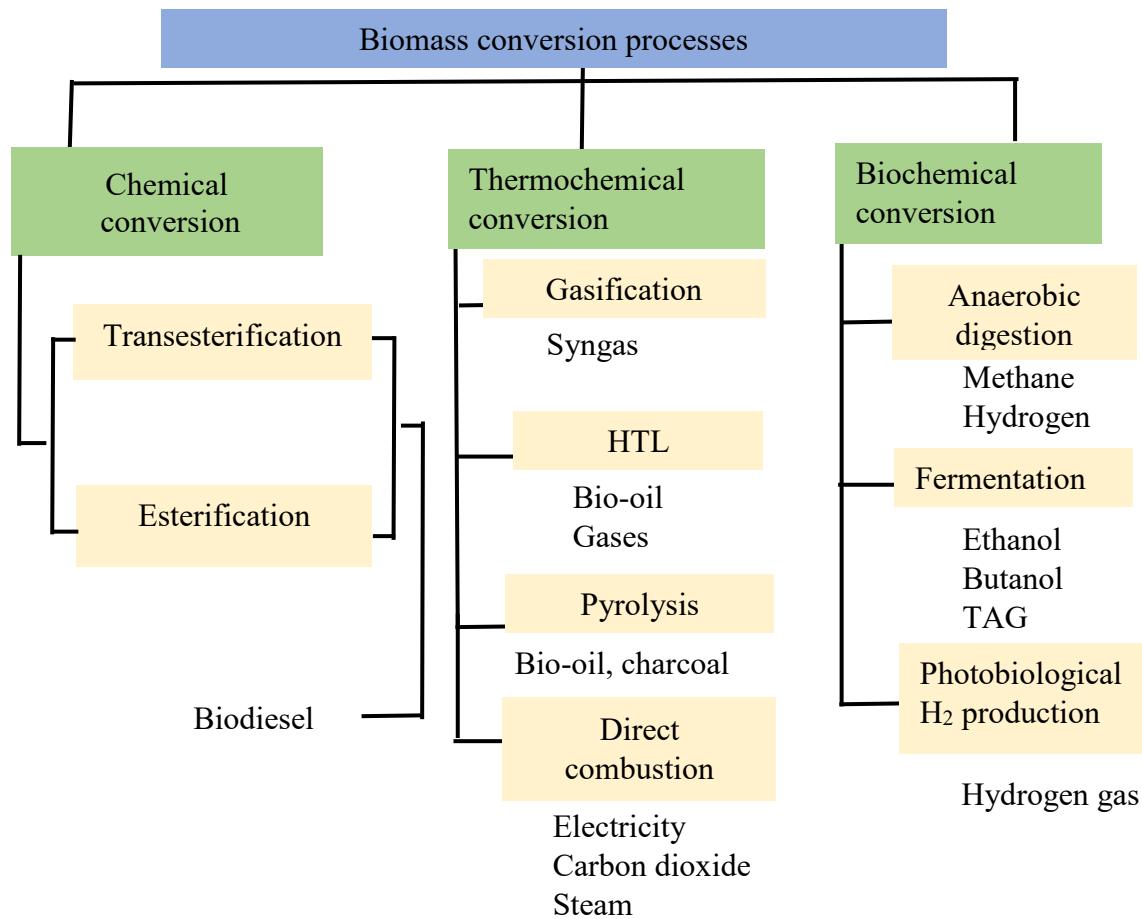


Figure 2.8. Microbial biomass conversion technologies to biofuels. Adopted in part from (Espinosa Gonzalez, 2014; H. Hassan et al., 2019; Medipally et al., 2015). TAG is triacylglyceride.

2.14.2.2 Thermochemical conversion

Thermochemical conversions are high-temperature deconstruction processes that use thermal decomposition to convert biomass to biofuel. This technique specifically uses high temperatures and pressure, with or without a catalyst, in the absence or presence of oxygen, to convert microbial biomass into biofuels and valuable products. Thermochemical conversion processes include gasification (high temperatures (800-1000°C) with steam), pyrolysis (high temperatures in the absence of oxygen), combustion (high temperatures in the presence of sufficient oxygen), and hydrothermal liquefaction (high temperatures, high pressures, with water) (H. Hassan et al., 2019; Ng et al., 2017; Raheem et al., 2015). These conversion techniques will be discussed in more detail below.

2.14.2.2.1 Pyrolysis

Pyrolysis is the thermal decomposition of biomass into gas, liquid (bio-oil), and solid (charcoal, biochar) products in the absence of oxygen at temperatures between 350 to 700°C (Chan et al., 2018; Espinosa Gonzalez, 2014; Kar, 2018; Karatzos et al., 2017; Kholkina et al., 2019; A. A. Lappas et al., 2009; Teixeira et al., 2017; W.-C. Wang & Lee, 2019). When pyrolysis is conducted at intermediate temperatures of about 500°C and in the absence of oxygen, a mixture of gases, char, and liquids (water, water-soluble, and water-insoluble organics, known as bio-oil) is produced (Karatzos et al., 2017). In fast pyrolysis, the heating is reduced to a short resident time in the pyrolytic system (i.e. a couple of seconds or less) to drive products to bio-oil (H. Hassan et al., 2019; Karatzos et al., 2017; Okafor & Daramola, 2020). The main benefit of fast pyrolysis is that the liquid product becomes more dominant compared to the gases and solids (Kazemi Shariat Panahi et al., 2019; Pinho et al., 2015; Remón et al., 2018; W.-C. Wang & Jan, 2018). The product

fraction of interest determines the optimum pyrolysis temperature and duration of time for the pyrolysis process (Okafor & Daramola, 2020).

One of the drawbacks of bio-oil from biomass is the amount of oxygen contained in the final product. The high oxygen content affects the acid number of the biofuel, leading to corrosiveness, high viscosity, etc. (Karatzos et al., 2017). Another downside of bio-oils produced from biomass is the nitrogen content of the final product. Other undesirable components of biofuels are sulfur, minerals, and salts, which lowers biofuel qualities and must be upgraded to meet approved fuel standard specifications (Gonzalez, 2014; Karatzos et al., 2017).

2.14.2.2.2 Gasification

Gasification partially oxidizes wet biomass to produce gas, which subsequently undergoes upgrading via chemical processes such as Fischer-Tropsch synthesis to yield chemicals such as methanol, which can be used directly or can be converted to ethanol. This process uses oxygen at elevated temperatures ($>700\text{ }^{\circ}\text{C}$) (H. Hassan et al., 2019; Karatzos et al., 2017). The combustion gas produced by gasification is known as syngas and it contains different concentrations of gases such as CO , H_2 , CO_2 , N_2 , and methane (CH_4) (H. Hassan et al., 2019). The gas generated by gasification may not necessarily be used directly as fuel except after upgrading (Karatzos et al., 2017). Gases that can be used directly as fuel include renewable hydrocarbon gases. Gasification studies using different algal biomasses have been mainly focused on optimizing conversion yields and driving the production of a particular gas, mostly H_2 . The reactions can also occur in the presence of a catalyst either to promote methane (gas) formation or to suppress it (H. Hassan et al., 2019; M. Hu et al., 2018; A. A. Lappas et al., 2009; A. Lappas & Heracleous, 2011, 2016; Nam et al., 2011; Pang, 2019; Prakash et al., 2015; Y. Shen et al., 2014; Singh et al., 2014; C.

Yang et al., 2019).

However, the main drawback in using the gasification technique is the formation of tar in the gasified product because this causes fouling of the pipes, turbines, gas engines, and filters (H. Hassan et al., 2019). The overall efficiency of gasification is reduced by the formation of tar. To remove the tar, two methods are applied. This includes dry methods that involve the use of filters, cyclones, and the likes to remove the tars, as well as wet methods that encompass the use of wet cyclones and spray towers to separate the tar (H. Hassan et al., 2019). The limitation of both methods is that they eliminate the tar instead of allowing the tar to be converted into syngas. The prevention/minimization of tar formation can be achieved through improved gasifier design, tuning the operating conditions (i.e. pressure, temperature, steam/biomass ratio, gasifying agent), and the use of catalysts (H. Hassan et al., 2019; Karatzos et al., 2017; Leibbrandt et al., 2013).

2.14.2.3 Direct Biomass Combustion

When microbial biomass is burned to produce gas in the presence of O₂, it is called direct biomass combustion (Gonzalez, 2014; Okafor & Daramola, 2020). The carbon is oxidized to CO₂ and hydrogen is oxidized to H₂O during biomass direct combustion (Banapurmath et al., 2019; Bwapwa et al., 2018; Laesecke et al., 2017; Voloshin et al., 2016). A direct conversion process is preferred if the moisture content of the biomass is < 50% (H. Hassan et al., 2019). Uses of direct biomass combustion include heat, biogas, or steam generation (Bwapwa et al., 2018; K. Chen et al., 2016; Dabros et al., 2018; Hilten et al., 2010; Laesecke et al., 2017; Q. Ren & Zhao, 2015; Ross et al., 2008; Velmurugan et al., 2014; Voloshin et al., 2016). Different types of biomass can be used for direct combustion such as wood biomass, municipal solid waste, and agricultural waste biomass (Espinosa Gonzalez, 2014; Okafor & Daramola, 2020). Some pre-processing steps such as drying

(to reduce moisture to the desired level) and size reduction (for the creation of more surface area) are required before using the biomass in the direct combustion technique (Espinosa Gonzalez, 2014; Okafor & Daramola, 2020). The major drawbacks associated with the direct biomass combustion technique are the costs incurred from size reduction and drying, as well as the generation of hazardous gases.

2.14.2.4 Thermochemical liquefaction

Thermochemical liquefaction is a technique that is applied to wet microbial biomass for their transformation into liquid fuel (H. Hassan et al., 2019). The temperature and pressure required to reach sub-critical conditions for thermochemical liquefaction are 200 to 350°C and 5 to 20 MPa, respectively (Espinosa Gonzalez, 2014). The combination of this temperature and pressure in thermochemical liquefaction leads to efficient conversion of heavy hydrocarbon chains to smaller molecules that have higher energy density (Espinosa Gonzalez, 2014; H. Hassan et al., 2019). This can be quickened by the use of a catalyst (Eibner et al., 2017; X. Huang et al., 2019). Bio-oil obtained from pyrolysis of biomass (bio-crude) contains $\geq 40\%$ of oxygen, making upgrading mandatory to improve the energy value (Karatzos et al., 2017). This includes deoxygenation as well as catalytic hydrogenation with metals of nickel, platinum, palladium, and their oxides (Ishida et al., 2021; Kostyniuk et al., 2021). The upgrading improves the biofuel quality to meet fuel standard specifications (Agarwal, 2007; Asomaning et al., 2014c; Baroutian et al., 2013; Grioui et al., 2019; Rabie et al., 2018; Wiggers et al., 2013; Xiaoyi Yang et al., 2016). The main goal of liquefaction is to obtain a higher-quality bio-oil than that obtained through pyrolysis, specifically in terms of obtaining higher heating values and lower oxygen content.

Liquefaction allows the use of wet biomass thereby eliminating the dewatering step making thermochemical liquefaction an attractive alternative to pyrolysis. Other names for the process used for the conversion of wet microbial biomass using high temperature and pressure are hydrothermal carbonization (200°C, 2 MPa) (Biller & Ross, 2016; X. Chen et al., 2018; Daful & R Chandraratne, 2018; Espinosa Gonzalez, 2014; He et al., 2018; Lin et al., 2016; Ma et al., 2019; Mathimani & Mallick, 2019; J. Zhang & Zhang, 2019; Zhuang et al., 2018), hydrothermal liquefaction (280 to 370°C, 10 to 25 MPa) (Castellví Barnés et al., 2015; Durak & Genel, 2018; Leng et al., 2018; López Barreiro et al., 2018; Pedersen et al., 2017; Vardon et al., 2012; C. (Charles) Xu et al., 2018), and hydrothermal gasification (400 to 700°C, 25 to 30 MPa) (Ciuta et al., 2018; Daful & R Chandraratne, 2018; Demirel, 2018; Espinosa Gonzalez, 2014; Lin et al., 2016; Mei Wu et al., 2014; Singh et al., 2014; C. (Charles) Xu et al., 2018; J. Zhang & Zhang, 2019).

2.14.3 Chemical conversion processes

Chemical conversion of oleaginous microbial biomass is done either by transesterification or esterification depending on the feedstock composition (Koutinas et al., 2014; Naik et al., 2010). One major requirement for chemical conversion is that the biomass must be composed of lipid consisting of 90 - 98% TAG, must contain traces of other residual materials, and moisture (H. Hassan et al., 2019). If the microbial biomass lipid contained an ample amount of free fatty acid or moisture, then esterification is preferred to transesterification to avoid saponification reactions (H. Hassan et al., 2019; Karmakar & Halder, 2019). Conversely, if the lipid contains less FFA and moisture, transesterification occurs (H. Hassan et al., 2019). This is so because the esterification reaction eliminates water molecules, formation of esters and water occurs when alcohols react with carboxylic acids (condensation reaction).

2.14.3.1 Transesterification

Transesterification refers to the process that changes the organic group of an ester to an organic group of alcohol (Martinez-Silveira et al., 2019; Meher et al., 2006; Reis et al., 2014). This reaction occurs in the formation of biodiesel when microbial lipids (specifically TAG) react with mono-alcohol in the presence of a catalyst. It is an equilibrium reaction that requires an excess alcohol /bio-oil ratio to switch to higher reaction rates (Louhasakul et al., 2018; Meher et al., 2006; Rezania et al., 2019; Schuchardt et al., 1998). The catalysts often in use for transesterification reactions are acids, bases, or enzymes. Two forms of transesterification reactions are homogenous and heterogenous transesterification (Karmakar & Halder, 2019; Schuchardt et al., 1998). Homogenous transesterification reactions are known for their fast reaction rate and low cost of the catalyst, whereas heterogeneous transesterification reactions are known for easy separation and regeneration of the catalyst, which makes it more feasible for industrial application (Karmakar & Halder, 2019; Meher et al., 2006; Rezania et al., 2019). Enzymatic transesterification reactions have gained great attention and have become one of the hot topics in research because of the ease of product separation, the absence of saponification, and the lower temperature required for its operation. Notwithstanding, operations of enzymatic transesterification reactions have not yet been optimized (Louhasakul et al., 2018; Martinez-Silveira et al., 2019; Rezania et al., 2019; Schuchardt et al., 1998).

Base catalyzed transesterification is the most common method for biodiesel production, which can be either homogenous or heterogeneous. When compared with acid and enzyme-catalyzed transesterification reactions, the base transesterification reaction is faster (Meher et al., 2006; Rezania et al., 2019). Potassium hydroxide (KOH) and sodium hydroxide (NaOH) are the common bases used in homogeneous base transesterification reactions for biodiesel commercial

production (Louhasakul et al., 2018; Meher et al., 2006; Schuchardt et al., 1998). For instance, waste oil was converted to biodiesel using homogeneous methyl alcohol and NaOH to yield 85% fatty acid methyl esters (FAME) after 30 minutes (Leung & Guo, 2006; Martinez-Silveira et al., 2019). Rapeseed (Rashid & Anwar, 2008), frying oil (Encinar et al., 2005), and plant oils and animal fats (Muniyappa et al., 1996) were also transformed to FAME using basic homogeneous transesterification reactions.

Acid-catalyzed transesterification reactions are different from the basic transesterification reactions, yielding about 95-99% of FAME at temperatures above 100 °C. However, comparatively higher alcohol to oil ratio of 9:1 to 166:1 is required to shift the equilibrium towards the product side (Campos et al., 2014). The increase in the amount of mono-alcohol required in the acidic transesterification reaction poses difficulties with separation. Nevertheless, the higher acidity in acidic transesterification reactions completely removed the risk of soap formation (saponification) due to the simultaneous occurrence of esterification and transesterification (Pathak, 2015). Common acids for homogeneous acid-catalyzed transesterification of microbial lipids are sulfuric acid (H_2SO_4) and hydrochloric acid (HCl) (Soriano Jr et al., 2009).

Enzyme catalyzed transesterification is achieved by using lipases to transesterify microbial lipids to biodiesel (Mateos et al., 2021). It is environmentally and economically a very friendly process able to lessen the problems associated with acidic and basic transesterification reactions. As a result of the numerous merits of producing biodiesel via enzyme-catalyzed transesterification, it is recently been referred to as the best sustainable option to replace petroleum diesel. More so, lipases as enzyme catalysts can be used in free form or immobilized form for homogeneous and heterogeneous transesterification reactions, respectively, to produce methyl esters.

2.14.3.2 Esterification

Esterification is a chemical reaction that involves carboxylic acid and alcohol groups, producing an ester. Conversely, transesterification discussed in section 2.6.4.1 modifies the ester produced by esterification. When lipids are hydrolyzed, free fatty acids (FFAs) are generated. This FFAs are esterified with methanol or ethanol in the presence of an acid catalyst such as HCl to produce FAMEs (Kyriakidis & Dionysopoulos, 1983; Mateos et al., 2021; Zullaikah et al., 2019). The acid catalyst promotes the nucleophilic attack of the alcohol to the carbonyl carbon that leads to water loss and FAME production (dos Santos et al., 2019).

2.14.4 Current microbial biomass conversion techniques

2.14.4.1 Microbial fuel cell (MFC) for electricity generation

An MFC is defined as a device that utilizes microorganisms for direct biomass degradation and metabolism, and then uses the products for power production (electricity) using electrochemical activity (Y. Wang et al., 2021). An MFC can only exist if there is an electroactive microorganism that will degrade the chemical organic matters present in the biomass for electron generation and deposition on the anode side (Moradian et al., 2021; Y. Wang et al., 2021). Electroactive microorganisms irreversibly attach to the electrode surface resulting in the formation of biofilm. This produced biofilm is called electroactive microorganisms (EAMs) biofilm (Moradian et al., 2021). A schematic diagram of the MFC process is shown in Figure 2.9. The electrons deposited at the anode migrate to the cathode side via an external circuit connected to the cathode thereby creating a current (Moradian et al., 2021; Y. Wang et al., 2021). The proton exchange membrane in the MFC allows protons to enter the cathode side for power generation.

Yadev *et al.*, (2020) developed a bioelectricity production strategy using a two-compartment

MFC where bacterium and microalgae synergistically collaborated to fulfill the need of each other while generating power in the MFC (Yadav et al., 2020). MFC conversion requires lower temperatures such as room temperature. Substrates for MFC include, but are not limited to, cow dung, fruit peels (mango, orange, and lemon peels), chitin, food wastes, kitchen wastes, corn-stover, wood, sewage, rice straw, and algal biomass (S. H. A. Hassan et al., 2014; Hui Li et al., 2016; S.-W. Li, He, et al., 2017; S.-W. Li, Zeng, et al., 2017; Moradian et al., 2020; Yadav et al., 2020). An MFC is an excellent multi-substrate utilization technique. The substrates/biomass used in an MFC sometimes needs to be pretreated to enable microorganisms to achieve complete hydrolysis of the biomass.

Electroactive microorganisms used in the MFC technique are *firmicutes* (*Clostridium butyricum*), *Actinobacteria* (*Actinoalloteichus cyanogriseus*), *proteobacteria* (*Geobacter sulfurreducens*), *archaea* (hyperthermophile *Pyrococcus furiosus*), and eukaryotes (*Cystobasidium slooffiae* JSUX1), respectively (S. H. A. Hassan et al., 2014; Moradian et al., 2020). Both Gram-positive and Gram-negative bacteria, as well as yeast and fungi, have been utilized as EAM (Moradian et al., 2020, 2021)

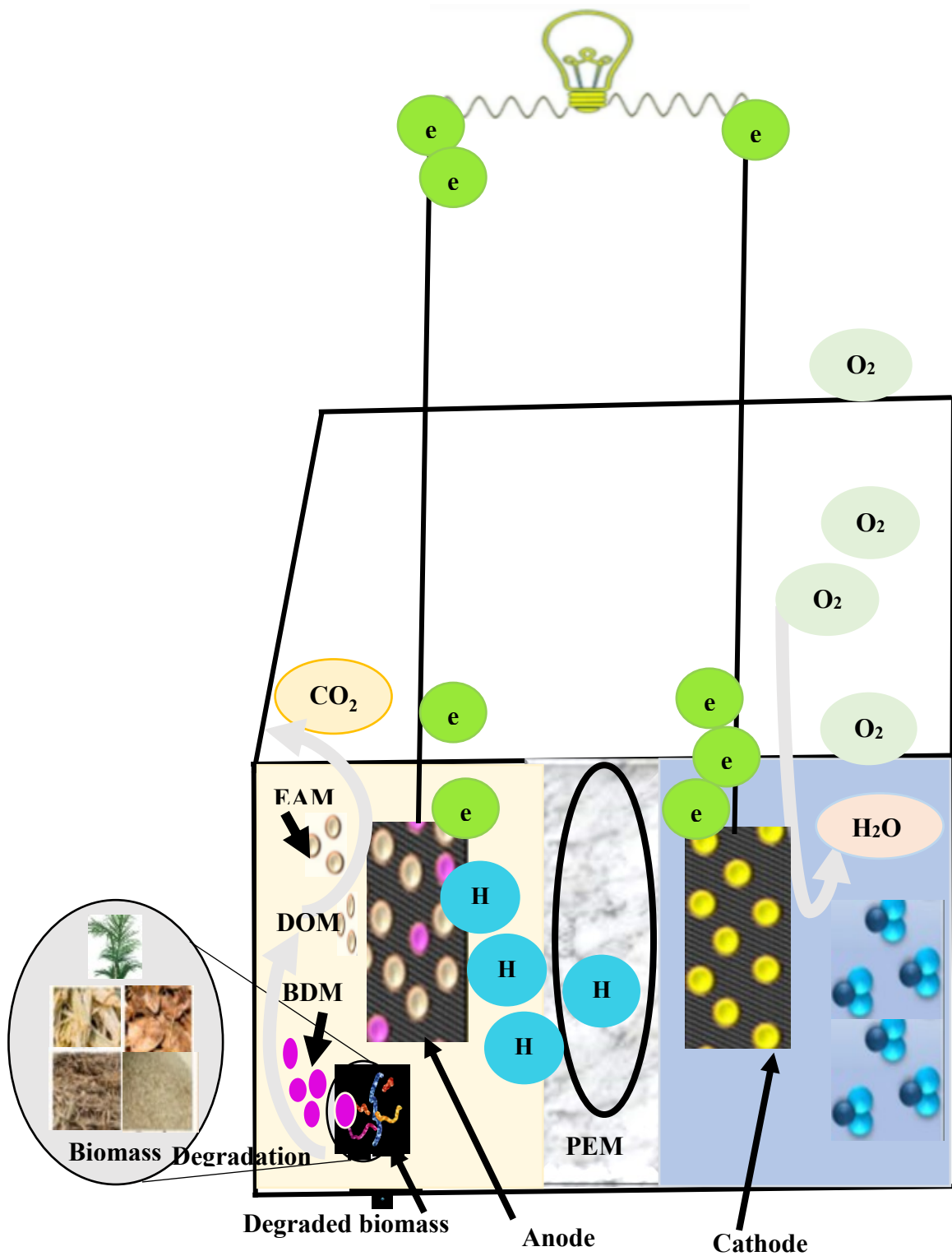


Figure 2.9: Microbial fuel cell process diagram. Adopted in part from (Moradian et al., 2021).

BDM: biomass-degrading microorganism, PEM: proton exchange membrane, EAM: electroactive microorganism, and DOM: dissolved organic matters.

2.14.4.2 Lipid-to-hydrocarbon (LTH) technology

The lipid-to-hydrocarbon technology (LTH) is a patented biofuel production technique developed in Dr. Bressler's laboratory. LTH involves the use of two thermal processes to hydrolyze and pyrolyze lipids from different sources in a reactor. The first thermal process is hydrolysis that liberates fatty acids from the glycerol backbone of glycerides to produce free fatty acids, which are recovered using hexane leaving glycerol as a by-product (Figure 2.10). The second thermal process is pyrolysis in a second reactor for the conversion of the recovered fatty acids into renewable hydrocarbons (Asomaning, 2014; Asomaning et al., 2014c; Espinosa-Gonzalez, Asomaning, et al., 2014; Maher et al., 2008). Outstanding features of this process are that it saves time in the sense that oleaginous slurry can be used directly circumventing the costs of dewatering (drying) (Asomaning et al., 2014c; Espinosa-Gonzalez, Asomaning, et al., 2014; Maher et al., 2008). The application of LTH and other hydrothermal conversion techniques for whole biomass processing is geared toward the production of liquid product fraction which is drop-in-fuels (renewable hydrocarbons). The glycerol waste from pyrolysis was valorized when it was a carbon source for oleaginous yeast cultivation (Espinosa-Gonzalez, Parashar, Chae, et al., 2014)

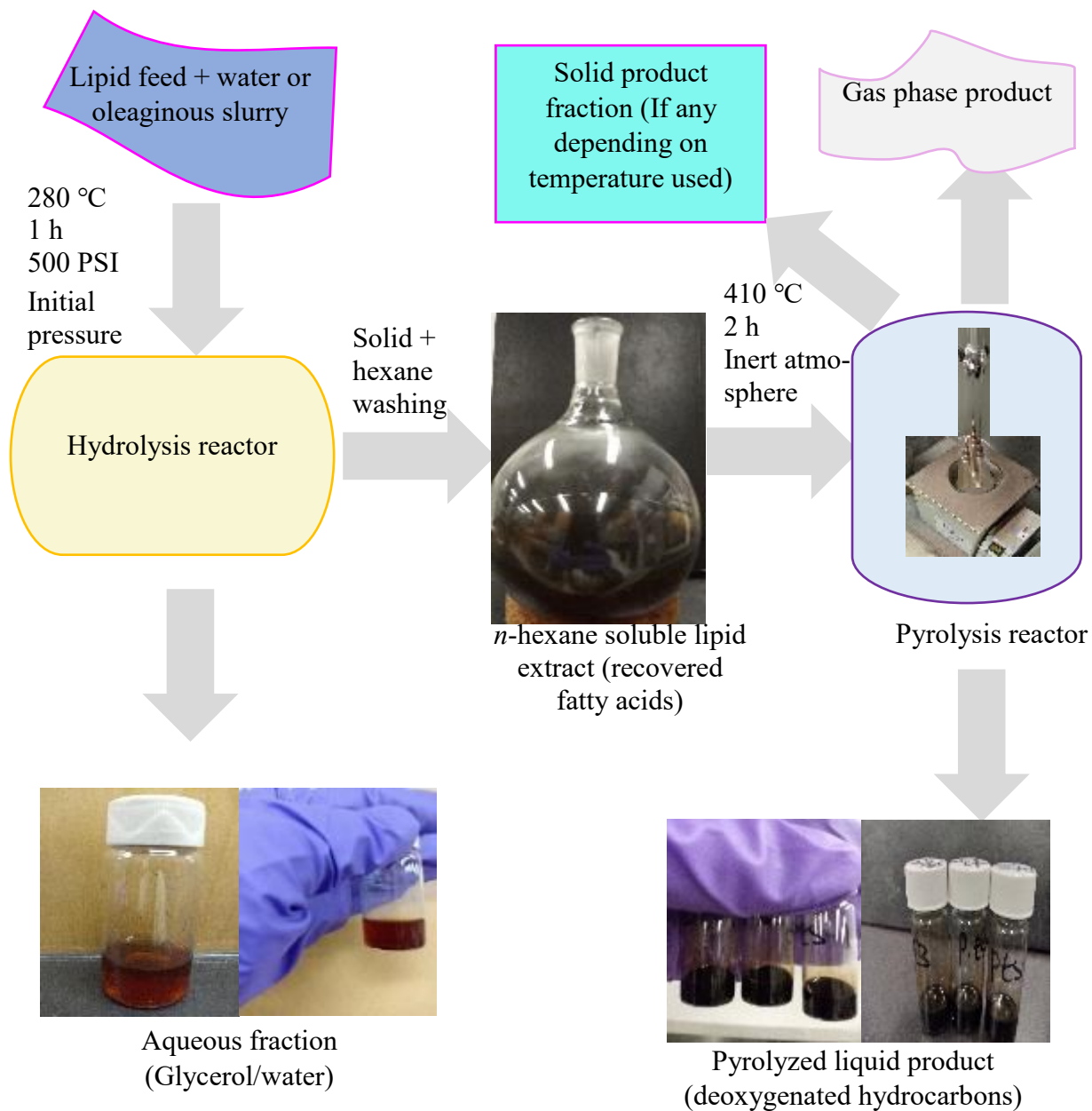


Figure 2.10 Lipid to hydrocarbon (LTH) process.

Chapter 3

3 Materials and methods

3.1 Materials

The yeasts *Pseudozyma hubeiensis* IPMI-10 (JCM 24585) and *Cystobasidium iriomotense* ISM28-8s^T (JCM 24594) were obtained from the Japan Collection of Microorganisms (JCM). *Pseudozyma tsukubaensis* (Onishi) Boekhout (ATCC 24555) was obtained from the American Type Culture Collection center (ATCC) (Manassas, VA). Glycerol stocks (25%) of *P. hubeiensis* IPMI-10, *C. iriomotense*, and *Pseudozyma tsukubaensis* were made for their long-term storage, which was then kept at -80°C. For short-term storage, the yeasts were streaked on yeast extract peptone dextrose (YEPD) agar plates, incubated at 30 °C for 3 days, then stored in a 4 °C fridge. A single colony from the short-term agar plate stocks was used for the cultivation experiments. Fresh YEPD agar plates were streaked with the glycerol stock every 3-4 weeks. Chemicals used in growth medium were purchased from Sigma-Aldrich (St. Louis, MO) and include magnesium sulfate heptahydrate (MgSO₄•7H₂O; 0.25 g/L), calcium chloride (CaCl₂; 0.15 g/L), biotin (C₁₀H₁₆N₂O₃S; 1 mg/L), thiamin (C₁₂H₁₇N₄OS⁺; 1 mg/L), sodium phosphate dibasic (anhydrous) (Na₂PO₄; 75.2 g/L), potassium phosphate monobasic (KH₂PO₄; 30 g/L), sodium chloride (NaCl; 5 g/L), ammonium chloride (NH₄Cl; 5 g/L), NaOH, ethylenediaminetetraacetic acid (EDTA; 5 g/L), iron (III) chloride hexahydrate (FeCl₃•6H₂O; 0.83 g/L), zinc chloride (ZnCl₂; 84 mg/L), manganese (II) chloride tetrahydrate (MnCl₂•4H₂O; 1.6 mg/L), copper (II) chloride dihydrate (CuCl₂•2H₂O; 13 mg/L), cobalt (II) chloride dihydrate (CoCl₂•2H₂O; 10 mg/L), boric acid (H₂BO₃; 10 mg/L). Triolein, diolein, monoolein, and oleic acid were used as model fatty acids, purchased from Thermo Fisher Scientific (Mississauga, ON) and Sigma-Aldrich (St. Louis, MO).

Glucose and xylose sugars were purchased from Sigma-Aldrich (St. Louis, MO). Chloramphenicol and ethanol were sourced from Sigma-Aldrich (St. Louis, MO). Sulfuric acid and hexane (HPLC grade) were obtained from Fisher Scientific (Fairlawn, NJ) and nitrogen (99.998%) was obtained from Praxair (Mississauga, ON). Fatty Acid Methyl Esters (FAME) were from the Nu-chek Prep (MN, USA) FAME standards Mixture GLC 483.

3.2 Methods

3.2.1 Yeast biomass production

3.2.1.1 Medium preparation

M9 mineral medium was prepared using seven stock solutions and sterilized water (867 ml). The seven stock solutions were: M9 mineral salt solution (100 ml/L), glucose and xylose (carbon sources) stock solution (equimolar amount of 15 g/L respectively), $\text{MgSO}_4 \cdot 7\text{H}_2\text{O}$ stock solution (1 ml/L), CaCl_2 stock solution (0.3 ml/L), biotin stock solution (1 ml/L), thiamine stock solution (1 ml/L), and trace mineral stock solution (10 ml/L). The preparation of these stock solutions is described below.

M9 salt stock solution was made by dissolving sodium phosphate dibasic (anhydrous) (Na_2PO_4 ; 75.2 g/L), potassium phosphate monobasic (KH_2PO_4 ; 30 g/L), sodium chloride (NaCl ; 5 g/L), and ammonium chloride (NH_4Cl ; 5 g/L) in Milli-Q water (800 ml). Then, the pH of the M9 salt solution was adjusted to 7.2 with NaOH and the final volume was brought up to 1 L with Milli-Q water before autoclaving at 121°C for 15 min. Glucose or xylose stock solutions were made by adding 15 g of each sugar in 70 ml Milli-Q water or an equimolar amount (15 g each) of both sugars in 140 mL Milli-Q water. The carbon sources solutions were autoclaved for 15 min at 121°C. The $\text{MgSO}_4 \cdot 7\text{H}_2\text{O}$ stock solution was prepared by dissolving 24.65 g in 87 mL of Milli-

Q water to make a 100 mL stock solution before autoclaving for 15 min at 121°C. The 100 mL stock solution of $\text{CaCl}_2 \cdot 2\text{H}_2\text{O}$ was prepared by dissolving 14.70 g in 94.5 mL Milli-Q water. The stock solution was autoclaved at 121°C for 15 min. The biotin stock solution was prepared by dissolving 50 mg of biotin in 45 mL Milli-Q water. Small aliquots of 1 N NaOH were added until biotin was completely dissolved and the final volume was brought up to 50 mL. The biotin stock solution was filter-sterilized through a 0.22 μm filter. Aliquots of 1 mL were prepared and stored at -20°C. The thiamin-HCl stock solution was prepared by dissolving 50 mg of thiamin-HCl in 45 mL of Milli-Q water, then brought up to 50 mL. This solution was sterilized through a 0.22 μm filter and stored at -20°C.

The trace elements solution was prepared by first dissolving ethylenediaminetetraacetic acid (EDTA; 5 g/L) in 800 mL Milli-Q water and then the pH was adjusted to 7.5 with NaOH. The following chemicals were then added to the EDTA solution: iron (III) chloride hexahydrate ($\text{FeCl}_3 \cdot 6\text{H}_2\text{O}$; 0.83 g/L), zinc chloride (ZnCl_2 ; 84 mg/L), manganese (II) chloride tetrahydrate ($\text{MnCl}_2 \cdot 4\text{H}_2\text{O}$; 1.6 mg/L), copper (II) chloride dihydrate ($\text{CuCl}_2 \cdot 2\text{H}_2\text{O}$; 13 mg/L), cobalt (II) chloride dihydrate ($\text{CoCl}_2 \cdot 2\text{H}_2\text{O}$; 10 mg/L), and boric acid (H_2BO_3 ; 10 mg/L). The volume was brought up to 1 L with Milli-Q water. The trace mineral solution was filter-sterilized through a 0.22 μm filter instead of autoclaving to prevent heat denaturation of heat-sensitive trace minerals and precipitation of trace metals. The chloramphenicol solution was prepared by adding 50 mg to 2 mL of 99% ethanol, followed by vortexing for 30 seconds, and in addition to the sterilizing 1 L of M9 mineral medium.

Milli-Q water (1 L) was sterilized for 30 min at 121°C and was allowed to cool down to room temperature (20-22 °C) in the biosafety cabinet before being used for medium production. The sterilized Milli-Q water was used for M9 mineral production throughout the whole

experiments when the sterilized Milli-Q water was no longer hot (at times left overnight at room temperature or kept in 4 °C fridges to be used the following day) to avoid the production of cloudy M9 mineral medium when calcium chloride was added. We observed that the addition of calcium chloride when the sterilized Milli-Q water was still hot resulted in precipitation formation and/or cloudy (unclear) M9 mineral medium. M9 mineral medium was prepared by adding 100 mL of M9 mineral salt stock solution to 867 mL of sterile water (Milli-Q water), followed by the addition of the equimolar of glucose and xylose stock solutions (15 g/L each), 1 mL MgSO₄•7H₂O stock solution, 1 mL biotin stock solution, 1 mL thiamine stock solution, and 10 mL of the trace mineral stock solution. These were thoroughly mixed before the addition of 0.3 mL CaCl₂ stock solution. Then, the chloramphenicol stock solution was added to a final concentration of 50 mg/L. The pH of the medium was adjusted to 6.2 ± 0.2 with 1 M NaOH. The final concentration of the two carbon sources together was 15 g/L each. Ammonium chloride (NH₄Cl) was used as the main nitrogen (N) source at a final concentration of 0.5 g/L (0.01 mol/L) to give a final C: N ratio of 100:1 (nitrogen-limited mixed sugar M9 mineral medium). Ammonium chloride (5 g/L) was one of the components of the M9 salt stock solution prepared and sterilized in the preceding paragraphs. Only 100 mL of the M9 salt stock was used for medium preparation indicating that only 0.5 g/L of ammonium chloride was used as the main nitrogen source. This 0.5 g/L of ammonium chloride used in the M9 mineral medium preparation provided the required 0.01 mol of nitrogen required for this research to create the nitrogen-limited M9 mineral media.

3.2.1.2 Growing the yeast cells

Yeast strains used in this research were first grown on solid yeast extract peptone dextrose (YEPD) agar plates that contained chloramphenicol to prevent bacterial contamination. A volume

of 1 L of yeast extract peptone dextrose agar was prepared by adding 20 g of Bacto™ peptone (Gibco™, Fisher Scientific, Maryland, USA), 10 g of yeast extract from Thermo Fisher Scientific (Mississauga, ON), 20 g of agar (molecular genetics powder) from Thermo Fisher Scientific (Mississauga, ON), and 20 g of dextrose to 1 L of deionized water, and sterilizing at 121°C for 20 min. A mass of 50 mg of chloramphenicol was thoroughly dissolved in 2 ml of 99 % ethanol and then added to the 1 L YEPD to a final concentration of 50 mg/L. The chloramphenicol was added to the sterilized YEPD after cooling and immediately before pouring into Petri dishes (Yarrow, 1998). When the YEPD agar solidified, *P. hubeiensis* IPM1-10, *C. iriomotense* ISM28-8s^T, and *P. tsukubaensis* were streaked on the antibiotic YEPD agar plates and kept at 30°C for 72 h. This streaking process was repeated five consecutive times to ensure that there was no bacterial contamination.

3.2.1.3 Starter culture preparation

The first seed culture was prepared by using one colony of *P. hubeiensis* IPM1-10, *C. iriomotense* ISM28-8s^T, or *P. tsukubaensis* to separately inoculate 15 mL of nitrogen-limited mixed sugar M9 mineral medium in 50 mL Erlenmeyer flasks. The single colony was obtained from agar plates as described in Section 3.1. The inoculated nitrogen-limited mixed sugar M9 mineral medium was cultivated overnight (24 h) at 30°C and 200 RPM shaking. The second seed culture was prepared by inoculating 95 mL of fresh nitrogen-limited mixed sugar M9 mineral medium with 5 mL of the first seed culture in 250 mL Erlenmeyer flasks. The second seed culture was allowed to grow to an OD₆₀₀ of 0.8-1.0 and was then used as a starter culture for subsequent experiments.

3.2.1.4 Shake flask fermentation

P. hubeiensis IPM1-10, *C. iriomotense* ISM28-8s^T, and *P. tsukubaensis* were cultured separately in 500 mL Erlenmeyer flasks with 200 mL nitrogen-limited M9 mineral media as described prepared in section 3.2.1.1. Flasks were inoculated with 5% v/v of the second seed starter culture. Cultures were grown at 30°C with agitation (200 rpm) for a total of 240 h. All experiments were done in triplicate. The cultures were examined under a microscope to assess for contamination.

3.2.1.5 Bioreactor fermentation

P. hubeiensis IPM1-10, *C. iriomotense*, and *P. tsukubaensis* were grown in batch mode, using fully automated 5 L Infors-HT bioreactors (Bottmingen, Switzerland). 3 L of M9 mineral media (section 3.2.1.1) was used to grow separately each of the oleaginous yeasts (Figure 3.1). Bioreactors were inoculated with 5% (v/v) starter culture (second seed culture). The aeration valve was turned on and the stirrer speed was set to 300 rpm to ensure air saturation. The rotameter measuring air-flow rate was kept between 2-3 vessel volumes per minute (vvm).

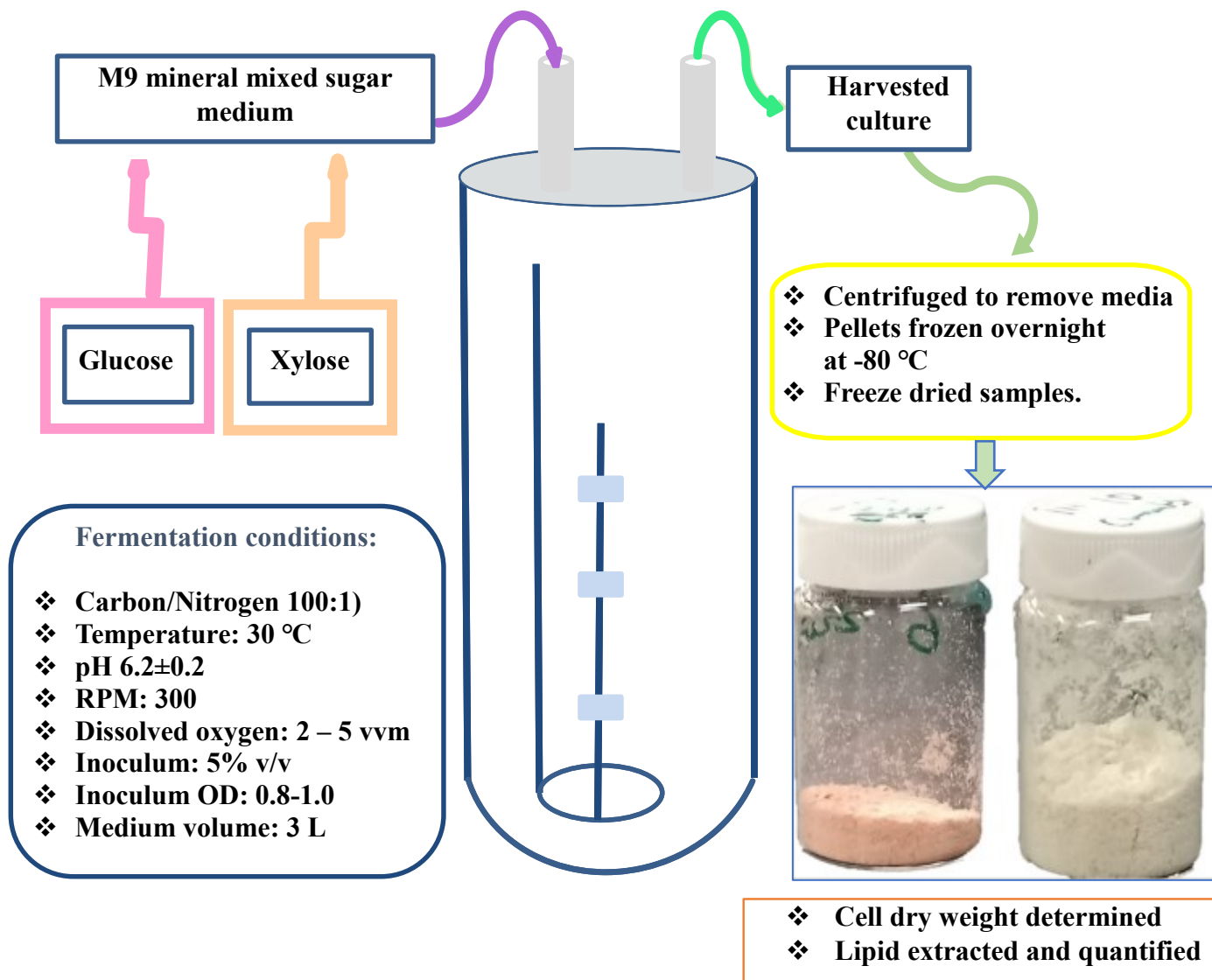


Figure 3.1: Schematic of the fermentation procedure for biofuel production

The dissolved oxygen saturation was set at a maximum value of 100% and a minimum value of 20%. After 72 hours when the dissolved oxygen saturation was shown to be reduced, the rotameter was increased to 5 vvm. Other bioreactor fermentation conditions are as follows: 1. The temperature of the bioreactor was set at 30 °C, with the same temperature entered for both the minimum and maximum setup values; 2. Two-point calibration of the pH probe (pH 4 and pH 7) was performed and the desired pH was set to 6.2 ± 0.2; 3. The stirrer rotation per minute (RPM)

was set to 300 and the same 300 rpm was set as the minimum and maximum values; 4. The base used for pH correction was 1 N NaOH and the base pump was set at 20 seconds with minimum and maximum readings set at 20 seconds as well to pump in the base when the pH dropped. 5. The antifoam used in this research was Silicone antifoam SAF-1397FGK from SILCHEM (ON, Canada) and it was prepared by mixing water and antifoam in 10:1 dilution. The antifoam pump was set at 10 and 5 seconds for the maximum and minimum values, respectively, to detect foam build-up/formation and pump in antifoam to retard the foam formation. These conditions were constant throughout the entire experiments.

Samples to assess OD₆₀₀, lipid content, residual sugar analysis, as well as cell dry weight (CDW) were taken at regular intervals. When samples of the three oleaginous yeasts were harvested, biomass was concentrated using an Avanti® J-26 XP centrifuge (Beckman Coulter centrifuge, Brea, CA) at 5,000 x g for 10 min. The cell pellets were stored in a freezer (-80 °C) until further use. For cell CDW and lipid content determination, the frozen yeast pellets were first lyophilized using a Labconco™ Console FreeZone™ freeze-dryer (MO, USA). All fermentations were done in triplicate. Yeast pellets were thawed, pooled from three batches, and homogenized before hydrolysis reactions to release the free fatty acids from the glycerol backbone for advanced biofuel production. It is important to mention that the oleaginous yeast slurry (frozen pellets) was not freeze-dried before hydrolysis.

3.2.2 Analysis of fermentations

2.2.2.1 Quantification of residual glucose and xylose sugars

Glucose and xylose concentrations were monitored using high-performance liquid chromatography (Agilent technologies 1200 series, CA, USA) with a refractive index detector

(RID), and an Aminex HPX-87H column (Bio-Rad, Richmond, CA, USA). The column oven temperature was set at 60°C and 0.005 M sulfuric acid was employed as the mobile phase with a flow rate of 0.6 mL/min (Espinosa-Gonzalez, Parashar, & Bressler, 2014a; Espinosa-Gonzalez, Parashar, Chae, et al., 2014). Respective sugar standards were used to prepare standard curves. The sugar standards used were 0.1 mg/mL, 0.4 mg/mL, 2 mg/mL, 8.9 mg/mL, 26.8 mg/mL, and 40 mg/mL showing that the range was between 0.1 - 40 mg/mL.

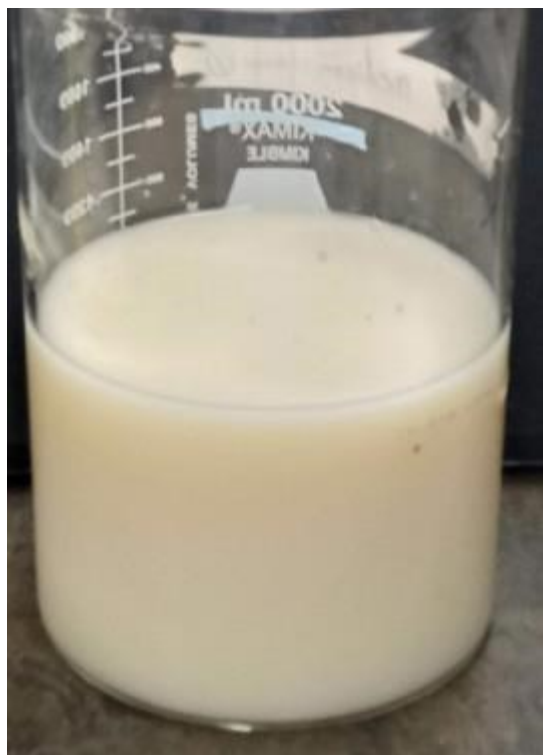
3.2.2.2 Growth

The growth of yeast cultures was assessed using OD(600 nm) readings taken using an Ultrospec 4300 Pro UV/Visible spectrophotometer instrument (Amersham Biosciences, Mississauga, ON, Canada). Measurements were taken in triplicate.

3.2.2.3 Cell dry weight determination

After harvest, 1 L of the oleaginous yeast culture was centrifuged using an Avanti JXN-26 centrifuge (Beckman Coulter, Brea, CA) at 10,000 x g for 10 min (Figure 3.2). The supernatant was separated from the pellets, and the yeast pellets were washed with 0.01 mM sodium phosphate buffer as described by Wang et al., 2020 (J. Wang et al., 2020). The washing was done twice and the supernatant was separated from the pellets. Yeast pellets were centrifuged again at 10,000 x g for 10 min and then freeze-dried for ten days until a constant dried weight was achieved. The supernatant was autoclaved to ensure proper waste disposal. The cell dry weight in g/L was calculated using Equations 3.1. See Equation 3.1 below

$$\text{Cell dry weight (g/L)} = \frac{(\text{weight of the tube and dry sample (g)} - \text{the weight of tube (g)})}{\text{sample volume (L)}}$$



Harvested oleaginous yeast culture

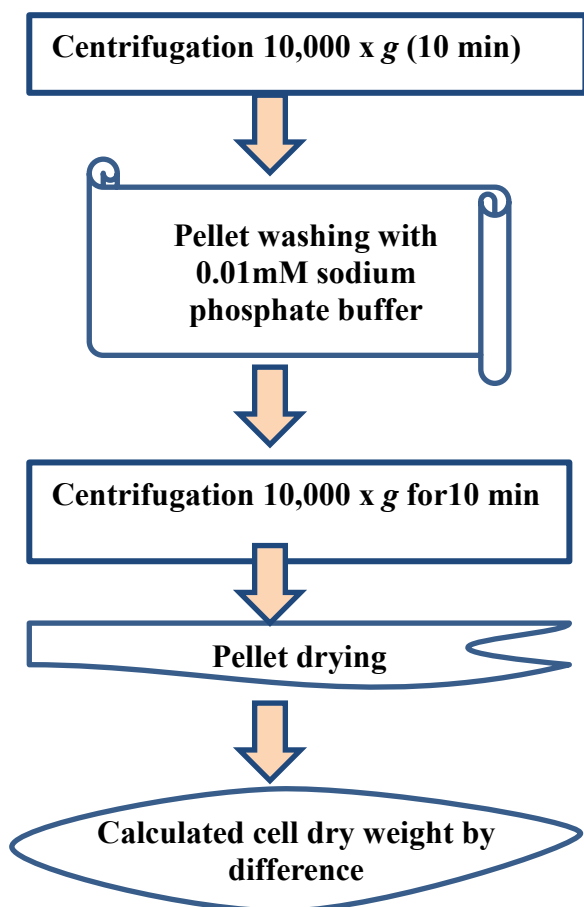


Figure 3.2: Schematic diagram of the cell dry weight determination protocol using *P. hubeiensis* culture

3.2.3 Microbial lipids quantification

Levels of microbial lipids in the freeze-dried samples were determined gravimetrically. First, the freeze-dried yeast biomass was crushed to create more surface area for solvent extraction using a mortar and pestle. The ground yeast powder (Figure 3.3) was added to chloroform: methanol (2:1) mixture according to the method of Folch et al. (Folch et al., 1957), with minor modification. The oleaginous yeast and solvent mixture was incubated in a Fisher Scientific ISOTEMP 228 water bath (ON, Canada) for 1 h at 60 °C. Then, it was centrifuged at 10500 x g for 10 min, followed by 20% water addition. The methanol/water upper phase was removed using a glass pipette. The extraction process was repeated three times. A rotary evaporator (Rotovapor® Büchi, Flawil,

Switzerland) was used for solvent evaporation; the vacuum pressure was stabilized in the range of 200 - 210 millibar and the water bath temperature was set at 50°C. The rotary evaporator was used to concentrate the lipid by solvent evaporation. Residual chloroform in the lipid was removed using gaseous nitrogen in the fume hood.

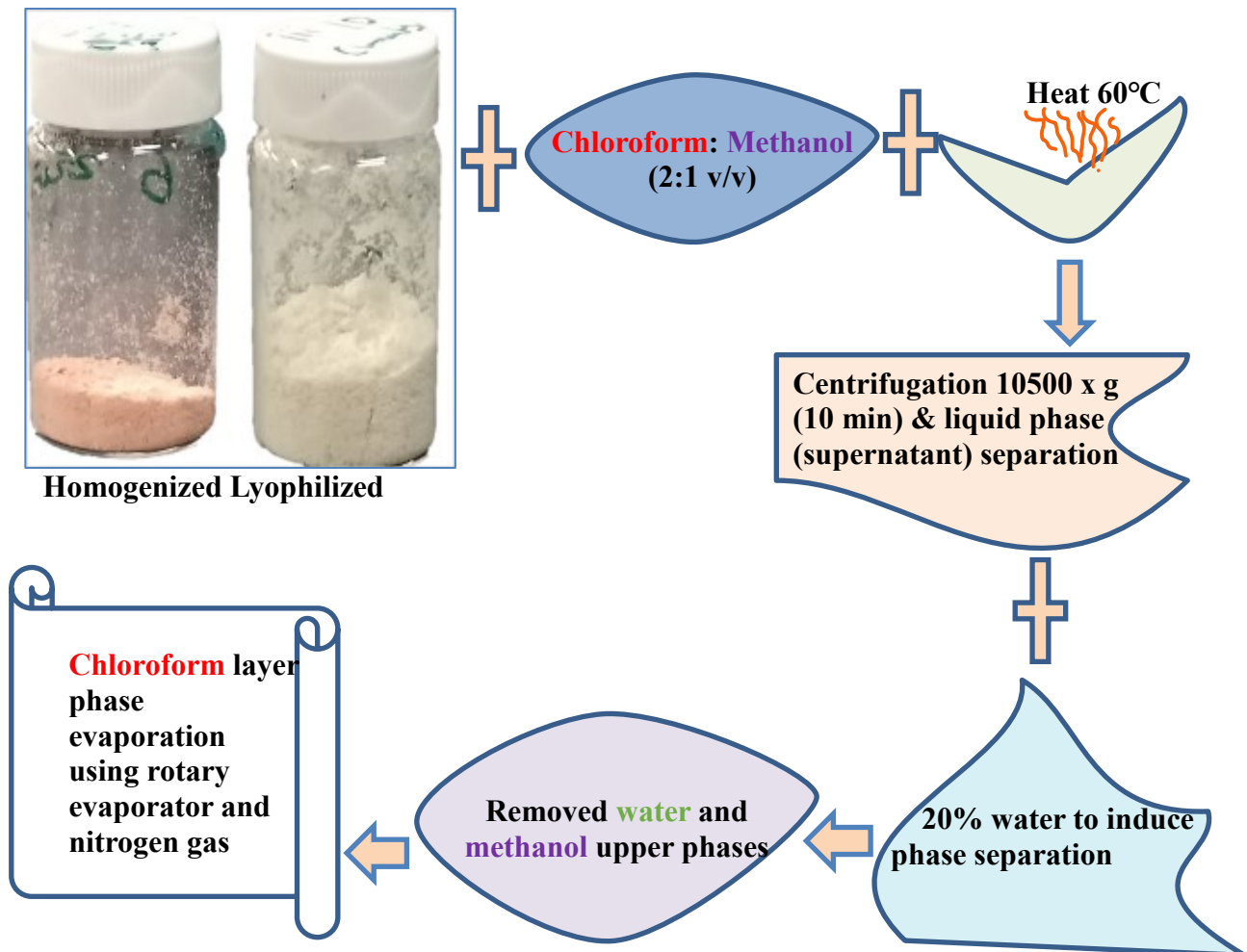


Figure 3.3: Schematic diagram of the lipid extraction procedure in freeze-dried oleaginous yeasts

3.2.4 Fatty acid methyl ester production

The extracted oleaginous lipids (TAG) before hydrolysis was first derivatized to form fatty acid methyl esters (FAME) using 3 N methanolic HCl (Sigma Aldrich, St Louis, MO). Methyl nonadecanoate (C19:0) was used as an internal standard (Figure 3.4). Briefly, 3 mL of the 3 N methanolic HCl was added to 0.1 g of the extracted lipid and the mixture was incubated for 2 h in a water bath at 50 °C with 5-10 second vortexing intermittently (every 30 min). The esterified or derivatized mixture was cooled for 20 min at room temperature before the addition of 100 µL of water, 1 mL of C19:0 internal standard stock solution, and 4 mL of *n*-hexane. This was followed by centrifugation and removal of the *n*-hexane top layer (FAME). The drying of the residual water present in the *n*-hexane soluble fraction was done using a pinch of anhydrous sodium sulfate and another centrifugation before analysis. Fatty acid profile analysis was done using an Agilent 7890 gas chromatography (GC) instrument with an autosampler coupled with a Restek Rt-2560 column (100m x 0.25mm x 2µm) and flame ionization detector (FID) (Saint-Laurent, QC, Canada). The injection temperature was 250°C, and the injection volume was 1 µL. The oven program started with a hold at 80°C for 4 min, ramped to 250°C at 2°C/min, and held for 20 min, for a total run time of 2.5 h. The carrier gas was hydrogen at a constant flow rate of 1.37 mL/min. The GC-FID temperature was kept constant at 250°C. This protocol was also used to derivatize the fatty acids recovered from *n*-hexane solubles after hydrolysis to form fatty acid methyl esters (FAME) and then followed by the quantification using the same GC-FID.

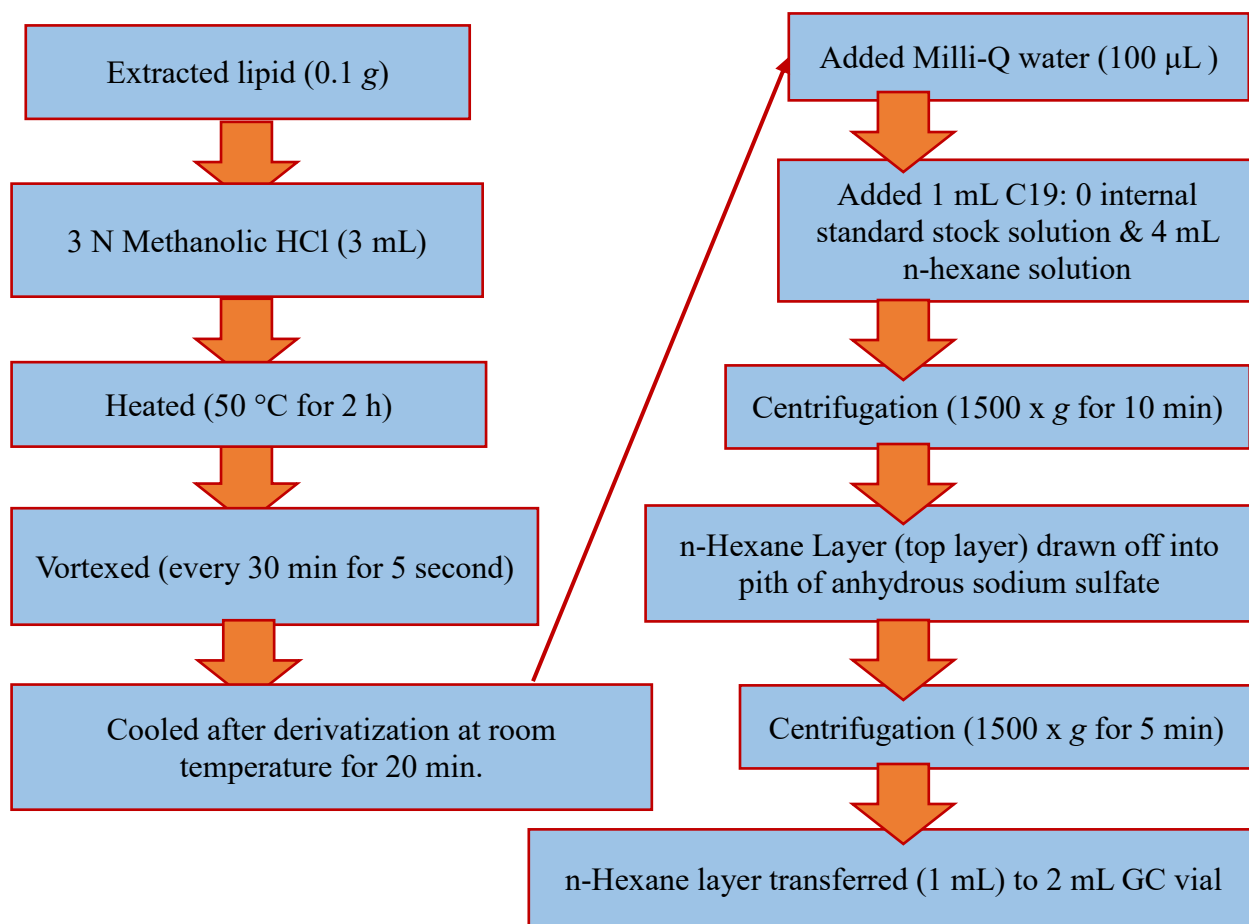


Figure 3.4: Schematic diagram of the derivatization of oleaginous extracted lipids (TAG) to fatty acid methyl esters.

3.2.5 Gram staining

Pure yeast cultures of *P. hubeiensis* IPM1-10, *C. iriomotense* ISM28-8s^T, and *P. tsukubaensis* were separately Gram stained. This was performed as per the instructional manual from the BD Gram stain kit, from Fisher Scientific (Ottawa, ON, Canada). First, the heat-fixed yeast cultures on glass slides were flooded with Gram crystal violet for 1 min and washed with water into a 250 ml beaker. Then, the washed glass slides were overlaid with Gram's iodine mordant for 1 min, and then the slide was flooded with Gram's decolorizing agent for 10-30

seconds before being rinsed with water again. Finally, the cells were counter-stained with 99% Gram's safranin and washed with water again. The glass slides were blot dried and examined under Zeiss Primo Star microscope, Carl Zeiss Canada Ltd (Toronto, ON, Canada).

3.2.6 Hydrolysis

Hydrolysis of oleaginous yeast slurries was carried out in 15 mL and 25 mL reactors to obtain sufficient quantities of hydrolyzed oleaginous yeast biomass required for the determination of product distribution. In this experiment, three 25 mL stainless steel reactors were loaded with 16.2 g of oleaginous yeast slurries (giving a total of 48.6 g of yeast slurry) for one yeast strain at a time. The loaded reactors were purged with nitrogen to achieve the initial pressure of 500 psi and this was done three times for each reactor to ensure a completely inert atmosphere in the reactors. The 15 mL and 25 mL reactors containing yeast slurries were heated in a fluidized sand bath (Techne model SBS-4) equipped with a Techne TC-8D temperature controller (Burlington, NJ) (Asomaning et al., 2014c; Espinosa-Gonzalez, Asomaning, et al., 2014; Espinosa-Gonzalez, Parashar, & Bressler, 2014b; Maher et al., 2008). For hydrolysis, the temperature controller was set at 280°C and the heater was turned on. When the sand bath temperature was at 280°C, the reactors were inserted inside the sand bath and heated for 1 h with an initial pressure of 500 psi as previously described (Asomaning et al., 2014c; Espinosa-Gonzalez, Parashar, & Bressler, 2014b; Maher et al., 2008). The time of the reaction was counted starting from the time the set temperature was reached. At the end of the reactions, the heating was turned off and the reactors were brought out, submerged into cold water cooling unit for 60 seconds, and shaken to remove sand particles on the reactors.

3.2.6.1 Post-hydrolysis treatment

3.2.6.2 Harvesting the products contained in the hydrolyzed reactors

After the hydrolysis reaction was completed, the gas fraction samples were collected from the reactors by releasing the pressure from the reactor into the air sacks. The air sacks were vacuumed and tested for leaks before storing gas samples in them. Other hydrolysis products (i.e. liquid and solid fractions) were collected separately using dry, clean glass containers. Briefly, a Büchner funnel containing a fiber Whatman GF/C filter paper, size 1.2 μm , (Whatman, Maidstone, Kent) was placed into a filter flask fitted with the house vacuum pump and used to initially separate the liquid fraction from the solid fraction. Then, the separated solid fraction was washed with de-ionized water to remove glycerol. Glycerol is completely miscible with water and 5 water washes were performed while the solid fraction was still inside the Buchner funnel attached to the vacuum filtration setup. A subsequent washing was performed using hexane and the filtrates were collected in separate glass containers. Hexane washing was also performed five times. Employing a rotary evaporator, the hexane soluble fractions were recovered after hexane evaporation. The hexane solubles were dried at 105°C for 2 h using a convection oven. The insoluble solid fraction that remained in the Buchner funnel after hexane wash was also dried in a convection oven at 105°C to a constant weight. The washed and dried solid fraction was referred to as insoluble solids. The composition of the gas fraction was analyzed using GC-TCD and GC-FID following the method described by (Asomaning et al., 2014b; Espinosa-Gonzalez, Asomaning, et al., 2014).

3.2.7 Pyrolysis of hexane soluble fraction from oleaginous yeast slurry

Pyrolysis reactions were conducted in 15 mL batch stainless steel microreactors manufactured from $\frac{3}{4}$ inch Swagelok stainless steel tube and fittings (AB, Canada) (Espinosa-

Gonzalez, Parashar, & Bressler, 2014b; Maher et al., 2008; Omidghane et al., 2017, 2020). Briefly, microreactors were properly fixed, fastened, washed with water, and rinsed with distilled water and acetone to ensure that they were completely clean and then dried thoroughly with compressed air. Exactly 1 g of hexane soluble lipids were loaded into clean and dry microreactors. The microreactors were closed, connected to a nitrogen purge system, pressurized to 500 psi, examined for leaks, purged with nitrogen three times and the microreactor valve was then sealed. The microreactor was disconnected from the purge system, attached to the accurate thermal systems rod that holds the microreactor in a vertical position in the pyrolysis chamber, and finally lowered to the center of the sand bath (Techne, Burlington, New Jersey, USA), which was heated at 410°C to start the reaction. The pyrolysis reaction occurred for 2 h under constant agitation. At the end of the pyrolysis, the reaction was stopped by submerging the microreactors immediately in a bucket of water at room temperature. The next step that followed was the cleaning of the microreactor surfaces using compressed air to remove traces of sand on the surface of the microreactor. The reactors were opened in the fume hood for the collection of the gas products fraction formed during the reactions in a gasbag. After venting, the liquid product fraction was collected into a pre-weighed glass vial with a Teflon cap.

3.2.8 Analysis of products

3.2.8.1 Chemical characterization of the hydrocarbon gaseous products

The gas product fraction was analyzed using a PerkinElmer Clarus 690 gas chromatography coupled with a thermal conductivity detector /flame ionization detector (GC-TCD/FID) and a packed column and capillary column, respectively. The GC oven temperature program started at 60°C for 8.5 min and ramped at 10°C/min to 200°C and was then held for 1 min. Gas samples were collected

from the gas bag for analysis by inserting a closed 5 mL glass syringe and needle assembly into the gas bag. The inserted 5-mL vacutainer was opened, gas was drawn, and released three times without bringing the syringe out from the gas bag to ensure a homogeneous gas mixture. The 5 ml vacutainer was then filled with 5 ml of the gas sample and injected into the gas analyzer manually for a complete analysis of the gases.

3.2.8.2 Chemical characterization of the hydrocarbon liquid products

The characterization of the hydrocarbon liquid products was done using gas chromatography with mass spectrophotometry and flame ionization detectors (GC-MS/FID) for proper peak identification and peak quantitation, respectively. The method used for the preparation of the liquid product for analysis is a new in-house optimized method in Dr. Bressler's laboratory (not published yet). Briefly, 200 μL of the pyrolyzed liquid fraction was weighed into a glass vial that contained 5 μL of carbon disulfide solvent (CS_2) and 3 mg of methyl nonadecanoate as the internal standard. The entire mixture was vortexed and transferred to a micro insert in a GC vial. The analysis was done using a PerkinElmer Clarus 690 GC with autosampler coupled with a PerkinElmer Clarus SQ 8 T EI/CI MS instrument operated in electron ionization (EI) mode. The injection temperature was 300°C, and the injection volume was 1 μl in the split mode of 1:10. Two capillary columns were used in series for the analysis, the first one being an Agilent DB-35ms column (30 m X 0.53 mm X 0.50 μm , Agilent Technologies, Santa Clara, CA, USA), followed by a Restek Stabilwax-DA column (14 m X 0.53 mm X 0.5 μm , Restek Corporation, Centre County, PA, USA). A PerkinElmer S-Swafer micro-channel flow splitting device was used at the end of the capillary column to split the flow to the FID and MS detectors. The oven program started with a 5 min hold at 40°C, ramped to 192°C at 8°C/min, then ramped to 250°C at 10°C/min, and held for 20.2 min, for a total run time

of 50 min. The carrier gas was helium at a constant flow rate of 8 mL/min. The analysis was operated independently but the detectors use the same sample at the same time. The gas chromatography (GC) - mass spectrometry detector (MSD) transfer line was at a temperature of 300°C, the MS source was at 230°C, and MSD was scanned from 35 to 550 m/z. The GC-FID temperature was kept constant at 300°C.

3.2.8.3 Lipids profile analysis

Qualitative analysis of lipid classes was performed using thin layer chromatography Whatman polyester silica plate (Maidstone, Kent) with standards of triolein, diolein, monoolein, and oleic acid in hexane and hexane:ether:acetic acid (80:20:1) as the mobile phase (Espinosa-Gonzalez, Parashar, & Bressler, 2014a; Gonzalez, 2014). Hexane soluble lipid classes were determined using the thin-layer chromatography (TLC) method on a Whatman polyester silica plate (Figure 3:5). The silica gel coated on the rigid plastic (polyester) was the stationary phase. After the mixture of the solvent (mobile phase) was poured into the TLC transparent vessel, the samples were applied on the stationary phase (polyester silica plate) and they were placed inside the TLC vessel with the mobile phase. The samples were drawn up the top of the plate (solvent front) utilizing capillary action and were separated at different points on the solid adsorbent coated on the plastic stationary support (polyester silica plate) based on the affinity of the samples with the mobile and stationary phases. The more the affinity of the sample, the lesser the distance it can travel and the more it adheres to the adsorbent. The higher the distance the sample travels on the stationary phase, the lower the affinity. The traveled sample spots were made visible by blowing the stationary phase with warm air from electric hand dryer for 30 minutes until the spots were clearly visible.

To determine the total fatty acid profile in both the freeze-dried yeast biomass slurry and hexane extracts, the lipids were first derivatized by esterification with 3 N methanolic HCl (Sigma-Aldrich, St. Louis, MO) following the manufacturer's instructions. Nonadecanoic acid methyl ester was an internal standard to compensate for the variabilities or losses that may be encountered in the preparation and analysis of the sample. Then, the derivatized samples were analyzed using GC-FID/MS (Agilent 7890 GC with 5975C MSD). Quantification of the fatty acid was done using a 100 m X 0.25 mm X 0.20 μ m Restek Rt-2560 column (Saint-Laurent, QC, Canada). The beginning injection temperature was 80°C, held for 4 mins, ramped to 250°C at 2°C/min, and held over 20 min. The injection flow rate was 1.37 mL/min. The carrier gas was hydrogen. To identify the products, their retention times were compared to the retention times of FAME from the Nu-chek Prep (MN, USA) FAME standards Mixture GLC 483. The Nonadecanoic acid methyl ester was used for calibration by plotting the ratio of the derivatized sample FAME signal to the internal standard signal as a function of the sample concentration of the standards. The ratio of the samples was used to get the concentration of the sample FAME from the calibration curve. Also, the identified FAMES were confirmed via further identification by comparing the electron ionization (EI) mass spectra in GC-MS to the National Institute of Standards and Technology (NIST) database. For product quantification, the peak areas of the products were compared to the area of the internal standard (C19:0). Fourier-transform infrared (FTIR) spectroscopy in conjunction with attenuated total reflectance (ATR) with diamond-Zinc-Selenide crystals apparatus, (Universal ATR FT-IR Frontier, PerkinElmer; MA, USA) was used to analyze the hexane soluble fractions. The wavenumbers were expressed in cm^{-1} in the range of 4000-650 cm^{-1} with a scan number of 8.

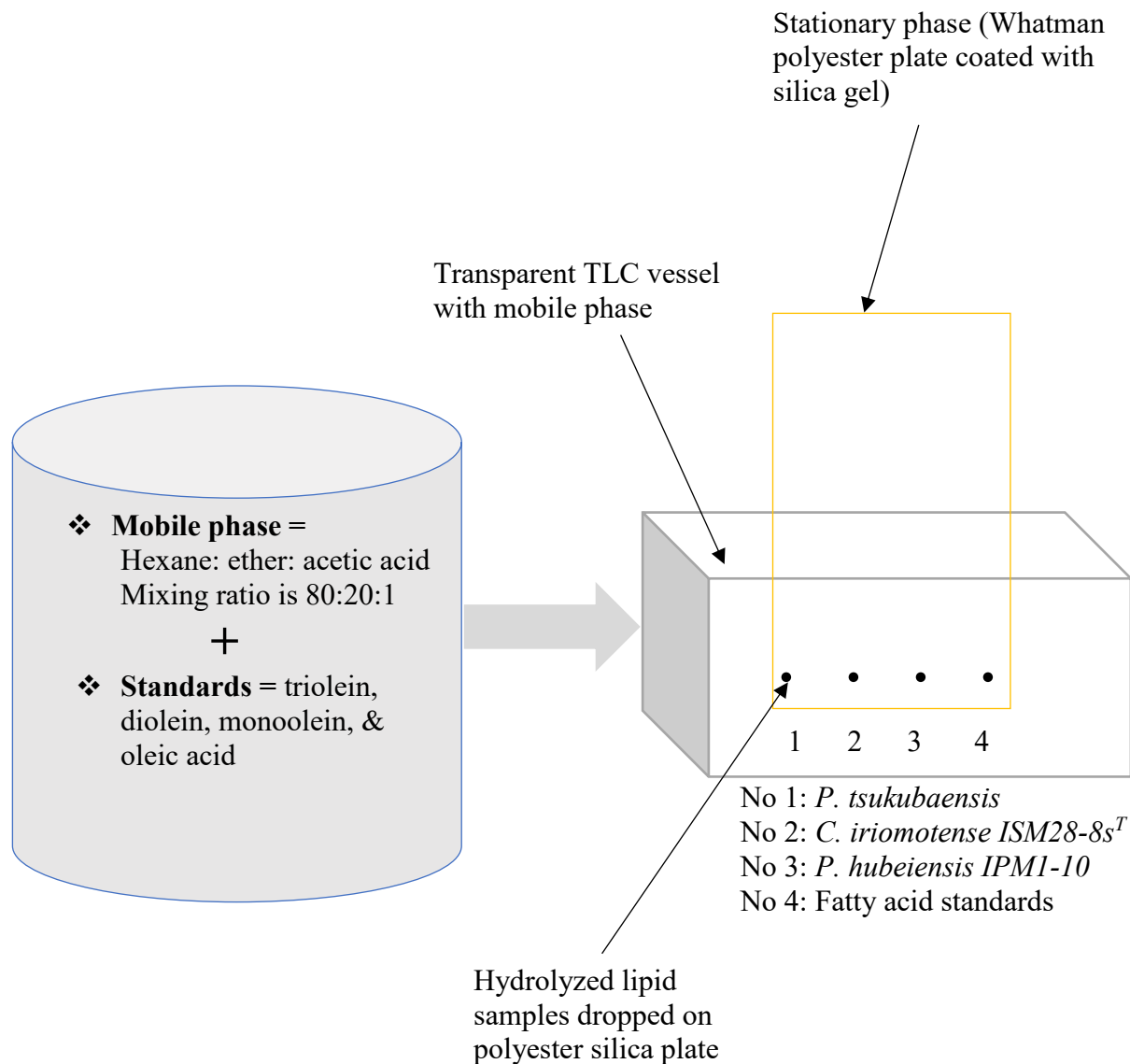


Figure 3.5: Schematic of thin-layer chromatography

3.2.9 Statistical analysis

Statistical analysis was conducted using analysis of variance (ANOVA) with Tukey post hoc test at a 95 % confidence level using Statgraphics centurion XVI version statistical software (Statgraphics Technologies, Inc., Virginia, USA).

Chapter 4

4 Results and Discussion

4.1 Gram-stained oleaginous yeast strains

To ensure that pure strains were being used for subsequent experiments, a single colony of *Pseudozyma hubeiensis* IPM1-10, *Cystobasidium iriomotense*, and *Pseudozyma tsukubaensis* from separate yeast extract peptone dextrose agar plates containing 50 mg chloramphenicol were grown individually in nitrogen-limited M9 mineral medium. The overnight culture of each organism was then Gram-stained and visualized using a Zeiss Primo Star microscope. The photomicrographs of the yeasts are shown in Figures 4.1, 4.2, and 4.3 for *Pseudozyma hubeiensis* IPM1-10, *Pseudozyma tsukubaensis*, and *C. iriomotense* ISM28-8s^T, respectively. One remarkable feature regarding the morphology of the three oleaginous yeasts grown in the limiting nitrogen medium is the cell elongation pattern observed, which is also known as pseudohyphal growth. This observed cell elongation pattern has also been reported to occur in *S. cerevisiae* during nitrogen starvation (Gancedo, 2001; Henrici, 1914).

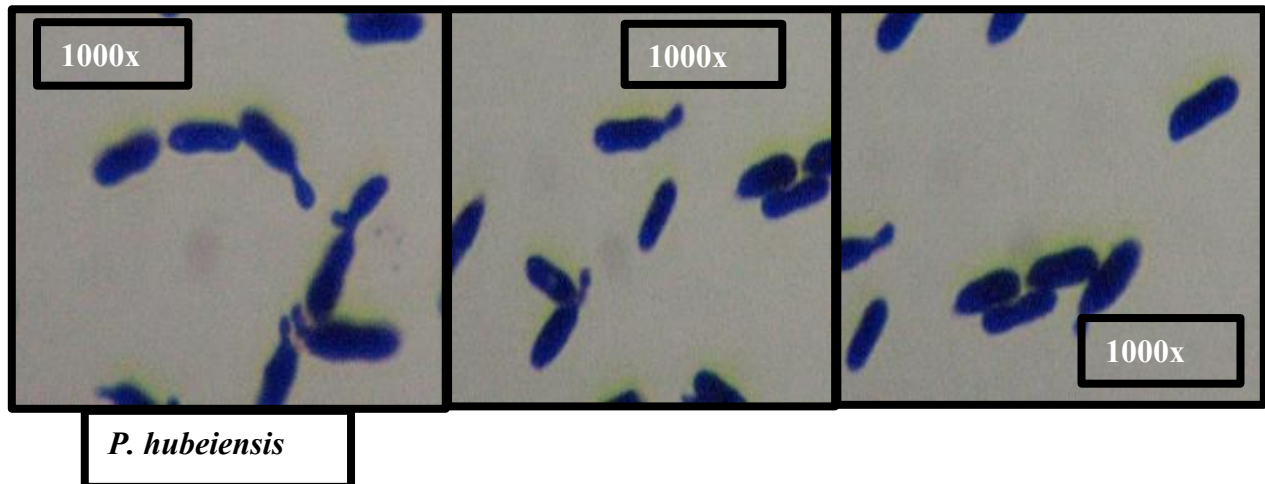


Figure 4.1: Micrographs of Gram-stained *P. hubeiensis* IPM1-10

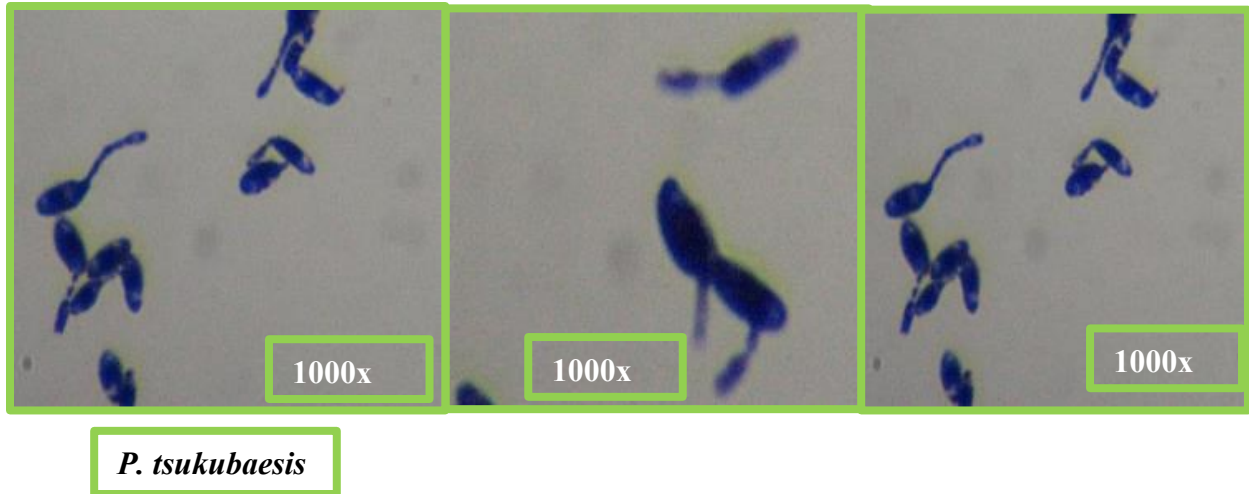


Figure 4.2: Micrographs of Gram-stained *P. tsukubaensis*

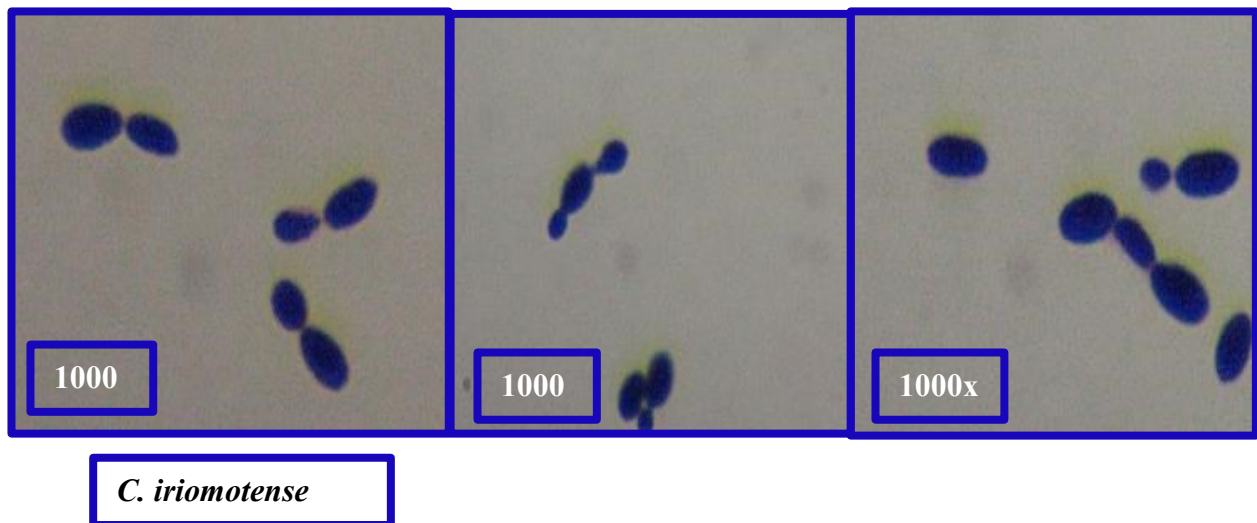


Figure 4.3: Micrographs of Gram-stained *C. iriomotense* ISM28-8s^T

4.2. Characterization of oleaginous organisms grown in shake flasks

4.2.1 Growth of *P. hubeiensis* in 500 mL shake flasks

Cultivation of *P. hubeiensis* IPM1-10 was carried out using a phosphate-buffered M9 mineral medium amended with equimolar amounts of glucose and xylose (15 g/L each) and 0.5

g/L ammonium chloride to give a final C: N ratio of 100:1. Then, the flasks were inoculated and incubated as indicated in section 3.2.1.3. The growth of *P. hubeiensis* IPM1-10 over time (Figure 4.4) and the sugar depletion pattern (Figure 4.5) were monitored for a period of 240 h. The OD₆₀₀ of the *P. hubeiensis* IPM1-10 cultures in shake flasks reached ~29. The growth curve had three phases: the lag phase, exponential phase, and stationary phase (Figure 4.4). The lag phase was observed within the first 8 h, with the exponential phase being more pronounced between 24 h – 144 h, after which the onset into the stationary phase was observed at 168 h. A diauxic growth pattern (multiple growth phases) was not seen in the growth curve of *P. hubeiensis* IPM1-10 when grown in a medium containing both glucose and xylose, indicating that glucose repression did not occur in *P. hubeiensis* IPM1-10. This was confirmed by the sugar consumption pattern observed in the culture (Figure 4.5). These data are in agreement with previous reports that *P. hubeiensis* can simultaneously utilize C5 and C6 sugars (Adsul et al., 2009; Digambar Gokhale, 2018; A Tanimura et al., 2016).

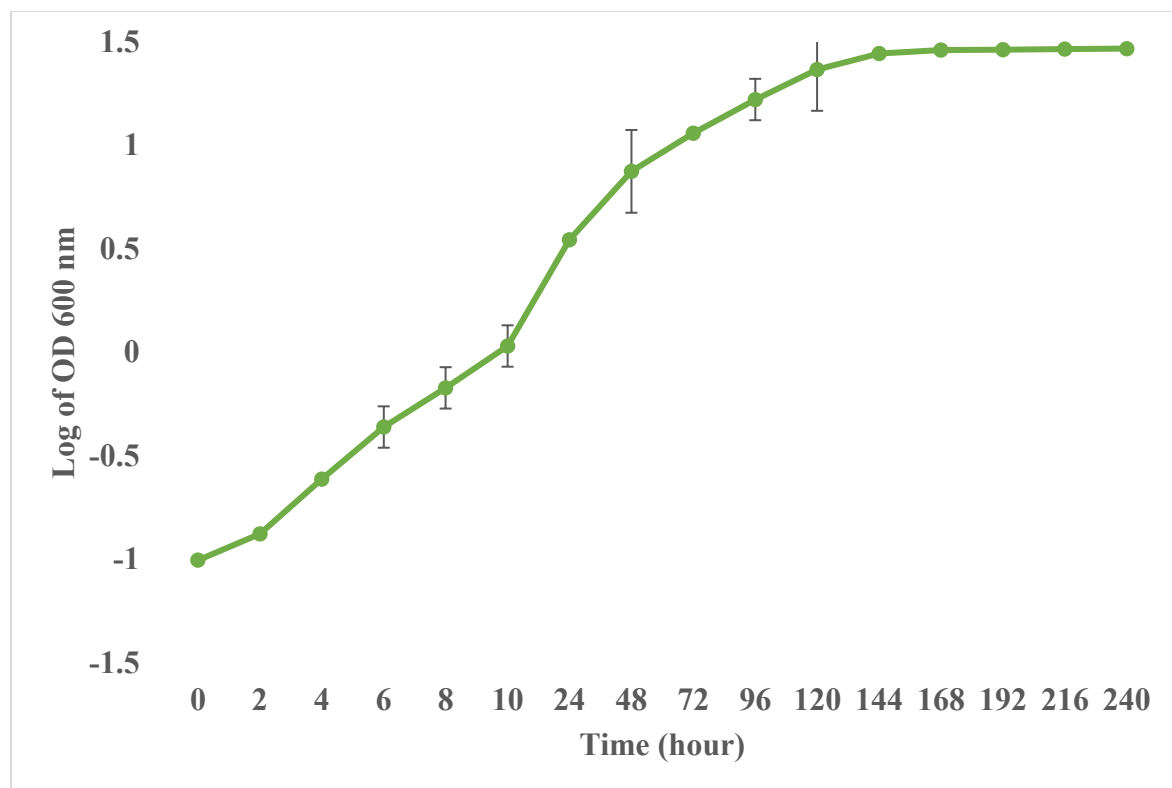


Figure 4.4: Growth curve for *P. hubeiensis* IPM1-10 in 500 mL Erlenmeyer shake flasks for 240 h using glucose and xylose as the carbon sources at a final concentration of 30 g/L (15 g/L each) and ammonium chloride at 0.5 g/L. The carbon to nitrogen ratio for these studies was 100:1. Data are presented as the means \pm standard deviation (error bars) of triplicate experiments.

4.2.2. Time course of sugar consumption by *P. hubeiensis* IPM1-10

As shown in Figure 4.5, *P. hubeiensis* IPM1-10 simultaneously utilized both sugars. Glucose present in the medium was completely consumed by 192 h while consumption of xylose was completed by 240 h (Figure 4.5). The lack of residual sugars in the shake flask experiments with *P. hubeiensis* IPM1-10 in this present study is not in agreement with the previous report by Tanimura et al., (2016), who cultivated *P. hubeiensis* IPM1-10 for 10 days in a 100 mL mixed sugar medium that contained three carbon sources (glucose 20 g/L, xylose 10 g/L, and arabinose

5 g/L) and two nitrogen sources (ammonium sulfate 1g/L and yeast extract 0.5 g/L) using shake flask (Ayumi Tanimura et al., 2016). This previous study had a higher amount of nitrogen relative to carbon when compared to the present study, and as a result, may have created a sense of satiety and comfortability to the organisms (stress-free environment), hence, the carbon sources became unused completely at the end of 240 hours. Also, there may be a possibility of a pH drop in the shake flask previous study by Tanimura *et al.*, 2016 (though not reported in the paper) to the point that further metabolism was not possible. Furthermore, the complete carbon utilization seen in this present study with *P. hubeiensis* IPM1-10 may have to do with the nitrogen source used in the research because Gobert et al., (2017) and Roca-Mesa et al., (2020) reported that that nitrogen sources affected non-*Saccharomyces* yeasts carbon metabolism, growth, and performance during winemaking. Since non-conventional yeasts are nitrogen source consumption specific (nitrogen source preferential) (Gobert et al., 2017; Roca-Mesa et al., 2020), then it is reasonable to deduce that possibly, the yeast extract made a difference in nitrogen in the present and previous studies may have contributed to the lack of residual carbon observed in this present study. Ideally, this should promote complete carbon utilization as it is nutrient-rich.

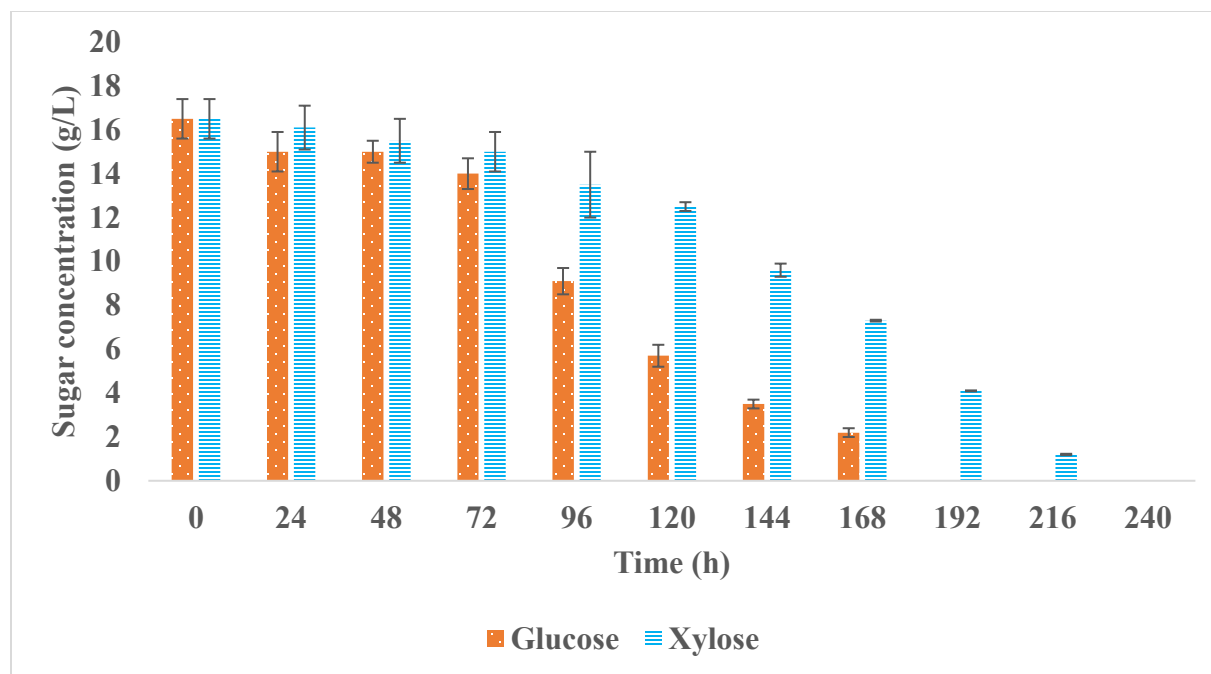


Figure 4.5: A time course of sugar consumption by *P. hubeiensis* IPM1-10 in 500 mL Erlenmeyer shake flasks for 240 h using glucose and xylose as the carbon sources at a final concentration of 30 g/L (15 g/L each) and ammonium chloride at 0.5 g/L. The carbon to nitrogen ratio for these studies was 100:1. Data are presented as the means \pm standard deviation (error bars) of triplicate experiments.

4.2.3 Biomass and lipid accumulation in small-batch shake flask by *P. hubeiensis* IPM1-10

At 120 h of fermentation, the level of the accumulated lipid in *P. hubeiensis* IPM1-10 was determined. This time point was chosen for the lipid accumulation test because previous researchers reported that 5 days of cultivation is the apt time to test for lipid accumulation up to 20% of CDW in yeasts (test for oleaginiccity in yeasts) (Rossi et al., 2009; Thancharoen et al., 2017). Moreover, 120 h is the timepoint in the exponential phase that had the highest OD. The data revealed that the lipid content of *P. hubeiensis* IPM1-10 was 49 ± 1 % on a cell dry weight (CDW)

basis. Thus, *P. hubeiensis* IPM1-10 was confirmed to generate high levels of lipid when grown using a mixture of C5 and C6 sugars. In terms of biomass accumulation, after 240 h, the cells harvested from the shake flask cultures had a cell dry weight of 10 ± 1 g/L.

4.2.4 Growth of *P. tsukubaensis* in 500 mL shake flasks

P. tsukubaensis was cultivated as described for *P. hubeiensis* IPM1-10 in a mixture of 15 g/L glucose and 15 g/L xylose (total of 30 g/L) as the carbon sources in a phosphate-buffered medium at $\text{pH } 6.2 \pm 0.2$ using 500 mL Erlenmeyer flasks. The growth of *P. tsukubaensis* was monitored for a period of 240 h (Figure 4.6). Using a spectrophotometer, the cell growth of *P. tsukubaensis* was measured and the culture reached a maximum OD_{600nm} of 26.9 ± 0.3 . The lag phase (0-10 h) was followed by an intensive sugar consumption phase (log phase) from around 24 to 168 h before the onset of the stationary phase at 192 h.

4.2.5 Time course sugar utilization profile of *P. tsukubaensis*

As shown in Figure 4.7, *P. tsukubaensis* simultaneously utilized both xylose and glucose in the small-scale shake flasks, with complete sugar consumption observed by 168 h and 240 h, respectively. As observed with *P. hubeiensis* IPM1-10, the gradual consumption of both sugars by *P. tsukubaensis* resulted in no residual sugars by the end of the experiment (Figure 4.7). Significantly, there was no preferential assimilation of C6 sugars over C5 sugars by *P. tsukubaensis*, suggesting that *P. tsukubaensis* is naturally endowed with transport system(s) and metabolic pathways for the simultaneous utilization of hexose and pentose sugars.

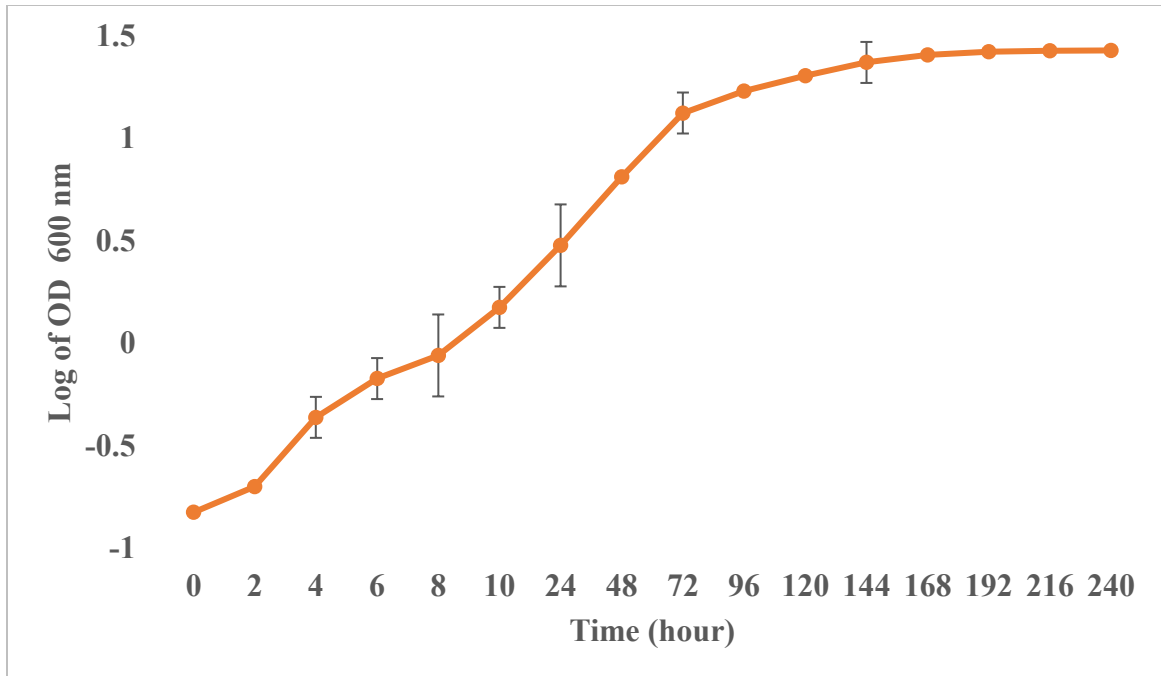


Figure 4.6: Growth curve of *P. tsukubaensis* in 500 mL Erlenmeyer shake flasks over a 240 h period using glucose and xylose as the carbon sources at a final concentration of 30 g/L (15 g/L each) and ammonium chloride at 0.5 g/L. The initial carbon to nitrogen ratio of the medium was 100:1. Data are presented as the means \pm standard deviation (error bars) of triplicate experiments.

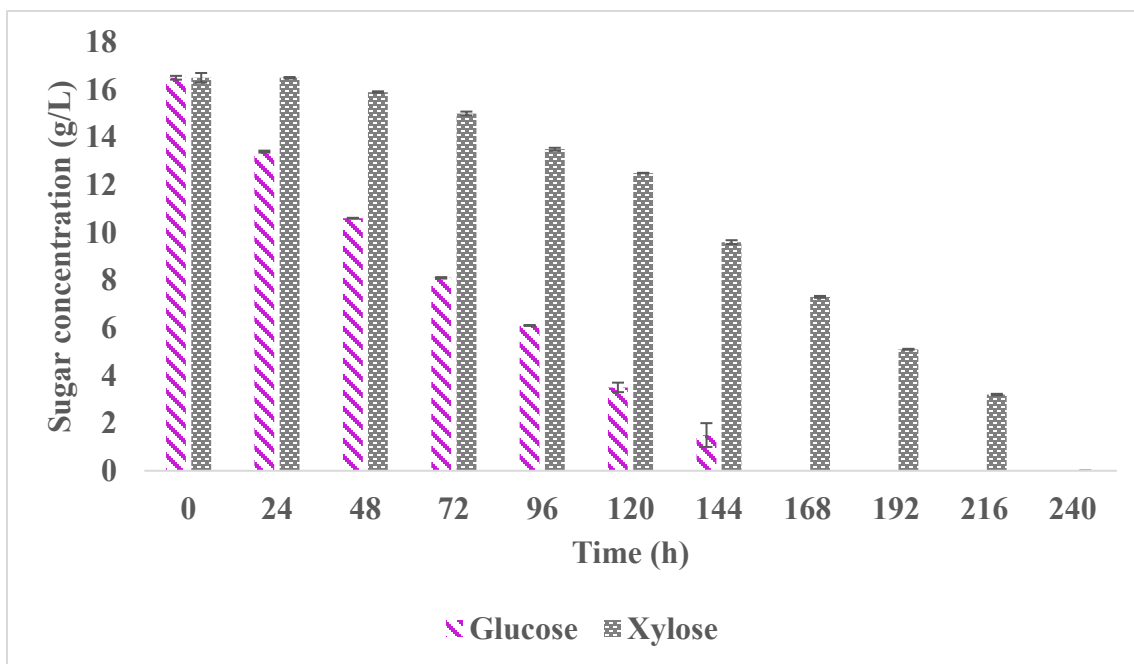


Figure 4.7: The time course sugar consumption profile of *P. tsukubaensis* when grown in 500 mL Erlenmeyer shake flasks for 240 h using glucose (15 g/L) and xylose (15 g/L) as the carbon sources at a final sugar concentration of 30 g/L and ammonium chloride at 0.5 g/L. The initial carbon to nitrogen ratio of the medium was 100:1. Data are presented as the means \pm standard deviation (error bars) of triplicate experiments.

4.2.6 Biomass and lipid accumulation by *P. tsukubaensis*

Similar to what was observed for *P. hubeiensis* IPM1-10, the lipid content observed in samples taken after 120 h of growth reached levels higher than 40% (43 ± 3 %) of cell dry weight, indicating that this organism is indeed oleaginous. While the OD_{600nm} observed for *P. tsukubaensis* after 240 h was similar to that of *P. hubeiensis* IPM1-10, the dry cell weight observed for *P. tsukubaensis* was nearly 50% lower (10 ± 1 g/L vs. 4.5 ± 0 g/L). The high OD with low dry cell weight in *P. tsukubaensis* may be attributed to the impact of the rich deep yellowish cream color of the culture which is different from that of *P. hubeiensis* IPM1-10 whitish cream culture. Also, *P. tsukubaensis* could be releasing different secondary metabolites that may result in OD differences.

4.2.7 Growth curve of *C. iriomotense* ISM28-8s^T in 500 mL shake flasks

C. iriomotense ISM28-8s^T was cultivated in the same manner as described above for *P. hubeiensis* IPM1-10 and *P. tsukubaensis*. While the growth patterns for *P. tsukubaensis* and *P. hubeiensis* IPM1-10 were similar, the growth observed for *C. iriomotense* ISM28-8s^T was quite different (Figure 4.8). A longer lag phase was observed for *C. iriomotense* ISM28-8s^T (i.e. over 24 h), which was in contrast with what was observed in *P. hubeiensis* IPM1-10 and *P. tsukubaensis*.

The log phase of growth was observed from around 48 h to 144 h. At 240 h, an OD₆₀₀ of 4.5 ± 0.2 was achieved by *C. iriomotense* ISM28-8s^T via simultaneous assimilation of glucose and xylose sugars. This was substantially lower than the OD₆₀₀ achieved by *P. tsukubaensis* and *P. hubeiensis* and can likely be explained after considering the sugar utilization data. It is important to mention here that the same medium was used for both the seed cultures and shake flasks for *C. iriomotense* ISM28-8s^T cultivation as well as for *P. tsukubaensis* and *P. hubeiensis* cultivation.

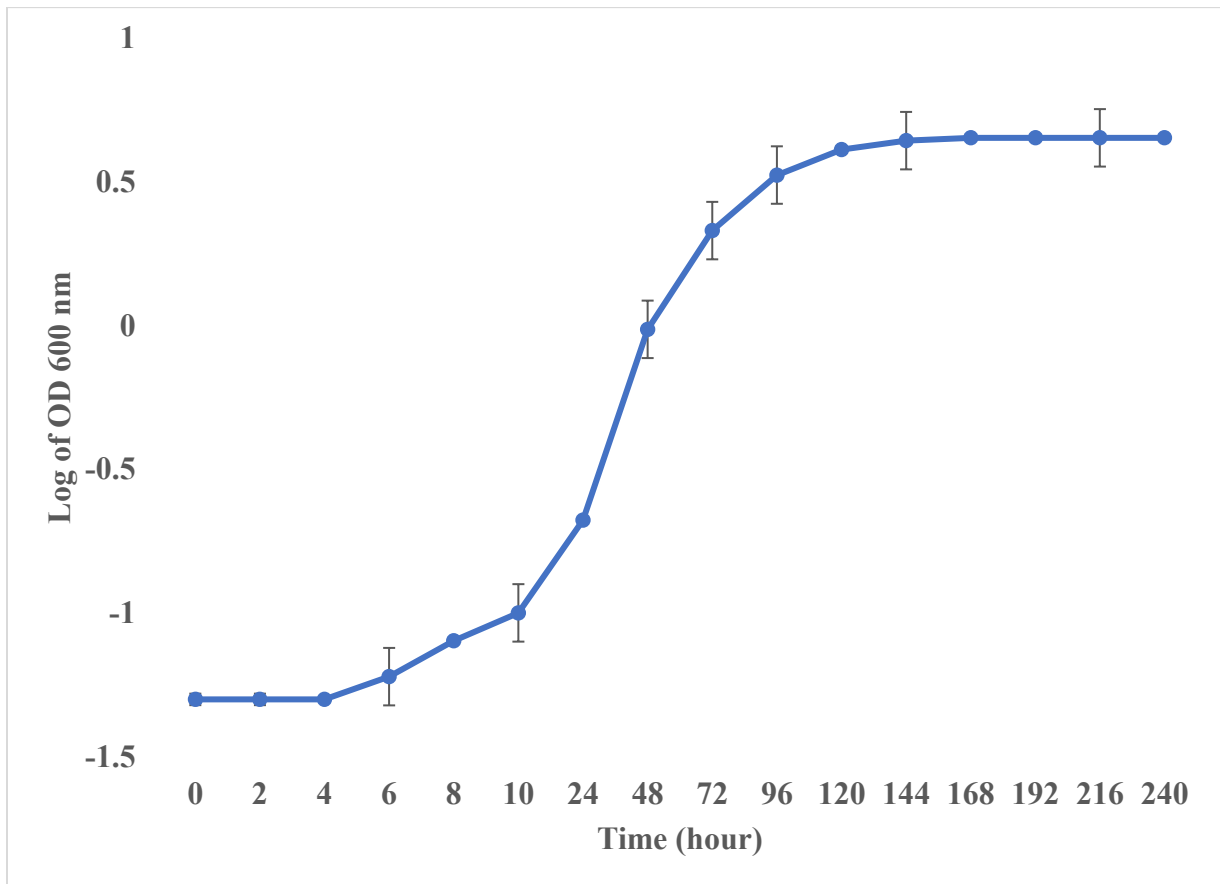


Figure 4.8: Growth curve of *C. iriomotense* ISM28-8s^T when grown in 500 mL Erlenmeyer shake flasks for 240 h using glucose and xylose as the carbon sources at a final concentration of 30 g/L (15 g/L each) and ammonium chloride at 0.5 g/L, achieving a carbon to nitrogen ratio of 100:1. Data are presented as the means \pm standard deviation (error bars) of triplicate experiments.

4.2.8 Time course utilization of glucose and xylose by *C. iriomotense* ISM28-8s^T

The time course profile of C5 and C6 sugar utilization by *C. iriomotense* ISM28-8s^T (Figure 4.9) demonstrated that although simultaneous use of the mixed sugars was observed, the sugar consumption was much slower than that observed for *P. tsukubaensis* and *P. hubeiensis*. In fact, only ~50% of the glucose and xylose sugars in the medium were consumed within the 240 h of this shake flask study. Residual sugar concentrations were 6.5 g/L and 8.5 g/L for xylose and glucose, respectively. Interestingly, *C. iriomotense* ISM28-8s^T utilized slightly more xylose than glucose, suggesting that *C. iriomotense* ISM28-8s^T may prefer using xylose to glucose. Residual sugars were also observed when *C. iriomotense* ISM28-8s^T was cultivated in 10 g/L of xylose and 10 g/L of glucose for a period of ten-day by Tanimura et al., (2018). In that study, 85.3% of the mixed sugars were consumed (Ayumi Tanimura et al., 2018).

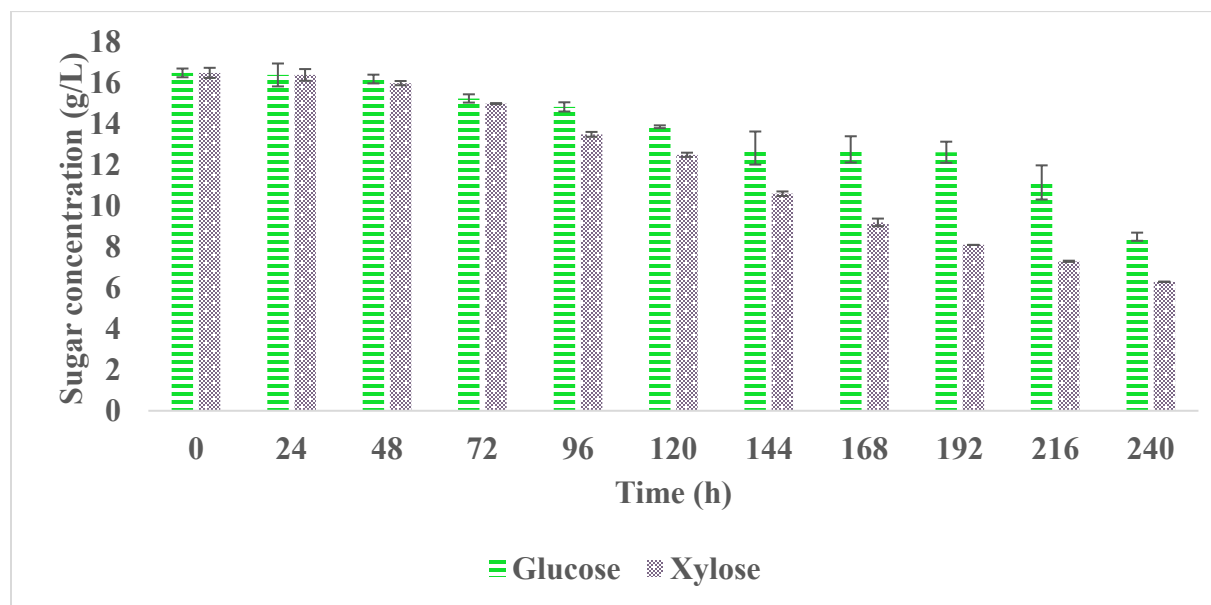


Figure 4.9: Time course sugar consumption profile of *C. iriomotense* ISM28-8s^T in 500 mL

Erlenmeyer shake flasks for 240 h using glucose and xylose as the carbon sources at a final concentration of 30 g/L (15 g/L each) and ammonium chloride at 0.5 g/L, achieving a carbon to

nitrogen ratio of 100:1. Data are presented as the means \pm standard deviation (error bars) of triplicate experiments.

4.2.9 Biomass and lipid accumulation by *C. iriomotense* ISM28-8s^T

The biomass generated from *C. iriomotense* ISM28-8s^T at the point of harvest (i.e. 240 h) was 1.3 ± 0 g/L, with lipid content of 21 ± 5 % on a cell dry weight (CDW) basis. These results were achieved with only 50.7% glucose and xylose consumption. Similarly, Tanimura et al. (2018) previously reported a lipid content (CDW basis) of 21%, through a higher sugar consumption (85.3%). However, those studies were performed using a medium with greater levels of nitrogen (Ayumi Tanimura et al., 2018). Higher sugar consumption and lower lipid accumulation in *C. iriomotense* ISM28-8s^T as observed by the previously reported study is an indication that the consumed sugars were geared toward biomass accumulation but less lipid per cell as a result of the higher nitrogen content relative to carbon their growth medium.

4.2.10 Summary of growth and lipid accumulation of oleaginous yeasts

The cell dry weights and lipid accumulation for *P. tsukubaensis*, *P. hubeiensis* IPM1-10, and *C. iriomotense* ISM28-8s^T are summarized in Table 4.1. Based on all of the data presented above, it is clear that the three oleaginous yeasts used in the shake flask experiments simultaneously utilized C5 and C6 sugars and were able to generate high levels of lipids. However, it is worth noting that *C. iriomotense* ISM28-8s^T could not efficiently utilize the sugars in the medium, resulting in substantial amounts of residual sugar at the point of harvest (240 h). One common characteristic exhibited by *P. tsukubaensis*, *P. hubeiensis* IPM1-10, and *C. iriomotense* ISM28-8s^T was the gradual utilization of glucose and xylose, though the rates at which the sugars

were consumed were specific to each organism.

Table 4.1. The % lipid and cell dry weight generated from shake flask cultivation

Oleaginous Yeast	Cell dry weight (CDW) in g/L at 240 h	% Lipid at 120 h
<i>P. hubeiensis</i> IPM1-10	10 ± 1 ^a	49 ± 1 ^a
<i>P. tsukubaensis</i>	4.5 ± 0 ^b	43 ± 3 ^a
<i>C. iriomotense</i> ISM28-8s ^T	1.3 ± 0 ^c	21 ± 5 ^b

Data used are mean ± standard deviation (error bars) of three assays. Within each column, values denoted with letters a, b, or c is significantly different (P<0.05).

4.3. Characterization of oleaginous organisms grown in 5 L bioreactors

As all three yeast strains demonstrated the ability to accumulate lipids when grown in a mixed-sugar, nitrogen-limiting medium, growth was scaled-up to the 5 L bioreactor scale. Similar to what was done for the shake flask experiments, strains were grown in a phosphate-buffered M9 mineral medium amended with an equimolar amount of glucose and xylose (15 g/L each) and 0.5g/L ammonium chloride to achieve a C: N ratio of 100:1. This limiting nitrogen condition is known to promote lipid production in some species of oleaginous yeasts such as *Lipomyces starkeyi*, *Cutaneotrichosporon dermatis*, and *Rhodospiridium. Toruloides* (L. Wang et al., 2020; Xiaobing Yang et al., 2014). Growth rates and sugar consumption were observed at various time points, and samples were analyzed to characterize lipid production, lipid profiles, as well as biomass accumulation. The results of these 5 L bioreactor experiments are discussed below.

4.3.1 Growth and time course of sugar utilization by *P. hubeiensis* IPM1-10 in bioreactors

The growth of *P. hubeiensis* IPM1-10 and the kinetics of sugar consumption throughout 240 h in an automated bioreactor were recorded (Figure 4.10). The *P. hubeiensis* IPM1-10 culture reached a maximum OD₆₀₀ of ~30, which was similar to what was achieved in shake flasks. Most importantly, diauxic growth was not observed, with levels of both glucose and xylose decreasing steadily throughout the entire growth period. This result indicates that glucose repression of xylose utilization did not occur in *P. hubeiensis* IPM1-10. This observation corroborates with a previous report showing that *P. hubeiensis* is a simultaneous utilizer of mixed sugars (Adsul et al., 2009; Digambar Gokhale, 2018; A Tanimura et al., 2016).

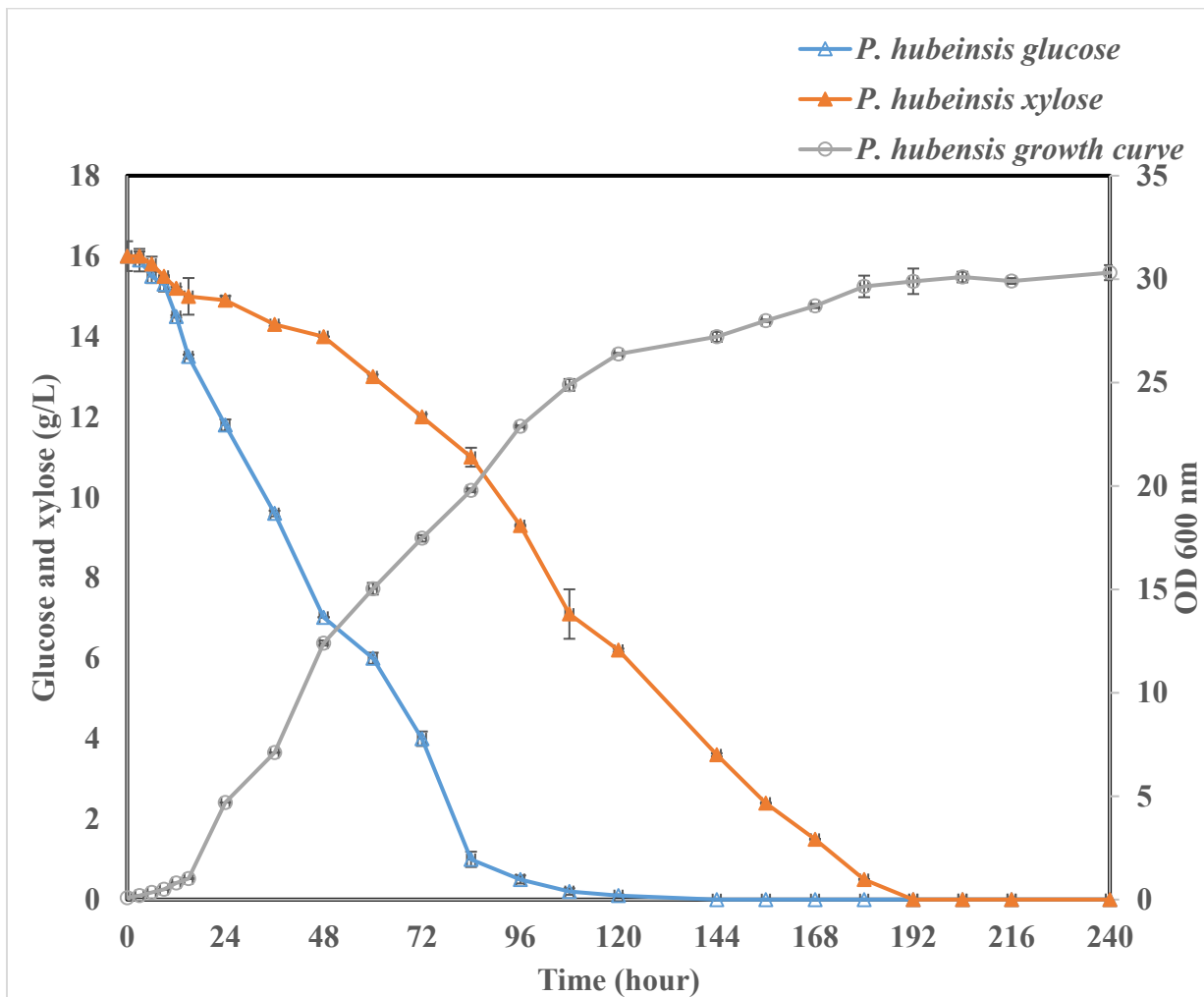


Figure 4.10 Substrate consumption by and growth profiles of *P. hubeiensis* IPM1-10 in a bioreactor. Cultures were grown for 240 h using an equimolar of glucose and xylose as the carbon sources at a final concentration of 30 g/L (15 g/L each) and ammonium chloride at 0.5 g/L for a carbon to nitrogen ratio of 100:1. Data are presented as the means \pm standard deviation (error bars) of triplicate experiments.

P. hubeiensis IPM1-10 completely and simultaneously utilized all of the sugar in the medium, with glucose and xylose being consumed by 120 h and 192 h, respectively, without leaving any residual sugar. Glucose and xylose simultaneous utilization in *P. hubeiensis* occurred at different rates and the overall average rate for substrate consumption in *P. hubeiensis* was 0.09 g/L/h for xylose and 0.17 g/L/h for glucose. It is important to note that the complete sugar consumption observed by *P. hubeiensis* IPM1-10 within 8 days of cultivation is contrary to previously reported data where only 93.06% of the mixed sugars were utilized by *P. hubeiensis* IPM1-10 when grown in shake flasks (Ayumi Tanimura et al., 2016). The lack of residual sugars seen in this research for both shake flask and large-scale bioreactor experiments could be attributed to the composition of the fermentation medium and cultivation conditions employed in this study.

Simultaneous utilization instead of sequential assimilation of the xylose and glucose sugars by *P. hubeiensis* IPM1-10 signifies that it is likely naturally endowed with efficient transport systems for both sugars. It could also be that the global regulatory mechanism that prevents the transcription of genes responsible for the expression/synthesis of enzymes responsible for secondary carbon (C5) utilization when preferred primary carbon (C6) is present is weak or completely lacking in this organism. More research needs to be carried out to determine and confirm the exact mechanism(s) and genes responsible for simultaneous C5 and C6 metabolism in

P. hubeiensis IPM1-10.

The medium composition, shaking speed, and temperature used in the present studies may have favored the growth and sugar consumption in *P. hubeiensis* IPM1-10 in both the bioreactor and shake flask, leading to complete and efficient sugar consumption. Inline monitoring of the pH (controlled pH), improved aeration, and better mixing may have facilitated higher lipid accumulation during *P. hubeiensis* IPM1-10 bioreactor cultivation.

4.3.2 Biomass and lipid accumulation by *P. hubeiensis* IPM1-10

After monitoring the fermentation for 192 h, the final volume of the *P. hubeiensis* IPM1-10 culture was 2.5 L and was harvested for biomass and lipid quantification. The total biomass generated after 192 h for *P. hubeiensis* IPM1-10 was 13.4 ± 0.5 g/L, with a lipid content of $59.0 \pm 2.3\%$ determined on a cell dry weight basis. Based on these numbers, the lipid concentration obtained by *P. hubeiensis* IPM1-10 was 7.9 ± 1.3 g/L. When expressed in terms of sugars consumed, the biomass and lipid yields obtained by *P. hubeiensis* IPM1-10 were 0.5 ± 0.1 g/g and 0.3 ± 0.1 g/g, respectively. Tanimura et al. (2016) have previously reported that when *P. hubeiensis* IPM1-10 was cultivated in shake flasks with 20 g/L of glucose, 10 g/L of xylose, and 5 g/L of arabinose, (i.e. a total of 35 g/L of mixed sugars), the cell dry mass was in the range of 6 - 8 g/L and the lipid concentration was between 1.2 g/L to 1.7 g/L (Ayumi Tanimura et al., 2016). In this present study, the lipid concentration of 7.9 ± 1.3 g/L calculated when *P. hubeiensis* IPM1-10 was cultivated in a limiting nitrogen medium was higher than that reported by Tanimura *et al.*, (2016), and is more similar to the lipid concentration of 9.53 ± 0.6 g/L reported by Wang *et al.*, (2020) (L. Wang et al., 2020) when *Cutaneotrichosporon dermatis* ZZ 46 was grown in glucose and xylose mixtures at the ratio of 2:1. Thus, compared to previous studies with *P. hubeiensis*

IPM1-10, our fermentation conditions resulted in improved carbon consumption (i.e. no residual sugars) and increased lipid accumulation (59%).

4.3.3 Lipid accumulation by *P. hubeiensis* over time

The lipid accumulation in *P. hubeiensis* IPM1-10 at various time points during the fermentation is shown in Figure 4.11. This result revealed that lipid accumulation increased from 120 h to 192 h but reduced to $31.3 \pm 0.2\%$ at 204 h. The reduction observed at 168 and 192 h was not statistically significantly different ($P \geq 0.05$). Since complete consumption of sugars was observed by 192 h (Figure 4.10), cells likely entered into the stationary phase at this point. During the stationary phase, yeast cells undergo morphological changes, such as the thickening of cell walls, which may require the use of stored lipids. Alternatively, it is possible that some cell lysis occurred during the stationary phase, leading to the loss of lipids to the culture supernatant and their subsequent separation from cells during centrifugation. The decrease in lipid content of cells once they reach the stationary phase will be an important consideration when designing continuous or fed-batch fermentation strategies for the cultivation of oleaginous organisms.

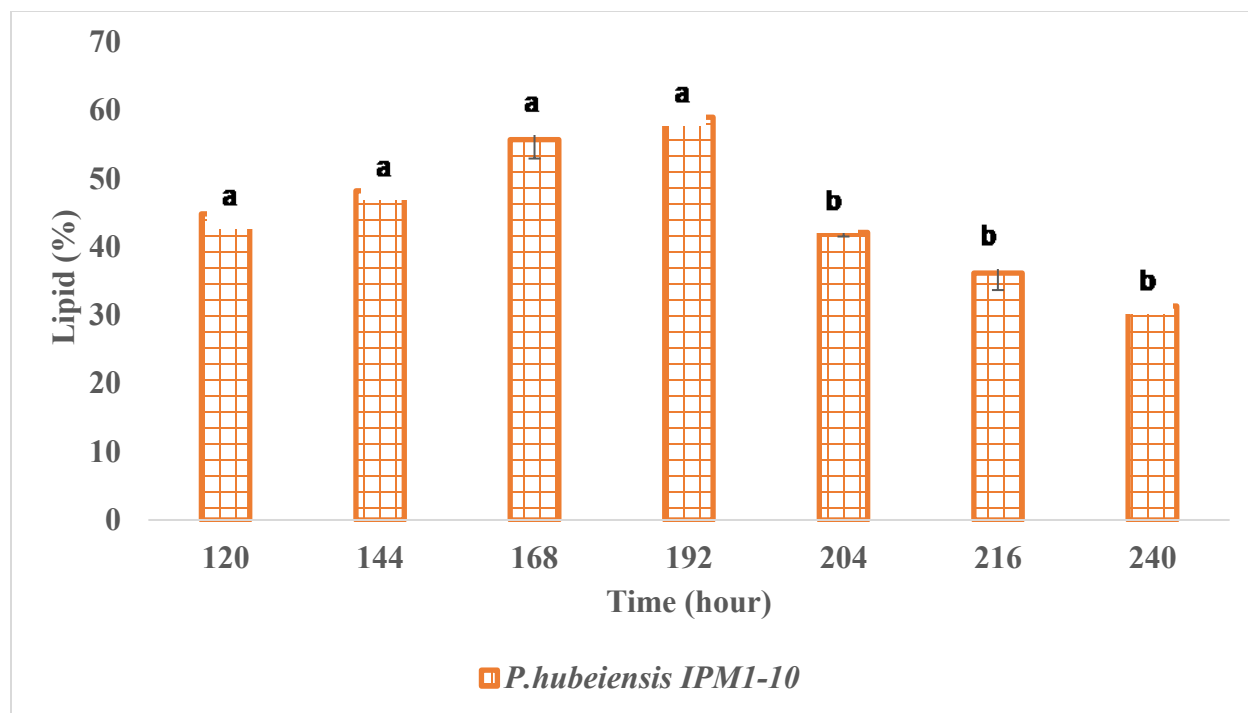


Figure 4.11: Lipid production in *P. hubeiensis* IPM1-10 from 120 h to 240 h. Cells were grown in a medium containing glucose and xylose in a 1:1 ratio (15 g/L each) in a 5 L bioreactor under limiting nitrogen conditions (0.5 g/L ammonium chloride). Bars denoted with different letters a or b is significantly different ($P < 0.05$).

4.3.4 Fatty acid composition of lipids from *P. hubeiensis* IPM1-10

GC/FID was used to determine the fatty acid profile of the extracted lipid from *P. hubeiensis* IPM1-10 (Figure 4.12). The dominant fatty acids present were palmitic acid (C16:0; $21.9 \pm 0.4\%$), stearic acid (C18:0; $9.2 \pm 0.5\%$), oleic acid (C18:1; $33.3 \pm 0.2\%$), linoleic acid (C18:2; $11.0 \pm 0.0\%$), and linolenic acid (C18:3; $15.6 \pm 0.6\%$). Small quantities of other fatty acids were detected. The quantified fatty acids in this study are similar to the overall fatty acid profile

as well as fatty acids that are more predominant as reported in *Rhodotorula glutinis* (known for palmitic, oleic, linoleic, and linolenic acids production) (Kot et al., 2016), *Candida sp* (known for myristic, palmitic, stearic, oleic, linoleic, and linolenic acids production) (Kobayashi et al., 1987), and *Trichosporon cutaneum* (known for palmitic, palmitoleic, oleic, and linoleic acids production) (Kolouchová et al., 2016), and in *Schwanniomyces occidentalis* (*Debaromyces occidentalis*) (Kolouchová et al., 2016; Lamers et al., 2016; Tezaki et al., 2017). The carbon number of the predominant fatty acids in *P. hubeiensis* IPM1-10 as observed in this study was from C16 to C22, specifically rich in long-chain fatty acids. This corroborates with similar reported observations in *Rhodotorula glutinis* and *Trichosporon cutaneum* (Kolouchová et al., 2016; Kot et al., 2016). The fatty acids of *P. hubeiensis* IPM1-10 were found to be 35.8% saturated and 64.5% unsaturated fatty acids, with polyunsaturated fatty acids (PUFA) and monounsaturated fatty acids (MUFA) representing 30.0% and 34.5% of the total lipid content, respectively. The C16 and C18 fatty acids accounted for 92.3% of the total fatty acids in *P. hubeiensis* IPM1-10 with the highest proportion (69.1%) coming from C18 fatty acids. Only 0.6% of the fatty acids were from C14, and 4.5% were from C20 fatty acids whereas 2.6% belongs to C22 fatty acids.

The relationship between fatty acid composition and the quality of biodiesel generated from these fatty acids showed that stearic and palmitic acids were the first to precipitate when liquid biodiesel is cooled, thereby forming the major component seen in recovered biodiesel clogged fuel filters (Lamaisri et al., 2015). Since fatty acids from *P. hubeiensis* are comprised of 35.8% of saturated fatty acids, it is possible that these specific fatty acids may generate fuel molecules that are known to clog engines. However, the fatty acids of *P. hubeiensis* IPM1-10 in this present study were shown to be composed of mainly unsaturated fatty acids (64.5%), which generate biodiesel molecules that are less prone to precipitation.

In addition, the viscosity of biodiesel increases as the chain length of the FAMES increases (Lamaisri et al., 2015). But when the long-chain FAMES have a *cis* double bond, the viscosity reduces whereas *trans* double bonds increase viscosity. An increase in the quantity of unsaturated FAMES lowers the cetane number and high levels of saturated FAMES increases the cetane number (Demirbas, 2007; Lage & Gentili, 2018; Lamaisri et al., 2015; X. Li et al., 2018; Menegazzo & Fonseca, 2019; Tamilselvan et al., 2020). Cetane number is the ability of a fuel to ignite (burn) when injected. The preferred FAMES for biodiesel production are those that give high cetane numbers because fuel quality specifications for petroleum diesel by the American Standard for Testing and Materials (ASTM) required that the cetane number must be at least 40 (ASTM D975-09). The presence of long-chain fatty acids (such as C20 and C22 and their isomers) shown in this study, which accounted for approximately 4.5% of the fatty acids, may likely lead to the production of better quality biodiesel. Overall, the fatty acid composition of *P. hubeienesis* IPM1-10 demonstrated that this oleaginous organism is a good candidate for biodiesel production.

The fatty acids generated by *P. hubeienesis* IPM1-10 are also a promising candidate for integration into the LTH process. Previous work by Asomaning *et al.*, (2014) demonstrated that fatty acid feed composition affected the composition of the pyrolysis product (Asomaning et al., 2014c). The majority of the fatty acids generated by *P. hubeienesis* IPM1-10 were in C16 to C22, which are excellent feedstocks for the LTH process for the generation of renewable diesel.

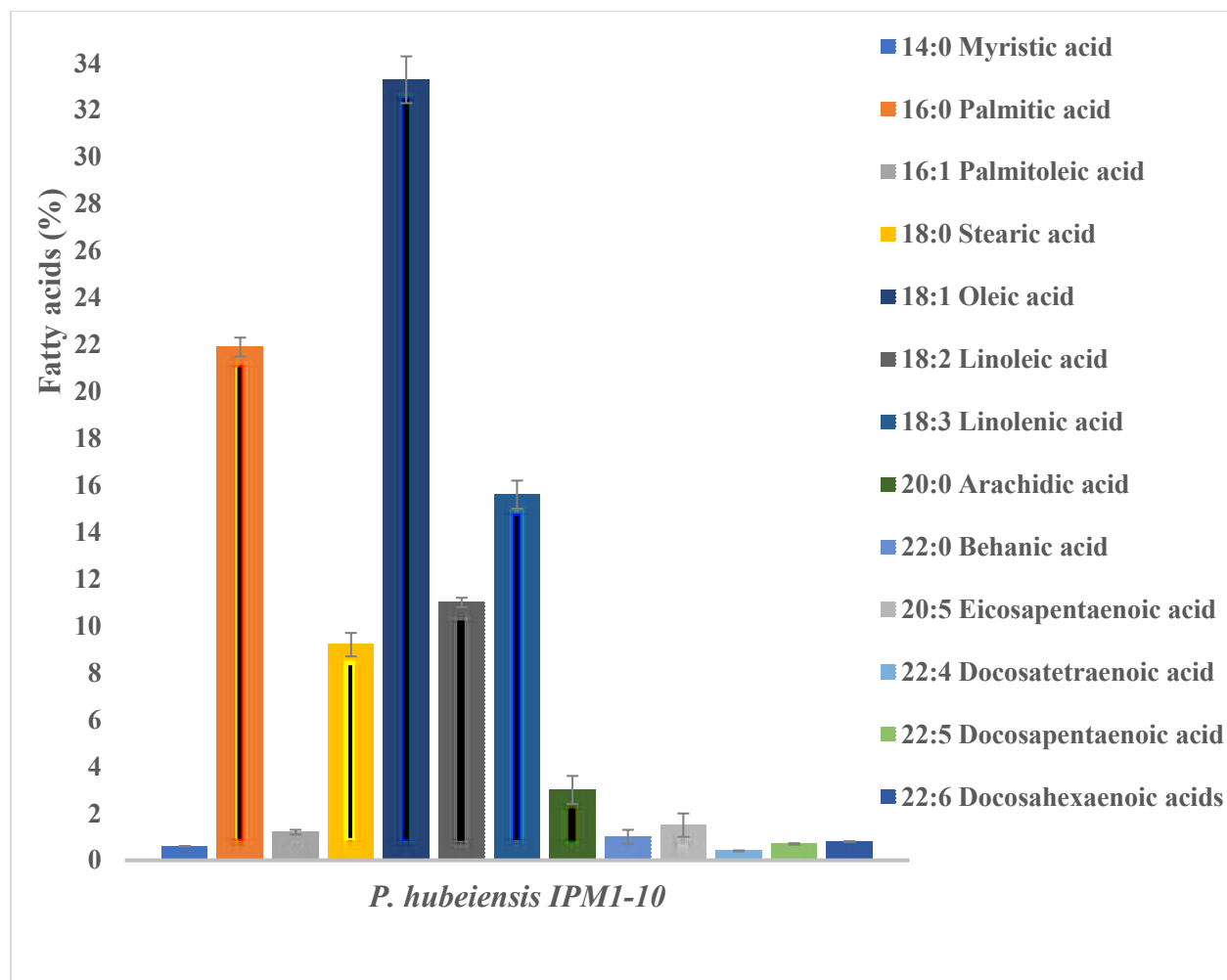


Figure 4.12: Fatty acid profile of the lipids accumulated in *P. hubeiensis* IPM1-10

4.3.5 Growth and time course of sugar utilization by *P. tsukubaensis* in bioreactors

Cultivation of *P. tsukubaensis* was performed as described for *P. hubeiensis* above. The growth of *P. tsukubaensis* over time and the kinetics of sugar consumption during a 240 h period are shown in Figure 4.13. The *P. tsukubaensis* culture reached a maximum OD₆₀₀ of 26 ± 0.1 at 204 h. Although *P. tsukubaensis* was shown to utilize both glucose and xylose simultaneously, the rate of glucose utilization during the earlier stages of the fermentation was much higher than that for xylose. Overall, *P. tsukubaensis* consumed glucose and xylose at a rate of 0.11 g/L/h and

0.08 g/L/h, respectively. The glucose present in the medium was fully consumed by 168 h and xylose was completely depleted from the medium by 216 h. The simultaneous utilization of C5 and C6 sugars by *P. tsukubaensis* highlights its great potential for uptake and metabolism of sugars from lignocellulosic feedstocks. The mechanism(s) in *P. tsukubaensis* for utilizing both sugars is still unknown, hence the need for further research.

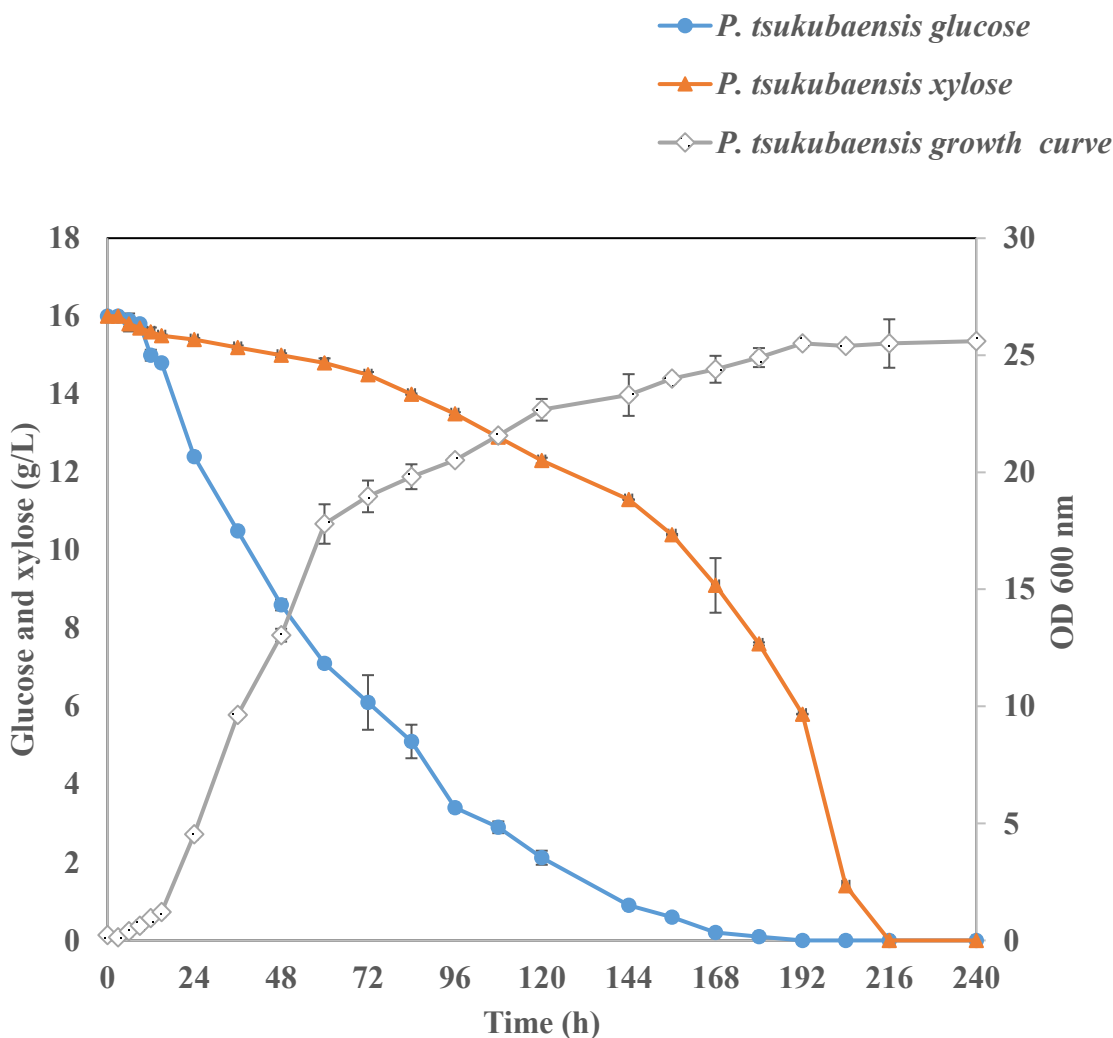


Figure 4.13: Substrate consumption by and growth profiles of *P. tsukubaensis* in a bioreactor for 240 h using glucose and xylose as the carbon source at a final concentration of 30 g/L (15 g/L

each) and ammonium chloride at 0.5 g/L for a carbon to nitrogen ratio of 100:1. Data are presented as the means \pm standard deviation (error bars) of triplicate experiments.

4.3.6. Biomass and lipid accumulation by *P. tsukubaensis*

The total biomass and lipid content generated based on the cell dry weight obtained for *P. tsukubaensis* after 204 h of cultivation in nitrogen limiting medium was 8.8 ± 0.9 g/L and $58.1 \pm 0.1\%$, respectively. Using these numbers, the lipid concentration was calculated to be 5.1 ± 1.9 g/L. Based on the amount of sugar consumed, biomass yields were 0.3 ± 0.0 g/g sugars and lipid yields were 0.2 ± 0.0 g/g.

Oleaginous yeasts are known for their excellent ability to produce lipids above 20% of their cell dry weight. For example, a previous study by Espinosa-Gonzalez *et al.*, (2014) showed that when the oleaginous yeast *Cryptococcus curvatus* was cultivated either in a batch mode or fed-batch mode under limiting nitrogen condition with glucose as the sole carbon source, the biomass generated and lipid content after 68 h in batch mode was 10 ± 1 g/L and 59 ± 2 g/L, respectively, on a cell dry weight basis. While for the fed-batch mode, biomass and lipid content (CDW) generated after 192 h of cultivation was 30 ± 3 g/L and $53 \pm 4\%$, respectively.

4.3.7. Time course of lipid accumulation in *P. tsukubaensis*

The lipid content in *P. tsukubaensis* increased from 120 h to 204 h, with levels decreasing by 240 h. There was no significant difference ($P \geq 0.05$) in lipid accumulation between 192 - 216 h. This was similar to what was observed for *P. hubeiensis*, though in this case, the maximum lipid content was observed at 192 h. As mentioned previously, the decrease in lipid content likely results from the transition to stationary phase, which is accompanied by morphological changes to the cell

and cell lysis. Both of these events may lead to lower lipid levels in harvested cell pellets.

There are ample works in the literature on the production of mannosylerythritol lipids (glycolipids), a biosurfactant, by *P. tsukubaensis* (Beck, Werner, et al., 2019; Konishi et al., 2007; Morita et al., 2007, 2010; Morita, Fukuoka, Imura, et al., 2015; Morita, Fukuoka, Kosaka, et al., 2015; Paulino et al., 2017; Saika et al., 2018; Yoshida et al., 2014). The information available on the use of *P. tsukubaensis* lipids include pharmaceutical (gene delivery, anti-bacterial, anti-tumor, and anti-oxidant activities), food, and cosmetics (human skin repair) applications (Morita, Fukuoka, Kosaka, et al., 2015; Paulino et al., 2017; Saika et al., 2018). However, this is the first report of using a mixed sugar and nitrogen limiting medium to generate lipids using *P. tsukubaensis*.

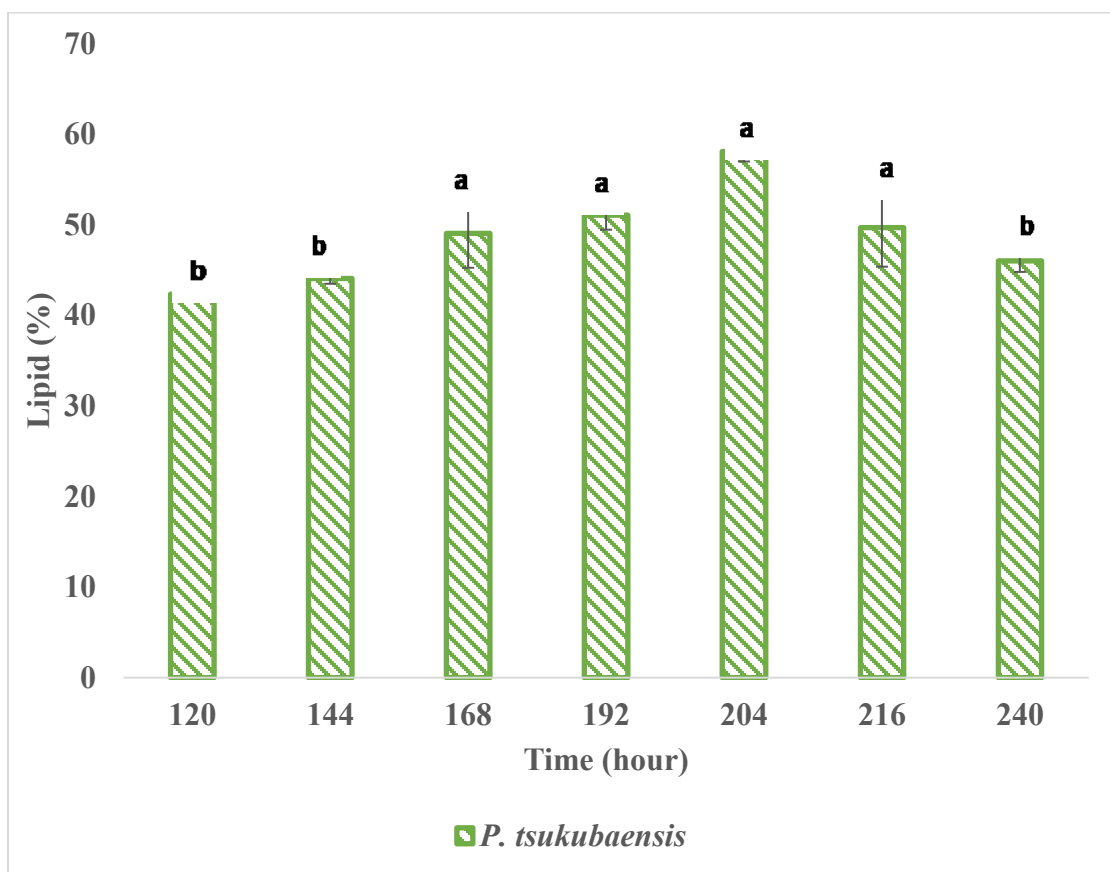


Figure 4.14: Time course experiment to monitor lipid production by *P. tsukubaensis* from simultaneous utilization of glucose and xylose in the ratio of 1:1 (15 g/L each) in a 5 L scale bioreactor under limiting nitrogen conditions (0.5 g/L ammonium chloride). Data are presented as the means \pm standard deviation (error bars) of triplicate experiments. Bars denoted with different letters a or b is significantly different ($P < 0.05$).

4.3.8 Fatty acid composition of lipids generated by *P. tsukubaensis*

The fatty acid profile of the lipids extracted from *P. tsukubaensis* was analyzed using GC/FID after the derivatization of the microbial lipids (TAG) to FAMES. The predominant fatty acids generated by *P. tsukubaensis* were palmitic acid (C16:0; $8.9 \pm 0\%$), oleic acid (C18:1; $43.2 \pm 0\%$), linoleic acid (C18:2; $24.4 \pm 1\%$), and linolenic acid (C18:3; $19.2 \pm 1\%$) (Figure 4.15). Other fatty acids were present in the profile at lower concentrations. The fatty acids produced by *P. tsukubaensis* were predominantly in the C16 to C24 range, which corresponds with data obtained from other oleaginous yeasts (Johnravindar et al., 2018; Kolouchová et al., 2016; Xiaobing Yang et al., 2015). The C16 and C18 fatty acids accounted for 9.2% and 88.7% of the total fatty acids in *P. tsukubaensis*, respectively. The vast majority of fatty acids from *P. tsukubaensis* were unsaturated (87.5%), with only 12.6% being saturated. The unsaturated fatty acids were evenly distributed between polyunsaturated (PUFA) and monounsaturated fatty acids, making up 44.3% and 43.2% of the total fatty acids, respectively. Thus, the fatty acids of *P. tsukubaensis* are similar to vegetable oil fatty acids, thereby predisposing it as an excellent source for renewable fuel production.

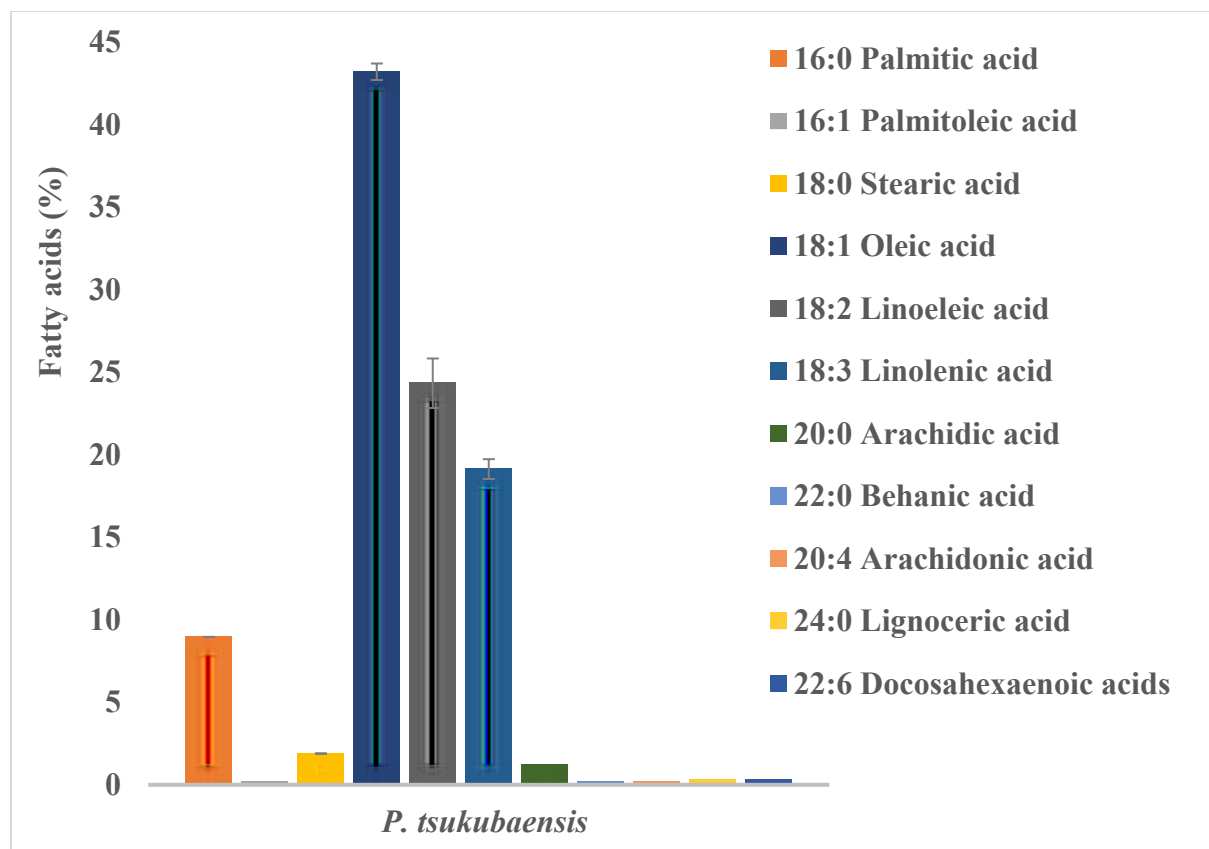


Figure 4.15: Fatty acid profile of *P. tsukubaensis* before hydrolysis

4.3.9. Growth and time course of sugar utilization by *C. iriomotense* ISM28-8s^T in bioreactors

C. iriomotense ISM28-8s^T was cultivated in the same manner as described for *P. hubeiensis* IPM1-10 and *P. tsukubaensis* above. While *P. hubeiensis* IPM1-10 and *P. tsukubaensis* displayed similar growth patterns, *C. iriomotense* ISM28-8s^T displayed poorer growth and sugar utilization. A substantial lag phase was observed (0-80 h) when culturing *C. iriomotense* ISM28-8s^T in bioreactors (Figure 4.16). Cultures of *C. iriomotense* ISM28-8s^T reached a maximum OD₆₀₀ of 5.3 ± 0.2 through the simultaneous assimilation of glucose and xylose sugars, which was much lower than the OD₆₀₀ of ~30 observed for *P. hubeiensis* IPM1-10 and *P. tsukubaensis*.

It should be noted that although simultaneous utilization of glucose and xylose was observed in these experiments, substantial amounts of residual sugar were observed (8.3 g/L glucose and 6.5 g/L xylose). Thus, *C. iriomotense* ISM28-8s^T only consumed 50.7% of total sugars in the medium during the 240 h experiment, correlating with sugar consumption rates of 0.03 g/L/h and 0.04 g/L/h for glucose and xylose, respectively. The amount of residual sugars in this experiment did not align with the report of Tanimura *et al.*, (2018) who observed that when *C. iriomotense* ISM28-8s^T was grown for 10 days in a medium amended with 10 g/L of xylose and 10 g/L of glucose, with no nitrogen limitation, about 85.3% of the amended sugars were consumed. It is possible that in the current experiment, another nutrient (i.e. trace mineral) was limiting. Future work should focus on optimizing the growth medium for *C. iriomotense* ISM28-8s^T to help promote full carbon utilization.

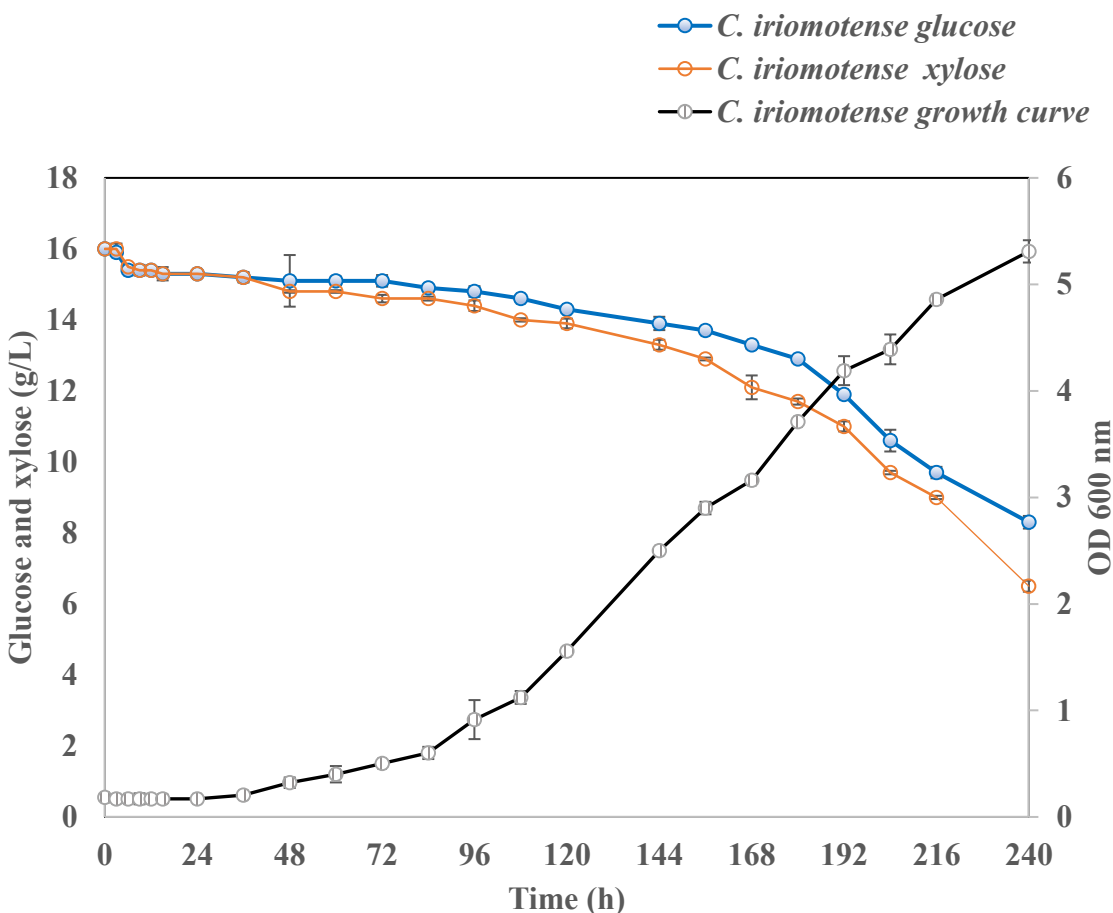


Figure 4.16: Substrate consumption by and growth profiles of *C. iriomotense* ISM28-8s^T in a 5 L bioreactor over a 240 h period. The medium contained equal amounts of glucose and xylose (15 g/L each, for a total of 30 g/L) and 0.5 g/L ammonium chloride, establishing a carbon to nitrogen ratio of 100:1. Data are mean \pm standard deviation (error bars) of three assays. Data are presented as the means \pm standard deviation (error bars) of triplicate experiments.

4.3.10. Biomass and lipid accumulation by *C. iriomotense*

At the point of harvest, the biomass generated from *C. iriomotense* ISM28-8s^T was 3.3 ± 0.4 g/L with a lipid content of $27.0 \pm 0.7\%$ on a cell dry weight basis, resulting in a lipid concentration of 0.9 ± 0.0 g/L. The lipid content obtained in this experiment was higher than the

21% observed previously by Tanimura et al. (2018). However, in that study, the medium was not nitrogen limited. Thus, a higher degree of sugar consumption (85.3%) and biomass accumulation (4.3 g/L) was observed. Biomass yields from *C. iriomotense* ISM28-8s^T were 0.2 ± 0.0 g/g sugar consumed and lipid yield was 0.1 g/g sugar consumed.

4.3.11. Time course of lipid accumulation in *C. iriomotense* ISM28-8s^T

A time course of lipid accumulation in *C. iriomotense* ISM28-8s^T (Figure 4.17) revealed that the lipid content showed an upward trend from 120 h to 240 h. Lipid accumulation increased from 120 h to 240 h, but there is no significant difference ($p \geq 0.5$) in lipid accumulation between 216 and 240 h. Given that the OD was still rising at 240 h and that there were substantial amounts of glucose and xylose still in the growth medium, it is possible that the cells were still in exponential phase at 240 h and that prolonged culturing may have resulted in the depletion of sugars, additional lipid accumulation, and the onset of stationary phase. Further experiments may be required using extended timepoints. Alternatively, optimization of the growth medium for *C. iriomotense* ISM28-8s^T may improve growth and lipid accumulation.

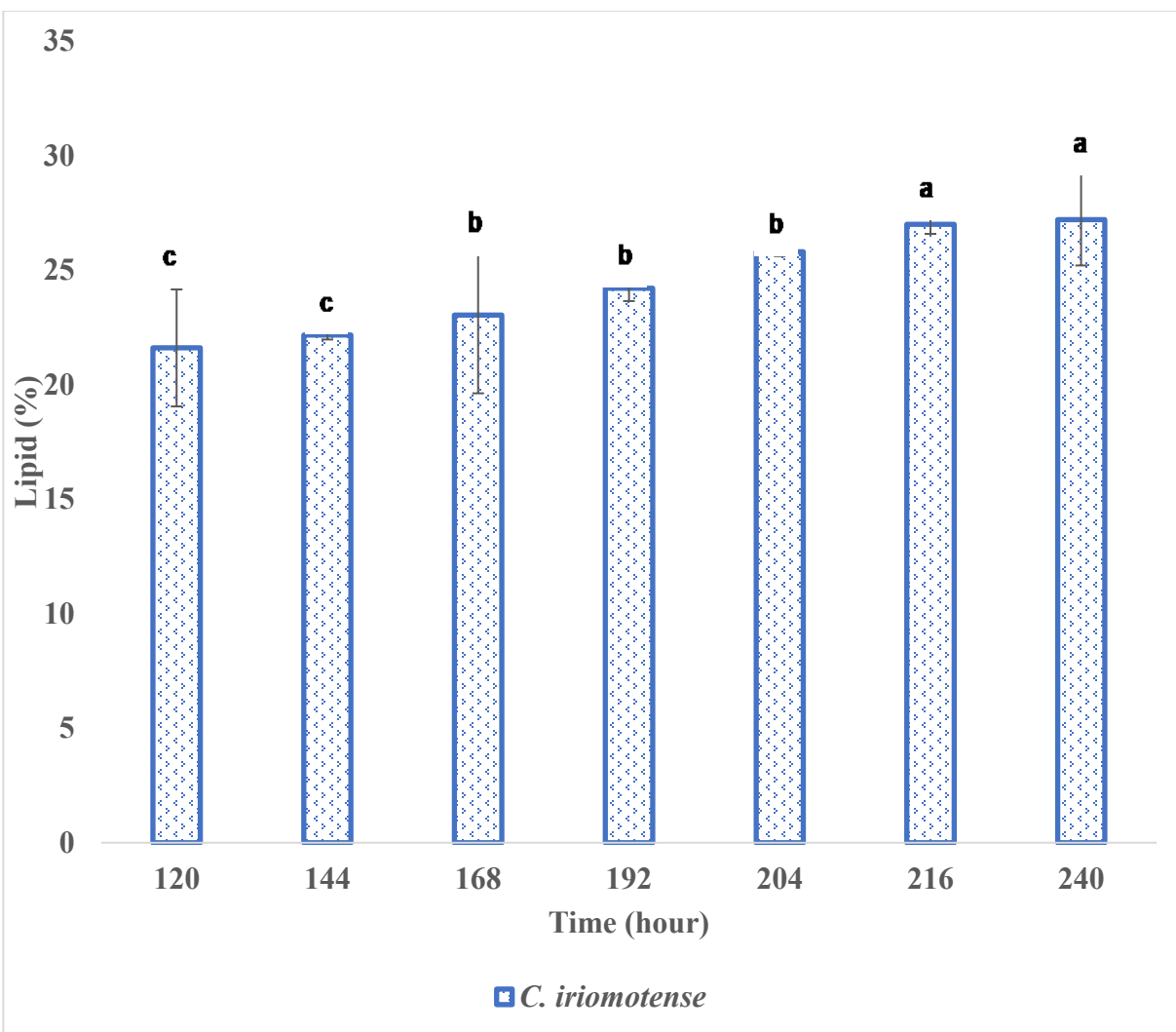


Figure 4.17: Time course of lipid production from 120 h to 240 h by *C. iriomotense* ISM28-8s^T from simultaneous utilization of glucose and xylose in the ratio of 1:1 (15 g/L each) in a 5 L scale bioreactor under limiting nitrogen conditions (0.5 g/L ammonium chloride). Bars are all denoted with an indicating that they are statistically similar ($P < 0.05$).

4.3.12. Fatty acid profile of lipid produced by *C. iriomotense* ISM28-8s^T

The fatty acid composition of the lipids generated by *C. iriomotense* ISM28-8s^T was determined via GC/FID. The fatty acids of *C. iriomotense* ISM28-8s^T were comprised predominantly of palmitic acid (C16:0; $26.8 \pm 1\%$), stearic acid (C18:0; 8.7 ± 0.0), oleic acid

(C18:1; $40.1 \pm 0.8\%$), linoleic acid (C18:2; $18.0 \pm 0.3\%$), and linolenic acid (C18:3; $3.2 \pm 0\%$). The C16 and C18 fatty acids were the predominant fatty acids in *C. iriomotense* ISM28-8s^T accounting for 96.7% of the total fatty acids, with 26.7% and 70.0% coming from C16 and C18 fatty acids, respectively. Generally, the carbon number of fatty acids present in *C. iriomotense* ISM28-8s^T ranged from C14 – C20, with 62.0% of the fatty acids being unsaturated and 38.0% saturated. Interestingly, polyunsaturated fatty acids (PUFA) accounted for only 21.2% of the total fatty acids whereas monounsaturated fatty acids accounted for 40.8%.

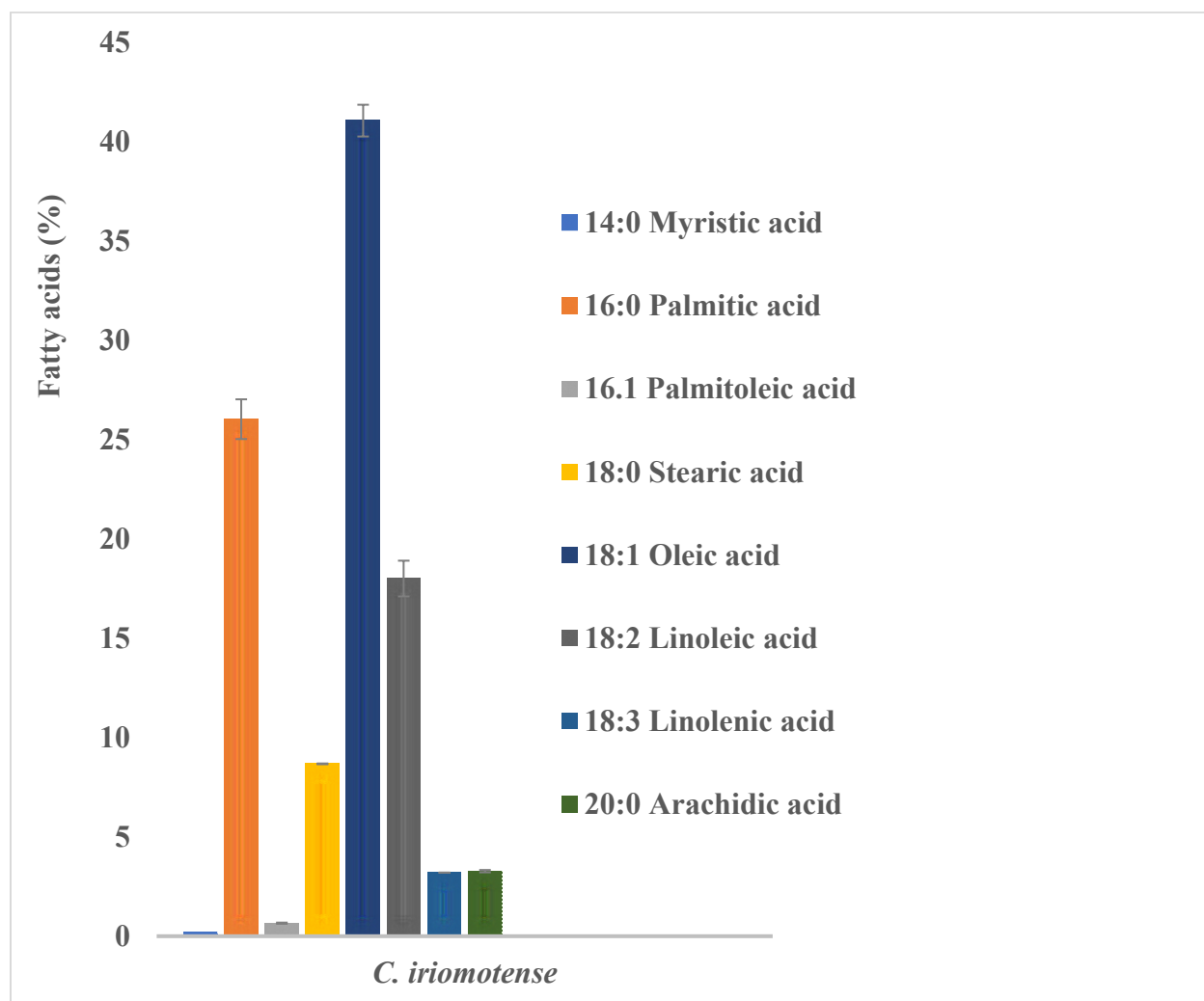


Figure 4.18: Fatty acid profile of *C. iriomotense* ISM28-8s^T

4.3.13. Comparison of yeast growth and lipid accumulation in 5 L bioreactors

The data obtained from the three oleaginous yeast strains cultivated in 5 L bioreactors are summarized in Table 4.2. All three strains were shown to simultaneously utilize the C5 and C6 sugars, though the consumption rates varied amongst the oleaginous yeasts. Although the glucose consumption rate was higher than that of xylose in *P. hubeiensis* and *P. tsukubaensis*, the opposite was true for *C. iriomotense*. Furthermore, *C. iriomotense* did not consume all of the sugars present in the medium, whereas *P. hubeiensis* and *P. tsukubaensis* did, which explains why significantly higher ODs were observed for the latter two strains when grown in 5 L bioreactors (i.e. ~30 vs. ~5)

The total lipid accumulation also varied among the three strains of oleaginous yeasts. The lowest lipid accumulation was observed for *C. iriomotense*; the lipid content of *P. hubeiensis* and *P. tsukubaensis* were statistically similar. However, it should be noted that all three yeast strains were confirmed to be oleaginous as they displayed lipid contents >20%. Generally, the fatty acid composition of *P. tsukubaensis* had a higher unsaturated content (86.8%) when compared to that of *P. hubeiensis* (64.8%) and *C. iriomotense* (56.4%). The oleaginous yeast with the highest levels of polyunsaturated fatty acids was *P. tsukubaensis* (43.6%) compared to *P. hubeiensis* (26.4%) and *C. iriomotense* (0.15%). Monounsaturated fatty acids were highest in *C. iriomotense* (56.3%) followed by *P. tsukubaensis* (43.2%) and *P. hubeiensis* (38.4%).

Based on the data shown in Table 4.2, *P. hubeiensis* and *P. tsukubaensis* have greater potential than *C. iriomotense* for the production of lipids for biofuel applications. However, it should be noted that further studies with *C. iriomotense* may reveal strategies to improve growth rates and/or lipid accumulation to necessary levels. Thus, all three strains were applied as lipid

feedstocks for the LTH technology to determine whether they could be used to generate hydrocarbon fuels.

Table 4.2: Summary of results obtained from three oleaginous yeasts grown in 5 L bioreactors.

Oleaginous yeasts	Cell dry weight (g/L)	% Lipid of cell dry weight	Lipid concent ration (g/L)	Biomass yield (g/g)	Lipid yield (g/g)	Sugar consum ed (g/L)	Culture harvest time (h)
<i>P. hubeiensis</i>	13.4 ± 0.5 ^a	59.0 ± 2.3 ^a	7.9 ± 1.3 ^a	0.5 ± 0.1 ^a	0.3 ± 0.0 ^a	30.0	192
<i>P. tsukubaensis</i>	8.8 ± 0.9 ^b	58.1 ± 0.1 ^a	5.11 ± 1.9 ^b	0.3 ± 0.0 ^b	0.2 ± 0.1 ^b	30.0	204
<i>C. iriomotense</i>	3.3 ± 0.4 ^c	27.0 ± 0.7 ^b	0.9 ± 0.0 ^c	0.21 ± .0 ^b	0.1 ± 0.0 ^c	15.2	240

Data are reported as the mean ± standard deviation of triplicate experiments. Within each column, values denoted with a different letter (i.e. a, b, or c) are statistically significantly different (P<0.05).

4.4 Characterization of the hydrolysis product generated from yeast slurries

4.4.1 Product distribution within yeast hydrolysates

Slurries of *P. hubeiensis*, *P. tsukubaensis*, and *C. iriomotense* were hydrolyzed separately as the first step of the LTH process. This procedure facilitates the hydrolysis of lipids into glycerol and fatty acids, the latter of which serves as the feedstock for the second step (i.e. pyrolysis) of the

LTH technology. The distribution of solids, gases, and aqueous fractions in the yeast hydrolysates is shown in Table 4.3. *P. hubeiensis* and *C. iriomotense* generated similar amounts of solids (>80%) whereas *P. tsukubaensis* produced much less solid products ($53.8 \pm 1\%$). Conversely, *P. tsukubaensis* generated the greatest amount of liquid product, followed by *P. hubeiensis*, with *C. iriomotense* producing the smallest amount of aqueous fraction. Very low levels of gas were generated through hydrolysis of the three yeast slurries, though *P. hubeiensis* produced slightly less than the other two organisms.

Table 4.3: Characterization of hydrolysis products generated from yeast slurries

Oleaginous yeasts	Weight % product distribution		
	Solid fraction	Aqueous fraction	Gas fraction
<i>P. hubeiensis</i>	83.0 ± 1^a	15.5 ± 1^b	1.2 ± 0.1^b
<i>P. tsukubaensis</i>	53.8 ± 1^b	44.2 ± 2^a	2.1 ± 0.1^a
<i>C. iriomotense</i>	89.8 ± 1^a	8.2 ± 1^c	2.0 ± 0.1^a

Data are reported as the mean \pm standard deviation of triplicate experiments. Within each column, values denoted with a different letter (i.e. a, b, or c) are statistically significantly different ($P < 0.05$).

4.4.2 Assessment of lipid classes in yeast hydrolysates through thin layer chromatography

The hexane soluble lipids recovered from the washing of only the solid hydrolysis products from the three yeasts were examined using thin-layer chromatography (TLC) on a Whatman polyester silica plate to visualize the lipid classes present. The TLC chromatogram (Figure 4.19) showed that fatty acids were predominantly found in all the hexane soluble products from *P. hubeiensis*, *P. tsukubaensis*, and *C. iriomotense*. The samples derived from the hydrolysates of the

three oleaginous yeasts (Figure 4.19, lanes 1-3) were devoid of triacylglycerol (i.e. triolein, an asymmetrical triacylglyceride). This is in agreement with previous studies by Asomaning et al. (2014) and Espinosa-Gonzalez et al. (2014) that reported the absence of triacylglycerides in the thin layer chromatogram analysis of hydrolyzed lipids. The lack of TAGs and abundance of free fatty acids observed through TLC is a clear indication that efficient hydrolysis of lipids to free fatty acids occurred in these experiments.

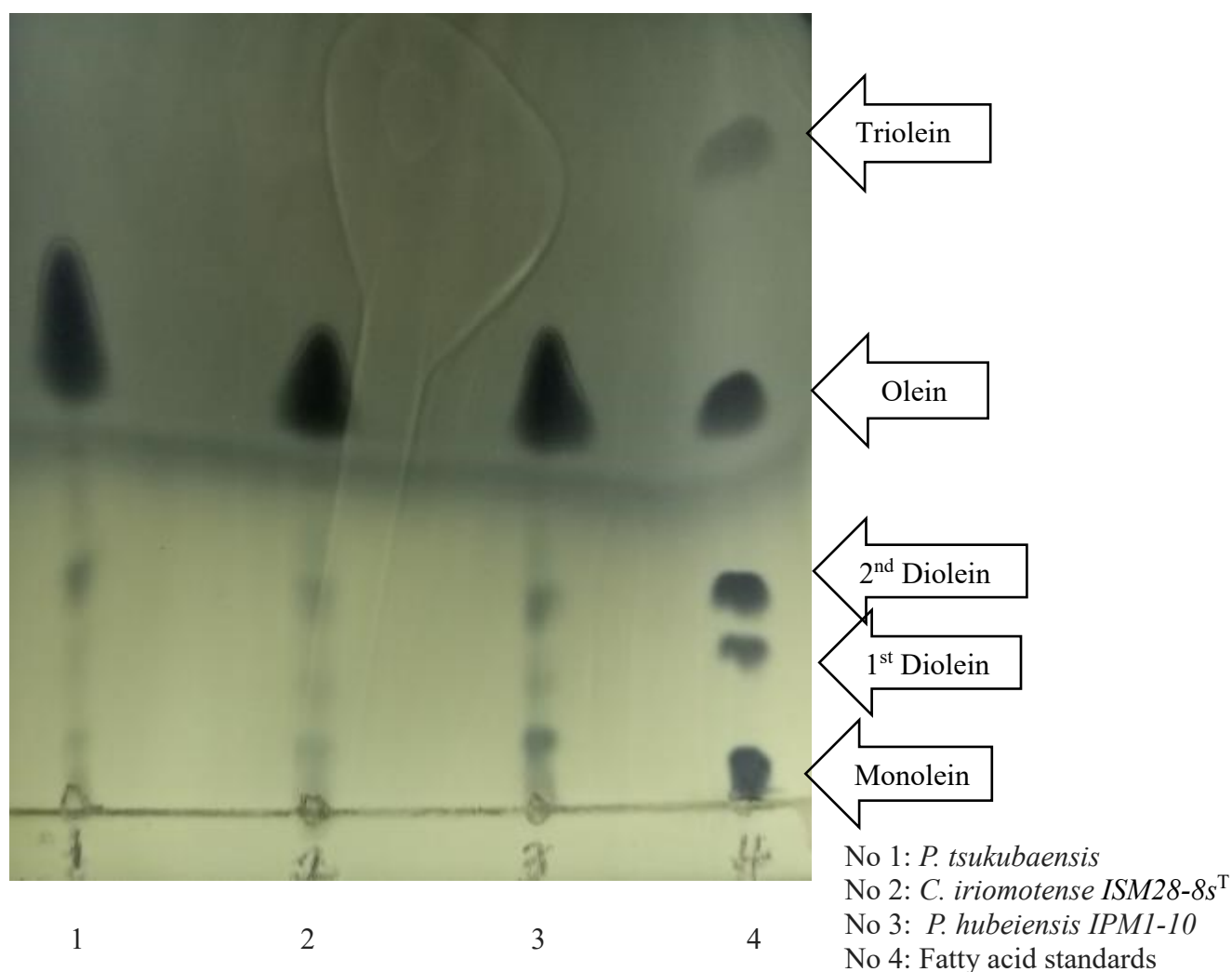


Figure 4.19. Thin-layer chromatography of yeast lipids after hydrolysis. The mobile phase was hexane, ether, and acetic acid in the ratio of 80:20:1.

4.4.3 Characterization of fatty acids extracted from yeast hydrolysates

The fatty acids present in the three yeast hydrolysates were isolated through hexane extraction and were then analyzed via GC-FID/MS. The distribution of fatty acids in these purified fractions is shown in Figure 4.20. While there were small differences between the oleaginous yeasts concerning the fatty acid distribution observed, the purified fatty acid fractions obtained from all three strains were shown to contain relatively high levels of oleic, palmitic, stearic, linoleic acids. A similar fatty acid profile was observed in the fatty acid stream obtained through hexane extraction of *Chlorella protothecoides* hydrolysates (Espinosa-Gonzalez, Asomaning, et al., 2014).

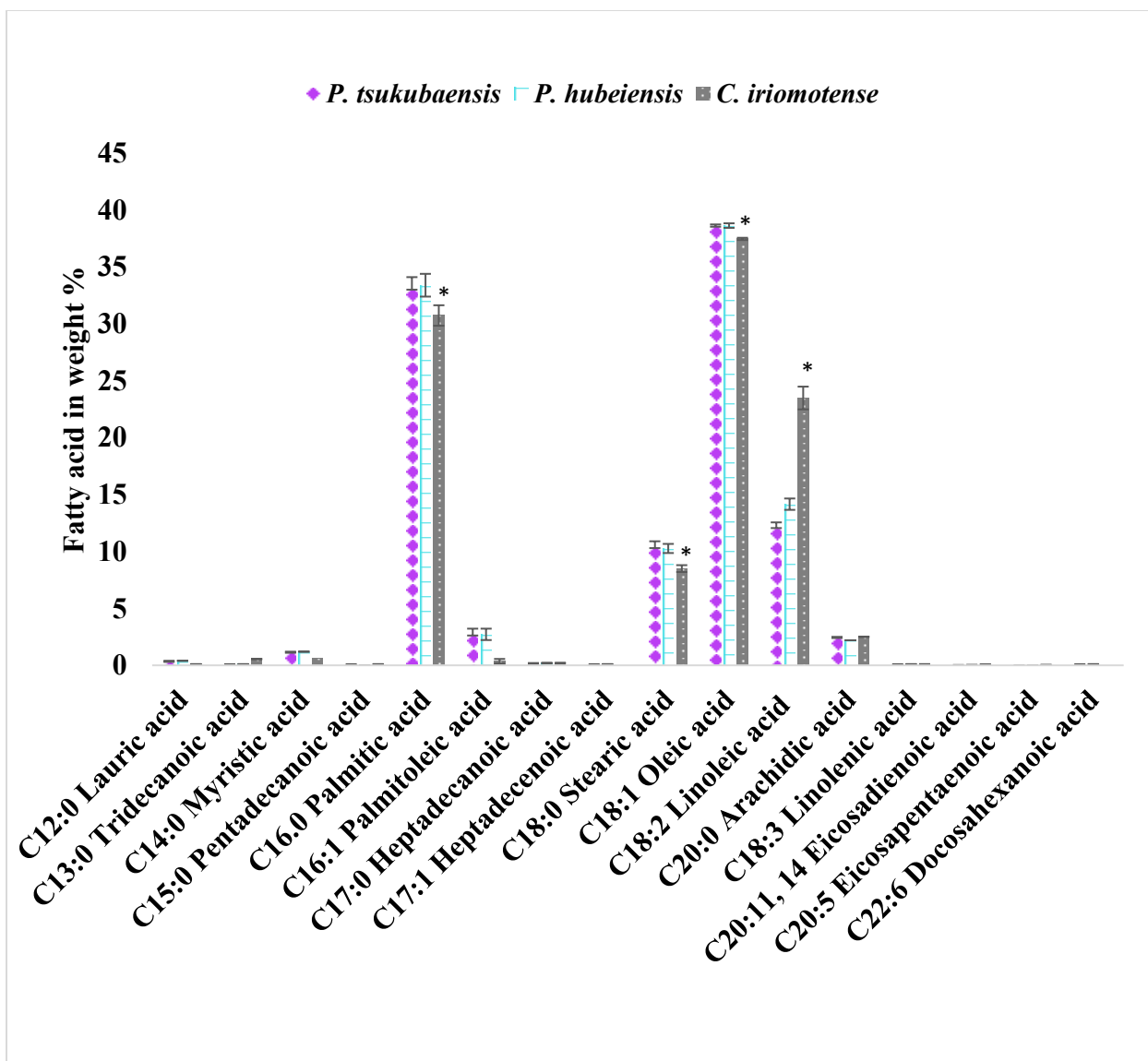


Figure 4.20: The fatty acid composition of the product obtained through hexane extraction of yeast hydrolysates. The three oleaginous yeast strains were grown in a 5 L bioreactor. Data are reported as the mean \pm standard deviation of triplicate experiments. For *C. iriomotense*, bars annotated with an asterisk represent values (i.e. weight %) that are significantly different ($P < 0.05$) from those observed for *P. tsukubaensis* and *P. hubeiensis*. For those fatty acids, there was no statistical difference between the values obtained for the latter two strains.

Comparison of the fatty acid profiles of *P. tsukubaensis*, *P. hubeiensis*, and *C. iriomotense* before and after hydrolysis highlighted several changes in fatty acids (Table 4.3). For instance, there was no lauric acid (C12:0), tridecanoic acid (C13:0), heptadecanoic acid (C17:0), or heptadecenoic acid (C17:1) in the profiles of all the three organisms before hydrolysis. Conversely, these fatty acids were detected in the fatty acids fractions from all three oleaginous yeasts after hydrolysis, albeit at very low levels (<1%). It is possible that the hydrolysis conditions resulted in some cracking of fatty acids to generate these new species. While this phenomenon has not been observed in past LTH experiments, it is possible that complex microbial systems contain salts or metals that could potentially catalyze such cracking.

Table 4.4: Fatty acid profiles before and after hydrolysis of oleaginous yeasts

Fatty acids	Composition (%) before hydrolysis			Composition (%) after hydrolysis		
	<i>P. tsukubaensis</i>	<i>P. hubeiensis</i>	<i>C. iriomotense</i>	<i>P. tsukubaensis</i>	<i>P. hubeiensis</i>	<i>C. iriomotense</i>
C12:0				0.4 ± 0.0	0.4 ± 0.0	0.1 ± 0.0
C13:0				0.1 ± 0.0	0.1 ± 0.0	0.6 ± 0.0
C14:0		0.6 ± 0.0	0.2 ± 0.0	1.2 ± 0.0	1.2* ± 0.0	0.6* ± 0.0
C15:0				0.1 ± 0.0	0.1 ± 0.0	0.1 ± 0.0
C16:0	9.0* ± 0.0	22.0* ± 0.4	26.0* ± 1	33.0* ± 0.4	33.4* ± 0.4	31.0 * ± 0.9
C16:1	0.2* ± 0.0	1.3* ± 0.1	0.7* ± 0.0	2.8* ± 0.0	2.8 * ± 0.0	0.4* ± 0.2
C17:0				0.2 ± 0.0	0.2 ± 0.0	0.2 ± 0.0
C17:1				0.1 ± 0.0	0.1 ± 0.0	
C18:0	1.9* ± 0.0	9.2* ± 0.5	8.7 ± 0.0	10.4* ± 0.5	10.3* ± 0.4	8.5 ± 0.3
C18:1	43.2* ± 0.3	33.3* ± 0.2	40.1* ± 0.1	35.3* ± 0.2	35.8* ± 0.5	33.9* ± 0.5
C18:2	24.4 ± 1.5*	13.1 ± 0.0	18.0 ± 0.3	13.0 ± 0.2*	13.0 ± 0.4	21.9 ± 0.3
C18:3	19.2* ± 0.6	15.6* ± 0.6	3.2* ± 0.0	0.1* ± 0.0	0.1* ± 0.0	0.1 ± 0.0

C20.0	1.2* ± 0.0	3.0 *± 0.0	3.3* ± 0.0	2.5* ± 0.0	2.2* ± 0.0	2.5* ± 0.0
C20.2				0.1* ± 0.0	0.1* ± 0.0	0.1* ± 0.0
C20.4	0.2* ± 0.0					
C20.5		1.5 ± 0.0*		0.1 ± 0.0	0.1* ± 0.0	0.1 ± 0.0
C22.4		0.4 ± 0.0				
C22.5		0.7 ± 0.0				
C22.0	0.2* ± 0.0	1.0 ± 0.0		0.5* ± 0.0		
C22.6	0.3* ± 0.0	0.8* ± 0.0		0.1 ± 0.0	0.1*± 0.0	
C24.0	0.3 ± 0.0					

*Significantly different ($\alpha=0.05$). The fatty acid composition for each organism was statistically compared before and after hydrolysis. The absence of an asterisk on a single fatty acid for *P. tsukubaensis*, *P. hubeiensis*, or *C. iriomotense* before and after hydrolysis is an indication of a lack of significant differences statistically.

while there was no significant difference in the palmitoleic acid content before and after hydrolysis.

There were many other differences between the fatty acid compositions before and after hydrolysis (Table 4.3). For example, levels of palmitic acid significantly increased after hydrolysis for all three oleaginous organisms. Palmitoleic acid statistically significantly increased ($p < 0.01$) after hydrolysis for *P. tsukubaensis*, *P. hubeiensis*, and *C. iriomotense*. There was a significant difference statistically in the palmitoleic acid content before and after hydrolysis for *P. tsukubaensis*, *P. hubeiensis*, and *C. iriomotense*. Stearic acid significantly increased after hydrolysis for *P. tsukubaensis* and *P. hubeiensis*, yet the P-value of 0.32 showed that no significant differences statistically were observed for *C. iriomotense* ($P \geq 0.05$). Comparison of oleic acid showed that there was a significant decrease after hydrolysis for *P. tsukubaensis*, *P. hubeiensis*,

and *C. iriomotense* ($P < 0.01$). These observed variations in fatty acid profiles before and after hydrolysis could be possibly because microbial lipids were derivatized before hydrolysis for fatty acid quantification while recovered fatty acids (no glycerol present) after hydrolysis were derivatized for fatty acids quantification. While the mechanism responsible for these changes is not understood, the data demonstrate that the fatty acids isolated from all three oleaginous organisms are comprised of molecules that are excellent substrates for the LTH process (Asomaning et al., 2014b; Espinosa-Gonzalez, Asomaning, et al., 2014).

4.5. Characterization of products generated through pyrolysis of hexane-extracted fatty acids

4.5.1. Quantification of liquid and gas fractions

After confirming that fatty acids could be isolated from the hydrolysates of the three oleaginous organisms, the three fatty acid feedstocks were integrated into the second step (i.e. pyrolysis) of the LTH process to generate hydrocarbon fuels. The pyrolysis step led to the formation of a liquid product and a gaseous product, with no formation of a solid product fraction. A similar distribution between the liquid and gaseous products was observed in all three experiments (Table 4.5), with liquid and gas products accounting for roughly 75% and 25%, respectively. It should be noted that the liquid product fractions were determined by weighing samples, while the gas fractions were calculated by difference.

Table 4.5: Pyrolysis product distribution

Source of hexane-extracted fatty acids	Weight % of feed	
	Liquid product fraction	Gas product fraction
<i>P. tsukubaensis</i>	73.6 ± 1.6 ^a	26.4 ± 1.5 ^a
<i>P. hubeiensis</i>	78.2 ± 1.3 ^a	21.8 ± 1.3 ^b
<i>C. iriomotense</i>	75.8 ± 8.8 ^a	24.2 ± 8.8 ^a

Data are generated from triplicate experiments and reported as the mean ± standard deviation. Within each column, values denoted with a different letter (i.e. a, b, or c) are statistically significantly different ($P < 0.05$).

4.5.2 Characterization of the gas fractions obtained through pyrolysis

The characterization of the gas product fractions generated through pyrolysis was performed using GC-FID and TCD. The gases present in the gas fraction were alkanes, alkenes, carbon monoxide, carbon dioxide, and hydrogen gases (Figure 4.21, 4.22, and Table 4.6). Other than nitrogen, which comprised the headspace for the pyrolysis reactions, the C1-C4 alkanes represented the largest class of gas product for experiments performed using *P. hubeiensis* ($19.3 \pm 0.04\%$) and *P. tsukubaensis* ($29.8 \pm 0.04\%$). A closer look at the peaks in the FID chromatogram (Figure 4.21) confirmed that among the C1-C4 alkane gases, ethane was the most abundant hydrocarbon present, followed by methane, propane, and finally butane. It should also be noted that there were no statistical differences observed amongst the C1-C4 gases obtained in experiments with *P. tsukubaensis* and *P. hubeiensis*. This was anticipated as the fatty acids isolated through hexane extraction of the two yeast hydrolysates were shown to be virtually identical

(Figure 4.20). Interestingly, the gas fraction obtained in experiments with *C. iriomotense* produced relatively low levels of C1-C4 alkanes (methane, ethane, propane, and butane). This observation may be attributed to the variations in fatty acid content due to yeast varietal differences when comparing *C. iriomotense* to *P. tsukubaensis* and *P. hubeiensis*. Nitrogen content in the gas fraction of *C. iriomotense* was up to 70%, significantly greater than the nitrogen present in the gas fractions of *P. tsukubaensis* and *P. hubeiensis* (Table 4.6 and Figure 4.22). Recall that nitrogen was used to purge the reactors three times at 500 psi to create an inert atmosphere in the pyrolysis reactors before commencing pyrolysis properly, it could be possible that the effect of varietal differences may have led to the nitrogen being diffused, trapped, and retained in *C. iriomotense* but not in *P. tsukubaensis* and *P. hubeiensis* since the procedure applied was the same. Different amounts of C2-C4 alkenes and C5+ alkanes/alkenes were also observed in the gas pyrolysis products generated in experiments with the three yeast strains. (Asomaning et al., 2014c, 2014a; Chew & Bhatia, 2008; Sotoudehniakarani et al., 2019; Wen et al., 2019). The observed nitrogen in the gas fraction was previously reported by Asomaning *et al* (2014) and Maher *et al* (2008) and was attributed as a result of the manual injection of the gas fraction to the gas analyzer. This observed high nitrogen content could possibly be part of the result of manual injection effects aside from the effects of varietal differences.

Table 4.6: Gas fraction components generated through pyrolysis of hexane-extracted fatty acids

Gas components	Weight percentage (%)		
	<i>P. tsukubaensis</i>	<i>P. hubeiensis</i>	<i>C. iriomotense</i>
C1-C4 alkane	29.8 ± 0.04*	19.3 ± 0.04	6.4 ± 0.04*
C2-C4 alkene	12.3 ± 0.02*	7.8 ± 0.02	3.4 ± 0.02*
C5+ alkanes/alkenes	7.6 ± 0.01	4.7 ± 0.01	1.9 ± 0.01
Carbon monoxide	9.5 ± 0.04*	5.5 ± 0.04	3.8 ± 0.04*
Carbon dioxide	11.9 ± 0.07	16.2 ± 0.07	11.7 ± 0.07
Hydrogen	0.5 ± 0.00*	0.3 ± 0.00	0.1 ± 0.00*
Nitrogen	29.1 ± 0.05*	43.2 ± 0.05	70.7 ± 0.05*
Oxygen	0.3 ± 0.01	3.0 ± 0.01	2.0 ± 0.01

*Significantly different ($\alpha=0.05$)

Data are generated from triplicate experiments and reported as the mean ± standard deviation. The gas component for *P. tsukubaensis*, *P. hubeiensis*, and *C. iriomotense* with a star symbol (*) denotes that there is a statistically significant difference ($P < 0.05$) between the starred organisms. A lack of a star symbol for a particular gas component for an organism denotes no statistical differences. There is no significant difference between samples that are unstarred.

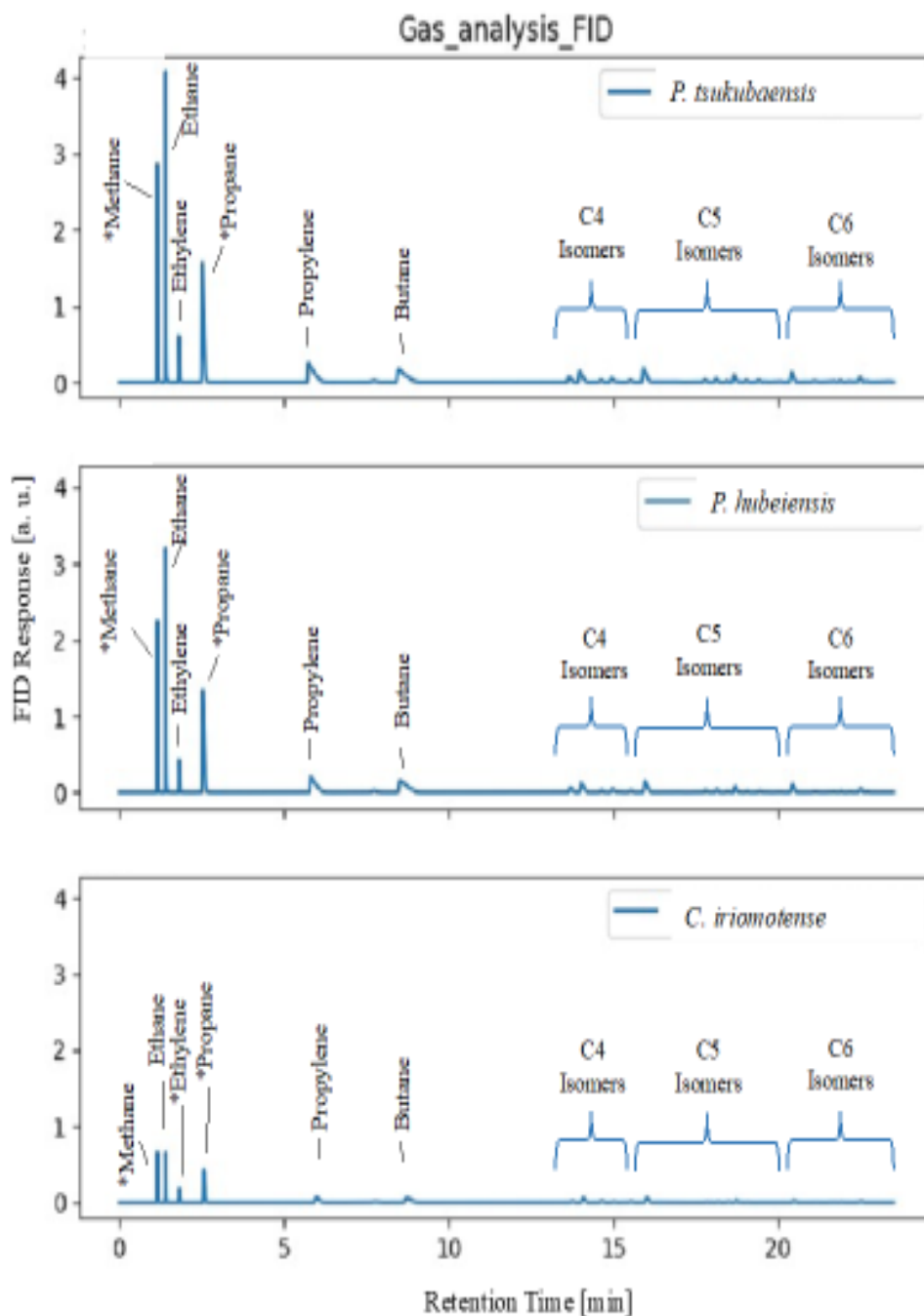


Figure 4.21: The GC-FID chromatograms of hydrocarbons in the gas fraction generated through pyrolysis (410 °C) of the hexane-extracted fatty acids obtained from *P. hubeiensis*, *P. tsukubaensis*, and *C. iriomotense* hydrolysates.

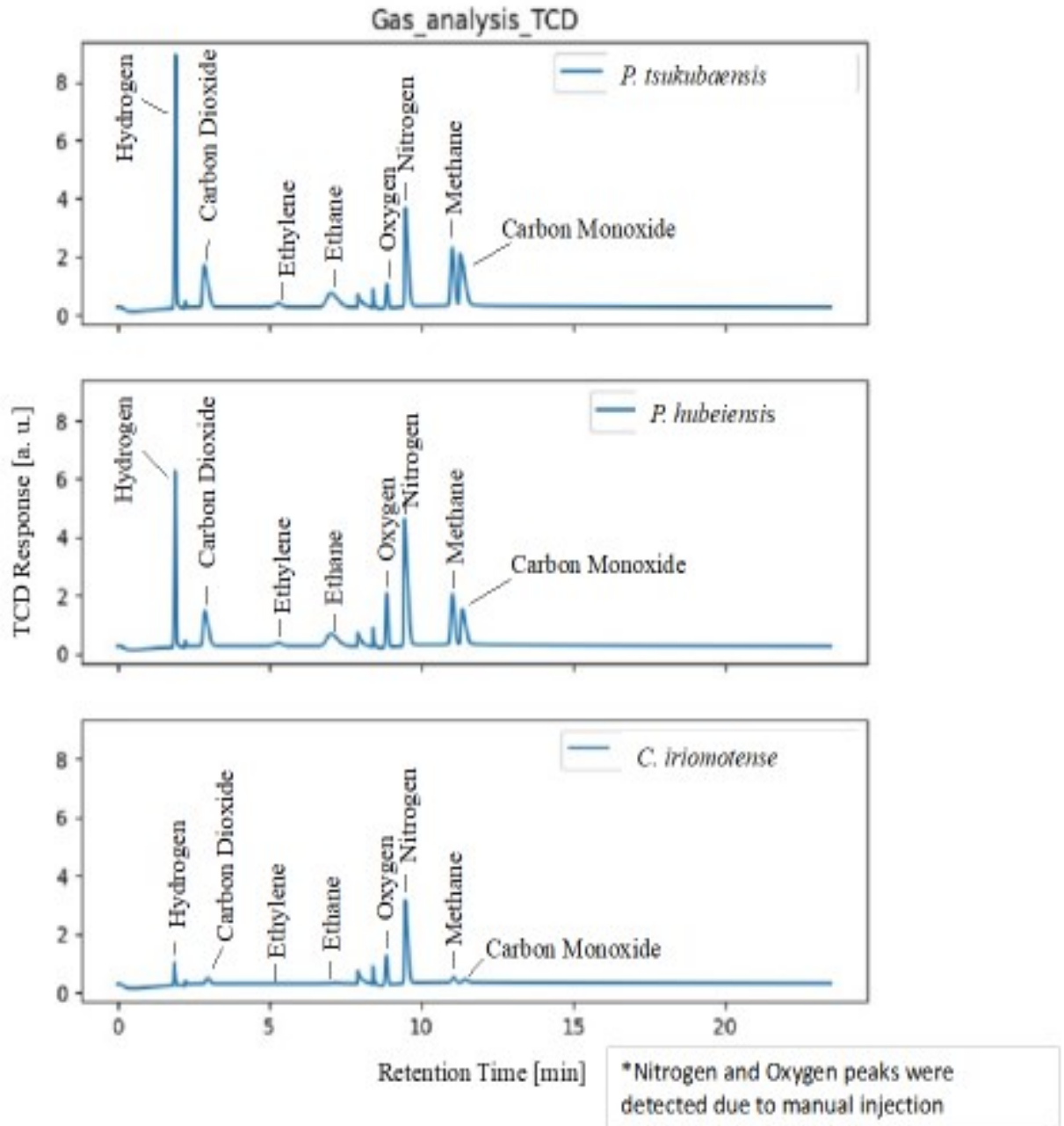


Figure 4.22: The GC-TCD chromatograms of hydrocarbons in the gas fraction generated through pyrolysis (410 °C) of the hexane-extracted fatty acids obtained from *P. hubeiensis*, *P. tsukubaensis*, and *C. iriomotense* hydrolysates.

Carbon dioxide (CO₂) and carbon monoxide (CO) were present in the gas fractions obtained using lipids derived from all three organisms (Table 4.6). The presence of CO in the pyrolytic gas fraction signifies the occurrence of deoxygenation via a decarbonylation reaction and CO₂ formation showed that deoxygenation occurred through decarboxylation reactions (Asomaning et al., 2014a). Other authors reported that CO and CO₂ were seen in the gas product fraction after pyrolysis of TAG and saturated/unsaturated fatty acids (Asomaning, 2014; Asomaning et al., 2014a, 2014c, 2014b, 2016; Espinosa-Gonzalez, Asomaning, et al., 2014; Omidghane et al., 2020).

Small amounts of H₂ gas were observed in all three experiments and may have resulted from a reaction between CO and water leading to the formation of H₂ and CO₂ via a water gas shift reaction (Asomaning et al., 2014a; Omidghane et al., 2017, 2020). Alternatively, hydrogen formation may result from dehydrogenation reactions and polymerization reactions that occur during the formation of aromatic compounds but were not observed in the pyrolysis conditions used in this research. Similarly, small levels of oxygen were observed in all three gas fractions, though this likely resulted from the manual injection of the gas fractions to the GC for characterization. This observation corroborates with the findings of previous researchers. Purging of the reactors with nitrogen created nitrogen headspace in the reactor before pyrolysis, so a higher quantity of nitrogen after hydrolysis possibly may signal a lesser quantity of gaseous hydrocarbon in the gas fraction as indicated in the chromatogram from TCD and FID (Figure 4.20 and 4.21) but not necessarily an indication of lack of pyrolysis reaction but possibly a varietal response to pyrolysis reaction.

4.5.3 Characterization of the liquid fractions obtained through pyrolysis

The liquid fractions generated from pyrolysis of hexane-extracted lipids obtained from the three oleaginous yeasts were characterized using GC-FID/MS. The peaks generated were matched by comparison with the National Institute of Standards and Technology (NIST) mass spectral library to facilitate their identification. The classes of compound identified were *n*-alkanes, 1-alkenes, internal alkenes, branched hydrocarbons, cyclic hydrocarbons, fatty acids, and aromatic hydrocarbons (Figure 4.23). It should be noted that some products could not be accurately identified or were unaccounted for, though the amounts varied depending on the experiment.

The chromatograms clearly showed that the products generated from fatty acids from all three organisms ranged in carbon number from C4 to C17 (Figure 4.23). Of the identified compounds, alkanes comprised the largest fraction within the liquid products: $37.3 \pm 0.02\%$ for *P. tsukubaensis*, $47.8 \pm 0.02\%$ for *P. hubeiensis*, and $31.6 \pm 0.02\%$ for *C. iriomotense*. The high content of the *n*-alkane class in the liquid product fraction corroborated with the reported findings of other researchers (Asomaning et al., 2014c; Espinosa-Gonzalez, Asomaning, et al., 2014; Maher et al., 2008).

It is important to mention that the chromatogram distinctively indicated the spike in C15 and C17 hydrocarbons (Figure 4.23). This observation was also reported by other researchers (Asomaning et al., 2014c; Espinosa-Gonzalez, Asomaning, et al., 2014; Omidghane et al., 2017, 2020), who confirmed that it was caused by direct deoxygenation of C16 and C18 fatty acids to C15 and C17 hydrocarbons during pyrolysis. As discussed previously, fatty acid profiling revealed the predominance of C16 and C18 fatty acids in *P. tsukubaensis* and *C. iriomotense*, *P. hubeiensis* (Figures 4.12, 4.15, and 4.18).

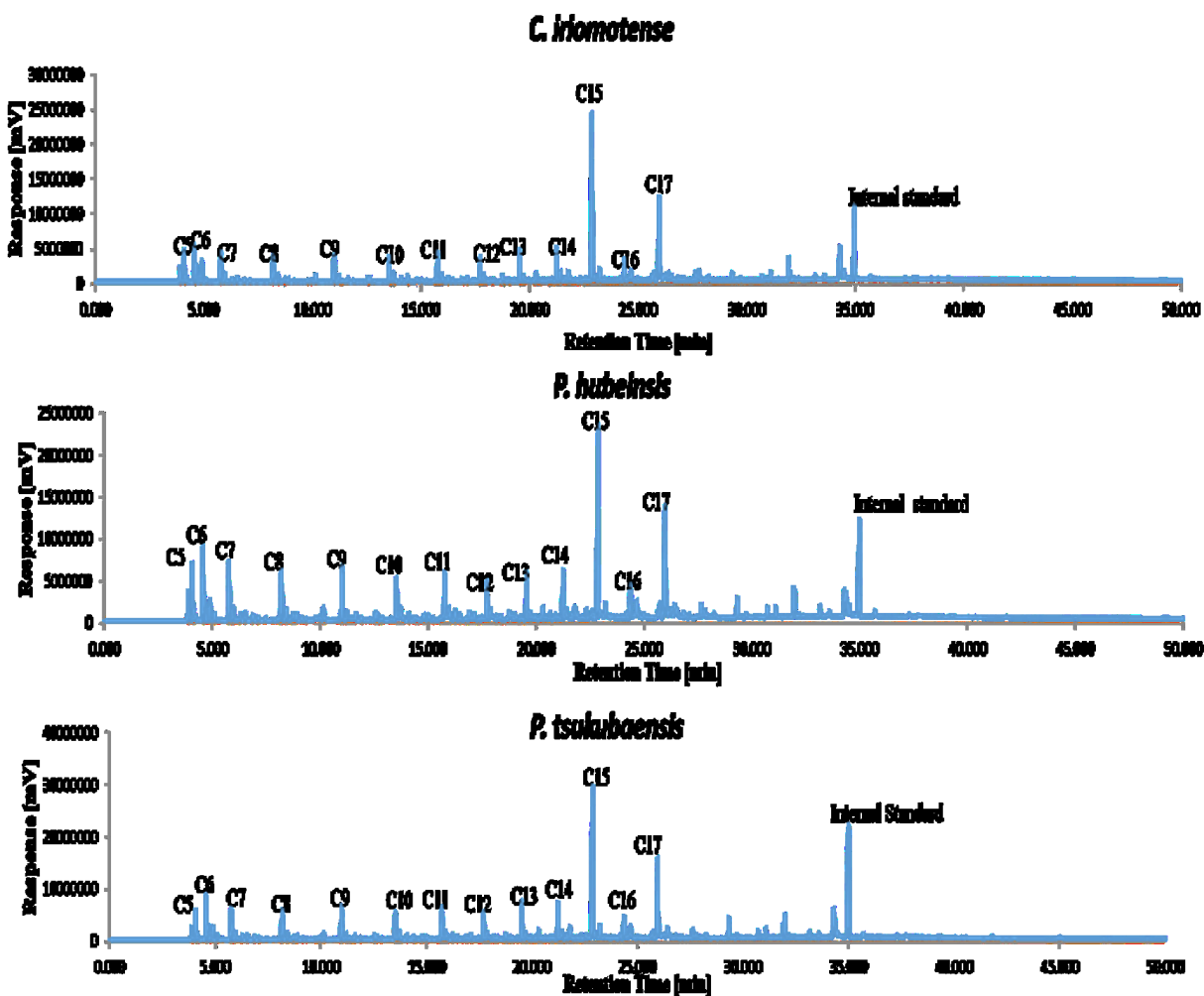


Figure 4.23: The GC-FID chromatograms of hydrocarbons in the liquid fractions generated through pyrolysis (410 °C) of the hexane-extracted fatty acids obtained from *P. hubeiensis*, *P. tsukubaensis*, and *C. iriomotense* hydrolysates.

Relatively low levels of 1-alkenes, internal alkenes, branched hydrocarbons, cyclic hydrocarbons, and aromatic hydrocarbons were observed in the liquid pyrolysis products generated from fatty acids sourced from the three oleaginous yeasts (Figure 4.24). For 1-alkenes, cyclic hydrocarbons, and aromatic hydrocarbons, there were no statistical differences observed between the three different experiments. Conversely, there were small yet statistical differences between the levels of internal alkenes and branched hydrocarbons in the liquid product generated

from the three different yeasts. Nevertheless, the overall trends observed from these categories of molecules were comparable in all three liquid pyrolysis products.

It should be noted that fatty acids were observed in the liquid pyrolysis product: $10.2 \pm 0.1\%$ for *P. tsukubaensis*, $5.4 \pm 0.1\%$ for *P. hubeiensis*, and $9.8 \pm 0.1\%$ for *C. iriomotense*. It is likely that these values represent unreacted fatty acids from the original pyrolysis feedstock. Thus, it is possible that further optimization of pyrolysis conditions for the fatty acids extracted from the three different yeast hydrolysates could result in the improved conversion of fatty acids to hydrocarbon fuels.

Other sets of the liquid fraction class were the unaccounted and unidentified classes. The unidentified class belongs to peaks that were eluted but could not be identified using the NIST mass spectral library. While the class of compound referred to as unaccounted alludes to the class that was not eluted in the chromatogram, which probably escaped detection because they are lower molecular weight compounds or higher molecular weight compounds. In all three experiments, there were substantial amounts of unidentified compounds, though the amounts depended on the organism from which the fatty acids were sourced, ranging from $13.5 \pm 0.2\%$ to $27.9 \pm 0.02\%$. Similarly, high levels of the unaccounted class were shown, ranging from $10.1 \pm 0.02\%$ to $36.4 \pm 0.02\%$, again depending on which oleaginous yeast was used in the experiments. Further optimization of pyrolysis conditions, as well as protocols and columns used for GC, may help to reduce the amount of unaccounted and unidentified classes. Nevertheless, characterization of the liquid product generated through the pyrolysis of fatty acids derived from *P. hubeiensis*, *P. tsukubaensis*, and *C. iriomotense* has confirmed the great potential of integrating these oleaginous yeast strains into the LTH process for the production of renewable biofuels.

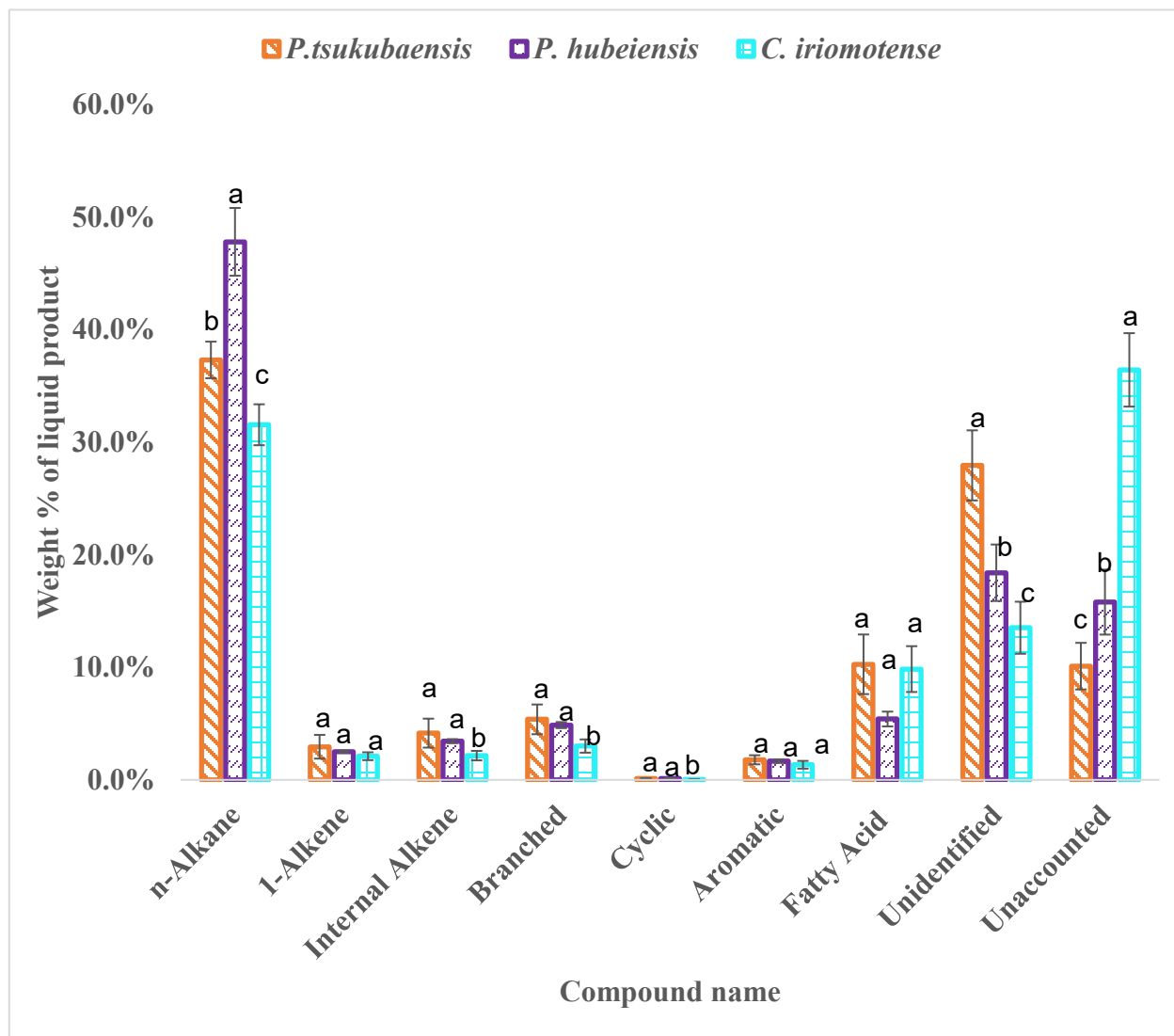


Figure 4.24: Classes of compounds in the liquid pyrolysis product generated from hexane-extracted fatty acids from *P. hubeiensis*, *P. tsukubaensis*, and *C. iriomotense*. Within each class, values denoted with different letters a, b, or c is significantly different ($P < 0.05$).

4.5.4. Characterization of the liquid pyrolysis product through FTIR-ATR

The liquid fractions generated through pyrolysis of fatty acids derived from oleaginous yeasts were subjected to FTIR-ATR to facilitate further characterization (Figure 4.25). The

presence of the C=O functional groups (stretch) at 1710 – 1720 cm^{-1} and C-O stretches at 1250 cm^{-1} (Figure 4.25) confirm that complete deoxygenation of fatty acids did not occur. This was anticipated given that a substantial amount of residual fatty acids were identified in the liquid pyrolysis product through GC-MS.

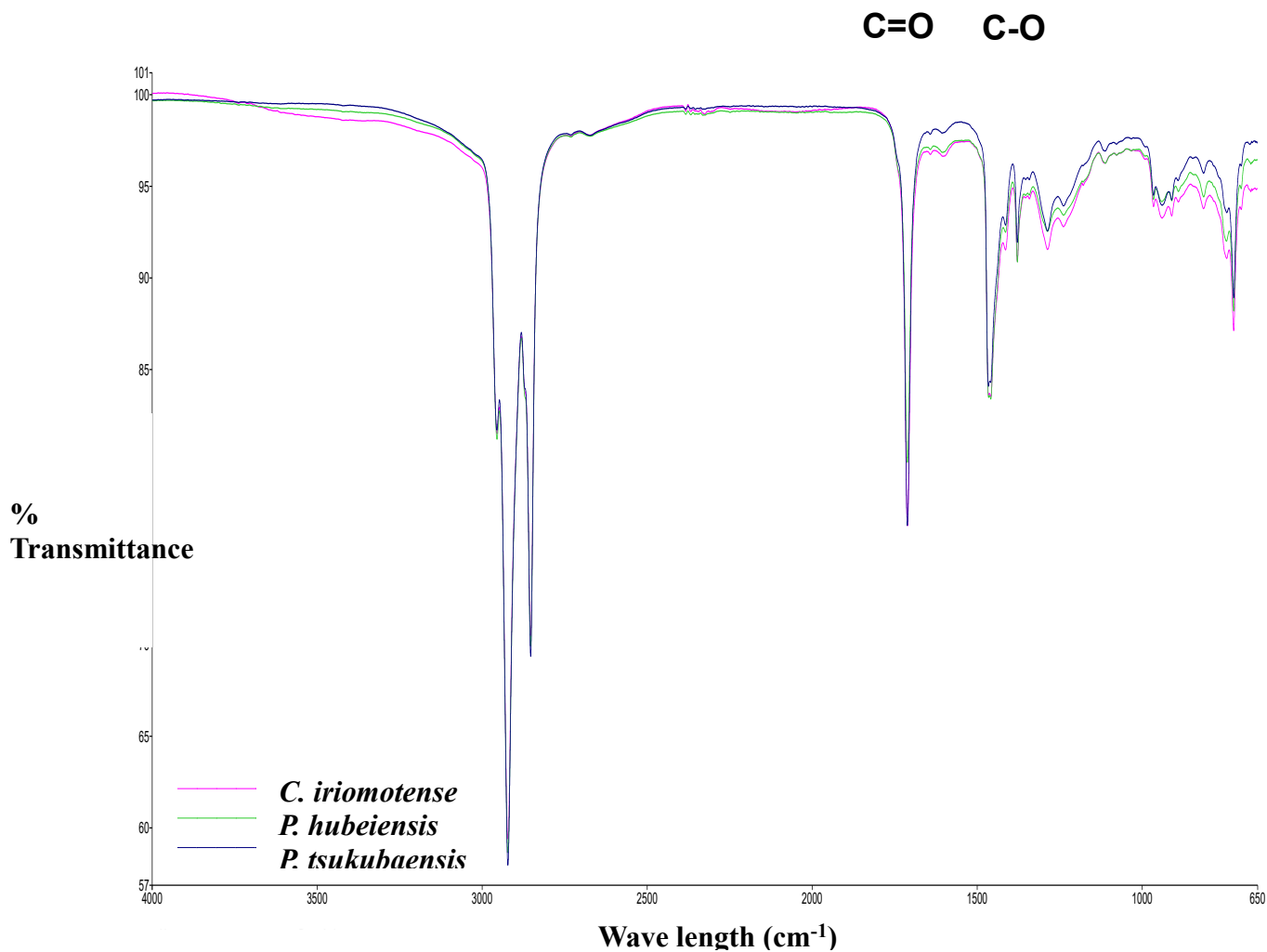


Figure 4.25: FTIR spectra of the liquid product generated through pyrolysis of fatty acids derived from *P. hubeiensis*, *P. tsukubaensis*, or *C. iriomotense*

4.6 Overall conclusions from of the integration of oleaginous yeasts into the LTH process

The hydrolysis of slurries of the three oleaginous yeasts was shown to successfully produce fatty acids that could be isolated through simple hexane extraction. Although the absolute levels of the various fatty acids did vary depending on the yeast, in all three cases, the most abundant fatty acids after hydrolysis were oleic acid, linoleic acid, palmitic acid, and stearic acid. These C16 and C18 fatty acids have been shown to be excellent substrates for the LTH process, thus demonstrating the promise of *P. hubeiensis*, *P. tsukubaensis*, or *C. iriomotense* for the production of lipids for biofuel applications. Furthermore, pyrolysis of the three different fatty acid feedstocks generated a hydrocarbon stream rich in alkanes and other fuel molecules. Taken together, the data presented in this section provide proof of concept that the lipids generated by *P. hubeiensis*, *P. tsukubaensis*, and *C. iriomotense* through growth on mixed C5 and C6 sugars can serve as a feedstock for the LTH technology.

Chapter 5 General conclusions, recommendations, and future directions

5.1. General conclusions

Simultaneous consumption of C5 and C6 sugars for lipid production was achieved by *P. hubeiensis*, *P. tsukubaensis*, and *C. iriomotense*. This study demonstrated that *P. hubeiensis* and *P. tsukubaensis* utilized glucose and xylose in the medium efficiently and are preferred to *C. iriomotense* for the production of lipids in both shake flask and bioreactor studies. Nevertheless, it should be mentioned that further optimization of growth conditions and/or medium could improve sugar consumption and lipid accumulation in *C. iriomotense*. The high levels of lipid accumulation

observed in the nitrogen-limiting medium containing both glucose and xylose may offer an opportunity and significant interest for biofuel producers that want to utilize lignocellulosic feedstocks that are rich in C5 and C6 sugars. For such industrial applications, the data presented in this thesis highlight the need to characterize growth and lipid accumulation in the oleaginous organism of choice as the onset of the stationary phase may likely reduce overall lipid yields.

The hydrolysis of the microbial slurries successfully broke down the TAGs, resulting in the formation of free fatty acids and glycerol. The fatty acid profiles observed from experiments with all three oleaginous organisms resembled that of vegetable oil, which is also characterized by having high levels of palmitic acid, stearic acid, oleic acid, and linoleic acid. Subsequent pyrolysis of the fatty acids extracted from yeast hydrolysates using hexane generated a liquid product with promising biofuel applications. This includes the presence of *n*-alkanes, *1*-alkenes, internal alkenes, branched hydrocarbons, aromatic hydrocarbons, and cyclic hydrocarbons.

Taken together, this research has successfully demonstrated that three different oleaginous yeasts, *P. hubeiensis*, *P. tsukubaensis*, and *C. iriomotense*, can simultaneously utilize glucose and xylose to generate high levels of lipids. Furthermore, the lipids generated by these yeasts can serve as the lipid feedstock for the LTH process towards the generation of hydrocarbons. Thus, the data presented in this thesis provides foundational work for using microbes for the bioconversion of lignocellulosic materials for the production of renewable drop-in fuels.

5.2 Recommendations and future directions

Future work in this space should focus on the optimization of various stages within the overall process. For example, with regards to the cultivation of oleaginous organisms, different growth mediums should be assessed to determine their impact on growth and lipid accumulation.

This includes examining different carbon to nitrogen ratios, varying the levels of minerals and salts, and even altering the medium pH. These studies may identify strategies to improve growth and lipid accumulation in *P. tsukubaensis* and *P. hubeiensis* and may result in complete sugar utilization by *C. iriomotense*. In addition, it would be very interesting to cultivate these oleaginous organisms in sugar streams derived from the hydrolysis of actual lignocellulosic substrates.

In addition, the conditions used for the pyrolysis of the fatty acids derived from the oleaginous organisms should also be examined further as a substantial amount of fatty acids were observed in the liquid pyrolysis product. Although pyrolysis conditions have been optimized for model fatty acids, the complex nature of lipids extracted from complex microbial systems has an impact on the pyrolysis step. These studies will need to be performed using fatty acids from all three yeasts as there could be differences between these three feedstocks.

This work addresses fuel/energy security in the sense that it would be able to reduce overdependence on fossil fuel if employed on industrial-scale production thereby conserving fossil fuel/energy. Converting lignocellulose to hydrolysates (sugars) for microbial consumption for TAG production for onward transformation to fatty acids as feedstock for renewable hydrocarbon production (drop-in fuel) via pyrolysis is a form of energy resource supplementation. Though a substantial portion of the feedstock may be lost during all the conversion steps the quality of the drop in fuel is equivalent to fossil fuel, reliable, accessible, readily available, acceptable, and viable. In terms of economic viability based on carbon usage, it is viable as industry nationally and globally would benefit from this research work as an alternative technological source for drop-in fuel production using microbes which will save us when the impending doom (imminent danger) of complete depletion of fossil fuel reservoir strikes.

Finally, since *P. tsukubaensis*, *P. hubeiensis*, and *C. iriomotense* can simultaneously utilize

glucose and xylose they must have a unique transporter for the assimilation of these sugars. Thus, the transport mechanism(s) should be investigated as this may lead to the development of other yeast strains that can simultaneously utilize glucose and xylose. Furthermore, a better understanding of the metabolic pathway(s) responsible for the simultaneous utilization of hexose and pentose sugars in non-conventional yeasts could also promote the development of genetic engineering strategies to generate superior microbes for bioconversion of lignocellulosic materials.

By engaging in these further studies, there will be a better understanding of how to grow microbes using lignocellulosic feedstocks to produce lipids. While lipids have tremendous applications in biofuel industries, there are also other applications for lipids in the nutraceutical and cosmetic industries. Thus, these studies may have far-reaching applications to other industries, and may even facilitate the development of biorefining strategies that will generate multiple value-added products from a single feedstock, which in turn will help to advance the bio-industrial sector as a whole.

References

- Abas, N., Khan, N., Haider, A., Iqbal, S., & Shahbaz, M. (2018). CO₂ Utilization Drivers, Opportunities and Conversion Challenges. In *Reference Module in Materials Science and Materials Engineering*. Elsevier. <https://doi.org/10.1016/B978-0-12-803581-8.10494-1>
- Abdel-Mawgoud, A. M., & Stephanopoulos, G. (2018). Simple glycolipids of microbes: Chemistry, biological activity and metabolic engineering. *Synthetic and Systems Biotechnology*, 3(1), 3–19. <https://doi.org/10.1016/j.synbio.2017.12.001>
- Abdullah, B., Muhammad, S. A. F. S., Shokravi, Z., Ismail, S., Kassim, K. A., Mahmood, A. N., & Aziz, M. M. A. (2019). Fourth generation biofuel: A review on risks and mitigation strategies. *Renewable and Sustainable Energy Reviews*, 107, 37–50.
- Adams, C., Godfrey, V., Wahlen, B., Seefeldt, L., & Bugbee, B. (2013). Understanding precision nitrogen stress to optimize the growth and lipid content tradeoff in oleaginous green microalgae. *Bioresource Technology*, 131, 188–194.
- Adegboye, M. F., Ojuederie, O. B., Talia, P. M., & Babalola, O. O. (2021). Bioprospecting of microbial strains for biofuel production: metabolic engineering, applications, and challenges. *Biotechnology for Biofuels*, 14(1), 5. <https://doi.org/10.1186/s13068-020-01853-2>
- Adnan, M., Zheng, W., Islam, W., Arif, M., Abubakar, Y. S., Wang, Z., & Lu, G. (2018). Carbon Catabolite Repression in Filamentous Fungi. In *International Journal of Molecular Sciences* (Vol. 19, Issue 1). <https://doi.org/10.3390/ijms19010048>
- Adsul, M. G., Bastawde, K. B., & Gokhale, D. V. (2009). Biochemical characterization of two xylanases from yeast *Pseudozyma hubeiensis* producing only xylooligosaccharides. *Bioresource Technology*, 100(24), 6488–6495. <https://doi.org/10.1016/j.biortech.2009.07.064>
- Agarwal, A. K. (2007). Biofuels (alcohols and biodiesel) applications as fuels for internal combustion engines. *Progress in Energy and Combustion Science*, 33(3), 233–271. <https://doi.org/10.1016/j.peccs.2006.08.003>
- Akhundi, A., Habibi-Yangjeh, A., Abitorabi, M., & Rahim Pourn, S. (2019). Review on photocatalytic conversion of carbon dioxide to value-added compounds and renewable fuels by graphitic carbon nitride-based photocatalysts. *Catalysis Reviews*, 61(4), 595–628.
- Alalwan, H. A., Alminshid, A. H., & Aljaafari, H. A. S. (2019). Promising evolution of biofuel generations. Subject review. *Renewable Energy Focus*, 28, 127–139. <https://doi.org/10.1016/j.ref.2018.12.006>
- Amaniampong, P. N., Asiedu, N. Y., Fletcher, E., Dodoo-Arhin, D., Olatunji, O. J., & Trinh, Q. T. (2020). Conversion of Lignocellulosic Biomass to Fuels and Value-Added Chemicals Using Emerging Technologies and State-of-the-Art Density Functional Theory Simulations Approach. In *Valorization of Biomass to Value-Added Commodities* (pp. 193–220). Springer.

- Ami, D., Posterì, R., Mereghetti, P., Porro, D., Doglia, S. M., & Branduardi, P. (2014). Fourier transform infrared spectroscopy as a method to study lipid accumulation in oleaginous yeasts. *Biotechnology for Biofuels*, 7(1), 12. <https://doi.org/10.1186/1754-6834-7-12>
- Anastasi, A., Varese, G. C., Bosco, F., Chimirri, F., & Marchisio, V. F. (2008). Bioremediation potential of basidiomycetes isolated from compost. *Bioresource Technology*, 99(14), 6626–6630.
- Annamalai, N., Sivakumar, N., & Oleskowicz-Popiel, P. (2018). Enhanced production of microbial lipids from waste office paper by the oleaginous yeast *Cryptococcus curvatus*. *Fuel*, 217, 420–426.
- Arvindnarayan, S., Sivagnana Prabhu, K. K., Shobana, S., Kumar, G., & Dharmaraja, J. (2017). Upgrading of micro algal derived bio-fuels in thermochemical liquefaction path and its perspectives: A review. *International Biodeterioration & Biodegradation*, 119, 260–272. <https://doi.org/10.1016/j.ibiod.2016.08.011>
- Asomaning, J. (2014). *Thermal cracking of lipids to produce renewable fuels and platform chemicals*.
- Asomaning, J., Mussone, P., & Bressler, D. C. (2014a). Pyrolysis of polyunsaturated fatty acids. *Fuel Processing Technology*, 120, 89–95. <https://doi.org/10.1016/j.fuproc.2013.12.007>
- Asomaning, J., Mussone, P., & Bressler, D. C. (2014b). Thermal deoxygenation and pyrolysis of oleic acid. *Journal of Analytical and Applied Pyrolysis*, 105, 1–7.
- Asomaning, J., Mussone, P., & Bressler, D. C. (2014c). Two-stage thermal conversion of inedible lipid feedstocks to renewable chemicals and fuels. *Bioresource Technology*, 158, 55–62. <https://doi.org/10.1016/j.biortech.2014.01.136>
- Asomaning, J., Omidghane, M., Chae, M., & Bressler, D. C. (2016). Thermal processing of algal biomass for biofuel production. *Current Opinion in Green and Sustainable Chemistry*, 2, 1–5. <https://doi.org/10.1016/j.cogsc.2016.08.005>
- Atsonios, K., Kougioumtzis, M.-A., Panopoulos, K., & Kakaras, E. (2015). Alternative thermochemical routes for aviation biofuels via alcohols synthesis: Process modeling, techno-economic assessment and comparison. *Applied Energy*, 138, 346–366. <https://doi.org/10.1016/j.apenergy.2014.10.056>
- Baloch, H. A., Nizamuddin, S., Siddiqui, M. T. H., Riaz, S., Jatoi, A. S., Dumbre, D. K., Mubarak, N. M., Srinivasan, M. P., & Griffin, G. J. (2018). Recent advances in production and upgrading of bio-oil from biomass: A critical overview. *Journal of Environmental Chemical Engineering*, 6(4), 5101–5118. <https://doi.org/10.1016/j.jece.2018.07.050>
- Banapurmath, N. R., Yaliwal, V. S., Adaganti, S. Y., & Halewadimath, S. S. (2019). Chapter 11 - Power Generation From Renewable Energy Sources Derived From Biodiesel and Low Energy Content Producer Gas for Rural Electrification. In D. Barik (Ed.), *Energy from Toxic Organic Waste for Heat and Power Generation* (pp. 151–194). Woodhead Publishing. <https://doi.org/10.1016/B978-0-08-102528-4.00011-0>
- Baroutian, S., Aroua, M. K., Raman, A. A. A., Shafie, A., Ismail, R. A., & Hamdan, H. (2013).

- Blended aviation biofuel from esterified *Jatropha curcas* and waste vegetable oils. *Journal of the Taiwan Institute of Chemical Engineers*, 44(6), 911–916.
<https://doi.org/10.1016/j.jtice.2013.02.007>
- Bartley, M. L., Boeing, W. J., Dungan, B. N., Holguin, F. O., & Schaub, T. (2014). pH effects on growth and lipid accumulation of the biofuel microalgae *Nannochloropsis salina* and invading organisms. *Journal of Applied Phycology*, 26(3), 1431–1437.
<https://doi.org/10.1007/s10811-013-0177-2>
- Bastawde, K. B., Puntambekar, U. S., & Gokhale, D. V. (1994). Optimization of cellulase-free xylanase production by a novel yeast strain. *Journal of Industrial Microbiology*, 13(4), 220–224. <https://doi.org/10.1007/BF01569752>
- Beck, A., Haitz, F., Grunwald, S., Preuss, L., Rupp, S., & Zibek, S. (2019). Influence of microorganism and plant oils on the structure of mannosylerythritol lipid (MEL) biosurfactants revealed by a novel thin layer chromatography mass spectrometry method. *Journal of Industrial Microbiology & Biotechnology*, 46(8), 1191–1204.
- Beck, A., Werner, N., & Zibek, S. (2019). *Chapter 4 - Mannosylerythritol Lipids: Biosynthesis, Genetics, and Production Strategies* (D. G. Hayes, D. K. Y. Solaiman, & R. D. B. T.-B. S. (Second E. Ashby (eds.); pp. 121–167). AOCs Press.
<https://doi.org/10.1016/B978-0-12-812705-6.00004-6>
- Ben-Iwo, J., Manovic, V., & Longhurst, P. (2016). Biomass resources and biofuels potential for the production of transportation fuels in Nigeria. *Renewable and Sustainable Energy Reviews*, 63, 172–192. <https://doi.org/10.1016/j.rser.2016.05.050>
- Bender, D. A. (2003). *TRICARBOXYLIC ACID CYCLE* (B. B. T.-E. of F. S. and N. (Second E. Caballero (ed.); pp. 5851–5856). Academic Press.
<https://doi.org/10.1016/B0-12-227055-X/01363-8>
- Bender, R. A. (2013). *Glycolysis* (S. Maloy & K. B. T.-B. E. of G. (Second E. Hughes (eds.); pp. 346–349). Academic Press. <https://doi.org/10.1016/B978-0-12-374984-0.00659-8>
- Bertilsson, M., Bertilsson, M., Andersson, J., Andersson, J., Lidén, G., & Lidén, G. (2008). Modeling simultaneous glucose and xylose uptake in *Saccharomyces cerevisiae* from kinetics and gene expression of sugar transporters. *Bioprocess and Biosystems Engineering*, 31(4), 369–377. <https://doi.org/10.1007/s00449-007-0169-1>
- Bhagavan, N. V., & Ha, C. E. (2015). Lipids I: Fatty acids and eicosanoids. *Essentials of Medical Biochemistry*, 2, 269–297.
- Biller, P., & Ross, A. B. (2016). 17 - Production of biofuels via hydrothermal conversion. In R. Luque, C. S. K. Lin, K. Wilson, & J. Clark (Eds.), *Handbook of Biofuels Production (Second Edition)* (pp. 509–547). Woodhead Publishing.
<https://doi.org/10.1016/B978-0-08-100455-5.00017-5>
- Blanco, A., & Blanco, G. (2017). *Chapter 14 - Carbohydrate Metabolism* (A. Blanco & G. B. T.-M. B. Blanco (eds.); pp. 283–323). Academic Press.
<https://doi.org/10.1016/B978-0-12-803550-4.00014-8>

- Boekhout, T., Fonseca, Á., Sampaio, J. P., Bandoni, R. J., Fell, J. W., & Kwon-Chung, K. J. (2011). Chapter 100 - Discussion of Teleomorphic and Anamorphic Basidiomycetous Yeasts. In *The Yeasts* (Fifth Edit, pp. 1339–1372). Elsevier B.V. <https://doi.org/10.1016/B978-0-444-52149-1.00100-2>
- Bratby, J. (2016). *Coagulation and flocculation in water and wastewater treatment*. IWA publishing.
- Britannica, T. (2020). of Encyclopaedia (2020). *LL Zamenhof. Encyclopedia Britannica*.
- Bruder, S., Hackenschmidt, S., Moldenhauer, E. J., & Kabisch, J. (2018). Chapter 12 - Conventional and Oleaginous Yeasts as Platforms for Lipid Modification and Production. In U. T. Bornscheuer (Ed.), *Lipid Modification by Enzymes and Engineered Microbes* (pp. 257–292). AOCS Press. <https://doi.org/10.1016/B978-0-12-813167-1.00012-8>
- Bueno, J. G. R., Borelli, G., Corrêa, T. L. R., Fiamenghi, M. B., José, J., de Carvalho, M., de Oliveira, L. C., Pereira, G. A. G., & Dos Santos, L. V. (2020). Novel xylose transporter Cs4130 expands the sugar uptake repertoire in recombinant *Saccharomyces cerevisiae* strains at high xylose concentrations. *Biotechnology for Biofuels*, *13*(1), 1–20.
- Bwapwa, J. K., Anandraj, A., & Trois, C. (2018). Microalgae processing for jet fuel production. *Biofuels, Bioproducts & Biorefining*, *12*(4), 522–535. <https://doi.org/10.1002/bbb.1878>
- Cakmak, T., Angun, P., Demiray, Y. E., Ozkan, A. D., Elibol, Z., & Tekinay, T. (2012). Differential effects of nitrogen and sulfur deprivation on growth and biodiesel feedstock production of *Chlamydomonas reinhardtii*. *Biotechnology and Bioengineering*, *109*(8), 1947–1957.
- Campos, D. C., Dall'Oglio, E. L., de Sousa Jr, P. T., Vasconcelos, L. G., & Kuhnen, C. A. (2014). Investigation of dielectric properties of the reaction mixture during the acid-catalyzed transesterification of Brazil nut oil for biodiesel production. *Fuel*, *117*, 957–965.
- Caporusso, A., Capece, A., & De Bari, I. (2021). Oleaginous yeasts as cell factories for the sustainable production of microbial lipids by the valorization of agri-food wastes. *Fermentation*, *7*(2), 1–33. <https://doi.org/10.3390/fermentation7020050>
- Carsanba, E., Papanikolaou, S., & Erten, H. (2018). Production of oils and fats by oleaginous microorganisms with an emphasis given to the potential of the nonconventional yeast *Yarrowia lipolytica*. *Critical Reviews in Biotechnology*, *38*(8), 1230–1243. <https://doi.org/10.1080/07388551.2018.1472065>
- Castellví Barnés, M., Lange, J.-P., van Rossum, G., & Kersten, S. R. A. (2015). A new approach for bio-oil characterization based on gel permeation chromatography preparative fractionation. *Journal of Analytical and Applied Pyrolysis*, *113*, 444–453. <https://doi.org/10.1016/j.jaap.2015.03.005>
- Catchpole, O., Moreno, T., Montañes, F., & Tallon, S. (2018). Perspectives on processing of high value lipids using supercritical fluids. *The Journal of Supercritical Fluids*, *134*, 260–268. <https://doi.org/10.1016/j.supflu.2017.12.001>
- Cattaneo, S., Stucchi, M., Villa, A., & Prati, L. (2019). Gold Catalysts for the Selective Oxidation of Biomass-Derived Products. *ChemCatChem*, *11*(1), 309–323.

- Celenza, JOHN L, & Carlson, M. (1989). Mutational analysis of the *Saccharomyces cerevisiae* SNF1 protein kinase and evidence for functional interaction with the SNF4 protein. *Molecular and Cellular Biology*, 9(11), 5034.
- Celenza, John L, Marshall-Carlson, L., & Carlson, M. (1988). The yeast SNF3 gene encodes a glucose transporter homologous to the mammalian protein. *Proceedings of the National Academy of Sciences*, 85(7), 2130–2134.
- Chan, Y. H., Quitain, A. T., Yusup, S., Uemura, Y., Sasaki, M., & Kida, T. (2018). Liquefaction of palm kernel shell in sub- and supercritical water for bio-oil production. *Journal of the Energy Institute*, 91(5), 721–732. <https://doi.org/10.1016/j.joei.2017.05.009>
- Chen, Chen, Luo, Z., & Yu, C. (2019). Release and transformation mechanisms of trace elements during biomass combustion. *Journal of Hazardous Materials*, 380, 120857.
- Chen, Chunyi, Pan, G., Shi, W., Xu, F., Techtmann, S. M., Pfiffner, S. M., & Hazen, T. C. (2018). Clay flocculation effect on microbial community composition in water and sediment. *Frontiers in Environmental Science*, 6, 60.
- Chen, K., Zhang, L., Gholizadeh, M., Ai, N., Hasan, M. D. M., Mourant, D., Li, C.-Z., & Jiang, S. P. (2016). Feasibility of tubular solid oxide fuel cells directly running on liquid biofuels. *Chemical Engineering Science*, 154, 108–118. <https://doi.org/10.1016/j.ces.2016.04.024>
- Chen, W.-H., & Lin, B.-J. (2019). Chapter 13 - Thermochemical conversion of microalgal biomass. In A. Basile & F. Dalena (Eds.), *Second and Third Generation of Feedstocks* (pp. 345–382). Elsevier. <https://doi.org/10.1016/B978-0-12-815162-4.00013-6>
- Chen, X., Ma, X., Peng, X., Lin, Y., Wang, J., & Zheng, C. (2018). Effects of aqueous phase recirculation in hydrothermal carbonization of sweet potato waste. *Bioresource Technology*, 267, 167–174. <https://doi.org/10.1016/j.biortech.2018.07.032>
- Cheng, J. (2017). *Biomass to renewable energy processes*. CRC press.
- Chew, T. L., & Bhatia, S. (2008). Catalytic processes towards the production of biofuels in a palm oil and oil palm biomass-based biorefinery. *Bioresource Technology*, 99(17), 7911–7922. <https://doi.org/10.1016/j.biortech.2008.03.009>
- Chintagunta, A. D., Zuccaro, G., Kumar, M., Kumar, S. P. J., Garlapati, V. K., Postemsky, P. D., Kumar, N. S. S., Chandel, A. K., & Simal-Gandara, J. (2021). Biodiesel Production From Lignocellulosic Biomass Using Oleaginous Microbes: Prospects for Integrated Biofuel Production. *Frontiers in Microbiology*, 12.
- Cho, H. U., & Park, J. M. (2018). Biodiesel production by various oleaginous microorganisms from organic wastes. *Bioresource Technology*, 256, 502–508.
- Chreptowicz, K., Mierzejewska, J., Tkáčová, J., Mlynek, M., & Čertik, M. (2019). Carotenoid-producing yeasts: Identification and Characteristics of Environmental Isolates with a Valuable Extracellular Enzymatic Activity. *Microorganisms (Basel)*, 7(12), 653. <https://doi.org/10.3390/microorganisms7120653>
- Ciuta, S., Tsiamis, D., & Castaldi, M. J. (2018). Chapter Two - Fundamentals of Gasification and

- Pyrolysis. In S. Ciuta, D. Tsiamis, & M. J. Castaldi (Eds.), *Gasification of Waste Materials* (pp. 13–36). Academic Press. <https://doi.org/10.1016/B978-0-12-812716-2.00002-9>
- Compagno, C., Dashko, S., & Piškur, J. (2014). Introduction to Carbon Metabolism in Yeast. In J. Piškur & C. Compagno (Eds.), *Molecular Mechanisms in Yeast Carbon Metabolism* (pp. 1–19). Springer Berlin Heidelberg. https://doi.org/10.1007/978-3-642-55013-3_1
- da Cunha-Pereira, F., Hickert, L. R., Sehnem, N. T., de Souza-Cruz, P. B., Rosa, C. A., & Ayub, M. A. Z. (2011). Conversion of sugars present in rice hull hydrolysates into ethanol by *Spathaspora arborariae*, *Saccharomyces cerevisiae*, and their co-fermentations. *Bioresource Technology*, *102*(5), 4218–4225.
- Da Silva, P. D. M. P., Lima, F., Alves, M. M., Bijmans, M. F. M., & Pereira, M. A. (2016). Valorization of lubricant-based wastewater for bacterial neutral lipids production: Growth-linked biosynthesis. *Water Research*, *101*, 17–24. <https://doi.org/10.1016/j.watres.2016.05.062>
- Dabros, T. M. H., Stummann, M. Z., Høj, M., Jensen, P. A., Grunwaldt, J.-D., Gabrielsen, J., Mortensen, P. M., & Jensen, A. D. (2018). Transportation fuels from biomass fast pyrolysis, catalytic hydrodeoxygenation, and catalytic fast hydrolysis. *Progress in Energy and Combustion Science*, *68*, 268–309. <https://doi.org/10.1016/j.pecs.2018.05.002>
- Daful, A. G., & R Chandraratne, M. (2018). Biochar Production From Biomass Waste-Derived Material. In *Reference Module in Materials Science and Materials Engineering*. Elsevier. <https://doi.org/10.1016/B978-0-12-803581-8.11249-4>
- Danquah, M. K., Ang, L., Uduman, N., Moheimani, N., & Forde, G. M. (2009). Dewatering of microalgal culture for biodiesel production: exploring polymer flocculation and tangential flow filtration. *Journal of Chemical Technology & Biotechnology: International Research in Process, Environmental & Clean Technology*, *84*(7), 1078–1083.
- Davoli, P., & Weber, R. W. S. (2002). Carotenoid pigments from the red mirror yeast, *Sporobolomyces roseus*. *Mycologist*, *16*(3), 102–108.
- De Bhowmick, G., Sarmah, A. K., & Sen, R. (2018). Lignocellulosic biorefinery as a model for sustainable development of biofuels and value added products. *Bioresource Technology*, *247*, 1144–1154. <https://doi.org/10.1016/j.biortech.2017.09.163>
- De Bhowmick, G., Sarmah, A. K., & Sen, R. (2019). Zero-waste algal biorefinery for bioenergy and biochar: a green leap towards achieving energy and environmental sustainability. *Science of The Total Environment*, *650*, 2467–2482.
- Demirbas, A. (2007). Progress and recent trends in biofuels. *Progress in Energy and Combustion Science*, *33*(1), 1–18. <https://doi.org/10.1016/j.pecs.2006.06.001>
- Demirel, Y. (2018). 1.22 Biofuels. In I. Dincer (Ed.), *Comprehensive Energy Systems* (pp. 875–908). Elsevier. <https://doi.org/10.1016/B978-0-12-809597-3.00125-5>
- Deng, X., Fei, X., & Li, Y. (2011). The effects of nutritional restriction on neutral lipid accumulation in *Chlamydomonas* and *Chlorella*. *African Journal of Microbiology Research*, *5*(3), 260–270.

- Deutscher, J. (2008). The mechanisms of carbon catabolite repression in bacteria. *Current Opinion in Microbiology*, 11(2), 87–93.
- Dong, T., Knoshaug, E. P., Pienkos, P. T., & Laurens, L. M. L. (2016). Lipid recovery from wet oleaginous microbial biomass for biofuel production: A critical review. *Applied Energy*, 177, 879–895. <https://doi.org/10.1016/j.apenergy.2016.06.002>
- dos Santos, L. K., Hatanaka, R. R., de Oliveira, J. E., & Flumignan, D. L. (2019). Production of biodiesel from crude palm oil by a sequential hydrolysis/esterification process using subcritical water. *Renewable Energy*, 130, 633–640. <https://doi.org/10.1016/j.renene.2018.06.102>
- Dourou, M., Aggeli, D., Papanikolaou, S., & Aggelis, G. (2018). Critical steps in carbon metabolism affecting lipid accumulation and their regulation in oleaginous microorganisms. *Applied Microbiology and Biotechnology*, 102(6), 2509–2523. <https://doi.org/10.1007/s00253-018-8813-z>
- Du, Y., Schuur, B., Kersten, S. R. A., & Brilman, D. W. F. (2015). Opportunities for switchable solvents for lipid extraction from wet algal biomass: An energy evaluation. *Algal Research*, 11, 271–283. <https://doi.org/10.1016/j.algal.2015.07.004>
- Duarte, S., Lv, P., Almeida, G., Rolón, J. C., & Perré, P. (2017). Alteration of physico-chemical characteristics of coconut endocarp — *Acrocomia aculeata* — by isothermal pyrolysis in the range 250–550°C. *Journal of Analytical and Applied Pyrolysis*, 126, 88–98. <https://doi.org/10.1016/j.jaap.2017.06.021>
- Dulermo, T., Lazar, Z., Dulermo, R., Rakicka, M., Haddouche, R., & Nicaud, J.-M. (2015). Analysis of ATP-citrate lyase and malic enzyme mutants of *Yarrowia lipolytica* points out the importance of mannitol metabolism in fatty acid synthesis. *BBA - Molecular and Cell Biology of Lipids*, 1851(9), 1107–1117. <https://doi.org/10.1016/j.bbali.2015.04.007>
- Durak, H., & Genel, Y. (2018). Hydrothermal conversion of biomass (*Xanthium strumarium*) to energetic materials and comparison with other thermochemical methods. *The Journal of Supercritical Fluids*, 140, 290–301. <https://doi.org/10.1016/j.supflu.2018.07.005>
- Dutta, K., Daverey, A., & Lin, J.-G. (2014). Evolution retrospective for alternative fuels: First to fourth generation. *Renewable Energy*, 69, 114–122.
- Eibner, S., Margeriat, A., Broust, F., Laurenti, D., Geantet, C., Julbe, A., & Blin, J. (2017). Catalytic deoxygenation of model compounds from flash pyrolysis of lignocellulosic biomass over activated charcoal-based catalysts. *Applied Catalysis B: Environmental*, 219, 517–525. <https://doi.org/10.1016/j.apcatb.2017.07.071>
- Encinar, J. M., Gonzalez, J. F., & Rodríguez-Reinares, A. (2005). Biodiesel from used frying oil. Variables affecting the yields and characteristics of the biodiesel. *Industrial & Engineering Chemistry Research*, 44(15), 5491–5499.
- Erni, B., & Zanolari, B. (1986). Glucose-permease of the bacterial phosphotransferase system. Gene cloning, overproduction, and amino acid sequence of enzyme IIGlc. *Journal of Biological Chemistry*, 261(35), 16398–16403.
- Espinosa-Gonzalez, I., Asomaning, J., Mussone, P., & Bressler, D. C. (2014). Two-step thermal

- conversion of oleaginous microalgae into renewable hydrocarbons. *Bioresource Technology*, 158, 91–97. <https://doi.org/10.1016/j.biortech.2014.01.080>
- Espinosa-Gonzalez, I., Parashar, A., & Bressler, D. C. (2014a). Heterotrophic growth and lipid accumulation of *Chlorella protothecoides* in whey permeate, a dairy by-product stream, for biofuel production. *Bioresource Technology*, 155, 170–176.
- Espinosa-Gonzalez, I., Parashar, A., & Bressler, D. C. (2014b). Hydrothermal treatment of oleaginous yeast for the recovery of free fatty acids for use in advanced biofuel production. *Journal of Biotechnology*, 187, 10–15. <https://doi.org/10.1016/j.jbiotec.2014.07.004>
- Espinosa-Gonzalez, I., Parashar, A., Chae, M., & Bressler, D. C. (2014). Cultivation of oleaginous yeast using aqueous fractions derived from hydrothermal pretreatments of biomass. *Bioresource Technology*, 170, 413–420. <https://doi.org/10.1016/j.biortech.2014.08.006>
- Espinosa Gonzalez, M. I. (2014). *Development of technological alternatives to produce renewable fuels from oleaginous microorganisms.*
- Fai, A. E. C., da Silva, J. B., de Andrade, C. J., Bution, M. L., & Pastore, G. M. (2014). Production of prebiotic galactooligosaccharides from lactose by *Pseudozyma tsukubaensis* and *Pichia kluyveri*. *Biocatalysis and Agricultural Biotechnology*, 3(4), 343–350. <https://doi.org/10.1016/j.bcab.2014.04.005>
- Fakas, S. (2017). Lipid biosynthesis in yeasts: A comparison of the lipid biosynthetic pathway between the model nonoleaginous yeast *Saccharomyces cerevisiae* and the model oleaginous yeast *Yarrowia lipolytica*. *Engineering in Life Sciences*, 17(3), 292–302.
- Fakhry, E. M., & El Maghraby, D. M. (2015). Lipid accumulation in response to nitrogen limitation and variation of temperature in *Nannochloropsis salina*. *Botanical Studies*, 56(1), 1–8.
- Farwick, A., Bruder, S., Schadeweg, V., Oreb, M., & Boles, E. (2014). Engineering of yeast hexose transporters to transport D-xylose without inhibition by D-glucose. *Proceedings of the National Academy of Sciences*, 111(14), 5159–5164.
- Feher, J. (2012). *2.9 - ATP Production I: Glycolysis* (J. B. T.-Q. H. P. Feher (ed.); pp. 171–179). Academic Press. <https://doi.org/10.1016/B978-0-12-382163-8.00020-7>
- Feng, Q., Liu, Z. L., Weber, S. A., & Li, S. (2018). Signature pathway expression of xylose utilization in the genetically engineered industrial yeast *Saccharomyces cerevisiae*. *PLoS One*, 13(4), e0195633. <https://doi.org/10.1371/journal.pone.0195633>
- Flores, C.-L., Rodríguez, C., Petit, T., & Gancedo, C. (2000). Carbohydrate and energy-yielding metabolism in non-conventional yeasts. *FEMS Microbiology Reviews*, 24(4), 507–529.
- Folch, J., Lees, M. J., & Stanley, G. H. S. (1957). A simple method for the isolation and purification of total lipides from animal tissues. *Journal of Biological Chemistry*, 226(1), 497–509.
- Fonseca, F. G., Funke, A., Niebel, A., Soares Dias, A. P., & Dahmen, N. (2019). Moisture content as a design and operational parameter for fast pyrolysis. *Journal of Analytical and*

- Applied Pyrolysis*, 139, 73–86. <https://doi.org/10.1016/j.jaap.2019.01.012>
- Furimsky, E. (2013). Hydroprocessing challenges in biofuels production. *Catalysis Today*, 217, 13–56. <https://doi.org/10.1016/j.cattod.2012.11.008>
- Galafassi, S., Cucchetti, D., Pizza, F., Franzosi, G., Bianchi, D., & Compagno, C. (2012). Lipid production for second generation biodiesel by the oleaginous yeast *Rhodotorula graminis*. *Bioresource Technology*, 111, 398–403. <https://doi.org/10.1016/j.biortech.2012.02.004>
- Gancedo, J. M. (1998). Yeast carbon catabolite repression. *Microbiology and Molecular Biology Reviews*, 62(2), 334–361.
- Gancedo, J. M. (2001). Control of pseudohyphae formation in *Saccharomyces cerevisiae*. *FEMS Microbiology Reviews*, 25(1), 107–123.
- Gao, M., Ploessl, D., & Shao, Z. (2018). Enhancing the Co-utilization of Biomass-Derived Mixed Sugars by Yeasts. *Frontiers in Microbiology*, 9, 3264. <https://doi.org/10.3389/fmicb.2018.03264>
- Gao, M., Ploessl, D., & Shao, Z. (2019). Enhancing the co-utilization of biomass-derived mixed sugars by yeasts. *Frontiers in Microbiology*, 9, 3264.
- Gárdonyi, M., Österberg, M., Rodrigues, C., Spencer-Martins, I., & Hahn-Hägerdal, B. (2003). High capacity xylose transport in *Candida intermedia* PYCC 4715. *FEMS Yeast Research*, 3(1), 45–52. <https://doi.org/10.1111/j.1567-1364.2003.tb00137.x>
- Ge, S., Champagne, P., Plaxton, W. C., Leite, G. B., & Marazzi, F. (2017). Microalgal cultivation with waste streams and metabolic constraints to triacylglycerides accumulation for biofuel production. *Biofuels, Bioproducts and Biorefining*, 11(2), 325–343. <https://doi.org/10.1002/bbb.1726>
- Gobert, A., Tourdot-Maréchal, R., Morge, C., Sparrow, C., Liu, Y., Quintanilla-Casas, B., Vichi, S., & Alexandre, H. (2017). Non-Saccharomyces Yeasts Nitrogen Source Preferences: Impact on Sequential Fermentation and Wine Volatile Compounds Profile . In *Frontiers in Microbiology* (Vol. 8, p. 2175). <https://www.frontiersin.org/article/10.3389/fmicb.2017.02175>
- Gokhale, Digambar. (2018). Pseudozyma hubeiensis, an unexplored yeast: It's potential in biomass conversion to value added products. *Journal of Bacteriology & Mycology: Open Access*, 6(2). <https://doi.org/10.15406/jbmoa.2018.06.00181>
- Gokhale, D. V., Patil, S. G., & Bastawde, K. B. (1998). Potential application of yeast cellulase-free xylanase in agrowaste material treatment to remove hemicellulose fractions. *Bioresource Technology*, 63(2), 187–191. [https://doi.org/10.1016/S0960-8524\(97\)00062-X](https://doi.org/10.1016/S0960-8524(97)00062-X)
- Goldberg, S. (2008). Mechanical/physical methods of cell disruption and tissue homogenization. *2D PAGE: Sample Preparation and Fractionation*, 3–22.
- Gomes, T. A., Zanette, C. M., & Spier, M. R. (2020). An overview of cell disruption methods for intracellular biomolecules recovery. *Preparative Biochemistry & Biotechnology*, 50(7), 635–654. <https://doi.org/10.1080/10826068.2020.1728696>

- Goncalves, D. L., Matsushika, A., Belisa, B., Goshima, T., Bon, E. P. S., & Stambuk, B. U. (2014). Xylose and xylose/glucose co-fermentation by recombinant *Saccharomyces cerevisiae* strains expressing individual hexose transporters. *Enzyme and Microbial Technology*, *63*, 13–20.
- Gonzalez, M. I. E. (2014). *Development of Technological Alternatives to Produce Renewable Fuels from Oleaginous Microorganisms*. University of Alberta.
- Gouveia, L., & Passarinho, P. C. (2017). Biomass conversion technologies: biological/biochemical conversion of biomass. In *Biorefineries* (pp. 99–111). Springer.
- Grioui, N., Halouani, K., & Agblevor, F. A. (2019). Assessment of upgrading ability and limitations of slow co-pyrolysis: Case of olive mill wastewater sludge/waste tires slow co-pyrolysis. *Waste Management*, *92*, 75–88.
<https://doi.org/10.1016/j.wasman.2019.05.016>
- Gujjari, P., Suh, S.-O., Coumes, K., & Zhou, J. J. (2011). Characterization of oleaginous yeasts revealed two novel species: *Trichosporon cacaoliposimilis* sp. nov. and *Trichosporon oleaginosus* sp. nov. *Mycologia*, *103*(5), 1110–1118.
- Günerken, E., D'Hondt, E., Eppink, M. H. M., Garcia-Gonzalez, L., Elst, K., & Wijffels, R. H. (2015). Cell disruption for microalgae biorefineries. *Biotechnology Advances*, *33*(2), 243–260.
- Guo, H., Duerh, A., Su, Y., Hensen, E. J. M., Qi, X., & Smith Jr, R. L. (2020). Mechanistic role of protonated polar additives in ethanol for selective transformation of biomass-related compounds. *Applied Catalysis B: Environmental*, *264*, 118509.
- Halim, R., Danquah, M. K., & Webley, P. A. (2012). Extraction of oil from microalgae for biodiesel production: A review. *Biotechnology Advances*, *30*(3), 709–732.
- Hall, M. J., & Ratledge, C. (1977). Lipid accumulation in an oleaginous yeast (*Candida* 107) growing on glucose under various conditions in a one- and two-stage continuous culture. *Applied and Environmental Microbiology*, *33*(3), 577–584.
<https://doi.org/10.1128/aem.33.3.577-584.1977>
- Hamacher, T., Becker, J., Gardonyi, M., Hahn-Hagerdal, B., & Boles, E. (2002). Characterization of the xylose-transporting properties of yeast hexose transporters and their influence on xylose utilization. *Microbiology*, *148*(9), 2783–2788.
<https://doi.org/10.1099/00221287-148-9-2783>
- Hao, X., Suo, H., Zhang, G., Xu, P., Gao, X., & Du, S. (2021). Ultrasound-assisted enzymatic preparation of fatty acid ethyl ester in deep eutectic solvent. *Renewable Energy*, *164*, 937–947. <https://doi.org/10.1016/j.renene.2020.09.114>
- Harrison, S. T. L. (1991). Bacterial cell disruption: A key unit operation in the recovery of intracellular products. *Biotechnology Advances*, *9*(2), 217–240.
[https://doi.org/10.1016/0734-9750\(91\)90005-G](https://doi.org/10.1016/0734-9750(91)90005-G)
- Hassan, H., Lim, J. K., & Hameed, B. H. (2019). Catalytic co-pyrolysis of sugarcane bagasse and waste high-density polyethylene over faujasite-type zeolite. *Bioresource Technology*, *284*, 406–414. <https://doi.org/10.1016/j.biortech.2019.03.137>

- Hassan, M., Blanc, P. J., Pareilleux, A., & Goma, G. (1994). Production of single-cell oil from prickly-pear juice fermentation by *Cryptococcus curvatus* grown in batch culture. *World Journal of Microbiology & Biotechnology*, *10*(5), 534–537.
- Hassan, S. H. A., El-Rab, S. M. F. G., Rahimnejad, M., Ghasemi, M., Joo, J.-H., Sik-Ok, Y., Kim, I. S., & Oh, S.-E. (2014). Electricity generation from rice straw using a microbial fuel cell. *International Journal of Hydrogen Energy*, *39*(17), 9490–9496.
- He, C., Tang, C., Li, C., Yuan, J., Tran, K.-Q., Bach, Q.-V., Qiu, R., & Yang, Y. (2018). Wet torrefaction of biomass for high quality solid fuel production: A review. *Renewable and Sustainable Energy Reviews*, *91*, 259–271.
<https://doi.org/10.1016/j.rser.2018.03.097>
- Heidenreich, S., Müller, M., & Foscolo, P. U. (2016). Chapter 5 - Advanced Process Combination Concepts. In S. Heidenreich, M. Müller, & P. U. Foscolo (Eds.), *Advanced Biomass Gasification* (pp. 55–97). Academic Press. <https://doi.org/10.1016/B978-0-12-804296-0.00005-1>
- Heiland, S., Radovanovic, N., Höfer, M., Winderickx, J., & Lichtenberg, H. (2000). Multiple hexose transporters of *Schizosaccharomyces pombe*. *Journal of Bacteriology*, *182*(8), 2153–2162.
- Henrici, A. T. (1914). The staining of yeasts by Gram's method. *The Journal of Medical Research*, *30*(3), 409.
- Hewavitharana, G. G., Perera, D. N., Navaratne, S. B., & Wickramasinghe, I. (2020). Extraction methods of fat from food samples and preparation of fatty acid methyl esters for gas chromatography: A review. *Arabian Journal of Chemistry*, *13*(8), 6865–6875.
<https://doi.org/10.1016/j.arabjc.2020.06.039>
- Hilten, R., Speir, R., Kastner, J., & Das, K. C. (2010). Production of fuel from the catalytic cracking of pyrolyzed poultry DAF skimmings. *Journal of Analytical and Applied Pyrolysis*, *88*(1), 30–38. <https://doi.org/10.1016/j.jaap.2010.02.007>
- Ho, C. S., Khadka, N. K., She, F., Cai, J., & Pan, J. (2016). Polyglutamine aggregates impair lipid membrane integrity and enhance lipid membrane rigidity. *Biochimica et Biophysica Acta (BBA) - Biomembranes*, *1858*(4), 661–670.
<https://doi.org/10.1016/j.bbamem.2016.01.016>
- Höfer, M., & Misra, P. C. (1978). Evidence for a proton/sugar symport in the yeast *Rhodotorula gracilis* (glutinis). *Biochemical Journal*, *172*(1), 15–22.
- Hossain, S. M. Z. (2019). Biochemical conversion of microalgae biomass into biofuel. *Chemical Engineering & Technology*, *42*(12), 2594–2607.
- Hou, J., Qiu, C., Shen, Y., Li, H., & Bao, X. (2017a). Engineering of *Saccharomyces cerevisiae* for the efficient co-utilization of glucose and xylose. *FEMS Yeast Research*, *17*(4).
- Hou, J., Qiu, C., Shen, Y., Li, H., & Bao, X. (2017b). Engineering of *Saccharomyces cerevisiae* for the efficient co-utilization of glucose and xylose. *FEMS Yeast Research*, *17*(4).
<https://doi.org/10.1093/femsyr/fox034>

- Hrnčič, M. K., Kravanja, G., & Knez, Ž. (2016). Hydrothermal treatment of biomass for energy and chemicals. *Energy*, *116*, 1312–1322. <https://doi.org/10.1016/j.energy.2016.06.148>
- Hu, C., Wu, S., Wang, Q., Jin, G., Shen, H., & Zhao, Z. K. (2011). Simultaneous utilization of glucose and xylose for lipid production by *Trichosporon cutaneum*. *Biotechnology for Biofuels*, *4*, 25. <https://doi.org/10.1186/1754-6834-4-25>
- Hu, M., Laghari, M., Cui, B., Xiao, B., Zhang, B., & Guo, D. (2018). Catalytic cracking of biomass tar over char supported nickel catalyst. *Energy*, *145*, 228–237. <https://doi.org/10.1016/j.energy.2017.12.096>
- Huang, C., Guo, H., Zhang, H., Xiong, L., Li, H., & Chen, X. (2019). A new concept for total components conversion of lignocellulosic biomass: a promising direction for clean and sustainable production in its bio-refinery. *Journal of Chemical Technology & Biotechnology*, *94*(8), 2416–2424.
- Huang, X., Kudo, S., & Hayashi, J. (2019). Two-step conversion of cellulose to levoglucosenone using updraft fixed bed pyrolyzer and catalytic reformer. *Fuel Processing Technology*, *191*, 29–35. <https://doi.org/10.1016/j.fuproc.2019.03.014>
- Ishida, N., Kamae, Y., Ishizu, K., Kamino, Y., Naruse, H., & Murakami, M. (2021). Sustainable System for Hydrogenation Exploiting Energy Derived from Solar Light. *Journal of the American Chemical Society*, *143*(5), 2217–2220.
- Isikgor, F. H., & Becer, C. R. (2015). Lignocellulosic biomass: a sustainable platform for the production of bio-based chemicals and polymers. *Polymer Chemistry*, *6*(25), 4497–4559. <https://doi.org/10.1039/c5py00263j>
- Janda, S., Kotyk, A., & Tauchová, R. (1976). Monosaccharide transport systems in the yeast *Rhodotorula glutinis*. *Archives of Microbiology*, *111*(1), 151–154.
- Javed, M. R., Bilal, M. J., Ashraf, M. U. F., Waqar, A., Mehmood, M. A., Saeed, M., & Nashat, N. (2019). *Microalgae as a Feedstock for Biofuel Production: Current Status and Future Prospects*.
- Jeffries, T. W. (2006). Engineering yeasts for xylose metabolism. *Current Opinion in Biotechnology*, *17*(3), 320–326. <https://doi.org/10.1016/j.copbio.2006.05.008>
- Jiang, Y., Shen, Y., Gu, L., Wang, Z., Su, N., Niu, K., Guo, W., Hou, S., Bao, X., Tian, C., & Fang, X. (2020). Identification and Characterization of an Efficient d-Xylose Transporter in *Saccharomyces cerevisiae*. *Journal of Agricultural and Food Chemistry*, *68*(9), 2702–2710. <https://doi.org/10.1021/acs.jafc.9b07113>
- Jin, J., Dupré, C., Legrand, J., & Grizeau, D. (2016). Extracellular hydrocarbon and intracellular lipid accumulation are related to nutrient-sufficient conditions in pH-controlled chemostat cultures of the microalga *Botryococcus braunii* SAG 30.81. *Algal Research*, *17*, 244–252. <https://doi.org/10.1016/j.algal.2016.05.007>
- Jin, M., Slininger, P. J., Dien, B. S., Waghmode, S., Moser, B. R., Orjuela, A., Sousa, L. da C., & Balan, V. (2015). Microbial lipid-based lignocellulosic biorefinery: feasibility and challenges. *Trends in Biotechnology*, *33*(1), 43–54.

<https://doi.org/https://doi.org/10.1016/j.tibtech.2014.11.005>

- Jin, Y.-S., Laplaza, J. M., & Jeffries, T. W. (2004). Saccharomyces cerevisiae Engineered for Xylose Metabolism Exhibits a Respiratory Response. *Applied and Environmental Microbiology*, 70(11), 6816–6825. <https://doi.org/10.1128/AEM.70.11.6816-6825.2004>
- Johnravindar, D., Karthikeyan, O. P., Selvam, A., Murugesan, K., & Wong, J. W. C. (2018). Lipid accumulation potential of oleaginous yeasts: A comparative evaluation using food waste leachate as a substrate. *Bioresource Technology*, 248, 221–228. <https://doi.org/https://doi.org/10.1016/j.biortech.2017.06.151>
- Johnson, E. A. (2013a). Biotechnology of non-Saccharomyces yeasts—the ascomycetes. *Applied Microbiology and Biotechnology*, 97(2), 503–517.
- Johnson, E. A. (2013b). Biotechnology of non-Saccharomyces yeasts—the basidiomycetes. *Applied Microbiology and Biotechnology*, 97(17), 7563–7577.
- Johnson, E. A., & Echavarri-Erasun, C. (2011). Chapter 3 - Yeast Biotechnology. In C. P. Kurtzman, J. W. Fell, & T. Boekhout (Eds.), *The Yeasts (Fifth Edition)* (pp. 21–44). Elsevier. <https://doi.org/https://doi.org/10.1016/B978-0-444-52149-1.00003-3>
- Johnson, V., Singh, M., Saini, V. S., Sista, V. R., & Yadav, N. K. (1992). Effect of pH on lipid accumulation by an oleaginous yeast: Rhodotorula glutinis IIP-30. *World Journal of Microbiology and Biotechnology*, 8(4), 382–384.
- Jojima, T., Jojima, T., Omumasaba, C., Omumasaba, C., Inui, M., Inui, M., Yukawa, H., & Yukawa, H. (2010). Sugar transporters in efficient utilization of mixed sugar substrates: current knowledge and outlook. *Applied Microbiology and Biotechnology*, 85(3), 471–480. <https://doi.org/10.1007/s00253-009-2292-1>
- Jump, D. B. (2009). Mammalian fatty acid elongases. *Methods in Molecular Biology (Clifton, N.J.)*, 579, 375–389. https://doi.org/10.1007/978-1-60761-322-0_19
- Kamrad, S., Grossbach, J., Rodríguez-López, M., Mülleder, M., Townsend, S., Cappelletti, V., Stojanovski, G., Correia-Melo, C., Picotti, P., & Beyer, A. (2020). Pyruvate kinase variant of fission yeast tunes carbon metabolism, cell regulation, growth and stress resistance. *Molecular Systems Biology*, 16(4), e9270.
- Käppeli, O. (1987). *Regulation of Carbon Metabolism in Saccharomyces cerevisiae and Related Yeasts* (A. H. Rose & D. W. B. T.-A. in M. P. Tempest (eds.); Vol. 28, pp. 181–209). Academic Press. [https://doi.org/https://doi.org/10.1016/S0065-2911\(08\)60239-8](https://doi.org/https://doi.org/10.1016/S0065-2911(08)60239-8)
- Kar, Y. (2018). Catalytic cracking of pyrolytic oil by using bentonite clay for green liquid hydrocarbon fuels production. *Biomass and Bioenergy*, 119, 473–479. <https://doi.org/https://doi.org/10.1016/j.biombioe.2018.10.014>
- Karatzos, S., van Dyk, J. S., McMillan, J. D., & Saddler, J. (2017). Drop-in biofuel production via conventional (lipid/fatty acid) and advanced (biomass) routes. Part I. *Biofuels, Bioproducts and Biorefining*, 11(2), 344–362. <https://doi.org/10.1002/bbb.1746>
- Karhumaa, K., Hahn-Hägerdal, B., & Gorwa-Grauslund, M. (2005). Investigation of limiting metabolic steps in the utilization of xylose by recombinant Saccharomyces cerevisiae using

- metabolic engineering. *Yeast*, 22(5), 359–368. <https://doi.org/10.1002/yea.1216>
- Karim, A., Islam, M. A., Khalid, Z. Bin, Faizal, C. K. M., Khan, M. M. R., & Yousuf, A. (2020). *Chapter 9 - Microalgal Cell Disruption and Lipid Extraction Techniques for Potential Biofuel Production* (A. B. T.-M. C. for B. P. Yousuf (ed.); pp. 129–147). Academic Press. <https://doi.org/https://doi.org/10.1016/B978-0-12-817536-1.00009-6>
- Karmakar, B., & Halder, G. (2019). Progress and future of biodiesel synthesis: Advancements in oil extraction and conversion technologies. *Energy Conversion and Management*, 182, 307–339. <https://doi.org/https://doi.org/10.1016/j.enconman.2018.12.066>
- Kawashima, A., Akihiro, H., Morita, H., Fukuoka, M., Honda, K., & Morita, M. (2011). Dioxin-like polychlorinated biphenyl adsorbent obtained from enzymatic saccharification residue of lignocellulose. *Bioresource Technology*, 102(7), 4682–4687. <https://doi.org/https://doi.org/10.1016/j.biortech.2011.01.033>
- Kayikci, O. mur, & Nielsen, J. (n.d.). *Glucose repression in Saccharomyces cerevisiae*. <https://doi.org/10.1093/femsyr/fov068>
- Kayikci, Ö., & Nielsen, J. (2015). Glucose repression in *Saccharomyces cerevisiae*. *FEMS Yeast Research*, 15(6), fov068.
- Kazemi Shariat Panahi, H., Tabatabaei, M., Aghbashlo, M., Dehghani, M., Rehan, M., & Nizami, A.-S. (2019). Recent updates on the production and upgrading of bio-crude oil from microalgae. *Bioresource Technology Reports*, 7, 100216. <https://doi.org/https://doi.org/10.1016/j.biteb.2019.100216>
- Keasling, J., Garcia Martin, H., Lee, T. S., Mukhopadhyay, A., Singer, S. W., & Sundstrom, E. (2021). Microbial production of advanced biofuels. *Nature Reviews Microbiology*, 19(11), 701–715. <https://doi.org/10.1038/s41579-021-00577-w>
- Kholkina, E., Kumar, N., Ohra-aho, T., Lehtonen, J., Lindfors, C., Perula, M., Peltonen, J., Salonen, J., & Murzin, D. Y. (2019). Transformation of industrial steel slag with different structure-modifying agents for synthesis of catalysts. *Catalysis Today*. <https://doi.org/https://doi.org/10.1016/j.cattod.2019.04.033>
- Kobayashi, K., Suginaka, H., & Yano, I. (1987). Analysis of fatty acid composition of *Candida* species by gas-liquid chromatography using a polar column. *Microbios*, 51(206), 37–42.
- Kolouchová, I., Mat'átková, O., Sigler, K., Masák, J., & Řezanka, T. (2016). Lipid accumulation by oleaginous and non-oleaginous yeast strains in nitrogen and phosphate limitation. *Folia Microbiologica*, 61(5), 431–438. <https://doi.org/10.1007/s12223-016-0454-y>
- Konishi, M., Morita, T., Fukuoka, T., Imura, T., Kakugawa, K., & Kitamoto, D. (2007). Production of different types of mannosylerythritol lipids as biosurfactants by the newly isolated yeast strains belonging to the genus *Pseudozyma*. *Applied Microbiology and Biotechnology*, 75(3), 521–531. <https://doi.org/10.1007/s00253-007-0853-8>
- Kostyniuk, A., Bajec, D., & Likozar, B. (2021). Catalytic hydrogenation, hydrocracking and isomerization reactions of biomass tar model compound mixture over Ni-modified zeolite catalysts in packed bed reactor. *Renewable Energy*, 167, 409–424.

- Kot, A. M., Błażej, S., Kurcz, A., Gientka, I., & Kieliszek, M. (2016). *Rhodotorula glutinis*—potential source of lipids, carotenoids, and enzymes for use in industries. *Applied Microbiology and Biotechnology*, *100*(14), 6103–6117.
- Kot, A. M., Gientka, I., Bzducha-Wróbel, A., Błażej, S., & Kurcz, A. (2020). Comparison of simple and rapid cell wall disruption methods for improving lipid extraction from yeast cells. *Journal of Microbiological Methods*, *176*, 105999. <https://doi.org/https://doi.org/10.1016/j.mimet.2020.105999>
- Koutinas, A. A., Chatzifragkou, A., Kopsahelis, N., Papanikolaou, S., & Kookos, I. K. (2014). Design and techno-economic evaluation of microbial oil production as a renewable resource for biodiesel and oleochemical production. *Fuel*, *116*, 566–577.
- Krishnan, S., Ghani, N. A., Aminuddin, N. F., Quraishi, K. S., Azman, N. S., Cravotto, G., & Leveque, J.-M. (2020). Microwave-assisted lipid extraction from *Chlorella vulgaris* in water with 0.5%–2.5% of imidazolium based ionic liquid as additive. *Renewable Energy*, *149*, 244–252. <https://doi.org/https://doi.org/10.1016/j.renene.2019.12.063>
- Kumar, A., Anushree, Kumar, J., & Bhaskar, T. (2019). Utilization of lignin: A sustainable and eco-friendly approach. *Journal of the Energy Institute*. <https://doi.org/https://doi.org/10.1016/j.joei.2019.03.005>
- Kumari, A. (2018). *Chapter 2 - Citric Acid Cycle* (A. B. T.-S. B. Kumari (ed.); pp. 7–11). Academic Press. <https://doi.org/https://doi.org/10.1016/B978-0-12-814453-4.00002-9>
- Kurtzman, C., Fell, J. W., & Boekhout, T. (2011). *The yeasts: a taxonomic study*. Elsevier.
- Kurtzman, C. P., Fell, J. W., & Boekhout, T. (2011). Definition, classification and nomenclature of the yeasts. In *The yeasts* (pp. 3–5). Elsevier.
- Kuyper, M., Winkler, A. A., van Dijken, J. P., & Pronk, J. T. (2004). Minimal metabolic engineering of *Saccharomyces cerevisiae* for efficient anaerobic xylose fermentation: a proof of principle. *FEMS Yeast Research*, *4*(6), 655–664. <https://doi.org/10.1016/j.femsyr.2004.01.003>
- Kyriakidis, N. B., & Dionysopoulos, G. (1983). Preparation of fatty acid methyl esters from olive oil and other vegetable oils using aqueous hydrochloric acid-methanol. *Analyst*, *108*(1287), 738–741. <https://doi.org/10.1039/AN9830800738>
- Lackner, M. (2017). 3rd-Generation Biofuels: Bacteria and Algae as Sustainable Producers and Converters. In *Handbook of Climate Change Mitigation and Adaptation, Second Edition* (pp. 3173–3210). https://doi.org/10.1007/978-3-319-14409-2_90
- Laesecke, J., Ellis, N., & Kirchen, P. (2017). Production, analysis and combustion characterization of biomass fast pyrolysis oil – Biodiesel blends for use in diesel engines. *Fuel*, *199*, 346–357. <https://doi.org/https://doi.org/10.1016/j.fuel.2017.01.093>
- Lage, S., & Gentili, F. G. (2018). Quantification and characterisation of fatty acid methyl esters in microalgae: Comparison of pretreatment and purification methods. *Bioresource Technology*, *257*, 121–128. <https://doi.org/https://doi.org/10.1016/j.biortech.2018.01.153>
- Lagunas, R. (1993). Sugar transport in *Saccharomyces cerevisiae*. *FEMS Microbiology Reviews*,

10(3–4), 229–242.

- Lamaisri, C., Punsuvon, V., Chanprame, S., Arunyanark, A., Srinives, P., & Liangsakul, P. (2015). Relationship between fatty acid composition and biodiesel quality for nine commercial palm oils. *Songklanakarinn Journal of Science & Technology*, 37(4).
- Lamers, D., van Biezen, N., Martens, D., Peters, L., van de Zilver, E., Jacobs-van Dreumel, N., Wijffels, R. H., & Lokman, C. (2016). Selection of oleaginous yeasts for fatty acid production. *BMC Biotechnology*, 16(1), 45. <https://doi.org/10.1186/s12896-016-0276-7>
- Laoteng, K., Čertík, M., & Cheevadhanark, S. (2011). Mechanisms controlling lipid accumulation and polyunsaturated fatty acid synthesis in oleaginous fungi. *Chemical Papers*, 65(2), 97–103. <https://doi.org/10.2478/s11696-010-0097-4>
- Lappas, A. A., Bezergianni, S., & Vasalos, I. A. (2009). Production of biofuels via co-processing in conventional refining processes. *Catalysis Today*, 145(1), 55–62. <https://doi.org/10.1016/j.cattod.2008.07.001>
- Lappas, A., & Heracleous, E. (2011). 19 - Production of biofuels via Fischer-Tropsch synthesis: biomass-to-liquids. In R. Luque, J. Campelo, & J. Clark (Eds.), *Handbook of Biofuels Production* (pp. 493–529). Woodhead Publishing. <https://doi.org/10.1533/9780857090492.3.493>
- Lappas, A., & Heracleous, E. (2016). 18 - Production of biofuels via Fischer-Tropsch synthesis: Biomass-to-liquids. In R. Luque, C. S. K. Lin, K. Wilson, & J. Clark (Eds.), *Handbook of Biofuels Production (Second Edition)* (pp. 549–593). Woodhead Publishing. <https://doi.org/10.1016/B978-0-08-100455-5.00018-7>
- Leandro, M. J., Gonçalves, P., & Spencer-Martins, I. (2006). Two glucose/xylose transporter genes from the yeast *Candida intermedia*: first molecular characterization of a yeast xylose-H⁺ symporter. *Biochemical Journal*, 395(3), 543–549. <https://doi.org/10.1042/BJ20051465>
- Lee, J. W., Yook, S., Koh, H., Rao, C. V., & Jin, Y.-S. (2021). Engineering xylose metabolism in yeasts to produce biofuels and chemicals. *Current Opinion in Biotechnology*, 67, 15–25. <https://doi.org/10.1016/j.copbio.2020.10.012>
- Lee, R. A., & Lavoie, J.-M. (2013). From first- to third-generation biofuels: Challenges of producing a commodity from a biomass of increasing complexity. *Animal Frontiers*, 3(2), 6–11. <https://doi.org/10.2527/af.2013-0010>
- Lee, S.-M., Young, E. M., & Alper, H. S. (2015). Chapter 12 - Remaining Challenges in the *Metabolic Engineering of Yeasts for Biofuels* (M. E. B. T.-D. M. C. of B. to A. B. Himmel (ed.); pp. 209–237). Elsevier. <https://doi.org/10.1016/B978-0-444-59592-8.00012-9>
- Leibbrandt, N. H., Aboyade, A. O., Knoetze, J. H., & Görgens, J. F. (2013). Process efficiency of biofuel production via gasification and Fischer-Tropsch synthesis. *Fuel*, 109, 484–492. <https://doi.org/10.1016/j.fuel.2013.03.013>
- Leng, L., Li, H., Yuan, X., Zhou, W., & Huang, H. (2018). Bio-oil upgrading by emulsification/microemulsification: A review. *Energy*, 161, 214–232. <https://doi.org/10.1016/j.energy.2018.07.117>

- Leung, D. Y. C., & Guo, Y. (2006). Transesterification of neat and used frying oil: Optimization for biodiesel production. *Fuel Processing Technology*, *87*(10), 883–890.
- Li, Hao, Liu, Z., Zhang, Y., Li, B., Lu, H., Duan, N., Liu, M., Zhu, Z., & Si, B. (2014). Conversion efficiency and oil quality of low-lipid high-protein and high-lipid low-protein microalgae via hydrothermal liquefaction. *Bioresource Technology*, *154*, 322–329. <https://doi.org/10.1016/j.biortech.2013.12.074>
- Li, Hui, Tian, Y., Zuo, W., Zhang, J., Pan, X., Li, L., & Su, X. (2016). Electricity generation from food wastes and characteristics of organic matters in microbial fuel cell. *Bioresource Technology*, *205*, 104–110.
- Li, S.-W., He, H., Zeng, R. J., & Sheng, G.-P. (2017). Chitin degradation and electricity generation by *Aeromonas hydrophila* in microbial fuel cells. *Chemosphere*, *168*, 293–299.
- Li, S.-W., Zeng, R. J., & Sheng, G.-P. (2017). An excellent anaerobic respiration mode for chitin degradation by *Shewanella oneidensis* MR-1 in microbial fuel cells. *Biochemical Engineering Journal*, *118*, 20–24.
- Li, X., Luo, X., Jin, Y., Li, J., Zhang, H., Zhang, A., & Xie, J. (2018). Heterogeneous sulfur-free hydrodeoxygenation catalysts for selectively upgrading the renewable bio-oils to second generation biofuels. *Renewable and Sustainable Energy Reviews*, *82*, 3762–3797. <https://doi.org/10.1016/j.rser.2017.10.091>
- Li, X., Park, A., Estrela, R., Kim, S.-R., Jin, Y.-S., & Cate, J. H. D. (2016). Comparison of xylose fermentation by two high-performance engineered strains of *Saccharomyces cerevisiae*. *Biotechnology Reports*, *9*(C), 53–56. <https://doi.org/10.1016/j.btre.2016.01.003>
- Liang, H., & Gaber, R. F. (1996). A novel signal transduction pathway in *Saccharomyces cerevisiae* defined by Snf3-regulated expression of HXT6. *Molecular Biology of the Cell*, *7*(12), 1953–1966.
- Lin, Y., Ma, X., Peng, X., Yu, Z., Fang, S., Lin, Y., & Fan, Y. (2016). Combustion, pyrolysis and char CO₂-gasification characteristics of hydrothermal carbonization solid fuel from municipal solid wastes. *Fuel*, *181*, 905–915. <https://doi.org/10.1016/j.fuel.2016.05.031>
- Lindquist, R. N., & Horton, H. R. (1993). *Problems and solutions for Horton" Principles of biochemistry"*. N. Patterson Publ.: Prentice Hall.
- Lindsey, R. (2020). Climate change: atmospheric carbon dioxide. *NOAA Climate. Gov, Maryland, News and Features, Understanding Climate*, *14*.
- Liu, D., Ding, L., Sun, J., Boussetta, N., & Vorobiev, E. (2016). Yeast cell disruption strategies for recovery of intracellular bio-active compounds — A review. *Innovative Food Science & Emerging Technologies*, *36*, 181–192. <https://doi.org/10.1016/j.ifset.2016.06.017>
- Liu, Z., Quek, A., Kent Hoekman, S., & Balasubramanian, R. (2013). Production of solid biochar fuel from waste biomass by hydrothermal carbonization. *Fuel*, *103*, 943–949. <https://doi.org/10.1016/j.fuel.2012.07.069>

- Lopes, M., Gomes, A. S., Silva, C. M., & Belo, I. (2018). Microbial lipids and added value metabolites production by *Yarrowia lipolytica* from pork lard. *Journal of Biotechnology*, 265, 76–85.
- López Barreiro, D., Martín-Martínez, F. J., Torri, C., Prins, W., & Buehler, M. J. (2018). Molecular characterization and atomistic model of biocrude oils from hydrothermal liquefaction of microalgae. *Algal Research*, 35, 262–273. <https://doi.org/10.1016/j.algal.2018.08.034>
- Louhasakul, Y., Cheirsilp, B., Maneerat, S., & Prasertsan, P. (2018). Direct transesterification of oleaginous yeast lipids into biodiesel: Development of vigorously stirred tank reactor and process optimization. *Biochemical Engineering Journal*, 137, 232–238.
- Lü, J., Sheahan, C., & Fu, P. (2011). Metabolic engineering of algae for fourth generation biofuels production. *Energy & Environmental Science*, 4(7), 2451–2466.
- Lynd, L. R., Wyman, C. E., & Gerngross, T. U. (1999). Biocommodity Engineering. *Biotechnology Progress*, 15(5), 777–793. <https://doi.org/10.1021/bp990109e>
- Ma, J., Luo, H., Li, Y., Liu, Z., Li, D., Gai, C., & Jiao, W. (2019). Pyrolysis kinetics and thermodynamic parameters of the hydrochars derived from co-hydrothermal carbonization of sawdust and sewage sludge using thermogravimetric analysis. *Bioresource Technology*, 282, 133–141. <https://doi.org/10.1016/j.biortech.2019.03.007>
- Maddi, B. (2019). Extraction Methods Used to Separate Lipids from Microbes. In *Microbial Lipid Production* (pp. 151–159). Springer.
- Maher, K. D., Kirkwood, K. M., Gray, M. R., & Bressler, D. C. (2008). Pyrolytic Decarboxylation and Cracking of Stearic Acid. *Industrial & Engineering Chemistry Research*, 47(15), 5328–5336. <https://doi.org/10.1021/ie0714551>
- Manu, H. A., Meena, H. R., & Priyanka, B. N. (2020). Likelihood of Consuming Cloned Animal Products: Ordered Logistic Regression Model. *Int. J. Curr. Microbiol. App. Sci*, 9(1), 479–485.
- Martinez-Silveira, A., Villarreal, R., Garmendia, G., Rufo, C., & Vero, S. (2019). Process conditions for a rapid in situ transesterification for biodiesel production from oleaginous yeasts. *Electronic Journal of Biotechnology*, 38, 1–9.
- Masri, M. A., Garbe, D., Mehlmer, N., & Brück, T. B. (2019). A sustainable, high-performance process for the economic production of waste-free microbial oils that can replace plant-based equivalents. *Energy & Environmental Science*, 12(9), 2717–2732.
- Mateos, P. S., Navas, M. B., Morcelle, S. R., Ruscitti, C., Matkovic, S. R., & Briand, L. E. (2021). Insights in the biocatalyzed hydrolysis, esterification and transesterification of waste cooking oil with a vegetable lipase. *Catalysis Today*, 372, 211–219. <https://doi.org/10.1016/j.cattod.2020.09.027>
- Mathimani, T., & Mallick, N. (2019). A review on the hydrothermal processing of microalgal biomass to bio-oil - Knowledge gaps and recent advances. *Journal of Cleaner Production*, 217, 69–84. <https://doi.org/10.1016/j.jclepro.2019.01.129>

- Mathiyazhagan, M., & Ganapathi, A. (2011). Factors affecting biodiesel production. *Research in Plant Biology*, 1(2).
- Maza, D. D., Viñarta, S. C., Su, Y., Guillamón, J. M., & Aybar, M. J. (2020). Growth and lipid production of *Rhodotorula glutinis* R4, in comparison to other oleaginous yeasts. *Journal of Biotechnology*, 310, 21–31. <https://doi.org/https://doi.org/10.1016/j.jbiotec.2020.01.012>
- Mbuyane, L. L., Bauer, F. F., & Divol, B. (2021). The metabolism of lipids in yeasts and applications in oenology. *Food Research International*, 141, 110142. <https://doi.org/https://doi.org/10.1016/j.foodres.2021.110142>
- McHugh, M., & Krukoniš, V. (2013). *Supercritical fluid extraction: principles and practice*. Elsevier.
- McWilliams, A. (2018). The global market for carotenoids. *BCC Research: Wellesley, MA, USA*.
- Medipally, S. R., Yusoff, F. M., Banerjee, S., & Shariff, M. (2015). Microalgae as Sustainable Renewable Energy Feedstock for Biofuel Production. *BioMed Research International*, 2015, 519513. <https://doi.org/10.1155/2015/519513>
- Meeuwse, P., Sanders, J. P. M., Tramper, J., & Rinzema, A. (2013). Lipids from yeasts and fungi: Tomorrow's source of biodiesel? *Biofuels, Bioproducts and Biorefining*, 7(5), 512–524. <https://doi.org/10.1002/bbb.1410>
- Meher, L. C., Sagar, D. V., & Naik, S. N. (2006). Technical aspects of biodiesel production by transesterification—a review. *Renewable and Sustainable Energy Reviews*, 10(3), 248–268.
- Mehta, S. V, Patil, V. B., Velmurugan, S., Lobo, Z., & Maitra, P. K. (1998). Std1, a gene involved in glucose transport in *Schizosaccharomyces pombe*. *Journal of Bacteriology*, 180(3), 674–679.
- Mei Wu, L., Hui Zhou, C., Shen Tong, D., & Hua Yu, W. (2014). Chapter 15 - Catalytic Thermochemical Processes for Biomass Conversion to Biofuels and Chemicals. In V. K. Gupta, M. G. Tuohy, C. P. Kubicek, J. Saddler, & F. Xu (Eds.), *Bioenergy Research: Advances and Applications* (pp. 243–254). Elsevier. <https://doi.org/https://doi.org/10.1016/B978-0-444-59561-4.00015-2>
- Menegazzo, M. L., & Fonseca, G. G. (2019). Biomass recovery and lipid extraction processes for microalgae biofuels production: A review. *Renewable and Sustainable Energy Reviews*, 107, 87–107. <https://doi.org/https://doi.org/10.1016/j.rser.2019.01.064>
- Meng, X., Yang, J., Xu, X., Zhang, L., Nie, Q., & Xian, M. (2009). Biodiesel production from oleaginous microorganisms. *Renewable Energy*, 34(1), 1–5.
- Mercer, P., & Armenta, R. E. (2011). Developments in oil extraction from microalgae. *European Journal of Lipid Science and Technology*, 113(5), 539–547.
- Mhetras, N., Liddell, S., & Gokhale, D. (2016). Purification and characterization of an extracellular β -xylosidase from *Pseudozyma hubeiensis* NCIM 3574 (PhXyl), an unexplored yeast. *AMB Express*, 6(1). <https://doi.org/10.1186/s13568-016-0243-7>
- Mirza, U. K., Ahmad, N., & Majeed, T. (2008). An overview of biomass energy utilization in

- Pakistan. *Renewable and Sustainable Energy Reviews*, 12(7), 1988–1996.
- Monedero, V., Yebra, M. J., Poncet, S., & Deutscher, J. (2008). Maltose transport in *Lactobacillus casei* and its regulation by inducer exclusion. *Research in Microbiology*, 159(2), 94–102.
- Monlau, F., Sambusiti, C., Antoniou, N., Barakat, A., & Zabaniotou, A. (2015). A new concept for enhancing energy recovery from agricultural residues by coupling anaerobic digestion and pyrolysis process. *Applied Energy*, 148, 32–38.
<https://doi.org/10.1016/j.apenergy.2015.03.024>
- Moradian, J. M., Fang, Z., & Yong, Y.-C. (2021). Recent advances on biomass-fueled microbial fuel cell. *Bioresources and Bioprocessing*, 8(1), 1–13.
- Moradian, J. M., Xu, Z., Shi, Y., Fang, Z., & Yong, Y. (2020). Efficient biohydrogen and bioelectricity production from xylose by microbial fuel cell with newly isolated yeast of *Cystobasidium slooffiae*. *International Journal of Energy Research*, 44(1), 325–333.
- Morita, T., Fukuoka, T., Imura, T., & Kitamoto, D. (2015). Mannosylerythritol Lipids: Production and Applications. *Journal of Oleo Science*, 64, 133–141.
<https://doi.org/10.5650/jos.ess14185>
- Morita, T., Fukuoka, T., Kosaka, A., Imura, T., Sakai, H., Abe, M., & Kitamoto, D. (2015). Selective formation of mannosyl-1-arabitol lipid by *Pseudozyma tsukubaensis* JCM16987. *Applied Microbiology and Biotechnology*, 99(14), 5833–5841.
<https://doi.org/10.1007/s00253-015-6575-4>
- Morita, T., Konishi, M., Fukuoka, T., Imura, T., Kitamoto, H. K., & Kitamoto, D. (2007). Characterization of the genus *Pseudozyma* by the formation of glycolipid biosurfactants, mannosylerythritol lipids. *FEMS Yeast Research*, 7(2), 286–292.
<https://doi.org/10.1111/j.1567-1364.2006.00154.x>
- Morita, T., Ogura, Y., Takashima, M., Hirose, N., Fukuoka, T., Imura, T., Kondo, Y., & Kitamoto, D. (2011). Isolation of *Pseudozyma churashimaensis* sp. nov., a novel ustilaginomycetous yeast species as a producer of glycolipid biosurfactants, mannosylerythritol lipids. *Journal of Bioscience and Bioengineering*, 112(2), 137–144.
<https://doi.org/10.1016/j.jbiosc.2011.04.008>
- Morita, T., Takashima, M., Fukuoka, T., Konishi, M., Imura, T., & Kitamoto, D. (2010). Isolation of basidiomycetous yeast *Pseudozyma tsukubaensis* and production of glycolipid biosurfactant, a diastereomer type of mannosylerythritol lipid-B. *Applied Microbiology and Biotechnology*, 88(3), 679–688. <https://doi.org/10.1007/s00253-010-2762-5>
- Moysés, D. N., Reis, V. C. B., de Almeida, J. R. M., de Moraes, L. M. P., & Torres, F. A. G. (2016). Xylose Fermentation by *Saccharomyces cerevisiae*: Challenges and Prospects. *International Journal of Molecular Sciences*, 17(3), 207.
<https://doi.org/10.3390/ijms17030207>
- Mukherjee, A., Verma, J. P., Gaurav, A. K., Chouhan, G. K., Patel, J. S., & Hesham, A. E.-L. (2020). Yeast a potential bio-agent: future for plant growth and postharvest disease management for sustainable agriculture. *Applied Microbiology and Biotechnology*, 104(4),

1497–1510.

- Muniyappa, P. R., Brammer, S. C., & Nouredini, H. (1996). Improved conversion of plant oils and animal fats into biodiesel and co-product. *Bioresource Technology*, *56*(1), 19–24.
- Mus, F., Toussaint, J.-P., Cooksey, K. E., Fields, M. W., Gerlach, R., Peyton, B. M., & Carlson, R. P. (2013). Physiological and molecular analysis of carbon source supplementation and pH stress-induced lipid accumulation in the marine diatom *Phaeodactylum tricornutum*. *Applied Microbiology and Biotechnology*, *97*(8), 3625–3642.
- Naghdi, F. G., Bai, X., Thomas-Hall, S. R., Sharma, K., & Schenk, P. M. (2016). Lipid extraction from wet *Chaetoceros muelleri* culture and evaluation of remaining defatted biomass. *Algal Research*, *20*, 205–212. <https://doi.org/10.1016/j.algal.2016.10.011>
- Naik, S. N., Goud, V. V., Rout, P. K., & Dalai, A. K. (2010). Production of first and second generation biofuels: a comprehensive review. *Renewable and Sustainable Energy Reviews*, *14*(2), 578–597.
- Nair, A., & Sarma, S. J. (2021). The impact of carbon and nitrogen catabolite repression in microorganisms. *Microbiological Research*, 126831.
- Nam, L. T. H., Vinh, T. Q., Loan, N. T. T., Tho, V. D. S., Yang, X.-Y., & Su, B.-L. (2011). Preparation of bio-fuels by catalytic cracking reaction of vegetable oil sludge. *Fuel*, *90*(3), 1069–1075. <https://doi.org/10.1016/j.fuel.2010.10.060>
- Nandy, S. K., & Srivastava, R. K. (2018). A review on sustainable yeast biotechnological processes and applications. *Microbiological Research*, *207*, 83–90. <https://doi.org/10.1016/j.micres.2017.11.013>
- Ndikubwimana, T., Zeng, X., Murwanashyaka, T., Manirafasha, E., He, N., Shao, W., & Lu, Y. (2016). Harvesting of freshwater microalgae with microbial bioflocculant: a pilot-scale study. *Biotechnology for Biofuels*, *9*(1), 47. <https://doi.org/10.1186/s13068-016-0458-5>
- Neto, J. M., Komesu, A., da Silva Martins, L. H., Gonçalves, V. O. O., de Oliveira, J. A. R., & Rai, M. (2019). Third generation biofuels: an overview. In *Sustainable Bioenergy* (pp. 283–298). Elsevier.
- New, A. M., Cerulus, B., Govers, S. K., Perez-Samper, G., Zhu, B., Boogmans, S., Xavier, J. B., & Verstrepen, K. J. (2014). Different levels of catabolite repression optimize growth in stable and variable environments. *PLoS Biology*, *12*(1), e1001764.
- Ng, D. K. S., Ng, K. S., & Ng, R. T. L. (2017). Integrated Biorefineries. In M. A. Abraham (Ed.), *Encyclopedia of Sustainable Technologies* (pp. 299–314). Elsevier. <https://doi.org/10.1016/B978-0-12-409548-9.10138-1>
- Nijland, J. G., & Driessen, A. J. M. (2020). Engineering of Pentose Transport in *Saccharomyces cerevisiae* for Biotechnological Applications . In *Frontiers in Bioengineering and Biotechnology* (Vol. 7, p. 464). <https://www.frontiersin.org/article/10.3389/fbioe.2019.00464>
- Nijland, J. G., Shin, H. Y., Boender, L. G. M., Waal, P. P. de, Klaassen, P., & Driessen, A. J. M. (2017). Improved Xylose Metabolism by a CYC8 Mutant of *Saccharomyces cerevisiae*.

Applied and Environmental Microbiology, 83(11), E00095.
<https://search.proquest.com/docview/1908306720>

- Octave, S., & Thomas, D. (2009). Biorefinery: Toward an industrial metabolism. *Biochimie*, 91(6), 659–664.
- Okafor, D. C., & Daramola, M. O. (2020). A Short Overview of Analytical Techniques in Biomass Feedstock Characterization. In *Valorization of Biomass to Value-Added Commodities* (pp. 21–46). Springer.
- Olatunji, O., Akinlabi, S., & Madushele, N. (2020). Application of Lignocellulosic Biomass (LCB). In *Valorization of Biomass to Value-Added Commodities* (pp. 3–19). Springer.
- Omidghane, M., Bartoli, M., Asomaning, J., Xia, L., Chae, M., & Bressler, D. C. (2020). Pyrolysis of fatty acids derived from hydrolysis of brown grease with biosolids. *Environmental Science and Pollution Research*, 27(21), 26395–26405.
- Omidghane, M., Jenab, E., Chae, M., & Bressler, D. C. (2017). Production of renewable hydrocarbons by thermal cracking of oleic acid in the presence of water. *Energy & Fuels*, 31(9), 9446–9454.
- Oncel, S. S. (2013). Microalgae for a macroenergy world. *Renewable and Sustainable Energy Reviews*, 26, 241–264. <https://doi.org/10.1016/j.rser.2013.05.059>
- Orr, V. C. A., & Rehmann, L. (2016). Ionic liquids for the fractionation of microalgae biomass. *Current Opinion in Green and Sustainable Chemistry*, 2, 22–27. <https://doi.org/10.1016/j.cogsc.2016.09.006>
- Osorio-González, C. S., Hegde, K., Brar, S. K., Kermanshahpour, A., & Avalos-Ramírez, A. (2019). Challenges in lipid production from lignocellulosic biomass using *Rhodospiridium* sp.; A look at the role of lignocellulosic inhibitors. *Biofuels, Bioproducts and Biorefining*, 13(3), 740–759. <https://doi.org/10.1002/bbb.1954>
- Özcan, S., & Johnston, M. (1999). Function and regulation of yeast hexose transporters. *Microbiology and Molecular Biology Reviews*, 63(3), 554–569.
- Pan, J., Muppaneni, T., Sun, Y., Reddy, H. K., Fu, J., Lu, X., & Deng, S. (2016). Microwave-assisted extraction of lipids from microalgae using an ionic liquid solvent [BMIM][HSO₄]. *Fuel*, 178, 49–55. <https://doi.org/10.1016/j.fuel.2016.03.037>
- Pang, S. (2019). Advances in thermochemical conversion of woody biomass to energy, fuels and chemicals. *Biotechnology Advances*, 37(4), 589–597. <https://doi.org/10.1016/j.biotechadv.2018.11.004>
- Papanikolaou, S., & Aggelis, G. (2011). Lipids of oleaginous yeasts. Part I: Biochemistry of single cell oil production. *European Journal of Lipid Science and Technology*, 113(8), 1031–1051. <https://doi.org/10.1002/ejlt.201100014>
- Park, J.-Y., Jeon, W., Lee, J.-H., Nam, B., & Lee, I.-G. (2018). Effects of supercritical fluids in catalytic upgrading of biomass pyrolysis oil. *Chemical Engineering Journal*. <https://doi.org/10.1016/j.cej.2018.11.010>

- Parsons, S., Chuck, C. J., & McManus, M. C. (2018). Microbial lipids: Progress in life cycle assessment (LCA) and future outlook of heterotrophic algae and yeast-derived oils. *Journal of Cleaner Production*, *172*, 661–672. <https://doi.org/10.1016/j.jclepro.2017.10.014>
- Patel, A., Karageorgou, D., Rova, E., Katapodis, P., Rova, U., Christakopoulos, P., & Matsakas, L. (2020). An overview of potential oleaginous microorganisms and their role in biodiesel and omega-3 fatty acid-based industries. *Microorganisms*, *8*(3), 434.
- Patel, A., & Matsakas, L. (2019). A comparative study on de novo and ex novo lipid fermentation by oleaginous yeast using glucose and sonicated waste cooking oil. *Ultrasonics Sonochemistry*, *52*, 364–374. <https://doi.org/10.1016/j.ultsonch.2018.12.010>
- Pathak, S. (2015). Acid catalyzed transesterification. *Journal of Chemical and Pharmaceutical Research*, *7*(3), 1780–1786.
- Patil, P. D., Dandamudi, K. P. R., Wang, J., Deng, Q., & Deng, S. (2018). Extraction of bio-oils from algae with supercritical carbon dioxide and co-solvents. *The Journal of Supercritical Fluids*, *135*, 60–68. <https://doi.org/10.1016/j.supflu.2017.12.019>
- Patil, P. D., Reddy, H., Muppaneni, T., & Deng, S. (2017). Biodiesel fuel production from algal lipids using supercritical methyl acetate (glycerin-free) technology. *Fuel*, *195*, 201–207. <https://doi.org/10.1016/j.fuel.2016.12.060>
- Paul, T., Sinharoy, A., Baskaran, D., Pakshirajan, K., Pugazhenti, G., & Lens, P. N. L. (2020). Bio-oil production from oleaginous microorganisms using hydrothermal liquefaction: a biorefinery approach. *Critical Reviews in Environmental Science and Technology*, 1–39.
- Paulino, B. N., Pessôa, M. G., Molina, G., Neto, A. A. K., Oliveira, J. V. C., Mano, M. C. R., & Pastore, G. M. (2017). Biotechnological production of value-added compounds by ustilaginomycetous yeasts. *Applied Microbiology and Biotechnology*, *101*(21), 7789–7809.
- Pedersen, T. H., Jensen, C. U., Sandström, L., & Rosendahl, L. A. (2017). Full characterization of compounds obtained from fractional distillation and upgrading of a HTL biocrude. *Applied Energy*, *202*, 408–419. <https://doi.org/10.1016/j.apenergy.2017.05.167>
- Pichler, H., & Emmerstorfer-Augustin, A. (2018). Modification of membrane lipid compositions in single-celled organisms – From basics to applications. *Methods*, *147*, 50–65. <https://doi.org/10.1016/j.ymeth.2018.06.009>
- Picó, E. A., López, C., Cruz-Izquierdo, Á., Munarriz, M., Iruretagoyena, F. J., Serra, J. L., & Llama, M. J. (2018). Easy reuse of magnetic cross-linked enzyme aggregates of lipase B from *Candida antarctica* to obtain biodiesel from *Chlorella vulgaris* lipids. *Journal of Bioscience and Bioengineering*, *126*(4), 451–457. <https://doi.org/10.1016/j.jbiosc.2018.04.009>
- Pinho, A. de R., de Almeida, M. B. B., Mendes, F. L., Ximenes, V. L., & Casavechia, L. C. (2015). Co-processing raw bio-oil and gasoil in an FCC Unit. *Fuel Processing Technology*, *131*, 159–166. <https://doi.org/10.1016/j.fuproc.2014.11.008>
- Posmanik, R., Cantero, D. A., Malkani, A., Sills, D. L., & Tester, J. W. (2017). Biomass conversion to bio-oil using sub-critical water: Study of model compounds for food

- processing waste. *The Journal of Supercritical Fluids*, 119, 26–35.
<https://doi.org/10.1016/j.supflu.2016.09.004>
- Prakash, A., Singh, R., Balagurumurthy, B., Bhaskar, T., Arora, A. K., & Puri, S. K. (2015). Chapter 16 - Thermochemical Valorization of Lignin. In A. Pandey, T. Bhaskar, M. Stöcker, & R. K. Sukumaran (Eds.), *Recent Advances in Thermo-Chemical Conversion of Biomass* (pp. 455–478). Elsevier. <https://doi.org/10.1016/B978-0-444-63289-0.00016-8>
- Rabie, A. M., Mohammed, E. A., & Negm, N. A. (2018). Feasibility of modified bentonite as acidic heterogeneous catalyst in low temperature catalytic cracking process of biofuel production from nonedible vegetable oils. *Journal of Molecular Liquids*, 254, 260–266.
<https://doi.org/10.1016/j.molliq.2018.01.110>
- Ragauskas, A. J., Williams, C. K., Davison, B. H., Britovsek, G., Cairney, J., Eckert, C. A., Frederick, W. J., Hallett, J. P., Leak, D. J., Liotta, C. L., Mielenz, J. R., Murphy, R., Templer, R., & Tschaplinski, T. (2006). *The path forward for biofuels and biomaterials*.
<http://opus.bath.ac.uk/34521>
- Raheem, A., Wan Azlina, W. A. K. G., Taufiq Yap, Y. H., Danquah, M. K., & Harun, R. (2015). Thermochemical conversion of microalgal biomass for biofuel production. *Renewable and Sustainable Energy Reviews*, 49, 990–999.
<https://doi.org/10.1016/j.rser.2015.04.186>
- Rashid, U., & Anwar, F. (2008). Production of biodiesel through optimized alkaline-catalyzed transesterification of rapeseed oil. *Fuel*, 87(3), 265–273.
- Ratledge, C. (2004). Fatty acid biosynthesis in microorganisms being used for Single Cell Oil production. *Biochimie*, 86(11), 807–815. <https://doi.org/10.1016/j.biochi.2004.09.017>
- Ratledge, C., & Cohen, Z. (2008). Microbial and algal oils: do they have a future for biodiesel or as commodity oils? *Lipid Technology*, 20(7), 155–160.
- Ratledge, C., & Wynn, J. P. (2002). The biochemistry and molecular biology of lipid accumulation in oleaginous microorganisms. *Advances in Applied Microbiology*, 51, 1–52.
- Rebello, S., Abraham, A., Madhavan, A., Sindhu, R., Binod, P., Karthika Bahuleyan, A., Aneesh, E. M., & Pandey, A. (2018). Non-conventional yeast cell factories for sustainable bioprocesses. *FEMS Microbiology Letters*, 365(21), fny222.
- Reece, J. B., Urry, L. A., Cain, M. L., Wasserman, S. A., Minorsky, P. V, & Jackson, R. B. (2011). Cellular respiration and fermentation. *Campbell Biology*, 163–183.
- Reis, E. M., Coelho, R. S., Grimaldi, R., Anschau, A., Cacia Ferreira Lacerda, L. M., Chaar, J., & Franco, T. T. (2014). In situ transesterification from oleaginous yeast biomass. *Ibic2014: 4th International Conference on Industrial Biotechnology*, 38, 319–324.
- Remón, J., Arcelus-Arillaga, P., García, L., & Arauzo, J. (2018). Simultaneous production of gaseous and liquid biofuels from the synergetic co-valorisation of bio-oil and crude glycerol in supercritical water. *Applied Energy*, 228, 2275–2287.
<https://doi.org/10.1016/j.apenergy.2018.07.093>

- Ren, C., Chen, T., Zhang, J., Liang, L., & Lin, Z. (2009). An evolved xylose transporter from *Zymomonas mobilis* enhances sugar transport in *Escherichia coli*. *Microbial Cell Factories*, 8(1), 66. <https://doi.org/10.1186/1475-2859-8-66>
- Ren, Q., & Zhao, C. (2015). Evolution of fuel-N in gas phase during biomass pyrolysis. *Renewable and Sustainable Energy Reviews*, 50, 408–418. <https://doi.org/10.1016/j.rser.2015.05.043>
- Rezaei, M., & Mehrpooya, M. (2018). Investigation of a new integrated biofuel production process via fast pyrolysis, co-gasification and hydrougrading. *Energy Conversion and Management*, 161, 35–52. <https://doi.org/10.1016/j.enconman.2018.01.078>
- Rezania, S., Oryani, B., Park, J., Hashemi, B., Yadav, K. K., Kwon, E. E., Hur, J., & Cho, J. (2019). Review on transesterification of non-edible sources for biodiesel production with a focus on economic aspects, fuel properties and by-product applications. *Energy Conversion and Management*, 201, 112155.
- Ritchie, H., & Roser, M. (2017). Fossil fuels. *Our World in Data*.
- Rivera, E. C., Montalescot, V., Viau, M., Drouin, D., Bourseau, P., Frappart, M., Monteux, C., & Couallier, E. (2018). Mechanical cell disruption of *Parachlorella kessleri* microalgae: Impact on lipid fraction composition. *Bioresource Technology*, 256, 77–85.
- Roca-Mesa, H., Sendra, S., Mas, A., Beltran, G., & Torija, M.-J. (2020). Nitrogen Preferences during Alcoholic Fermentation of Different Non-Saccharomyces Yeasts of Oenological Interest. In *Microorganisms* (Vol. 8, Issue 2). <https://doi.org/10.3390/microorganisms8020157>
- Ross, A. B., Jones, J. M., Kubacki, M. L., & Bridgeman, T. (2008). Classification of macroalgae as fuel and its thermochemical behaviour. *Bioresource Technology*, 99(14), 6494–6504. <https://doi.org/10.1016/j.biortech.2007.11.036>
- Rossi, M., Buzzini, P., Cordisco, L., Amaretti, A., Sala, M., Raimondi, S., Ponzoni, C., Pagnoni, U. M., & Matteuzzi, D. (2009). Growth, lipid accumulation, and fatty acid composition in obligate psychrophilic, facultative psychrophilic, and mesophilic yeasts. *FEMS Microbiology Ecology*, 69(3), 363–372. <https://doi.org/10.1111/j.1574-6941.2009.00727.x>
- Rouhollah, H., Iraj, N., Giti, E., & Sorah, A. (2007). Mixed sugar fermentation by *Pichia stipitis*, *Sacharomyces cerevisiaea*, and an isolated xylosefermenting *Kluyveromyces marxianus* and their cocultures. *African Journal of Biotechnology*, 6(9).
- Ruchala, J., & Sibirny, A. A. (2021). Pentose metabolism and conversion to biofuels and high-value chemicals in yeasts. *FEMS Microbiology Reviews*, 45(4), fuaa069. <https://doi.org/10.1093/femsre/fuaa069>
- Ryu, S., & Trinh, C. T. (2018). Understanding functional roles of native pentose-specific transporters for activating dormant pentose metabolism in *Yarrowia lipolytica*. *Applied and Environmental Microbiology*, 84(3).
- Saika, A., Koike, H., Fukuoka, T., & Morita, T. (2018). Tailor-made mannosylerythritol lipids: current state and perspectives. *Applied Microbiology and Biotechnology*, 102(16), 6877–6884. <https://doi.org/10.1007/s00253-018-9160-9>

- Saini, R., Hegde, K., Brar, S. K., & Soccol, C. R. (2020). Advances in Engineering Strategies for Enhanced Production of Lipid in *Rhodospiridium* sp. from Lignocellulosics and Other Carbon Sources. In *Valorization of Biomass to Value-Added Commodities* (pp. 507–519). Springer.
- Salazar, O., & Asenjo, J. A. (2007). Enzymatic lysis of microbial cells. *Biotechnology Letters*, 29(7), 985–994. <https://doi.org/10.1007/s10529-007-9345-2>
- Saloheimo, A., Rauta, J., Stasyk, V., Sibirny, A. A., Penttilä, M., & Ruohonen, L. (2007). Xylose transport studies with xylose-utilizing *Saccharomyces cerevisiae* strains expressing heterologous and homologous permeases. *Applied Microbiology and Biotechnology*, 74(5), 1041–1052.
- Scaife, M. A., Merckx-Jacques, A., Woodhall, D. L., & Armenta, R. E. (2015). Algal biofuels in Canada: Status and potential. *Renewable and Sustainable Energy Reviews*, 44, 620–642. <https://doi.org/10.1016/j.rser.2014.12.024>
- Schor, D., Maniscalco, S., Tuttle, M. M., Alligood, S., & Kapsak, W. R. (2010). Nutrition facts you can't miss: The evolution of front-of-pack labeling: Providing consumers with tools to help select foods and beverages to encourage more healthful diets. *Nutrition Today*, 45(1), 22–32.
- Schuchardt, U., Sercheli, R., & Vargas, R. M. (1998). Transesterification of vegetable oils: a review. *Journal of the Brazilian Chemical Society*, 9, 199–210.
- Seidl, P. R., & Goulart, A. K. (2016). Pretreatment processes for lignocellulosic biomass conversion to biofuels and bioproducts. *Current Opinion in Green and Sustainable Chemistry*, 2, 48–53. <https://doi.org/10.1016/j.cogsc.2016.09.003>
- Sha, Q. (2013). *A comparative study on four oleaginous yeasts on their lipid accumulating capacity*.
- Shankar, M., Chhotaray, P. K., Agrawal, A., Gardas, R. L., Tamilarasan, K., & Rajesh, M. (2017). Protic ionic liquid-assisted cell disruption and lipid extraction from fresh water *Chlorella* and *Chlorococcum* microalgae. *Algal Research*, 25, 228–236. <https://doi.org/10.1016/j.algal.2017.05.009>
- Sharma, B. K., Suarez, P. A. Z., Perez, J. M., & Erhan, S. Z. (2009). Oxidation and low temperature properties of biofuels obtained from pyrolysis and alcoholysis of soybean oil and their blends with petroleum diesel. *Fuel Processing Technology*, 90(10), 1265–1271. <https://doi.org/10.1016/j.fuproc.2009.06.011>
- Sharma, N. K., Behera, S., Arora, R., Kumar, S., & Sani, R. K. (2018). Xylose transport in yeast for lignocellulosic ethanol production: current status. *Journal of Bioscience and Bioengineering*, 125(3), 259–267.
- Sharrel, R., Aravind, M., & Arun Karthika, B. (2018). Non-conventional yeast cell factories for sustainable bioprocesses. *FEMS Microbiology Letters*, 365(21).
- Shen, M.-H., Song, H., Li, B.-Z., & Yuan, Y.-J. (2015). Deletion of D-ribulose-5-phosphate 3-epimerase (RPE1) induces simultaneous utilization of xylose and glucose in xylose-utilizing *Saccharomyces cerevisiae*. *Biotechnology Letters*, 37(5), 1031–1036.

- Shen, Y., Zhao, P., & Shao, Q. (2014). Porous silica and carbon derived materials from rice husk pyrolysis char. *Microporous and Mesoporous Materials*, *188*, 46–76. <https://doi.org/10.1016/j.micromeso.2014.01.005>
- Shields-Menard, S. A., Amirsadeghi, M., French, W. T., & Boopathy, R. (2018). A review on microbial lipids as a potential biofuel. *Bioresource Technology*, *259*, 451–460. <https://doi.org/10.1016/j.biortech.2018.03.080>
- Shields-Menard, S. A., AmirSadeghi, M., Green, M., Womack, E., Sparks, D. L., Blake, J., Edelmann, M., Ding, X., Sukhbaatar, B., Hernandez, R., Donaldson, J. R., & French, T. (2017). The effects of model aromatic lignin compounds on growth and lipid accumulation of *Rhodococcus rhodochrous*. *International Biodeterioration & Biodegradation*, *121*, 79–90. <https://doi.org/10.1016/j.ibiod.2017.03.023>
- Shokravi, Z., Shokravi, H., Aziz, M. A., & Shokravi, H. (2019). The Fourth-Generation Biofuel: A Systematic Review on Nearly Two Decades of Research from 2008 to 2019. *Fossil Free Fuels*, 213–251.
- Siegal, M. L. (2015). Shifting sugars and shifting paradigms. *PLoS Biology*, *13*(2), e1002068.
- Sijtsma, L., Anderson, A. J., & Ratledge, C. (2010). 7 - Alternative Carbon Sources for Heterotrophic Production of Docosahexaenoic Acid by the Marine Alga *Cryptocodinium cohnii*. In Z. Cohen & C. Ratledge (Eds.), *Single Cell Oils (Second Edition)* (pp. 131–149). AOCS Press. <https://doi.org/10.1016/B978-1-893997-73-8.50011-6>
- Sijtsma, L., Springer, J., Meesters, P. A. E. P., de Swaaf, M. E., & Eggink, G. (1998). Recent advances in fatty acid synthesis in oleaginous yeasts and microalgae. *Recent Research Developments in Microbiology* *2*, 219–232.
- Simpson-Lavy, K., & Kupiec, M. (2019). Carbon catabolite repression in yeast is not limited to glucose. *Scientific Reports*, *9*(1), 1–10.
- Singh, R., Bhaskar, T., & Balagurumurthy, B. (2014). Chapter 11 - Hydrothermal Upgradation of Algae into Value-added Hydrocarbons. In A. Pandey, D.-J. Lee, Y. Chisti, & C. R. Soccol (Eds.), *Biofuels from Algae* (pp. 235–260). Elsevier. <https://doi.org/10.1016/B978-0-444-59558-4.00011-5>
- Sitepu, I. R., Garay, L. A., Sestric, R., Levin, D., Block, D. E., German, J. B., & Boundy-Mills, K. L. (2014). Oleaginous yeasts for biodiesel: current and future trends in biology and production. *Biotechnology Advances*, *32*(7), 1336–1360.
- Sitepu, I., Selby, T., Lin, T., Zhu, S., & Boundy-Mills, K. (2014). Carbon source utilization and inhibitor tolerance of 45 oleaginous yeast species. *Journal of Industrial Microbiology & Biotechnology*, *41*(7), 1061–1070. <https://doi.org/10.1007/s10295-014-1447-y>
- Smallbone, K., Messiha, H. L., Carroll, K. M., Winder, C. L., Malys, N., Dunn, W. B., Murabito, E., Swainston, N., Dada, J. O., Khan, F., Pir, P., Simeonidis, E., Spasić, I., Wishart, J., Weichart, D., Hayes, N. W., Jameson, D., Broomhead, D. S., Oliver, S. G., ... Mendes, P. (2013). A model of yeast glycolysis based on a consistent kinetic characterisation of all its enzymes. *FEBS Letters*, *587*(17), 2832–2841. <https://doi.org/10.1016/j.febslet.2013.06.043>

- Soriano Jr, N. U., Venditti, R., & Argyropoulos, D. S. (2009). Biodiesel synthesis via homogeneous Lewis acid-catalyzed transesterification. *Fuel*, *88*(3), 560–565.
- Sotoudehniakarani, F., Alayat, A., & McDonald, A. G. (2019). Characterization and comparison of pyrolysis products from fast pyrolysis of commercial *Chlorella vulgaris* and cultivated microalgae. *Journal of Analytical and Applied Pyrolysis*, *139*, 258–273. <https://doi.org/10.1016/j.jaap.2019.02.014>
- Sreeharsha, R. V., & Mohan, S. V. (2020). Obscure yet Promising Oleaginous Yeasts for Fuel and Chemical Production. *Trends in Biotechnology (Regular Ed.)*, *38*(8), 873–887. <https://doi.org/10.1016/j.tibtech.2020.02.004>
- Stincone, A., Prigione, A., Cramer, T., Wamelink, M. M. C., Campbell, K., Cheung, E., Olin-Sandoval, V., Grüning, N., Krüger, A., & Tauqeer Alam, M. (2015). The return of metabolism: biochemistry and physiology of the pentose phosphate pathway. *Biological Reviews*, *90*(3), 927–963.
- Stülke, J., & Hillen, W. (1999). Carbon catabolite repression in bacteria. *Current Opinion in Microbiology*, *2*(2), 195–201.
- Su, C.-H., Chien, L.-J., Gomes, J., Lin, Y.-S., Yu, Y.-K., Liou, J.-S., & Syu, R.-J. (2011). Factors affecting lipid accumulation by *Nannochloropsis oculata* in a two-stage cultivation process. *Journal of Applied Phycology*, *23*(5), 903–908. <https://doi.org/10.1007/s10811-010-9609-4>
- Subhadra, B. (2011). Algal biorefinery-based industry: an approach to address fuel and food insecurity for a carbon-smart world. *Journal of the Science of Food and Agriculture*, *91*(1), 2–13.
- Subhadra, B. G. (2010). Sustainability of algal biofuel production using integrated renewable energy park (IREP) and algal biorefinery approach. *Energy Policy*, *38*(10), 5892–5901. <https://doi.org/10.1016/j.enpol.2010.05.043>
- Subtil, T., & Boles, E. (2012). Competition between pentoses and glucose during uptake and catabolism in recombinant *Saccharomyces cerevisiae*. *Biotechnology for Biofuels*, *5*(1), 14.
- Sumiyoshi, Y., Crow, S. E., Litton, C. M., Deenik, J. L., Taylor, A. D., Turano, B., & Ogoshi, R. (2017). Belowground impacts of perennial grass cultivation for sustainable biofuel feedstock production in the tropics. *GCB Bioenergy*, *9*(4), 694–709.
- Tager, H. S. (1993). Principles of Biochemistry. *JAMA*, *270*(16), 1989–1990.
- Takaku, H., Matsuzawa, T., Yaoi, K., & Yamazaki, H. (2020). Lipid metabolism of the oleaginous yeast *Lipomyces starkeyi*. *Applied Microbiology and Biotechnology*, *104*(14), 6141–6148. <https://doi.org/10.1007/s00253-020-10695-9>
- Takkellapati, S., Li, T., & Gonzalez, M. A. (2018). An Overview of Biorefinery Derived Platform Chemicals from a Cellulose and Hemicellulose Biorefinery. *Clean Technologies and Environmental Policy*, *20*(7), 1615–1630. <https://doi.org/10.1007/s10098-018-1568-5>
- Tamilselvan, P., Sassykova, L., Prabhakar, M., Bhaskar, K., Kannayiram, G., Subramanian, S., & Prakash, S. (2020). Influence of saturated fatty acid material composition in biodiesel on its performance in internal combustion engines. *Materials Today: Proceedings*, *33*, 1181–

1186. <https://doi.org/https://doi.org/10.1016/j.matpr.2020.07.626>

- Tanaka, E., & Honda, Y. (2017). Teleomorph–anamorph connection of *Macalpinomyces spermophorus* with *Pseudozyma tsukubaensis* and corresponding erythritol production. *Mycoscience*, 58(6), 445–451. <https://doi.org/10.1016/j.myc.2017.06.006>
- Tang, W., & Ho Row, K. (2020). Evaluation of CO₂-induced azole-based switchable ionic liquid with hydrophobic/hydrophilic reversible transition as single solvent system for coupling lipid extraction and separation from wet microalgae. *Bioresource Technology*, 296, 122309. <https://doi.org/https://doi.org/10.1016/j.biortech.2019.122309>
- Tanimura, A., Takashima, M., Sugita, T., Endoh, R., Ohkuma, M., Kishino, S., Ogawa, J., & Shima, J. (2016). Lipid production through simultaneous utilization of glucose, xylose, and L-arabinose by *Pseudozyma hubeiensis*: a comparative screening study. *AMB Express*, 6(58), (26 August 2016).
- Tanimura, Ayumi, Sugita, T., Endoh, R., Ohkuma, M., Kishino, S., Ogawa, J., Shima, J., & Takashima, M. (2018). Lipid production via simultaneous conversion of glucose and xylose by a novel yeast, *Cystobasidium iriomotense*. *PLoS One*, 13(9), e0202164. <https://doi.org/10.1371/journal.pone.0202164>
- Tanimura, Ayumi, Takashima, M., Sugita, T., Endoh, R., Ohkuma, M., Kishino, S., Ogawa, J., & Shima, J. (2016). Lipid production through simultaneous utilization of glucose, xylose, and l-arabinose by *Pseudozyma hubeiensis*: a comparative screening study. *AMB Express*, 6(1), 1–9. <https://doi.org/10.1186/s13568-016-0236-6>
- Teixeira, C. M., Fréty, R., Barbosa, C. B. M., Santos, M. R., Bruce, E. D., & Pacheco, J. G. A. (2017). Mo influence on the kinetics of jatropha oil cracking over Mo/HZSM-5 catalysts. *Catalysis Today*, 279, 202–208. <https://doi.org/https://doi.org/10.1016/j.cattod.2016.06.006>
- Tezaki, S., Iwama, R., Kobayashi, S., Shiwa, Y., Yoshikawa, H., Ohta, A., Horiuchi, H., & Fukuda, R. (2017). Δ 12-fatty acid desaturase is involved in growth at low temperature in yeast *Yarrowia lipolytica*. *Biochemical and Biophysical Research Communications*, 488(1), 165–170. <https://doi.org/https://doi.org/10.1016/j.bbrc.2017.05.028>
- Thancharoen, K., Malasri, A., Leamsingorn, W., & Boonyalit, P. (2017). Selection of oleaginous yeasts with lipid accumulation by the measurement of Sudan black B for benefits of biodiesel. *J Pharm Med Biol Sci*, 6(2), 37–53.
- Tonda, S., Kumar, S., Bhardwaj, M., Yadav, P., & Ogale, S. (2018). g-C₃N₄/NiAl-LDH 2D/2D hybrid heterojunction for high-performance photocatalytic reduction of CO₂ into renewable fuels. *ACS Applied Materials & Interfaces*, 10(3), 2667–2678.
- Tripathi, S., Choudhary, S., & Poluri, K. M. (2021). Insights into lipid accumulation features of *Coccomyxa* sp. IITRSTKM4 under nutrient limitation regimes. *Environmental Technology & Innovation*, 24, 101786.
- Uduman, N., Qi, Y., Danquah, M. K., Forde, G. M., & Hoadley, A. (2010). Dewatering of microalgal cultures: a major bottleneck to algae-based fuels. *Journal of Renewable and Sustainable Energy*, 2(1), 12701.
- Van der Ploeg, F. (2016). Fossil fuel producers under threat. *Oxford Review of Economic Policy*,

32(2), 206–222.

- Vardon, D. R., Sharma, B. K., Blazina, G. V, Rajagopalan, K., & Strathmann, T. J. (2012). Thermochemical conversion of raw and defatted algal biomass via hydrothermal liquefaction and slow pyrolysis. *Bioresource Technology*, *109*, 178–187. <https://doi.org/10.1016/j.biortech.2012.01.008>
- Velmurugan, A., Loganathan, M., & Gunasekaran, E. J. (2014). Experimental investigations on combustion, performance and emission characteristics of thermal cracked cashew nut shell liquid (TC-CNSL)–diesel blends in a diesel engine. *Fuel*, *132*, 236–245. <https://doi.org/10.1016/j.fuel.2014.04.060>
- Voloshin, R. A., Rodionova, M. V, Zharmukhamedov, S. K., Nejat Veziroglu, T., & Allakhverdiev, S. I. (2016). Review: Biofuel production from plant and algal biomass. *International Journal of Hydrogen Energy*, *41*(39), 17257–17273. <https://doi.org/10.1016/j.ijhydene.2016.07.084>
- Wagner, J. L., Ting, V. P., & Chuck, C. J. (2014). Catalytic cracking of sterol-rich yeast lipid. *Fuel*, *130*, 315–323. <https://doi.org/10.1016/j.fuel.2014.04.048>
- Wang, F., Ouyang, D., Zhou, Z., Page, S. J., Liu, D., & Zhao, X. (2021). Lignocellulosic biomass as sustainable feedstock and materials for power generation and energy storage. *Journal of Energy Chemistry*, *57*, 247–280. <https://doi.org/10.1016/j.jechem.2020.08.060>
- Wang, J., Chae, M., Bressler, D. C., & Sauvageau, D. (2020). Improved bioethanol productivity through gas flow rate-driven self-cycling fermentation. *Biotechnology for Biofuels*, *13*(1), 1–14.
- Wang, L., Wang, D., Zhang, Z., Cheng, S., Liu, B., Wang, C., Li, R., & Guo, S. (2020). Comparative Glucose and Xylose Coutilization Efficiencies of Soil-Isolated Yeast Strains Identify *Cutaneotrichosporon dermatis* as a Potential Producer of Lipid. *ACS Omega*, *5*(37), 23596–23603.
- Wang, W.-C., & Jan, J.-J. (2018). From laboratory to pilot: Design concept and techno-economic analyses of the fluidized bed fast pyrolysis of biomass. *Energy*, *155*, 139–151. <https://doi.org/10.1016/j.energy.2018.05.012>
- Wang, W.-C., & Lee, A.-C. (2019). The study of producing “drop-in” fuels from agricultural waste through fast pyrolysis and catalytic hydro-processing. *Renewable Energy*, *133*, 1–10. <https://doi.org/10.1016/j.renene.2018.10.022>
- Wang, Y., Van Le, Q., Yang, H., Lam, S. S., Yang, Y., Gu, H., Sonne, C., & Peng, W. (2021). Progress in microbial biomass conversion into green energy. *Chemosphere*, *281*, 130835.
- Wang, Z., Qu, L., Qian, J., He, Z., & Yi, S. (2019). Effects of the ultrasound-assisted pretreatments using borax and sodium hydroxide on the physicochemical properties of Chinese fir. *Ultrasonics Sonochemistry*, *50*, 200–207. <https://doi.org/10.1016/j.ultsonch.2018.09.017>
- Wen, S., Yan, Y., Liu, J., Buyukada, M., & Evrendilek, F. (2019). Pyrolysis performance, kinetic, thermodynamic, product and joint optimization analyses of incense sticks in N₂ and

- CO₂ atmospheres. *Renewable Energy*, *141*, 814–827.
<https://doi.org/10.1016/j.renene.2019.04.040>
- Wiggers, V. R., Zonta, G. R., França, A. P., Scharf, D. R., Simionatto, E. L., Ender, L., & Meier, H. F. (2013). Challenges associated with choosing operational conditions for triglyceride thermal cracking aiming to improve biofuel quality. *Fuel*, *107*, 601–608.
<https://doi.org/10.1016/j.fuel.2012.11.011>
- Wu, L., MingSun, L., LongYu, Z., YuSheng, L., YanLin, Z., ZiNiu, Y., ZongHua, M., & Qing, L. (2015). Simultaneous utilization of glucose and xylose for lipid accumulation in black soldier fly. *Biotechnology for Biofuels*, *8*(117), (14 August 2015).
- Wu, S., Zhao, X., Shen, H., Wang, Q., & Zhao, Z. K. (2011). Microbial lipid production by *Rhodospiridium toruloides* under sulfate-limited conditions. *Bioresource Technology*, *102*(2), 1803–1807.
- Xu, C. (Charles), Liao, B., Pang, S., Nazari, L., Mahmood, N., Tushar, M. S. H. K., Dutta, A., & Ray, M. B. (2018). 1.19 Biomass Energy. In I. Dincer (Ed.), *Comprehensive Energy Systems* (pp. 770–794). Elsevier. <https://doi.org/10.1016/B978-0-12-809597-3.00121-8>
- Xu, J., Du, W., Zhao, X., Zhang, G., & Liu, D. (2013). Microbial oil production from various carbon sources and its use for biodiesel preparation. *Biofuels, Bioproducts and Biorefining*, *7*(1), 65–77. <https://doi.org/10.1002/bbb.1372>
- Xu, S., Hu, Y., Wang, S., He, Z., Qian, L., Feng, Y., Sun, C., Liu, X., Wang, Q., Hui, C., & Payne, E. K. (2019). Investigation on the co-pyrolysis mechanism of seaweed and rice husk with multi-method comprehensive study. *Renewable Energy*, *132*, 266–277.
<https://doi.org/10.1016/j.renene.2018.08.002>
- Yadav, G., Sharma, I., Ghangrekar, M., & Sen, R. (2020). A live bio-cathode to enhance power output steered by bacteria-microalgae synergistic metabolism in microbial fuel cell. *Journal of Power Sources*, *449*, 227560.
- Yang, C., Li, R., Zhang, B., Qiu, Q., Wang, B., Yang, H., Ding, Y., & Wang, C. (2019). Pyrolysis of microalgae: A critical review. *Fuel Processing Technology*, *186*, 53–72.
<https://doi.org/10.1016/j.fuproc.2018.12.012>
- Yang, Xiaobing, Jin, G., Gong, Z., Shen, H., Song, Y., Bai, F., & Zhao, Z. K. (2014). Simultaneous utilization of glucose and mannose from spent yeast cell mass for lipid production by *Lipomyces starkeyi*. *Bioresource Technology*, *158*, 383–387.
<https://doi.org/10.1016/j.biortech.2014.02.121>
- Yang, Xiaobing, Jin, G., Wang, Y., Shen, H., & Zhao, Z. K. (2015). Lipid production on free fatty acids by oleaginous yeasts under non-growth conditions. *Bioresource Technology*, *193*, 557–562. <https://doi.org/10.1016/j.biortech.2015.06.134>
- Yang, Xiaoyi, Guo, F., Xue, S., & Wang, X. (2016). Carbon distribution of algae-based alternative aviation fuel obtained by different pathways. *Renewable and Sustainable Energy Reviews*, *54*, 1129–1147. <https://doi.org/10.1016/j.rser.2015.10.045>
- Yarrow, D. (1998). Methods for the isolation, maintenance and identification of yeasts. In *The*

- yeasts* (pp. 77–100). Elsevier.
- Yazan, D. M., van Duren, I., Mes, M., Kersten, S., Clancy, J., & Zijm, H. (2016). Design of sustainable second-generation biomass supply chains. *Biomass and Bioenergy*, *94*, 173–186. <https://doi.org/10.1016/j.biombioe.2016.08.004>
- Yellapu, S. K., Bharti, Kaur, R., Kumar, L. R., Tiwari, B., Zhang, X., & Tyagi, R. D. (2018). Recent developments of downstream processing for microbial lipids and conversion to biodiesel. *Bioresource Technology*, *256*, 515–528. <https://doi.org/10.1016/j.biortech.2018.01.129>
- Yoshida, S., Morita, T., Shinozaki, Y., Watanabe, T., Sameshima-Yamashita, Y., Koitabashi, M., Kitamoto, D., & Kitamoto, H. (2014). Mannosylerythritol lipids secreted by phyllosphere yeast *Pseudozyma antarctica* is associated with its filamentous growth and propagation on plant surfaces. *Applied Microbiology and Biotechnology*, *98*(14), 6419–6429.
- Younes, S., Bracharz, F., Awad, D., Qoura, F., Mehlmer, N., & Brueck, T. (2020). Microbial lipid production by oleaginous yeasts grown on *Scenedesmus obtusiusculus* microalgae biomass hydrolysate. *Bioprocess and Biosystems Engineering*, *43*(9), 1629–1638. <https://doi.org/10.1007/s00449-020-02354-0>
- Young, E. M., Comer, A. D., Huang, H., & Alper, H. S. (2012). A molecular transporter engineering approach to improving xylose catabolism in *Saccharomyces cerevisiae*. *Metabolic Engineering*, *14*(4), 401–411. <https://doi.org/10.1016/j.ymben.2012.03.004>
- Young, E. M., Tong, A., Bui, H., Spofford, C., & Alper, H. S. (2014). Rewiring yeast sugar transporter preference through modifying a conserved protein motif. *Proceedings of the National Academy of Sciences*, *111*(1), 131–136.
- Young, E., Poucher, A., Comer, A., Bailey, A., & Alper, H. (2011). Functional survey for heterologous sugar transport proteins, using *Saccharomyces cerevisiae* as a host. *Applied and Environmental Microbiology*, *77*(10), 3311–3319.
- Yousuf, A. (2012). Biodiesel from lignocellulosic biomass—Prospects and challenges. *Waste Management*, *32*(11), 2061–2067.
- Yuan, L., & Xu, Y.-J. (2015). Photocatalytic conversion of CO₂ into value-added and renewable fuels. *Applied Surface Science*, *342*, 154–167. <https://doi.org/10.1016/j.apsusc.2015.03.050>
- Yuzbasheva, E. Y., Agrimi, G., Yuzbashev, T. V., Scarcia, P., Vinogradova, E. B., Palmieri, L., Shutov, A. V., Kosikhina, I. M., Palmieri, F., & Sineoky, S. P. (2019). The mitochondrial citrate carrier in *Yarrowia lipolytica*: its identification, characterization and functional significance for the production of citric acid. *Metabolic Engineering*, *54*, 264–274.
- Zhang, B., Li, X., Fu, J., Li, N., Wang, Z., Tang, Y., & Chen, T. (2016). Production of acetoin through simultaneous utilization of glucose, xylose, and arabinose by engineered *Bacillus subtilis*. *PloS One*, *11*(7), e0159298.
- Zhang, G.-C., Kong, I. I., Wei, N., Peng, D., Turner, T. L., Sung, B. H., Sohn, J.-H., & Jin, Y.-S. (2016). Optimization of an acetate reduction pathway for producing cellulosic ethanol by engineered yeast. *Biotechnology and Bioengineering*, *113*(12), 2587–2596.

<https://doi.org/10.1002/bit.26021>

- Zhang, G.-C., Liu, J.-J., Kong, I. I., Kwak, S., & Jin, Y.-S. (2015a). Combining C6 and C5 sugar metabolism for enhancing microbial bioconversion. *Current Opinion in Chemical Biology*, 29, 49–57.
- Zhang, G.-C., Liu, J.-J., Kong, I. I., Kwak, S., & Jin, Y.-S. (2015b). Combining C6 and C5 sugar metabolism for enhancing microbial bioconversion. *Current Opinion in Chemical Biology*, 29, 49–57. <https://doi.org/10.1016/j.cbpa.2015.09.008>
- Zhang, J., & Zhang, X. (2019). 15 - The thermochemical conversion of biomass into biofuels. In D. Verma, E. Fortunati, S. Jain, & X. Zhang (Eds.), *Biomass, Biopolymer-Based Materials, and Bioenergy* (pp. 327–368). Woodhead Publishing. <https://doi.org/10.1016/B978-0-08-102426-3.00015-1>
- Zhang, Z., Cheng, J., Qiu, Y., Zhang, X., Zhou, J., & Cen, K. (2019). Competitive conversion pathways of methyl palmitate to produce jet biofuel over Ni/desilicated meso-Y zeolite catalyst. *Fuel*, 244, 472–478. <https://doi.org/10.1016/j.fuel.2019.02.036>
- Zhao, Z., Xian, M., Liu, M., & Zhao, G. (2020). Biochemical routes for uptake and conversion of xylose by microorganisms. *Biotechnology for Biofuels*, 13(1), 1–21. <https://doi.org/10.1186/s13068-020-1662-x>
- Zhou, W., Wang, Z., Alam, M. A., Xu, J., Zhu, S., Yuan, Z., Huo, S., Guo, Y., Qin, L., & Ma, L. (2019). Repeated Utilization of Ionic Liquid to Extract Lipid from Algal Biomass. *International Journal of Polymer Science*, 2019, 9209210. <https://doi.org/10.1155/2019/9209210>
- Zhou, X., Broadbelt, L. J., & Vinu, R. (2016). Chapter Two - Mechanistic Understanding of Thermochemical Conversion of Polymers and Lignocellulosic Biomass. *Advances in Chemical Engineering*, 49, 95–198. <https://doi.org/10.1016/bs.ache.2016.09.002>
- Zhuang, X., Zhan, H., Huang, Y., Song, Y., Yin, X., & Wu, C. (2018). Conversion of industrial biowastes to clean solid fuels via hydrothermal carbonization (HTC): Upgrading mechanism in relation to coalification process and combustion behavior. *Bioresource Technology*, 267, 17–29. <https://doi.org/10.1016/j.biortech.2018.07.002>
- Zullaikah, S., Utomo, A. T., Yasmin, M., Ong, L. K., & Ju, Y. H. (2019). 9 - Ecofuel conversion technology of inedible lipid feedstocks to renewable fuel. In K. Azad (Ed.), *Advances in Eco-Fuels for a Sustainable Environment* (pp. 237–276). Woodhead Publishing. <https://doi.org/10.1016/B978-0-08-102728-8.00009-7>
- Zuorro, A., Malavasi, V., Cao, G., & Lavecchia, R. (2018). Use of cell wall degrading enzymes to improve the recovery of lipids from *Chlorella sorokiniana*. *Chemical Engineering Journal*. <https://doi.org/10.1016/j.cej.2018.11.023>
- Żyłańczyk-Duda, E., Brzezińska-Rodak, M., Klimek-Ochab, M., Duda, M., & Zerka, A. (2017). *Yeast as a Versatile Tool in Biotechnology* (p. <https://www.intechopen.com/books/yeast-industrial>). <https://doi.org/10.5772/intechopen.70130>